Cerebral arteriovenous malformations: Radiosurgery-enhanced molecular targeting therapy

Saleh Rajab Kashba, MB ChB.

Department of Clinical Medicine, Faculty of Medicine and Health Sciences, Macquarie University, submitted in fulfilment of the requirements for the degree of Doctor of Philosophy.

Supervisor:

Professor Marcus Stoodley

June 2015

MACQUARIE University
SYDNEY·AUSTRALIA

This thesis is dedicated to my wife, Suad Alsamine, and daughters Sorour, Hadeel and Nurcine Kashba

Acknowledgements

Many great people have contributed to the production of this thesis. I owe my gratitude to all those people who have made this thesis possible, and will always remember and cherish them forever.

Firstly, I would like to thank my supervisor, Professor Marcus Stoodley. Marcus, you have been a role model to me to become an excellent doctor and researcher. Your patience, kindness and continuous support through all my research and my postgraduate neurosurgical training have been invaluable. You have been there in my darkest times and struggles in research, and I really appreciate everything you have done for me. I will always remember your generous invitations to all our lab members.

I would also like to extend my thanks to our laboratory members for being there for me during my PhD. I would especially like to thank Nirav J. Patel for supporting me with animal experiments, X. Song for helping me with immunostaining technique, M. Grace for radio-surgery assistance, our wonderful research assistant Vivienne S. for animal monitoring when required, and Sarah Hemley and Bowen Dempsey for their support.

My deep gratitude and thanks go to my friends Omar Z. Ameer and Ibrahim M. Salman who were always there for me during my PhD years. You never shut the door in my face whenever I knocked it – even at late hours. Your support and excellent advice helped me to excel in my research. I will always value your friendship and brotherhood.

My sincere thanks also goes to the former and current deans of the Australian School of advanced medicine, Prof. Michael Morgan, Prof. Bill McGaw and Prof. Simone Foote, for offering opportunities to excel in medical research and be surrounded by world class young scientist and achievers.

Lastly, I would like to thank my family members back home. To my mother, Sophia Mahmod, I thank you for your love and kindness. To my beloved father, Rajab Kashba, who passed away during the course of my PhD, you will always be in my heart and mind, and never forgotten. I also extend my appreciation to my brother Mohamed Kashba and uncle Ali Kashba. And, of course, this PhD would not have been possible without the continuous support of my lovely wife, Suad Alsamin, and three daughters, Sorour, Hadeel and Nurcine Kashba, to whom this thesis is dedicated to.

If I have forgotten anyone, I do sincerely apologies.

Saleh Kashba

List of publications and conference presentation

List publications arising from this thesis

Angiographic, hemodynamic and histological changes in an animal model of AVM treated with Gamma Knife radiosurgery. **S.R. KASHBA**, N.J. Patel, M. Grace, V.S. Lee, N. Raoufi-Rad, J.V. Amal Raj, T.T. Hong Duong, M. Stoodley (Published in the Journal of Neurosurgery – April 2015).

Characterization of Gamma-Knife induced histological changes in an animal model of AVM. **S.R. KASHBA**, N.J. Patel, X. Song, M, Grace, M.A. Stoodley. The Annual Scientific Meeting of the Neurosurgical Society of Australasia, 3-5th October 2013, Palmer Coolum Resort, Sunshine Coast, Queensland (Poster presentation).

Gamma Knife radiation-induced angiographic and haemodynamic changes in animal model of brain arteriovenous malformation. **S.R. KASHBA**, N.J. Patel, T.T. Hong Duong, M. Grace, V.S. Lee, N. Raoufi-Rad, J.V. Amal Raj, M.A. Stoodley. American Association of Neurological Surgeons (AANS), 27th April -1st May 2013, Ernest N. Morial Convention Centre, New Orleans, Louisiana (Poster presentation).

Gamma Knife radiation injury in animal model of arteiovenous malformation leads to differential regulation of vascular endothelial cell adhesion molecules. **S.R. KASHBA**, N.J. Patel, T.T. Hong Duong, M. Grace, S. Alsamin, M. A. Stoodley. American Association of Neurological Surgeons (AANS), 5-9th April 2014, Moscone Centre in San Francisco (Poster presentation).

Expression of thrombotic molecules after radiosurgery in an animal model of arteriovenous malformation**. S.R. KASHBA**, N.J. Patel, X. Song, M, Grace, M.A. Stoodley. (Has been accepted for verbal presentation at the Annual Scientific Meeting of the Neurosurgical Society of Australasia, Thursday 2 to Saturday 4 October 2014 Perth, Western Australia (verbal presentation)

List publications arising from the candidature

Irradiation induces molecular changes in endothelial cells of a rat AVM model. Newsha Raoufi-Rad, Zhenjun Zhao, Joshua McHattan, Vivienne S. Lee, Michael Grace, Thi Thuy Hong Duong, Marcus Stoodley, Nirav J. Patel, **Saleh R. Kashba**. World Molecular Imaging Congress, 2013. (Poster presentation).

Gamma radiation induced phosphatidylserine externalization on endothelial cells in a rat arteriovenous malformation model. Newsha Raoufi-Rad, Zhenjun Zhao, Hong T.T. Duong, Michael Grace, Nirav Patel, Vivienne Lee, **Saleh Kashba**, Jude Amal Raj and 1 Marcus A. Stoodley. Australian Vascular Biology Society meeting, 2013. (Poster presentation).

Abstract

Object

Cerebral arteriovenous malformations (AVMs) are a major cause of stroke in children and young adults. Surgery and stereotactic radiosurgery are treatment options for selected AVMs patients. However surgery is not suitable for larger deeply located AVMs. Radiosurgery has a long latency period and has a relatively low efficacy. Molecular targeting therapy to promote intravascular thrombosis is a new treatment strategy for high grade AVMs. This proposed treatment might improve the efficacy of radiosurgery in treating AVMs that not treatable with the current therapies. Non-ligand molecular therapy using lipopolysaccharides and tissue factor has been shown effectiveness in treating AVMs in an animal model. However, non-ligand therapy might be not safe in humans. Ligand-based therapies may overcome safety concerns of non-ligand therapy. Ligand based vascular targeting therapy for brain AVMs requires a specific endothelial cell surface molecule that distinguishes AVMs from the normal vessels. Unlike in tumours, endothelial cells of AVMs do not have specific markers that differentiate them from normal endothelial cells. Radiosurgery may have the ability to induce molecular endothelial changes sufficient to allow targeting.

Materials and methods

A Gamma Knife irradiated animal model of AVM was developed in this study. A specific animal frame was designed for this purpose. Identification of the created AVMs using 3D reconstructed CT images was achieved and the radiation treatment for each animal was planned using the Gamma Knife software. Responses of the AVM model to Gamma Knife radiation were studied using haemodynamic, morphological and histological techniques. Immunohistochemistry was used to investigate specific endothelial cell molecules in the animal model and their response to radiosurgery.

Results

Gamma Knife irradiation produced angiographic changes at 6 and 12 weeks, with statistically significant differences in the proximal and distal left external jugular vein diameters between the treatment group and the control group ($P < 0.05$).

Compared to the controls, the treated group had lower blood flow when assessed across all time points using ANOVA ($P < 0.001$). At 12 weeks, there was a significantly lower flow rate in the left common carotid artery and left external jugular vein in the treated group compared with the control group ($P < 0.001$) and ($P < 0.05$) respectively. Histologically, Gamma Knife radiosurgery induced concentric sub-endothelial cell growth. Intercellular adhesion molecule-1 (ICAM-1) expression significantly increased in the Gamma Knife treated group compared to the non-irradiated group ($P < 0.05$). Confocal analysis indicated that ICAM-1 expression was primarily confined to the endothelial cell surface. An increase in the expression of tissue factor in irradiated AVMs was identified at 1, 3, 6 and 12 weeks after radiation, however, this was not significant ($P>0.05$).

Conclusions

In the animal model of AVM, Gamma Knife irradiation induces angiographic, histological and haemodynamic responses may resemble that of human AVMs. This thesis shows that the Gamma Knife radiated animal model is suitable for studying methods to enhance radiation responses in AVMs. The study improves our understanding of the mechanism of radiosurgery for treating AVM. Moreover, radio surgery appears to induce specific molecular changes that discriminate AVM endothelium from normal endothelium, thus paving the way for targeted molecular therapy.

Declaration

This work contains no material that has been accepted for the award of any other degree or diploma in any university or tertiary institution and, to the best of my knowledge and belief, contains no material previously published or written by another person, except where due reference has been made in the text.

Saleh. Rajab. Kashba

June 2014

Table of Contents

Figures

Tables

Abbreviations

5FU	5 Fluorouracil
ALK-1	Activin receptor like kinase 1
Ang1 and Ang 2	Angiopoietin 1 and 2
ARDS	Acute respiratory distress syndrome
AVF	Arteriovenous fistula
AVMs	Arteriovenous malformations
CA4P	Combretastatin A-4 disodium phosphate
COX	Cyclooxygenase
CPP	Cerebral perfusion pressure
CT	Computed tomography
DIC	Disseminated intravascular coagulation
DVP	Draining vein pressure
ECM	Extracellular matrix
ECs	Endothelial cells
EGF	Epidermal growth factor
ENG	Endoglin
ET-1	Endothelin-1
FTI	Farnesyltransferase inhibitors
GKS	Gamma knife radiosurgery
Gy	Gray
HCAECs	Human coronary endothelial cells
HCMSMCs	Human coronary smooth muscle cells
HHT	Hereditary haemorrhagic telangiectasia
HPMEC	Human pulmonary micro-vascular endothelial cell
HUVECs	Human umbilical vein endothelial cells
ICAM-1	Intercellular adhesion molecule-1
ICH	Intracranial haemorrhage
Ig	Immunoglobulin
IL	Interleukin
IR	Ionised radiation
LCCA	Left common carotid artery
LEJV	Left external jugular vein
LINAC	Linear accelerator radiosurgery
LPS	Lipopolysaccharide
MAP	Mean arterial pressure
MHC class II	Major histocompatibility complex class II
MTD	Microtubule destabilizing agents
NO	Nitric oxide
PBMNCs	Human peripheral blood mononuclear cells
PBS	Phosphate buffered saline

PC	Pancreatic cancer
PDGF	Platelet-derived growth factor
PECAM-1, CD31	Platelet endothelial cell adhesion molecule-1
PGI2	Prostacyclin
RAS	Renin angiotensin system
RCC	Renal cell carcinoma
TKIs	Tyrosine kinase inhibitors
TM	Tissue factor
TNF	Tumor necrosis factor
TNF-α	Tissue necrosis factor-α
VCAM-1	Vascular cell adhesion molecule-1
VEGF	Vascular endothelial growth factor
VTAs	Vascular targeting agents
vWF	von Willebrand factor

Chapter 1

Cerebral vascular malformations

1.1 Epidemiology

Epidemiological information about cerebral arteriovenous malformations (AVMs) is unclear due to the scarcity of cerebral AVMs, prior reliance on angiography for diagnosis, biasing the data toward patients with haemorrhage, and late emergence of large and well-defined population studies [1]. A hospital-based autopsy study shows AVM prevalence ranges from 5 to 613 AVMs per 100,000 people [2-5]. A 27-year population-based retrospective study conducted in Olmsted County, Minnesota, found the incidence of haemorrhagic intracranial malformation to be 0.82 per 100,000; Jessurun found an annual incidence rate for symptomatic AVMs of 1.1 per 100,000 [6]. Another autopsy study conducted on 4530 people found 196 people had arteriovenous malformations of the brain (AMB), a rate of 4.3% [7]. A study performed in Perth, Australia between 1990 and 1996, found a detection rate of 0.89 per 100,000 persons per year [8]. More recently, between 2000 and 2002, a prospective epidemiological study carried out on around 10 million people found a detection rate of 1.34 per 100,000 people [1, 9]. AVM prevalence studies have rarely been conducted, although a Scottish community-based retrospective study reported a prevalence rate of less than 0.02% [10].

1.2 Pathogenesis

The exact factors that lead to the formation of AVMs are not well elucidated. Although de novo AVM formation has been reported [11, 12], recent studies suggest genetic factors contribute to the pathogenesis of sporadic brain AVMs [13, 14]. Many familial disorders leading to vascular malformations have been identified [15], such as Sturge-Weber disease,

Wyburn-Mason syndrome, and Osler-Weber-Rendu disease, also known as hereditary haemorrhagic telangiectasia (HHT).

HHT is an autosomal dominant disease characterised by multiple organ systems vascular malformations, including brain AVM malformation. HHT1 and HHT2 found to be caused by mutations in Endoglin (ENG) and Activin receptor-like kinase 1 (ALK-1) genes [16]. A polymorphism in ALK-1 reported to be associated with sporadic cerebral AVM susceptibility [17]. AVMs are believed to be linked to mutations in the ENG or mutations in Activin receptor-like kinase 1 gene (ACVRL1) [18, 19]. Mahmoud et al. reported that a deficiency inENG in the mouse leads to delayed remodelling of the capillary plexus and increased proliferation of endothelial cells leading to AVM formation [20]. In ACVRL1-deficient mice, it has been shown that ACVRL1 is required for angiogenesis and AVM development [21]. ACVRL1 acts to increase endothelial cell (EC) proliferation in mutated cranial vessels, and is believed to have a role in vessel malformations that may result in haemorrhage or stroke [22].

A study of the molecular feature of AVM tissue shows a highly antigenic milieu with increased EC turnover and inflammatory cell-mediated vascular remodelling [23, 24]. Chen et al. [25] demonstrated that neutrophils and macrophages are often identified in the vascular wall of AVM tissue; they suggest that inflammation is associated with AVM disease progression and rupture. Association of interleukin (IL) -1beta promoter with AVM susceptibility [13], presentation of intracranial haemorrhage (ICH) in AVM [24] and with new ICH after diagnosis [14], have suggested the role of inflammatory cytokines in AVM angiogenesis and formation.

The role of vasculogeneis in AVM formation has also been investigated. Many studies have shown that in AVM tissue, hypoxia inducible factor-1, vascular endothelial growth factor (VEGF), and VEGF receptors are increased [26, 27]; these factors and receptors are important in vasculogenesis during tissue ischemia [28, 29]. In the investigation of EC turnover in brain AVMs, Hashimoto et al. found a high EC turnover in AVM vessels compared to non-AVM tissue [30]. Matrix metalloproteinase–9 also increases in AVM tissue [23, 25], and this may lead to the release of endothelial progenitor cells (EPCs) and vasculogenesis [31].

1.3 Clinical presentation

Brain AVMs have haemorrhagic or non-haemorrhagic presentations. Haemorrhage is the most common clinical presentation, accounting for 38% to 75% of all AVMs [1]. With the introduction of non-invasive imaging technology such as MRI, the identification of incidental and un-ruptured AVMs has become more frequent, and is detected mainly in urban populations [9], a recent study shows that haemorrhage accounts for less than 50% of all AVM presentations [9] and detection of un-ruptured cerebral AVM occurs 2.5 times more than haemorrhagic presentation [9, 41-43].

Patients with a cerebral AVM present with seizures in 18–47% of cases [32-39], chronic headaches in 6–14% of cases and focal neurological deficit in 3–10% of cases [10, 36]. Non-specific symptoms and other incidental findings are reported in less than 15% of patients [40].

1.4 Natural history

Many studies report that rates of AVM haemorrhage range from 35–81% [44-48]. The haemorrhage site is mainly parenchymatous, subarachnoid, ventricular, or a combination of these locations. Intra-parenchymal locations are most likely to result in neurological deficits [44, 49]. In a cross-sectional prospective study from Columbia databank, 45% of subjects presented with intracranial haemorrhage [50]. In a prospective study from three different databases, cerebral haemorrhage was reported in 53% of the 1,289 AVM patients [51]. It has been reported that the annual risk of haemorrhage in patients with cerebral AVM ranges from 2–4% [36, 47, 49, 52, 53]. Re-bleeding seems to be higher in patients with initial haemorrhage presentation, suggesting the lesion becomes unstable and is subsequently more prone to re-bleeds [47, 53, 54].

Different groups have investigated the relationship between AVM size and the haemorrhage rate. Two groups found that small AVMs were associated with a haemorrhagic presentation

[55, 56], while other studies reported that lesions larger than 3 cm were related to haemorrhage [57]. Many researchers have found no relation between the bleeding of AVMs and their size [40, 58, 59].

Morbidity and mortality from bleeding as a consequence of AVM rupture have been studied. Different outcome measures, such as the scale of four grades of ‘good’, ‘fair’, ‘poor’, and ‘dead’ [38] or five grades being ‘no deficits’, ‘moderate disability’, ‘severe disability’, ‘persistent vegetative state’ and ‘death’ [32] have been used, making it difficult to interpret morbidity rates. Annual mortality rates from haemorrhage-related causes range from 0 to 4·7% [32, 38, 60, 61]. Brown et al. have documented that during 8 years of following 168 patients suffering from AVM, no severe disabling outcomes were documented and the overall risk of haemorrhage was 2.25% per year [36]; the Columbia Arteriovenous Malformations Study reports similar results [49]. More supporting studies have found that about 85% of patients retain a good quality of life following both first and second haemorrhages [46].

1.5 Pathology

1.5.1 AVM gross anatomy

Brain AVMs are collection of abnormal vessels including arteries and veins [62, 63]. The underlying structure of a cerebral AVM involves an immediate connection between arteries and abnormal tortuous dilated veins, which connect within what is referred to as the ‘nidus’ without an intervening with the capillary network **(Figure 1-1)** [62, 64]. The arteries which supply the AVM are called feeding arteries, and these may be circumferential, ‘en passage’, terminal or penetrating, according to their relation to the nidus. Feeding arteries vary in size, in number and in histological structure [65]. Four or fewer sizable feeding arteries can be seen, but the multiple small feeding arteries are less readily observed [66]. The nidus forms a wedge-shaped collection of vessels, usually in the subcortical area [67]. Communicating venules receive blood directly from the arteries or arterioles within the nidus, and drainage is to the nearby cerebral veins or dural venous sinus [67]. Several AVMs are tiny, only

detectable by angiography and they tend to affect the midbrain, pons, thalamus, or a small region of a cerebral lobe. Most AVMs are single lesions, but multiple AVMs have been documented [62].

Haemodynamic multicompartment of AVMs is a concept formulated from surgical experience and regional embolization of AVMs [68]. Angiographically, each compartment possesses intrinsic feeding arteries and draining veins [69]. Multicompartment AVMs larger than 3 cm have been found to have two or more feeding arteries and more than one draining vein. These tend to have multiple perforating blood supplies [67]. Inside the nidus, different compartments tend to be hemodynamically balanced with no inter-compartment transfer noted on angiography [67, 70]; however, inter-compartmentally connected venules may be present [71].

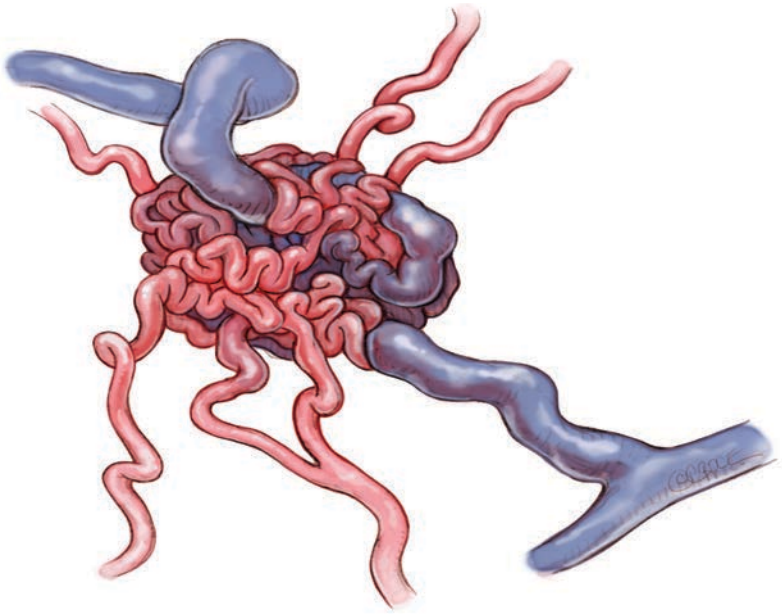

Figure 1-1 Schematic showing an AVM.

An AVM is a tangled bundle of blood vessels where arteries connect directly to veins with no capillary bed in between.

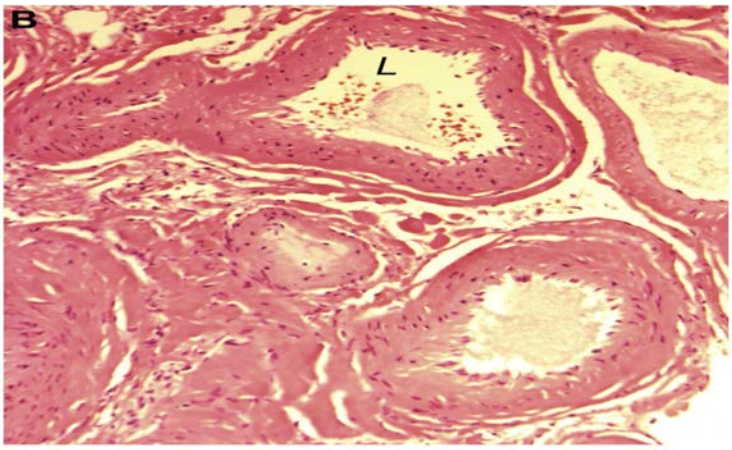

Figure 1-2 human arteriovenous malformation (AVM) nidus

A human AVM nidus (L = lumen) (haematoxylin and eosin stain; original magnification, **x** 400), adapted from Tu *et al*, 2010 [72].

1.5.2 Histopathology and ultrastructure

Under the light microscope, arteries and veins are not easy to differentiate among the dilated vessels of AVMs [73]. The AVM nidus has an abnormal structure without intervening normal brain tissue, and typically has a heterogeneous wall size and thickness [72]. A variably thickened endothelial layer, endothelial cushions, increased collagen deposition and lymphocyte infiltration in the vessel walls with hypertrophy of the medial layer may be observed **(Figure 1-2)** [62, 72]. Splitting of the elastic lamina has also been reported [72], as have thick-walled AVM vessels without an internal elastic lamina [73]. Thrombosis, contiguous gliosis, hemosiderin deposition and wall calcification are characteristic features [73]. Arterial wall thickening can be caused by proliferation of fibroblasts, muscle cells, and an increase in connective tissue. An increase in luminal size is also documented in the literature [63]. Aneurysm formation secondary to wall thinning is reported, together with the formation of arterialised veins, which tend to have a thickened wall caused by fibroblast proliferation. Occasionally, vessel wall structures are distinguishable, where arteries are characterised by the presence of smooth muscle cells and elastic lamina, and veins by the absence of muscle cells [74].

An incompetent blood brain barrier in the nidus has been noted under the electron microscope [72], and an endothelial discontinuity with the absence of both basement membrane and pericytes has been described. Endothelial cells of AVMs exhibit fenestrated processes, multiple filopodia and cytoplasmic vesicles, and subendothelial heterogeneous cells have also been detected [72]. In the nidus, no capillary bed has been observed. Perinidal capillaries observed 1-6 mm from the nidal border present with different sizes correlated with the nidus size. The main feature of perinidal capillaries is a dilated lumen that is almost 8–16 times that of the normal capillaries. Tu et al. have reported that the surrounding brain tissue has hemosiderin staining and that the endothelium of the perinidal capillaries is heterogeneous. Separation of the endothelium, and blood cell extravasation from the vascular wall, have also been documented. No basement membranes or astrocytic foot process have been observed. Fenestrated luminal surfaces and large gaps at the intercellular junction have been revealed, and Weibel-palade bodies identified in areas near inter-endothelial junctions. The endothelial cells of the perinidal capillaries demonstrate fenestrated processes, filopodia, lysosomes, cytoplasmic vesicles, and vacuoles with an average of one pericyte for every three ECs. An abundance of pinocytotic vessels, vacuoles and filaments have been observed in the pericytes [75].

1.6 Molecular expression

Several endothelial molecular proteins are detectable in the AVM vessels, including cell-adhesion molecules such as E-selecting, intercellular adhesion molecule-1 (ICAM-1), and platelet endothelial cell adhesion molecule-1 (PECAM). These are thought to participate in neovascularisation and vascular remodelling [76, 77]. Storer *et al* investigated the endothelial molecular expression in AVMs and observed the endothelium of AVM expressed P-selectin equivalent to that of normal endothelium. P-selectin was also expressed in the subendothelium of AVM, seen as faint staining. Storer et al. found that expression of E-selectin was markedly higher in AVMs than in normal controls, and that AVMs' ECs demonstrated ICAM-1 and vascular cell adhesion molecule 1 (VCAM-1) staining on their

endothelial cells [78]. In a rat model of AVM where endothelial molecular changes were investigated by Karunanyaka *et al* [77], E-selectin, P-selectin, and vascular endothelial growth factor were examined at several time points; E-selectin and P-selectin were expressed in different parts of the created fistulae.

Uranishi [79] investigated the presence of PECAM-1 (CD31) in the ECs of AVMs by immunohistochemistry to determine protein expression in frozen human AVM tissue. Uranishi found that the vast majority of tissues examined were positive for CD31 with two distinct antibodies. He also examined PECAM-1 expression using in-situ hybridisation; no statistically significant differences were found in CD31 protein or mRNA expression levels in AVMs. A marked decrease in the level of PECAM-1 mRNA in AVMs was documented in a study using human cerebrovascular malformations [80]. Expression of PECAM-1 on ECs was intense and was found generally co-localised with Von Willebrand factor (vWF) [78].

Expression of vascular endothelial growth factors (VEGF) A to D and their receptors in paraffin-embedded human AVM nidus were examined using an immunohistochemical technique [81]. The study indicated that 96.8% of AVMs patients stained positive for VEGF-A, 9.7% for VEGF-B, 54.5% for VEGF-C, and 51.6% for VEGF-D. It is believed that the VEGF–VEGF receptor system plays a role in the growth of intracranial AVMs. Increased expression of the transforming growth factor alpha, basic fibroblast growth factor and nitric oxide synthase in brain AVMs has been documented, supporting the contention that AVM are in a continuous angiogenic process [82, 83]. Sonstein et al. also found a high degree of astrocytic VEGF expression in children with recurrent AVMs [84].

Hashimoto et al. [85] investigated mRNA and protein expression of angiopoietin 1 (Ang1) and Ang2 in AVMs, with data showing that the level of Ang1 protein, Ang2 mRNA and Ang2 protein were 30% lower, 40% higher and 800% higher, respectively, in cerebral AVMs than in controls. They concluded that an abnormal balance in the angiopoietin and tyrosine kinase with immunoglobulin and endothelial growth factor-like domains 2 system may explain the aberrant vascular phenotype in the lesion.

1.7 Pathophysiology

The management of cerebral AVMs requires an understanding of AVM haemodynamic and the consequences of abnormal haemodynamic on the brain.

1.7.1 **Haemodynamic of the AVM nidus**

Flow resistance inside the nidus of AVMs is the most important factor in the determination of haemodynamic consequences. Many studies have found that the flow is mainly dependent on the cross-sectional area at the narrowest point in the fistula. As a significant proportion of AVMs have as their narrowest point vessels greater than 100 μm and some greater than 300 μm, they usually have a lower resistance than normal cerebral vasculature [86-88].

Turbulent flow is a characteristic feature of cerebral AVMs. The phenomenon results from an increase in velocity and lower resistance, an increase in diameter, and fluctuating vessel diameters found within the AVM nidus [89], and is believed to be responsible for venous varices found within or shortly beyond the nidus of the AVM, which cause structural fatigue and focal dilatation [90, 91]. Turbulent shear stresses as low as 1.5 dynes/cm^2 for as short a period as three hours were detected in an *in vitro* experiment. The stress was found to stimulate substantial endothelial DNA synthesis and endothelial turnover [92], which modulates endothelial transport, increases endothelial microfilament bundles, and makes ultrastructural changes in the subendothelial layer [93-95]. Both structural fatigue and pressure are responsible for rupture within the AVM nidus. In an experimental arteriovenous model, high shear stress produced platelet aggregation and red cell haemolysis in a dog model of AVM [96].

1.7.2 **Feeding arterial system of an AVM**

There is a tendency for AVMs and the terminal feeder to have a low-pressure measurement. Nornes and Grip measured the pressure in dilated feeding vessels and found the pressure

varied between 40 and 70 mmHg with flow reaching 550 ml per minute [91]. Another study found that the feeding artery pressure was about 45–62% that of the radial artery [97] and 67–71% that of the pressure in the femoral catheter [98, 99]. This is markedly less than normal distal pial arterial pressure, being around 90% of systemic arterial pressure. Pial arterial pressure on the side of the AVMs was 61% and 78% of the peripheral systemic pressure and the matched contralateral side respectively [100]. Fleischer et al. [101] investigated the relationship of transcranial Doppler flow velocities and AVM feeding artery pressures, finding that pressure in half of the cases was less than 50% of the femoral pressure. They concluded that as a result of high flow through the fistula, the dilated feeding arteries tend to have low measured pressure [102].

1.7.3 Draining venous system of AVMs

The pressure within the draining vein correlates with the pressure within feeding arteries but is inversely correlated to the AVM nidus size [102]. In human AVMs, a lack of intervening capillaries between artery and vein causes elevated pressure in the draining vein of AVMs [103]. In contrast to normal venous circulation, the flow within the draining vein of AVM has been reported to be pulsatile with high velocity [104]. The turbulent venous flow near the AVM nidus [91] and the greater pressure on the vein wall may be responsible for endothelial turnover and ultrastructural changes in the subendothelial layer of the AVM [93-95]. The risk of haemorrhage is reportedly increased when the venous resistance is increased secondary to venous drainage occlusion or stenosis.

1.8 Experimental animal model

Yassari et al. [105] described the angiographic, haemodynamic and histological characterisation of an arteriovenous fistula in rats. The model was created by anastomosing the end of the left external jugular vein (LEJV) to the side of the left common carotid artery (LCCA) in rats. The model allows a better description of histological changes in the dural

sinuses as well as in cortical vessels, demonstrating haemodynamic changes in the LCCA and LEJV. The angiographic study revealed that the proximal portion of the ipsilateral EJV and the distal ipsilateral EJV, and the diameter of the transverse sinus, increased significantly. The haemodynamic study showed a 68±4% increase in blood flow within the LCCA immediately post-fistula formation. However, no marked changes were observed in the flow through the fistula at different time points. Histologically, transverse sinus thickness increased slightly at 21 days post-AVM creation. Histological sections of the fistula showed fibrin deposition, proliferation of actin immunoreactive cells, apparent collagen infiltrated medial hyperplasia, well-organised smooth muscle layers, and discontinuous and elastin fragments. Yassari et al. concluded that the model is suitable for mechanistic and therapeutic studies of AVMs, and also indicate that the venous anatomy of the rat created a retrograde high flow in the jugular vein (arterialised feeder). The drawback of the model for this study is that the created AVM is not in the brain nor congenital **(Table 1-1).**

The same animal model was compared with human AVM. There were significant histopathological and ultrastructural similarities between human AVM vessels and the animal model, and the model became most representative of human AVMs when the blood flow reached its highest flow rate. It was concluded that the model shares haemodynamic, morphological and ultrastructural features with human AVMs, especially in the endothelial layer [72].

Massoud et al. [106] used a swine model of AVM to investigate histopathological characteristics. They developed AVM models from bilateral carotid retia mirabilia of swine after the surgical creation of large unilateral carotid-jugular fistulas. To ensure shunting of blood from the left to the right side of the neck and to induce high flow through both retia, the right occipital artery, the right external carotid artery and the muscular branch of the right ascending pharyngeal artery were deliberately occluded. At four days after AVM creation, there was angiographic evidence of vascular dilatation and tortuosity of the main arterial feeder and draining. These changes were most prominent in the 6-month-old model. The chronic models demonstrated disrupted elastic intimal hyperplasia that was focal and the presence of smooth muscle actin within cells in the tunica media of nidus vessels. In the

chronic vessels, histological study revealed increases in intimal hyperplasia and medial thickness.

Qian et al. [107] described a simplified AVM model in sheep. The model was created by anastomosing the CCA and the ipsilateral EJV. In their model they ligated the jugular vein above the anastomosis site and the proximal CCA below the anastomosis site. Extensive collateral flow through the rete mirabile into the distal segment of the external carotid artery above the ligature, with retrograde flow through the surgical anastomosis into the jugular vein was established. This model indicated that the vast majority of blood flow from the rete mirabile was diverted into the jugular vein through the created anastomosis.

Pietilä et al. [108] used dogs to create their AVM animal model. A bypass was created by interposing a superficial temporal artery segment between the middle cerebral artery (MCA) and the superior sagittal sinus. A vascularised muscle graft supplied by a side branch of the superficial temporal artery was implanted into the ischemic territory previously supplied by the middle cerebral artery. An angiographic study showed AVM-like formations with newly developed vessels in addition to the AV fistula. A histopathological study revealed a peri shunt parenchymal gliosis, proliferation of mesenchyme cells and fibroblasts. Capillary proliferation was also noted. They concluded that their animal model is comparable with the situation found in intracerebral AVM in humans.

Lemson et al. [109] investigated the role of intimal hyperplasia (IH) in the failure of arteriovenous (AV) fistulas of a goat model. The animals had a bridge graft AV fistula between the carotid artery and the jugular vein. Intimal hyperplasia displaying an abundant expression of α-smooth muscle actin was a prominent finding. Significantly, intimal hyperplasia also developed at the suture line. At the anastomosis, the hyperplastic lesions were usually not covered by endothelium and were instead overlaid with fibrin deposition. Frequently thrombus was present, particularly at the site of the anastomosis.

Several groups have considered carotid rete vascular arrangements as useful models that mimic human AVMs, and allow them to investigate effect of radiosurgery on their models [106, 110, 111]. The swine rete mirabile was used as a model of an AVM to explore the

effects of varying doses of radiosurgery. The mirabile received a single dose of radiation (20, 30, 40, 50, 60, 70, 80, and 90 Gray [Gy]) [110] and the effect was observed using angiography and histopathological examination. Progressive angiographic occlusion and marked thickening of the vessel wall, ultimately resulting in occlusion of the vascular lumen and associated thrombosis, were reported in the histological study; these changes correlated with the higher radiation doses. The major limitations of the use of the rete are that it is an arterio-arterial system with a much lower pressure gradient than exists in an AVM, and that the vessels have normal histological and molecular characteristics. Unlike human AVMs, there are no vein-like channels within the vascular network of the rete; nevertheless, the vascular changes in this model corresponded well to the histological changes described in irradiated AVMs. Several groups have modified the swine rete mirabile model to incorporate the high-flow features of AVMs by creation of a unilateral carotid-jugular fistula, with endovascular blocking of several side branches of the carotid to prevent collateral circulation, that induced high flow through both rete [106, 111].

Altschuler et al. [112] used a platform to deliver a dose of 50 Gy to an abdominal aorta vena caval fistula in the rat using a Gamma Knife machine. Targeting of the fistula was performed by leaving a small radiopaque clip at the site. The histological study of the irradiated tissue showed a venous endothelial proliferation that was not present in fistulae of non-irradiated animals.

Baker et al. [113] examined the effects of irradiating rat femoral arteries. They found that irradiation with 6000 R had no effect on the patency of the artery; the histological study demonstrated increased fibrosis and increased smooth muscle cell proliferation at the anastomosis site. Some arteries also exhibited endothelial proliferation.

The effects of intracranial venous hypertension in a rat model of arteriovenous fistula was investigated by Bederson et al. [114]. The fistula was created by anastomosing the proximal CCA to the distal EJV; the contralateral EJV was then occluded 24 hours later. The study revealed increased pressure in the transverse sinus and decreased mean arterial pressure, with a decrease in cerebral perfusion pressure. A histological examination of rats with permanent venous occlusion found venous infarction, severe brain oedema and subarachnoid

haemorrhage. Bederson et al. concluded that the model haemodynamically reproduced the haemorrhagic complication of the human AVM and explained the role of venous obstruction in the pathogenesis of congenital lesions.

The effect of chronic cerebral hypoperfusion associated with AVM has been investigated [115] using a model created via end-to-side anastomosis between the right distal EJV and the ipsilateral CCA, and ligation of left vein draining the left transverse sinus and bilateral external carotid arteries. Systemic mean arterial pressure (MAP), draining vein pressure (DVP), and CPP were measured. The results showed that fistula creation led to a significant decrease in MAP and cerebral perfusion pressure (CPP), and a significant increase in DVP in the AVF. Damage to the blood brain barrier, brain oedema and haemorrhage were also noticed.

Yamada et al. [116] examined the effect of cerebral venous hypertension on cerebral blood flow regulation in an animal model of dural AVMs. They connected the right CCA and right posterior facial vein, followed by left posterior facial vein ligation at seven weeks. They found that pressure in the superior sagittal sinus was around 9 mm Hg compared to 4 mm Hg in animals that had occluded fistulas. The pressure increases were mild when compared to other acute models of cerebral venous hypertension, and there were no alterations of the cerebrovascular response to hypercapnia and acute hypotension.

In a rabbit AVF model, Sho et al. [117] examined the consequences of sequential and prolonged exposure to high and low wall shear stress on arterial remodelling. They increased blood flow 17-fold to 20-fold by opening the created AVF. Dilatation, elongation, and tortuosity of the arterial wall were found to result from the increase in flow and wall shear stress. The length of the left CCA increased by 37% and 22% after the first and second exposures to high flow, with a further elongation of 10% after a third exposure. The luminal diameter throughout carotid segments exposed to high flow, with or without cycles of flow alteration, was greater than in the control animals; this indicated that the diameter increased and decreased during cycles of high flow and normal flow. Histological analysis revealed significant internal elastic lamina fragmentation, intimal thickening and spindle endothelial cells.

Another model to study the effect of disturbed venous outflow is a rat model of AVFs developed by Bederson et al.in which an anastomosis is created between the proximal CCA and the distal EJV. Orthograde blood flow from the CCA through the arteriovenous fistula (AVF) was observed. Drainage is through the contralateral EJV. Occlusion of this vein with an aneurysm clip led to intracranial venous hypertension. Histological examination one week after permanent venous outflow occlusion revealed venous infarction, subarachnoid haemorrhage, and severe brain oedema in those rats with an AVF but not in the control rats. In this model there was evidence that venous cerebral hypertension and arterial steal affect perfusion in the area around the shunt [114].

Scott et al. [118] investigated the vascular dynamics of cerebral arteriovenous shunt in an animal model. They created a carotid to jugular fistula model by performing a side-to-side anastomosis of the left CCA with the left internal jugular vein, followed by ligation of the proximal left CCA, in macaque monkeys. This generated a shunt through the Circle of Willis. They suggest that flow through the created arteriovenous shunt may be autoregulated to changes in the systemic arterial pressure, and is minimally responsive to changes in $PaCO_2$.

Morgan et al. [119] investigated the effects of hyperventilation on cerebral blood flow in the rat with an open and closed carotid-jugular fistula. They created a model of an AVF in the rat by establishing an end-to-end anastomosis of the internal carotid artery with the EJV. They created a functional fistula between the Circle of Willis and the venous system, which drained blood to the transverse sinus and also through an extracranial cervical route. The animals were divided into open fistula-low $PaCO_2$ and open fistula-intermediate $PaCO_2$; closed fistula-low $PaCO_2$ and closed fistula-intermediate $PaCO_2$ groups. The cerebral blood flow was markedly less in animals with the fistula but increased in animals where the fistula was closed immediately before they were sacrificed.

Stüer et al. [120] investigated the evidence for a predominant intrinsic sympathetic control of cerebral blood flow alterations in an animal model of cerebral AVM by creating an AVF in Sprague-Dawley rats, and found that the sympathetic nervous system down-regulates and provokes a cortical hyperperfusion condition.

Different animal models of AVM have been investigated; models of AVMs have been created in different animals including cats, dogs and swine rete. Many rat models were used to study the pathophysiology of the AVM. Yassari et al. [105] described the angiographic, haemodynamic and histological characterisation of an arteriovenous fistula in rat model of AVMs. Moreover, the histopathological characteristics of an AVM model rat models were explained; a study found that there are many histopathological and ultrastructural similarities between human AVM vessels and the animal model [72]. More importantly, details of molecular expression profile of the endothelium were also investigated in details. Yassari et al animal model is suitable to investigate the proposed molecular targeting therapy.

Table 1-1 Summarize the characteristics and results of various animal models.

Animal models	Characteristic features
Yassari et al. [105]	The animal model was created by anastomosing end of the left external jugular vein (LEJV) to the side of the left common carotid artery (LCCA) in rats. The results indicate that there was a significant histopathological and ultrastructural similarities between human AVM vessels and the created animal model [72]. They conclude that the model is suitable for therapeutic studies of AVMs. Storer et al [616] used the same model to investiagte expression of endothelial adhesion molecules after LINAC radiosurgery. He conclude that radiosurgery stimulates early expression of E-selectin and delayed up-regulation of vascular cell adhesion molecule-1 on the endothelial surface of the AVM model nidus. The same animal model was used to develop first molecular targeting therapy of the AVM using lipopolysaccharide and soluble tissue factor [198].
Massoud et al. [106]	A swine model of AVM: The group developed AVM models from bilateral carotid retia mirabilia of swine after the surgical creation of large unilateral carotid-jugular fistulas. There was angiographic evidence of vascular dilatation and tortuosity of the main arterial feeder and draining vein. There was a disrupted elastic intimal hyperplasia, intimal hyperplasia and medial thickness. Conclusion: the animal model is simulating human AVMs. Also this animal model can substantially reduce the cost of research and training radiosurgical management of AVMs. Swine rete mirabile was also used as a model of an AVM to explore the effects of varying doses of radiosurgery [110].
Pietilä et al. [108]	Dogs were used to create AVM animal model. A bypass between the middle cerebral artery (MCA) and the superior sagittal sinus. An AVM-like formation was clear on angiographic study. The histopathological study showed a peri shunt parenchymal gliosis, proliferation of mesenchyme cells and fibroblasts. Capillary proliferation was also noted. Conclusion: the animal model is similar to human AVMs.
Lemson et al. [109]	It is a goat model. AV fistula between the carotid artery and the jugular vein. The AV fistula model believed to be suitable to study intimal hyperplasia in human AV fistulas.
Sho et al. [117]	AVF model was created in rabbits. Histological analysis revealed a significant internal elastic lamina fragmentation, intimal thickening and spindle endothelial cells.

1.9 Treatment of cerebral AVMs

There are different modalities to treat cerebral AVM. These include endovascular embolization, microsurgery and stereotactic radiosurgery. Depending on the features of the AVM, these treatments may be used alone or in combination.

Improvements in microsurgery, endovascular surgery, and stereotactic radiation therapy, used alone or in combination, have increased the safety and effectiveness of brain AVM treatment [121].

1.9.1 Surgery

The history of AVM surgery began in 1928, when Cushing and Dandy published their experience with AVMs in 14 and 15 patients respectively [121]. Dandy believed that ligature of all vessels feeding the lesion, or total resection of the lesion itself, were the only curative options. AVM surgery was dangerous and largely unsuccessful.

Surgical resection involves a combination of dural opening and circumferential nidus dissection until complete AVM resection is achieved. The aim of resection is to eliminate the risk of haemorrhage [122]. Studies show that patients with complete excision have almost complete protection from long-term haemorrhagic complication, but that partial surgical removal does not prevent late re-bleeding [123].

Successful treatment outcomes have resulted from the advancement of understanding of the pathophysiology of AVM and the development of imaging techniques that include cerebral

angiography, computed tomography (CT) and magnetic resonance imaging. These are enhanced by improvements in surgical microscopes and microsurgical instruments [121].

The risk of surgical treatment for AVMs can be estimated using the Spetzler–Martin scale **(Table 1-1)**. This scale uses maximum diameter of the nidus, nidus location (within or outside eloquent cortex), and presence or absence of deep venous drainage to predict surgical outcomes [124]. Spetzler-Martin grades I and II cerebral AVMs are resected, with low morbidity and mortality; most cerebral AVMs of grades IV and V are not so treated [125]. The best results from surgery of cortical AVMs <10 ml demonstrate a 100% morphological cure with morbidity rates for Grades I through III of 0%, increasing to 21.9% in patients with Grade IV and 16.7% in patients with Grade V AVMs [126]. Angiographic cure following surgical resection ranges from 94–100%, with morbidity of 1·3–10·6% in small AVMs of 3·0 cm or less in diameter [126-128]. Pasqualin et al. demonstrated that of the operated AVMs with a nidus volume <10 ml, 27% had transient deficits, 4% new deficits, and 5% mortality; however, in patients subjected to resection of AVMs larger than 50 ml, they reported 28% new major deficits and 28% mortality [129].

Table 1-2 Determination of arteriovenous malformation grade (Spetzler and Martin) [123]

Graded Feature	Points Assigned
size of AVM	
small (< 3 cm)	**1**
medium (3–6 cm)	**2**
large (> 6 cm)	**3**
eloquence of adjacent brain	
non-eloquent	**0**
eloquent	**1**
pattern of venous drainage	
superficial only	**0**
deep	**1**

*Grade = [size] + [eloquence] + [venous drainage]; that is (1, 2, or 3) + (0 or 1) + (0 or 1).

1.9.2 Stereotactic radiosurgery

1.9.2.1 History of radiosurgery

Stereotactic radiosurgery evolved from the pioneering work reported in 1908 by Horsley and Clarke, who were able to insert a needle into a monkey brain with a tool that enabled them to localise intracranial structures in three dimensions. They were the first to report the stereotactic destruction of an intracranial target using electrode electrocoagulation [130, 131]. Interestingly, the tool was never used for other animal models [132].

In 1947, Spiegel and his co-workers at Temple Medical School in Philadelphia started developing the first stereotactic machine for human use [133]. In the 1950s several stereotactic machines were developed, and it was estimated that about 25,000 functional stereotactic procedures were carried out around the world [134].

Lars Leksell, the father of stereotactic radiosurgery, was born in 1907. His observations of morbidity and mortality associated with neurosurgery led him to apply stereotaxic techniques to radiation delivery. Based on the ideas of Horsley and Clarke, applied by Spiegel and Wycis, he developed an arc-centred stereotactic apparatus for intracerebral surgery in 1947 [135]. In 1951 he was first to illustrate the concept of stereotactic radiosurgery using collimated x-ray beams (gamma rays) [136]. In 1960, Leksell and colleagues [137] performed their first human stereotactic proton beam operation (a bilateral anterior capsulotomy). In the meantime, another research group introduced a cyclotron-based radiosurgery system and began irradiating pituitary lesions [138].

In 1984 Betti and Derechinsky [139] reported the first use of a linear accelerator radiosurgery (LINAC) -based radiotherapy system. The newly invented tool exploited many isocentric fixed radiation fields arrayed on different planes as the patient's head was rotated around a horizontal lateral axis. Later the multiple converging arc irradiation machines were developed. The quantification and dosimetry calculation in the LINAC-based system was not possible until Lutz and Winston [140] created the technology for a floor stand connected to the stereotactic frame, which overcame the mechanical inaccuracy of the LINAC.

The LINAC-based system has advantages over other radiation systems in that linear accelerators are more available and less expensive, and easy-to-use planning software has been produced. Adler and his co-workers developed Cyberknife, a LINAC based system, at Stanford University in California [141]. Cyberknife is a frameless stereotactic radiotherapy system that mounts a lightweight (59 kg) 6 mV linear accelerator on a highly mobile robotic arm. Cyber-knife determines the location of the skull or spine in the coordinate frame of the radiation delivery system by comparing digitally reconstructed CT phantoms obtained from the patient's treatment planning images, plus real-time oblique radiographs obtained during the procedure [142, 143]. Fiducials may be implanted within the target and used during image registration. The robot has the ability to make adjustments when the target moves by detecting the change, and so maintains accurate targeting [144]. Targeting the head, spine, chest, abdomen, and pelvis has become possible with this innovative system.

1.9.2.2 Stereotactic radiosurgery and AVM

In 1972 Steiner and his co-workers reported the use of stereotactic radiation for AVM treatment [145] and single-session stereotactic focused irradiation (radiosurgery) became a generally accepted treatment for cerebral AVMs [146]. According to the International Radiosurgery Association, stereotactic radiosurgery for AVM is a relatively high dose of focused radiation delivered precisely to the arteriovenous malformation, under the direct supervision of a medical team (neurosurgeon, radiation oncologist, registered nurse and medical physicist), in one surgical session [147]. Stereotactic radiosurgery is usually given in 1 fraction, and a marginal dose of AVM treatment ranges from 16 Gy to 25 Gy, accounting for 50 to 70% of the dose delivered to the centre of the AVM target [147].

Many studies have reported angiographic cures ranging from 65 to 85% in AVMs with a diameter of about 3 cm [148-151]; a lower obliteration rate is reported in larger AVMs [152, 153]. The results indicate that complete AVM obliteration is apparently not dependent on the device used, and the rate of obliteration is significantly affected by AVM-related factors such as nidus dimensions [154-156].

A drawback for using stereotactic radiosurgery for AVM treatment is that large AVMs cannot be irradiated safely as there is an increased probability of radiation-related adverse effects, while a reduction in the radiation dose decreases the success of complete AVM obliteration [157]. Patients remain exposed to the risk of haemorrhage in the ‘latency period’, which may extend for a period of months or even years, with dangerous or even lethal consequence [155, 158, 159].

1.9.2.2.1 Gamma Knife radiosurgery (GKS)

Gamma Knife machine contains 192 cobalt-60 sources in a hemispherical array. These produce photons (gamma rays), which carry high energy. Independent beams are created by each cobalt-60 source, and each individual beam, carrying a small dose, passes through brain via a unique path to target the lesion with little risk to normal brain tissue. The beams

converge at the target, producing a highly concentrated dose of radiation [160]. A retrospective study on patients who received a high dose of Gamma Knife radiation (at least 20–25 Gy) showed that AVM occlusion rates after one year varied from 33.7 to 39.5%, and between 79 and 86.5% two years post-radiation; angiographic obliteration rates at 1 year were reported at 76% [149, 161-163].

Yamamoto and colleagues [164] reported on 25 patients treated with GKS. They found that in AVMs that were completely covered by the radiosurgical field, the two-year thrombosis rate was 64%. One patient had complete thrombosis at three years and another at five years; the total cure rate was 73%. In another study, total cure was reported in 73% of cases. Of the patients studied, 64% had AVMs completely thrombosed at two years. Another study of 25 AVM patients treated with GKS found complete occlusion at three years in 5 patients, and another patient had his AVM thrombosis at five years [164].

A study by Lunsford et. al. [149] investigated 227 AVM patients who received GKS at a mean marginal dose of 21.2 Gy. Complete thrombosis was reported in 76.5%. Of those studied, 17 had angiography at one year. Of 75 patients followed for two years, 46 (61%) had follow-up angiography, and 37 of the 46 (80%) had complete angiographic obliteration.

Karlsson and co-workers [165] investigated the occlusion rate in 945 AVM patients treated with GKS, and found an overall occlusion rate of 56%. A 72% occlusion rate at three years after radiation has also been reported [166], and a 31% complete obliteration at one year post-radiation was reported in another study where obliteration rates were documented as more effective in superficially located AVMs, independent of AVM size [167].

1.9.2.2.2 Linear accelerator radiosurgery

Linear accelerators are devices that accelerate electrons to very high speeds by microwave energy. The energetic electrons collide with a heavy metal alloy in the head of the machine. Most of the collision energy is lost as heat, but a small percentage results in high-energy photon radiation (called x-rays because they are electronically produced). These photons are virtually identical to those produced by the spontaneous decay of radioactive cobalt in the

Gamma Knife. The photons are collimated and focused on the radiosurgical target. Linear accelerator systems rotate the beam around the patient from many angles, to create the hundreds-of-beams approach used by the Gamma Knife to provide high doses at the target but low doses to normal tissue [168].

Thrombosis rates after AVM treatment with LINAC have been investigated. Investigation of 66 AVMs treated with 40 Gy in 80% of patients in a linear accelerator radiosurgical system found a 66% two-year thrombosis rate. The rate increased when the maximum diameter of the lesion was less than 12 mm [160, 169, 170]. Complete nidus obliteration of 60.5% after a single radiosurgical treatment has also been documented [171].

One group used LINAC to treat 97 patients with AVMs with a dose ranging from 18.7 to 40 Gy. One-year angiographic follow-ups were done in 50 of the 56 patients. Fifty-two percent had complete angiographic obliteration, and of those followed up for two years, 75% had complete angiographic thrombosis. Small-sized AVMs were shown to have a high rate of cure [172]. A complete obliteration rate of 38% was seen one year after angiography with the use of a 50–55 Gy linear accelerator system [173]. The one-year total occlusion rate was 45%, and 73% was reported at two years after treatment with 15–25 Gy [174].

1.9.2.2.3 Particle beam radiosurgery

In particle beam radiosurgery facilities, charged subatomic particles are accelerated to very high speeds using cyclotron-like devices before directing them at patients. The Bragg peak effect has a unique physical property whereby most of the beam's energy is deposited at a predictable depth in tissue and there is little exit dose. This property is somewhat limited by the need to spread the peak to fit anatomic lesions, and by the restrictions in beam number compared with other radio-surgical methods; the high cost of particle beam radiosurgery systems is an additional problem with this method [160].

In a study conducted by Kjellberg et al. [175], 20% of AVM patients treated with stereotactic proton-beam therapy had complete nidus obliteration on follow-up angiography. Another

study reported 15.9% complete nidus obliteration. Steinberg and colleagues investigated the occlusion rate in 86 AVMs treated with a helium particle beam radiosurgical system and found thrombosis rates of 29%, 70% and 92% at one year, two years and three years' post-procedure [148].

1.9.2.3 Response of AVMs to radiosurgery

1.9.2.3.1 Histological response

Responses of AVMs to radiosurgery are highly variable: there is a latent period of months to years between delivered treatment and subsequent obliteration of an AVM. Under light microscopic studies, vessel occlusion and connective tissue stromal changes in AVMs pass through various parenchymal stages. Both proliferative and degenerative changes participate in the obliteration progression [176]. AVM obliteration may occur from a few months to 5 years post-treatment, and may not appear at all by the end of the follow-up period. It has been reported that post-radiosurgical vaso-occlusive effects are slowly progressive and maximised between one to two years after treatment [177].

Szeifert et al. [176] investigated histological and ultrastructural changes in AVMs after Gamma Knife surgery. Seven cerebral AVMs patients were enrolled in this study. All patients that had previously been treated with GKS suffered rebleeding 10 to 52 months after treatment. Proliferative and degenerative changes in irradiated AVM tissue were reported under light microscopy. Connective tissue stroma and a subendothelial region of irradiated AVM vessels had granulation tissue proliferation with inflammatory cells and spindle cell formation; intraluminal degenerated hyaline scar tissue was also identified. Under electron microscopy, the spindle cell population had different atypical features that could include oval nuclei, a smooth contour, and cisterns of endoplasmic reticulum, intracytoplasmic filaments and prominent nucleoli. In the extracellular matrix, the spindle cells were reported to be enclosed by enormous bundles of collagen fibres. They concluded that in the GKS-treated AVMs the ultrastructural and histological features of the spindle cell population in the GKS-

treated AVMs are similar to those myofibroblasts in wound healing processes and pathological fibromatoses, and that myofibroblasts may contribute to the shrinking process and final occlusion of AVMs after radiosurgery.

In another study [178], AVM tissue was taken from 18 patients; three of them had received a radiosurgical treatment dose ranging from 18 to 20 Gy using LINAC. Incomplete obliteration of the irradiated AVM tissue was found 33, 48, and 64 months after radiosurgery. Separation of the endothelial lining from the vessel wall with a subendothelial space containing proteinaceous material was observed. Luminal obliteration by coagulation of cytoplasmic debris and proteinaceous material leaking from the endothelium was also identified. Heterogeneous proteinaceous material and fibrin thrombi together with the loss of normal cellular structure were also evident in occluded vessels. Irradiated AVM vessels exhibited blood-brain barrier abnormalities, and irradiated AVM ECs displayed degeneration, which were more prominent 64 months after radiosurgical treatment. Proliferative thickening and luminal stenosis were seen in the intimal layer of feeding arteries. Within the tunica media, smooth muscle cell neoproliferation was evident with bundles of proliferating microfilaments, as well as large numbers of glycogen particles and surface vesicles in the cytoplasm. Endothelialised smooth muscle cell Weibel-Palade bodies were also identified [178, 179]. Un-discernible or fragmented elastic lamina in the obstructed vessels were reported and occasional clusters of lymphocytes were identified. Immunohistochemical techniques revealed an increased presence of collagen type III in irradiated vessels. Exudation of albuminous fluid in irradiated nidus tissues was also documented [180].

Schneider et al. [181] investigated the histopathology of AVMs after GKS **(Figure 1-3)**. They demonstrated that damage to the endothelial cells appears to be the first change to occur after irradiation. This was followed by progressive intimal thickening, secondary to smooth muscle cell proliferation that produces type IV collagen. Lastly, cellular degeneration and hyaline transformation occur.

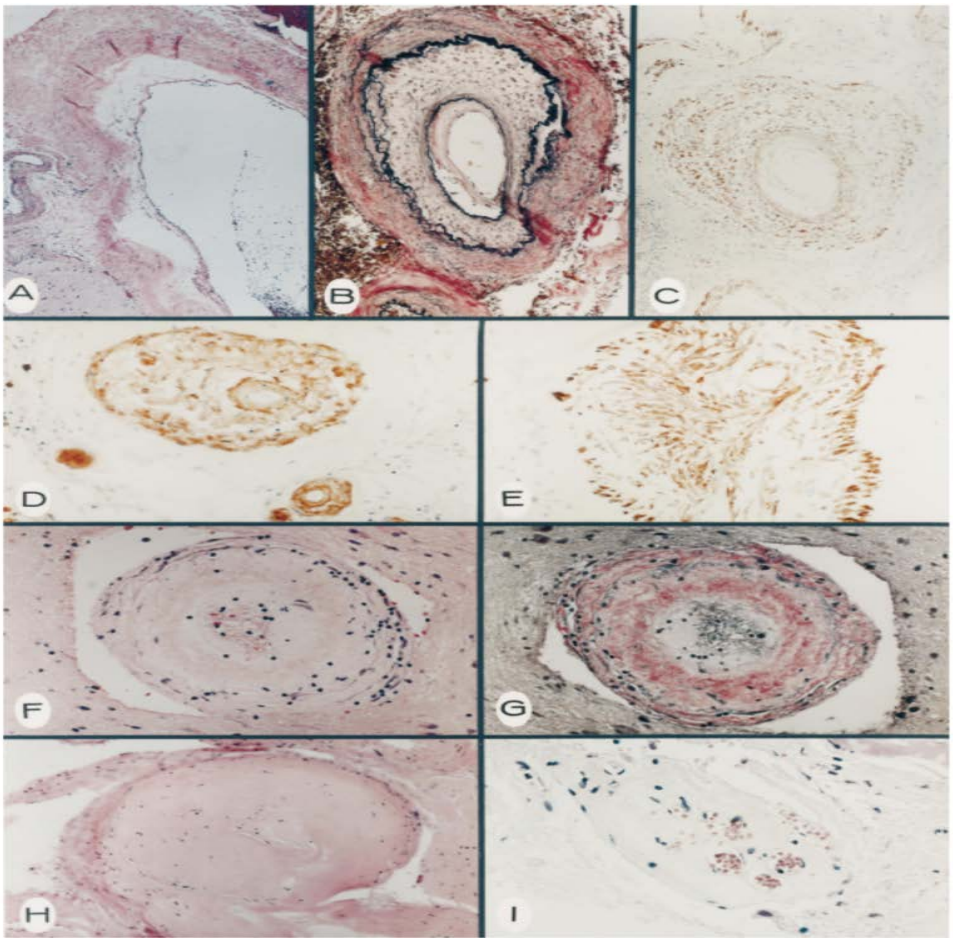

Figure 1-3. Photomicrographs displaying transverse sections of AVM vessels after GKS.

Photomicrographs illustrating the chronology of the occlusive process (A to I). A: Separation of the endothelial lining from the vessel wall, creating a subendothelial space containing proteinaceous material. H & E, original magnification × 20. B: Eccentric, proliferative thickening of the intimal layer and reduplication of the elastica. Elastin von Gieson, original magnification × 20. C: Robust reaction product within the cells of the thickened intimal layer in the same vessel shown in B, demonstrated by immunohistochemical staining for SMA, original magnification × 20. D: Reaction product is deposited in a diffuse extracellular pattern within the thickened intimal layer, shown by immunohistochemical staining for type IV collagen, original magnification × 20. E: In contrast to the extracellular pattern of collagen immunostaining (shown in D), SMA reaction product appears to be intracellular. Original magnification × 50. F: Markedly thickened wall with cellular degeneration evidenced by nuclear pyknosis, decreased cellularity, and a mild lymphocytic infiltrate. The lumen is occluded by a fibrin thrombus. H & E, original magnification × 50. G: Intensified intimal—medial staining, indicating deposition of dense fibrillar collagen following cellular degeneration. Hematoxylin von Gieson staining for collagen, original magnification × 50. H: Obliteration of the entire vascular structure with dense hyalinization, few remaining cell nuclei, and nuclear debris. H & E, original magnification × 33. I: End-stage vessel whose wall structure has been obliterated by dense hyalinization. Multiple endothelial cell—lined channels containing erythrocytes indicate recanalization. H & E, original magnification 366. Adapted from Schneider Bernard F 1997 [181]

1.9.2.3.2 Molecular response of cerebral AVM to radiation

In some irradiated vessels, marked expression of vWF has been noted in occlusive thrombi, although some irradiated vessels had no staining for vWF, indicating loss of the endothelial layer. No significant difference in thrombomodulin (TM) expression was seen in irradiated AVM tissue compared to non-irradiated tissue. Adventitial and perivascular expression of Tissue Factor (TF) was documented, with no endothelial or subendothelial TF staining seen in most of the tissue examined. Due to the lack of endothelial vWF expression, some irradiated vessels' TF appeared to be directly exposed to the luminal surface and was infrequently accompanied by occlusive thrombi [182]. Liu et al. [183], who investigated the expression of thrombotic molecules in cultured mouse brain endothelial cells exposed to radiation, found that TF expression was not changed by radiation. Their study demonstrated an upregulation of TM that increased with time after radiation exposure.

Simonian [184] used *in vitro* biotinylation and the Waters MS^E approach to measure membrane protein changes in the murine brain endothelial cells (bEnd.3). The expression levels of PECAM and cadherin 5 in bEnd.3 were increased at both 24 and 48 hours post-irradiation. Both integrin beta-1 and endothelial protein C receptor protein expression increased in the irradiated samples at 24 hours.

1.9.2.4 Limitation of radiosurgery

Many studies have been done to investigate causes of radiosurgical failure. A higher Spetzler-Martin grade, larger AVM size, and lower treatment dose have been found to be factors in the failure rate of radiosurgeical treatment. AVMs treated with a peripheral dose of less than 15 Gy had a high failure rate. In addition, a higher failure rate was found in patients with AVM volumes greater than 10 cm^3 [185]. Pollock and colleagues [186] found that the success of radiosurgeical treatment could be predicted by the following factors: low AVM volume, few draining veins, young age, and superficial location; they reported that previous embolisation of the AVM was negative predictive factor. In another study [187], radiosurgical

treatment failed to obliterate AVMs because the AVM nidus re-expanded after reabsorption of a prior haematoma that had compressed the vessels within the nidus, and the AVM recanalised after embolisation. Sometimes a definite cause for failure could not be determined, and the investigators suggested that the AVMs in these patients had some form of radiobiological resistance.

Predictive factors for radiosurgical obliteration of AVMs were studied by the Stockholm group [188], who found a higher radiosurgical dose shortened the latency to AVM obliteration. Another group found that failure to completely cover the whole nidus at the time of first treatment led to treatment failure [189]. AVM targeting error was another contributing factor: 59% of failures was attributed to inadequate targeting [190]. Zipfel and colleagues [191] investigated the importance of AVM angioarchitecture, finding that the response of AVMs to radiosurgery was affected by their morphology. Five variables were identified as related to an excellent outcome of radiosurgical treatment: AVM volume, patient age, AVM location, previous embolisation, and number of draining veins. The group found that all patients with an AVM score of less than one had excellent outcomes [192, 193].

1.10 Need for a new treatment

1.10.1 Possible improvements in AVM treatment

Improvement of the outcomes of current treatment modalities seems to be unlikely to lead to effective treatment of high grade AVMs [194, 195], although potential improvement in AVM treatment could arise from using radiosurgery [196]. In addition to improving physical radiation delivery methods, biologically enhancing the occlusive or thrombotic response to radiosurgery is theoretically attractive as a method for improving AVM treatment.

1.10.2 Vascular targeting therapy

A possible new treatment modality, described for many years in cancer therapy, is vascular targeting. The concept behind vascular targeting is to stimulate intravascular thrombosis. The

technique exploits natural differences between the endothelium of tumour vasculature and normal endothelial cells. Selective stimulation of thrombus formation inside abnormal vessels is achieved by using ligand or non-ligand targeting strategies. Ligand and non-ligand strategies result in widespread tumour vascular thrombosis, and necrosis of up to 95% of tumour cells is reported [197]. Administration of lipopolysaccharide (LPS) and soluble tissue factor has been reported as a trial treatment for AVM in animal models of AVM using a non-ligand strategy [198] that relies on the externalisation of phosphatidylserine from the internal endothelial cell membrane, which occurs not only in apoptosis but also in tumour vasculature [199] and endothelial cells after radiation [200].

The interaction of LPS–TF with externalised phosphatidylserine is a powerful stimulator of thrombosis [198]. Although thrombosis occurs particularly within regions receiving radiation in the animal model, it is still unclear if the method is safe and effective for use in humans. The LPS–TF methods may lack specificity, as it is not clear if changes that occur in chronically inflamed or neovascularising tissues also induce inappropriate thrombus formation [198]. Transient renal, hepatic toxicities, and constitutional effects such as fever, chills, and hypotension have been reported with administration of endotoxin (4 ng/kg) [201]. In animals, LPS is documented to induce disseminated intravascular coagulation (DIC) and septic shock syndrome [202]. A ligand-based vascular targeting strategy is the alternative technique to the non-ligand strategy, and may overcome these difficulties. The strategy uses a combination of a targeting moiety and an effector moiety. The targeting moiety is an antibody or peptide that binds to a selectively expressed tumour vessel endothelium marker, and the effector moiety induces thrombosis [197].

The inherent differences between tumour vessels and normal endothelial cells are sufficient to enable selective targeting without modification of the endothelium in cancer treatment [200]. Inducing vascular thrombosis in AVMs is an attractive new treatment, but endothelial cells of AVMs do not significantly differ from normal endothelial cells, and no marker has been detected that would be sufficiently discriminating in the case of tumour cells [75, 78, 182, 203, 204]. The vascular targeting of AVMs requires an induction or ‘priming’ technique that selectively changes expression of the endothelial cells’ surface molecules in AVMs without

affecting normal brain vessels [125]. Radiosurgery is a promising primer, not only because of its effects on endothelial cells but also for its precise spatial localisation [77, 205]. The spatial resolution of radiosurgery (in contrast to radiotherapy) has an accuracy of less than 1 mm. It is been reported in an animal model that there is no endothelial change and no thrombosis in the surrounding tissue or any organ other than in the targeted vessels using LINAC [77, 198].

1.10.3 Radiosensitisers

Radiosensitising is a process where an agent increases the susceptibility of cells or a tumour to the effects of radiation. The optimal radiation sensitiser would reach the targeted cells or tumour selectively in sufficient concentrations, and with minimal toxicity and less enhancement of radiation toxicity. Chemopotentiation is the process by which radiation increases the susceptibility of cells or a tumour to the effects of a chemotherapeutic agent.

In 1958 Heidelberger et al. established the concept of administering drugs and radiation simultaneously to augment the effect of radiation [206]. In 1974, Nigro trialled 5-fluorouracil (FU) in combination with Mitomycin C as a synchronised treatment with radiation for anal canal malignancy [207].

1.10.3.1 DNA targeting

One of the earliest agents to be used as a radiation sensitiser was 5-fluorouracil (5FU), which worked by affecting thymidilate synthase [208]. *In vitro* incubation of cells with noncytotoxic concentrations of 5FU before radiation increased radiation sensitivity. In pancreatic and rectal cancer, continuous intravenous infusion (CIVI) of 5FU with radiation has become the preferred therapy, because of the short half-life of 5FU in plasma [209, 210]. Capecitabine, an oral form of 5FU may make the combined modality therapy easier and safer.

Combination therapy is also used for different type of solid tumours. For example cisplatin, carboplatin, and oxaliplatin, which are platinum analogues, may be combined with

radiotherapy. It believed to work through several mechanisms when combined with radiation. These include formation of toxic platinum, inhibition of DNA repair, radiation-induced increase in cellular platinum uptake, and cell cycle arrest [211-213]. In cultured V79 cells, irradiation of these cells has been shown to increase cellular uptake of the chemotherapy agent carboplatin and enhance cell killing [214].

Another drug shown to have activity against human cancers that is a potent radiosensitiser is Gemcitabine (an analogue of cytarabine) [215-218]. Its sensitisation effect requires concurrent redistribution into S phase along with deoxyadenosine triphosphate pool depletion [218].

Camptothecin derivatives such as topotecan and irinotecan are Topoisomerase Inhibitors. The enzyme has roles in DNA metabolism, DNA replication, and the regulation of DNA supercoiling [219]. Chen et al. [220] indicate that, in cultured mammalian cells (Chinese hamster DC3F cells), when radiation is used concurrently with or immediately after camptothecin derivatives treatment, it enhances the cytotoxicity of radiation in a schedule-dependent manner.

1.10.3.2 Non DNA targeting

These types of drugs do not target the DNA, but work by their effect on apoptosis, tumour angiogenesis and cellular proliferation. The monoclonal antibody C225 (cetuximab) and the tyrosine-kinase inhibitor CI-1033 are new non-DNA targeting radiation sensitisers working through their anti-EGFR effect. *In vitro* use of C225 has been shown to enhance radiosensitivity and promote radiation-induced apoptosis [221]; it also has an antiproliferative effect and inhibits tumour cell growth kinetics. *In vivo* studies show that it also inhibits post radiation damage repair and downregulates tumour angiogenesis [222].

The presence of activated oncogene renin angiotensin system (RAS) is known to increase tumour cell resistance to radiation [223]. In human tumours, appeared that RAS gene mutations can be found in a variety of tumour types. The incidence varies from 30% in lung tumour up to 90% in adenocarcinomas of the pancreas [224]. RAS inhibition using

farnesyltransferase inhibitors (FTIs) has shown a radiosensitisation effect. In advanced head and neck cancer, and in non-small cell lung cancer, a high response rate was reported in a phase 1 trial of the FTI L-778-123 [225]. H-Ras transformed rat embryo fibroblasts cells (3.7 and 5R) and human tumour cells (T24 bladder cancer, HS578T breast cancer), after treatment with prenyltransferase inhibitors, showed a synergistic effect on radiation-induced cell killing [226, 227]. A significant and synergistic reduction in tumour cell survival was reported when a combination of FTI and irradiation was used to treat tumour cells in *in vivo* experiments [227].

It has been suggested that prostaglandins play a role in cell survival after ionizing radiation. The radio-protective ability of prostaglandins has been in reported in a number of cell types [228, 229]. However, indomethacin, a nonsteroidal anti-inflammatory drug, is reported to have radiopotentiating activity toward tumour cells [230, 231]. Cyclooxygenase (COX) enzyme 2 (COX-2) inhibitors are also known as radiosensitisers, and have an impact on the radiosensitivity of cells and tissues. Using nonspecific prostaglandin inhibitors such as nonsteroidal anti-inflammatory drugs has not been promising, as these drugs lack specificity against the targeted tumour. It has been reported that they have a tendency to cause toxicities in other proliferating host tissues such as gastrointestinal mucosa [232]. Highly selective COX enzyme 1 (COX-1) sparing drugs such as Celecoxib, which works through its selective inhibition of selective COX-2, have been reported to have radiosensitising and chemosensitising activities *in vitro*, and have been used in studies of non-small cell lung cancers and upper gastrointestinal tract cancers [225].

1.10.4 Targeting vascular growth factors

The mammalian vascular endothelial growth factor (VEGF) family consists of five glycoproteins, referred to as VEGFA, VEGFB, VEGFC, VEGF and placenta growth factor [233, 234]. Isolated from bovine pituitary follicular cells, they are heat- and acid-stable protein with a molecular weight of approximately 45,000 under non-reducing conditions and approximately 23,000 under reducing conditions [235]. Sengeret al. [236] identify the *VEGF*

gene as encoding the vascular permeability factor in tumour ascites, finding that the tumour ascites fluids of guinea pigs, hamsters, mice and a variety of other tumour cell lines *in vitro* contain activity that increases micro-vascular permeability significantly. Three VEGF receptors (VEGFR) have been discovered: VEGFR-1, VEGFR-2 and VEGFR-3. Both VEGFR-1 and VEGFR-2 control angiogenesis, whereas VEGFR-3 controls lymphangiogenesis [237] .

VEGF is known as one of the most important regulators of angiogenesis, active in embryonic development [238, 239], a potent inducer of vascular permeability in adults [240, 241], and present in the process of neovascularisation, such as wound healing or the menstrual cycle [242]. In cancer cells it plays a role in disease progression and decreased survival rate in cancer where it is overexpressed [243].

Tumour angiogenesis is known to be secondary to VEGF. It is a compound series of processes that includes classic sprouting angiogenesis, loss of pericyte–endothelial cell adhesion, increased permeability, vasodilation and the incorporation of bone marrow-derived endothelial progenitor cells [244-246]. Several VEGF-targeted agents have emerged from understanding the role of VEGF in the process of angiogenesis.

Numerous pro-survival pathways in endothelial cells are VEGF mediated, including the activation of BCL2, Akt, survivin and the inhibitor of apoptosis proteins [247, 248]. Blocking of VEGF signalling has been posited to lead to endothelial cell apoptosis as VEGF mediates endothelial cell survival functions.

Using VEGF-targeted therapies in murine models has shown that inhibition of VEGF signalling may cause endothelial cell apoptosis [249, 250]. Endothelial cell apoptosis secondary to VEGF-targeted therapy is also supported by clinical trial results [251], in which a 31% response rate after administration of sunitinib was observed. Tumour necrosis in 44% of patients after administration of axitinib, a selective VEGF receptor tyrosine kinase inhibitor (TKI), has also been reported.

VEGF-targeted agents can be divided into different subgroups including VEGF or VEGFR neutralising antibodies to soluble VEGF receptors or receptor hybrids, and TKIs with selectivity for VEGFRs [244, 246].

The anti-VEGF monoclonal antibody 'bevacizumab' was the first VEGF-targeted agent used in combination with chemotherapy to treat metastatic colorectal cancer (CRC), non-small cell lung cancer and metastatic breast cancer in combination with chemotherapy [252-254]. Studies since then have investigated the benefits of bevacizumab and many other VEGF-targeted therapies [252, 253, 255, 256].

VEGFR tyrosine kinase inhibitors TKIs are another type of VEGF-targeted agents. TKIs are 'multi-kinase' inhibitors, developed to target VEGF receptors selectively. In patients with advanced renal cell carcinoma (RCC), Sorafenib has shown good efficacy [255] as it also has with hepatocellular carcinoma [257] and in patients with RCC, where it is effective as a single agent. SU6668, a small molecule oxindole compound which selectively inhibits Flk-1/KDR, fibroblast and platelet-derived growth factor receptors (FGFR and PDGFR), exhibits strong *in vivo* antiangiogenic activity in intravital tumour microscopy studies [258]. SU5416, a specific blocker of VEGFR2 and shown to have an additive effect when combined with radiation in animal tumour models, is undergoing clinical trials for use in patients with lung cancer and malignant melanomas [259, 260]. Tivozanib is a potent TKI against VEGFR-1, -2 and -3, and minimal c-kit inhibition. Tivozanib demonstrated clinical activity in a phase II trial [261].

Endogenous inhibitors of angiogenesis, angiostatin and endostatin have been shown to have significant antitumour activity in tumour-bearing mice, particularly in combination with radiation [262-264], although the initial results of clinical trials have been disappointing and the large amounts of recombinant protein required have limited further work[265] . Similarly, while animal experiments with integrin antagonists [266, 267] and MMP inhibitors have been encouraging [268, 269], results from human trials have failed to demonstrate a significant survival benefit.

Targeting VEGF used in combination with metronomic chemotherapy has been described by

Kerbel et al. [270] who investigated a combination metronomic therapy using continuous low-dose chemotherapy given with concurrent VEGF-targeted therapy as a double attack on the tumour vascular bed. They found that the efficacy of metronomic chemotherapy was augmented when given in combination with specific anti-angiogenic drugs.

1.10.5 Gene therapy

Many groups in the literature who have used gene therapy for targeting tumour vasculature have reported that neural and mesenchymal stem cells can deliver genes to induce a significant antitumour reaction in animal models of intracranial tumour such as glioma, medulloblastoma, melanoma, brain metastasis, disseminated neuroblastoma and breast cancer lung metastasis. Up to a 90% a reduction in tumour volume and increased survival of the animals have been reported [271].

Selective delivery of genes to tumour endothelial cells using engineered retroviruses that can be coated with an antibody such as anti-VEGF has been reported [272]. This destroys the tumour endothelium, sparing normal tissues' angiogenic vessels by using tumour cell-specific cytotoxic T lymphocytes to deliver a retrovirus containing a gene encoding a VEGF-toxin fusion protein [273]. Treatment of a murine glioma model by intramuscular administration of an adeno-associated viral vector expressing angiostatin is described [274]. Other groups have used adenoviruses or modified adenoviruses to achieve delivery of anti-angiogenic compounds in glioma models. A study conducted in 2013 showed targeted therapy by gene transfer of a monovalent antibody in mice using intra-tumour or systemic techniques was followed by a therapeutic response [275].

Kantar et al. [276] investigated the potential role of stathmin1 genes in gastric cancer tumourigenesis. They used a lentiviral vector encoding a short hairpin RNA (shRNA) targeted against stathmin1 and reported significant inhibition of gastric cancer cell proliferation, migration and in tumourigenicity in xenograft animal models. Another group investigated gene therapy in pancreatic cancer (PC) to determine the anti-tumour effect of oncotic

adenovirus ZD55 harbouring IL-24 in immune-competent mice; they found that ZD55-IL-24 inhibited PC cell growth and induced PC apoptosis [277].

1.11 Vascular targeting and vascular targeting agents

In the early 1980s Juliana Denekamp described the concepts behind vascular targeting agents (VTAs) as a therapeutic approach to cancer [278, 279]. VTAs work in different ways from antiangiogenic agents **(Figure 1-4)**. The vascular targeting approach affects pre-existing blood vessels, to cause a fast selective shutdown of the blood supply to tumours to cause tumour cell death from ischemia. The method exploits the differences in the pathophysiology of tumour versus normal tissue vessels. Antiangiogenic agents prevent the formation of new blood vessels from existing vessels. In contrast to antiagiogenic agents, VTAs

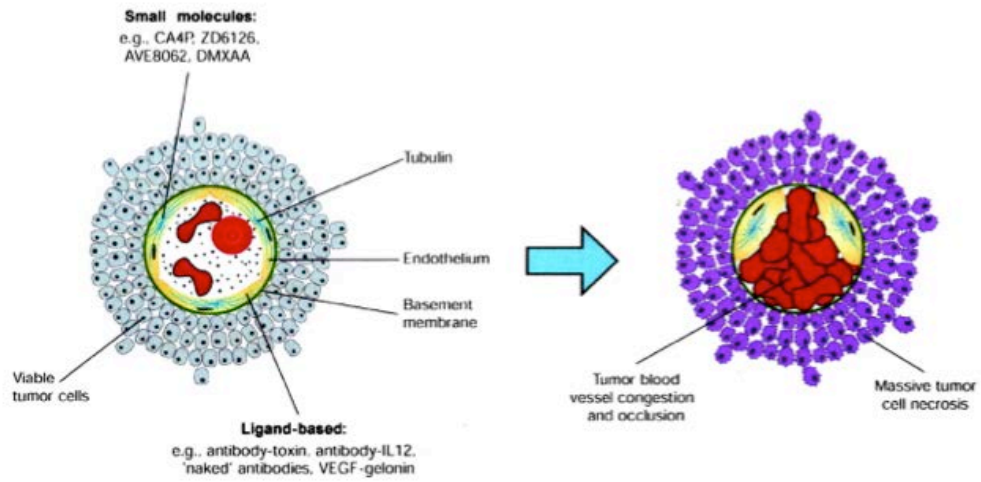

Figure 1-4 mechanism of action of vascular targeting agent (VTA) approaches.

VTAs exploit differences between tumour and normal tissue blood vessels, cause the selective and rapid occlusion of tumour vasculature, and lead to massive tumour cell necrosis. There are broadly two types of VTAs. The small molecules include combretastatin A-4 disodium phosphate (CA4P), ZD6126, AVE8062, and DMXAA. Ligand-based VTAs use antibodies, peptides, or growth factors to target tumour endothelial cells with agents that occlude blood vessels. Adapted from Thorpe 2004 [197]

are more effective in large tumours models, and can cause widespread central necrosis in experimental tumours [280, 281]. In contrast to direct-acting antitumour therapies and angiogenesis inhibitors, which usually work in the periphery of a tumour, VTAs are most effective in the high-interstitial pressure central area [282]. In experimental solid tumours, combining VTAs with anti-proliferative antitumour therapies or angiogenesis inhibitors can lead to synergistic activity [283-285].

1.11.1 Vascular targeting agents

VTAs are divided into two groups, which both cause acute vascular shutdown in tumours leading to widespread central necrosis [286]. Small molecule VTAs exploit pathophysiological differences between tumour and normal tissue endothelium such as increased proliferation or permeability, to selectively occlude tumour vessels [278, 287, 288]. The other group is ligand-directed, which use a targeting ligand to achieve selectivity in binding to and obstructing tumour vasculature.

1.11.1.1 Small molecule VTAs.

Small molecule VTAs are classified into two subgroups: microtubule destabilising agents (MTD) and cytokine inducers. MTD small VTAs interrupt quickly proliferating and non-mature tumour endothelial cells, grounded on their dependence on a tubulin cytoskeleton to maintain their cell morphology. Tubulin-binding small VTAs have antimitotic and antivascular abilities that lead to mitotic arrest and decrease the blood supply to tumour cells [289]. Direct tumour cell cytotoxicity via mitotic arrest is the main mechanism of action in of MTD.

Combretastatin A-4 is a small molecule VTA shown to have antivascular effects at doses below the maximum tolerated dose [290]. One example of a tubulin-binding agent is Combretastatin A-4 Disodium Phosphate (CA4P), which looks like colchicine in structure. It

has been reported that within one hour's treatment of experimental tumours with CA4P, fast selective and extensive vascular damage and subsequent tumour growth delay are apparent [290-293]. Tozer et al.[294] showed that there is a reduction of tumour blood flow of <5% of starting value one hour after drug administration [295]. In experimental models, CA4P enhances the effects of both radiation [296-300] and radio-immunotherapy [301, 302]. A new synthetic water-soluble combretastatin A4 derivative called AVE8062 has been proven to cause shape changes in proliferating endothelial cells, the rapid shutdown of tumour blood flow, and extensive necrosis [303, 304].

Dolastatin 10 and its derivative TZT-1027/Sonidotin are more tubulin-binding agents that have antivascular activity [305] and, later, potent antitumour activity [306, 307]. The phosphate prodrug ZD6126, which is another tubulin-binding agent, interrupts the tubulin cytoskeleton of endothelial cells [308, 309]. *In vivo* studies have shown that ZD6126 at a well-tolerated dose causes tumour endothelial cell retraction and widespread endothelial cell loss [310], dramatic decrease in tumour blood flow [311], and in animal tumour models massive necrosis [310, 312], inhibiting the metastatic progression of pulmonary metastatic adenocarcinomas in mice [313].

1.11.1.2 Ligand-directed VTA

In ligand targeting therapy, ligands are directed to bind selectively to tumour blood vessel components. They exploit the inherent differences between tumour vessel and normal endothelial cells [200]. Ligand-directed VTAs strategy is consist of a targeting moiety and effector moieties that are linked together, usually via chemical cross-linkers or peptide bonds. The targeting moiety is an antibody or peptide that binds to a marker that is selectively expressed on tumour vessel endothelium; the effector moiety induces thrombosis directly or kill endothelial cells to cause thrombosis indirectly [197].

Burrows et al. [314] investigated the antibody-directed targeting of mouse tumour endothelium using the cytokine gene transfection technique to induce the selective expression of an experimental marker, major histocompatibility complex class II (MHC class II) on

tumour vascular endothelial cells [314]. They injected nude mice with an antitumour endothelial cell immunotoxin (a ricin-conjugated antibody against the MHC class II antigen). Dramatic occlusion of tumour blood vessels and significant regression of tumour was reported [315].

The extracellular domain of the human coagulation-inducing protein has been targeted to tumor vessels to induce specific tumour vessel thrombosis. Tissue factor binds to antibody or peptides directed against tumour vessel markers such as MHC class II [316], cell adhesion molecule VCAM-1 [317], and prostate-specific membrane antigen [318]. All these studies are reported to selectively induce thrombosis to tumour vessels [197].

VEGF is another marker that has been used for ligand targeting molecular therapy as the marker expression in increased in the tumour endothelium. Human VEGF-A has also been used to target toxins to tumour vessels that show an upregulation of VEGF receptors on the tumour vessels. VEGF and diphtheria toxin [319] have been shown to induce regression of mouse models of tumour. Halin et al. [320] and Carnemolla et al. [321] showed that targeting the ED-B (an extracellular matrix marker of angiogenic vessels) domain of fibronectin with IL-2 or IL-12 fused to the L19 scFv was found to have a noticeable activity towards aggressive murine tumours.

1.12 Targeting irradiated vasculature

Radiation can be exploited to direct drugs to specific area such as neoplasms or aberrant blood vessels. Radiated blood vessels express a number of cell adhesion molecules and receptors that participate in different pathophysiological process. Radiation has been found to induce expression of molecules in blood vessels such as ICAM-1, E-selectin, P-selectin and the β_3 integrin [322]. Recently Hallahan et al. [322] demonstrated that peptides that bind to the beta 3 integrin can be used to deliver fluorochromes and radionuclides to irradiated tumours. They observed a three- to four-fold increase in peptide binding in tumour vessels over adjacent normal tissue.

In a mouse model of radiation-resistant human lung cancer, He et al. [323] examined the hypothesis that radiation therapy can enhance the antitumour effects of phosphatidylserine-targeting antibodies. They demonstrated that radiation therapy improves the localisation of anti-phosphatidylserine antibodies to lung tumour vasculature. Recently Storer et al. investigated radiation-induced molecular targeting therapy, showing that in animal models of AVM, radiation therapy could be used to localise the VTA effect to the desired area. Lipopolysaccharides and TF were successfully used to promote thrombosis in the nidus area [198].

Kiani et al. [324] investigated exploiting radiation-induced upregulated molecules to target drugs or genes to select segments of the endothelium, using microspheres coated with a mAb to ICAM-1 to target irradiated tissue. They found that the number of adherent microspheres on irradiated human umbilical vein endothelial cells (HUVECs) was significantly higher than in the control, perhaps related to the presence of red blood cells (20% haematocrit) in the medium. The results from the *in vivo* work were similar. In a rat model, the number of adherent anti-ICAM-1 microspheres in locally irradiated cerebral tissue was also significant.

1.13 Potential use of VTA for AVMs.

1.13.1 No discriminating molecule

Many studies have investigated the molecular characteristic of the ECs of the AVM. Several molecules have been found to increase expression in AVM ECs. Endothelial expression of P-selectin seen in AVMs was found to be similar to that in controls [78]. Although E-selectin in AVM tissue was reported to be upregulated, its expression was either faint or absent in the endothelium. Most of the vascular malformations had indistinct to moderate endothelial expression of ICAM-1, insufficient to characterise the EC of the AVM. There were no overall systematic differences in PECAM-1 and VCAM-1 in the intensity and pattern of expression in normal vessels when compared with AVMs. These findings were supported by a study by Shenkar, et al [203] which demonstrated that PECAM-1 gene expression is reduced in AVMs

compared with superficial temporal arteries. Hashimoto et al. [325] showed that the ICAM-1 gene is upregulated in AVMs, E-selectin is expressed only on activated endothelium, and ICAM-1 and VCAM-1 are constitutively expressed at low levels.

1.13.2 Need for primer

To induce selective occlusion of AVM vessels, an endothelial surface molecule that discriminates them from normal vessels is required. Although it has been shown that AVM endothelium differs from normal vasculature, no marker has been identified that would be sufficiently discriminating [78, 182, 203]. Successful application of vascular targeting to AVMs therefore requires a 'priming' technique that selectively alters the surface molecule expression of the endothelial cells in AVMs without affecting normal brain vessels.

1.13.2.1 Possible primers

AVM endothelial cells' molecular expression does not show a significant difference from normal endothelial cells. Using radiosurgery as primer might be a suitable choice for the ligand-directed molecular targeting therapy as radiosurgery has been shown to induce ECs molecular changes and is a potent stimulus for expression of these molecules [326-331]. Some of these changes are significant enough to discriminate AVM endothelial cells from normal endothelial [200]. As it has been used for decades, there are no significant limitations for its use in humans. A core hypothesis of this thesis is that the efficacy of radiosurgery can be augmented by use of an agent of antibody, or a combination of both, to enhance and target the pathophysiological changes that occur in AVM tissue after radiation treatment.

Upregulation of certain endothelial cell molecules secondary to radiation injury and micro-vascular dysfunction has been reported [332]. Post-radiation upregulation of endothelial adhesion molecules such as E-selectin, P-selectin and ICAM-1 have been well documented in both *in vivo* [332] and *in vitro* [333] studies. Voisard et al. [334] investigated the effect of low-dose γ-irradiation (LDI) on mRNA expressions of ICAM-1 in human coronary endothelial cells (HCAECs), human coronary smooth muscle cells (HCMSMCs) and

HUVEC, irradiating the cells at doses of 0.5 Gy, 1 Gy, 10 Gy, 20 Gy, and 30 Gy. In HCAECs and HCMSMCs at the different doses, ICAM-1 mRNA was seen to be upregulated. Radiation was also reported to cause endothelial cell activation and lead to over-expression of VEGF, phosphoinositide 3 kinase/protein kinase B (PI3k/Akt), cyclooxygenase 2, and integrin receptors [335].

1.14 Endothelial cells

Developing techniques to culture human endothelial cells in the 1970s allowed investigators to understand the function of endothelium in detail. Adult humans have about 1 to 6×10^{13} ECs covering a surface area of 1 to 7 m^2 [336]. The ECs line vessels and control the flow of nutrient substances, diverse biologically active molecules, and blood cells themselves. They play an important function in controlling blood flow by formation of an active antithrombotic surface, which helps the transit of plasma and cellular constituents throughout the vascular lumen.

1.14.1 Growth and proliferation

The role of ECs in growth and proliferation has been investigated through both angiogenesis and vasculogenesis. Angiogenesis is the process of the formation of new blood vessels from existing ones, believed to be important for tissue regeneration and wound healing, and a prerequisite for tumour growth [337]. The normal turnover period of ECs is from 2.5 to 3 years [279]; during angiogenesis, however, the ECs of capillaries are capable of dividing as often as every five days. On the other hand, in vascular development during embryonic growth, endothelial cell precursors undergo division, differentiation, and organisation into tubules, a process known as vasculogenesis [338]. Endothelial-cell-specific growth factors (VEGFs) have been found to be responsible for initiation and regulation of angiogenesis and vasculogenesis, and were found to nearly exclusively express endothelium [339].

Liu [340] investigated the role of hypoxia in the regulation of vascular endothelial growth factor gene expression in ECs. Liu found that VEGF expression was demonstrated in

pulmonary artery endothelial cells in response to hypoxia, which indicates that an autocrine mechanism may be responsible for the proliferation of ECs. Moreover, the release of VEGF from endothelial cells can be stimulated by platelet-derived growth factor (PDGF) acting through phosphatidylinositol 39-kinase [341]. This mechanism, therefore, couples the proliferative effects of VEGF to intracellular structures responsible for cellular migration on matrix proteins.

VEGF was also found to stimulate migration of ECs, perhaps stimulating the reorganisation of the endothelial cell microfilament cytoskeleton and the formation of stress fibres. VEGF signals for ECs cytoskeletal changes are conveyed from VEGFR-2 through enhancement of MAP kinases, ERK and p38. The end result of VEGFR-2-dependent activation of p38 is phosphorylation of MAP kinase-activated protein kinase-2/3 and phosphorylated hsp27 [339, 342, 343]. Hsp27 is thought to play important roles in ECs migration during angiogenic sprouting through the regulation of F-actin polymerisation and changes in actin-based microfilaments.

1.14.2 EC heterogeneity

Discrepancies in the appearance of capillary ECs from distinctive vascular sites have long been identified, and seem well placed to theorise differences in function. ECs in the brain and retina have been found to be continuous and connected by tight junctions that help to maintain the blood-brain barrier. However, discontinuous ECs are found in liver, spleen, and bone marrow sinusoids and allow cellular trafficking between intercellular gaps. Where selective permeability is required, as in intestinal villi, endocrine glands and kidneys, the ECs are identified as fenestrated [344]. ECs from different tissues are also heterogeneous in surface phenotype and protein expression; for example, vWF, a common marker for ECs, is not expressed consistently in cells from all types of vessels [345]. In vascular ECs, only 3% express tissue type plasminogen activator [346]. Microvascular ECs also vary in their vulnerability to undergo apoptosis [347]. Mitra et al. documented that plasma from thrombotic thrombocytopenic purpura and sporadic haemolytic-uraemic syndrome patients

was able to induce apoptosis and expression of the apoptosis-associated molecule Fas (CD95) in ECs of small vessel dermal, renal and cerebral origins. In contrast, microvascular ECs of pulmonary and hepatic origin in large vessels such as the coronary artery were resistant.

Expression of homing receptors involved in cell trafficking is another example of EC heterogeneity. For example, pulmonary postcapillary ECs and some splenic venules exclusively express lung-specific EC adhesion molecule [348]. Expression of mucosal addressin cell adhesion molecule-1 is primarily restricted to high endothelial venules in Peyer's patches of the small intestine [349], while bone marrow-derived microvascular ECs demonstrate an affinity for binding megakaryocytes and CD34+ progenitor cells and constitutively produce hematopoietic stimulating factors such as Kit-ligand, granulocyte colony-stimulating factor, granulocyte-macrophage colony-stimulating factor, and IL-6 which assist control trafficking, proliferation, and hematopoietic lineage-specific differentiation of ECs [350]. ECs also show distinct subsets within the same organ: two distinct sinusoidal EC phenotypes present in adult human liver show distinct protein expression: hepatic periportal vessels express PECAM-1 and CD34, whereas PECAM-1 and CD34 are not expressed in sinusoidal intrahepatic ECs [351].

1.14.3 Endothelial cells and shear stress

Mechanical stresses on a blood vessel are determined by two principal vectors, stress (stretch) and shear (friction). The former is directed perpendicular to the endothelial surface by blood pressure and transmitted across the entire vessel wall. The latter acts tangentially to the vessel wall, creating shear (frictional) stress at the endothelial cell luminal surface which is applied to the endothelial cells through blood flow. The normal human shear stress ranges from negative values up to approximately 50 dyn/ cm^2 [339, 352].

Endothelial cells respond to shear stress by undergoing marked structural changes, leading to elongated, spindle-shaped cells with their long axis oriented in the direction of flow. Gimbrone et al. [353] found that the morphological changes are accompanied by distinct

alterations in the actin cytoskeleton, and that elongation of the endothelial cell in response to shear markedly modifies surface topography, reducing fractional gradients across the cell surface [353]. Mechanical stimuli produce many genotypic and phenotypic changes in endothelium [354, 355]. Zhao et al. [354] studied the effect of physiological levels of shear stress and hoop stretch on endothelial cell morphology, finding that both shear stress and hoop stretch markedly change in the cytoskeleton, evidenced by the formation of stress fibres. Combinations of shear stress and cyclic circumferential strain have a synergistic effect on vascular endothelial cell remodelling processes, as Ziegler et al. [355], who studied the influence of unidirectional flow environments on the expression of endothelin and nitric oxide synthase, demonstrated: shear stress with pressure induced a greater expression of Endothelin-1 (ET-1) mRNA and a lesser expression of nitric oxide synthase (ecNOS) mRNA than unidirectional shear stress and pressure. The combination of pressure and oscillatory shear stress can downregulate ecNOS levels, as well as upregulate ET-1 expression compared with unidirectional shear stress.

Expansile force applied to ECs modifies the expression of endothelin-1 [356], prostacyclin (PGI2) [357], and tissue plasminogen activator [358]. Up-regulation of eNOS and increased NO production are documented as being secondary to cyclic strain forces on endothelial cells [359]. Shear stress stimulates the synthesis and secretion of various bioactive molecules, including PGI2, tissue plasminogen activator, PDGF [360], and NO synthase [361].

Chiu [362] investigated the effect of shear stress (20 dynes/cm2) on ECs before and after the addition of tumour necrosis factor -α (TNF-α). He found that shear stress increased the TNF-α–induced expression of ICAM-1 at both mRNA and surface protein levels but decreased the TNF-α–induced expression of VCAM-1 and E-selectin. In another study, oscillatory shear stress was found to increase expression of VCAM-1, ICAM-1 and E-selectin in cultured human endothelium [363].

Cui et al. [364] investigated endothelial cell differentiation marker expression in response to shear stress at 12 dyne/cm^2. In late endothelial progenitor cells isolated from rat bone marrow, shear stress was found to upregulate the expression of endothelial cell differentiation markers

such as vWF and CD31. Shear stress causes an increase in the expression of mRNA of integrin subunits β1 and β3. This increase leads to an up-regulation of vWF and CD31.

1.14.4 Molecular expression of EC

1.14.4.1 Intercellular adhesive molecule-1 (ICAM-1)

ICAM-1 is a cell surface immunoglobulin discovered by a monoclonal antibody that inhibits phorbol ester-stimulated leukocyte aggregation. Many experimental methods have been used to investigate expression in ICAM-1 such as immunofluorescence and flow cytometry. ICAM-1 is expressed in many different tissues such as the endothelial cells of the vascular system, fibroblasts, and in portions of the haemopoietic system such as macrophages, tonsils, lymph nodes and Peyer's patches **(Table 1-3)**. The expression is usually more profound in lymph nodes and tonsils with reactive hyperplasia, and to a lesser extent in peripheral blood leukocytes [365]**.**

Table 1-3 Distribution of ICAM-I in normal human tissues

1.14.4.1.1.1	Vascular endothelium
1.14.4.1.1.2	Germinal centre cells (dendritic reticulum cells, B cells), interdigitating reticulum cells, and macrophages in lymphoid tissue [tonsils, lymph nodes, Peyer's patches)
1.14.4.1.1.3	Fibroblast-like cells and dendritic cells in all organs including skin, intestine, kidney, liver and thymus
1.14.4.1.1.4	Epithelial cells (thymic epithelial cells, mucosal epithelia in tonsils and sometimes tubular epithelial cells in kidneys)

1.14.4.1.2 Structure

ICAM-1 is a single chain trans-membrane protein of 505 amino acids [366]. The molecular weight of ICAM-1 varies between 80–114 kDa [91] depending on its level of glycosylation; non-glycosylated ICAM-1 has a molecular weight of 60 kDa. The extracellular part of these adhesive molecules is composed of 453 amino acids, the vast majority of which are hydrophobic, and which form five immunoglobulin (Ig)-like domains. The extracellular part is bound to a solitary hydrophobic transmembrane region (24 residues) and a small cytoplasmic tail (28 residues). The Ig domain has a sheet structure, which is stabilised by disulfide bonds. The cytoplasmic tail lacks classical signalling motifs but has one tyrosine residue which may be important for signalling [367]. The gene sequence of ICAM-1 is composed of seven exons separated by six introns [367].

1.14.4.1.3 Function

ICAM-1 appears to play a role in neutrophil migration to the inflammation site. It is believed that ICAM-1 has an important immunological function in activating CD8T cells [368] and signalling between lymphoid cells [369, 370]. It is also believed to facilitate Human Immunodeficiency Virus -1 (HIV-1) fusion with PM-1 [371], and to elicit a specific and reversible cell-cell adhesion [372]. Mice with absent ICAM-1 are more protected from lethal septic shock caused by bacteria by decreasing leukocyte-endothelial cell interaction [373]. Studies show that ICAM-1 has a role in inflammatory response via leukocyte adhesion, endothelial transmigration and mediating leukocyte rolling [374, 375]. The role of ICAM-1 in leukocyte adhesion to endothelium is also well reported [376]. A significant reduction in leukocyte migration has been documented by using antibodies which block ICAM-1. ICAM-1 is believed to play a role in T lymphocyte maturation [377]. Another function is that of outside-in signalling. The activation of kinase pp60 src in the brain endothelial cell has been linked to ICAM-1 cross linking [378, 379].

IgM and ICAM-1 co-cross-linking on Burkitt lymphoma cells interfere with mobilisation on calcium [380], so, following cell-cell adhesion, ICAM-1 might have a signalling function [381-383]. In addition to its other roles, it is believed to have a potential role in haemostasis and thrombosis via initiation of the extrinsic coagulation pathways that convert fibrinogen to fibrin [384]. It also plays a role in myeloid cell lineage differentiation [385] and is believed to have a role in infection prevention. Soluble ICAM-1 has been reported to inhibit viral infection of the human cell [386] and to play a role in P. falciparum malaria [387].

In one study that investigated the role of ICAM-1 in the pathogenesis of bronchial asthma, results suggested that ICAM-1 may be important in the pathogenesis of airway hyperresponsiveness and asthma. It may also be implicated in the pathogenesis of other diseases such as chronic bronchitis, emphysema, idiopathic pulmonary fibrosis, eosinophil in infiltration rhinitis, nasal polyposis, chronic urticaria and atopic dermatitis [388].

1.14.4.1.4 ICAM-1 expression

Studies performed on human organs (thymus, lymph node, intestine, skin, kidney and liver) to discover distribution of the ICAM-1 found staining in all tissues' blood vessel endothelia. There was more staining in the interfollicular area in lymph nodes, tonsils and Peyer's patches than in the vessels in other organs [365].

Müller et al. [389] carried out a comparative study to investigate the expression of adhesion molecules in human micro-vascular and macro-vascular endothelial cells. They found 40% of un-stimulated HUVEC expressed mild to faint ICAM-1 staining. 100% of the studied tissues expressed ICAM-1 after stimulation with TNF-α and LPS at 18 hours. The stimulated cells expressed strong 80% to moderate 20% staining. They also found only 5% of the un-stimulated human pulmonary micro-vascular endothelial cell (HPMEC) had ICAM-1 expression. Eighteen hours after the cells were stimulated with TNF-α and LPS, all HPMEC showed staining. Müller et al. described the *in vivo* expression of ICAM-1 in normal lungs and in acute respiratory distress syndrome (ARDS) lungs: weak basal in the normal lungs, but

considerable increase in ARDS lungs. Upregulation of ICAM-1 is also documented in lung microvascular endothelial ECs of ARDS [390].

1.14.4.1.5 Response to radiation

ICAM-1 expression can be modulated by inflammatory and immune cytokines. A three- to four-fold increase in ICAM-1 expression on dermal fibroblast after exposure to IL1 or IFN α is well reported. ICAM-1 expression increases in atherosclerotic and transplant-associated atherosclerotic tissue and in animal models of atherosclerosis [367].

Many studies have reported that ICAM-1 plays a part in radiation-induced inflammation; ICAM-1 expression 24 hours after radiation has been documented in lungs [391]. Other studies have revealed upregulation of ICAM-1 in human umbilical cord as a response to radiation [392]; Sharp et al. showed the same result using human endothelial cells radiated by Gamma Knife [333]. Using 5 Gy is documented to increase ICAM-1 expression in HUVECs 24 hours post-radiation [327]. A four-fold increase in expression is seen in GKS-irradiated human brain endothelial cells [393]. Gaugler et al. [394] investigated the effect of low doses of radiation on cultured human bone marrow endothelial cells and found a significant increase of the cells' surface ICAM-1 up to seven days post-radiation. Further evidence of the upregulation of surface ICAM-1 is the increase of leukocyte rolling, adherence and migration; in addition, leakage of albumin increased at two, four and six hours after 20 Gy abdominal irradiation in rats [395]. In subsequent work, mesenteric venules irradiated with 10 Gy induced ICAM-1 expression when delivered at rate of 3Gy/min, but it did not show any significant difference when the rate was 0.9 Gy/min [396]. There was an increase in ICAM-1 expression on the lung microvascular endothelium when it was irradiated with 2 Gy at 24 hours post-radiation; this lasted for many days [329]. Serum levels of ICAM-1 were reported to increase in people suffering radiation pneumonitis [397]. Marked upregulation of ICAM-1 on the pulmonary vascular endothelium of mice 80 days after thoracic irradiation has been reported [398], and the immediate upregulation of ICAM-1 on the oral mucosa in patients treated with either 30 or 60 Gy radiotherapy for head and neck cancers is well reported [330].

Gamma Knife induces production of intracellular reactive oxygen species (ROS), which can be countered via administration of antioxidants which decrease the cytotoxic effect resulting from ROS increase. Endothelial adhesive molecules' mobilisation can be interfered with by an antioxidant or agent that increases antioxidant status [399, 400]. Another important step in Endothelial Cell Adhesion Molecules (ECAMs) transduction is the production of an oxidant second messenger, which may lead to activation of poly-adenosin diphosphate ribose polymerase (PARP) [401]. Cell dysfunction, increased endothelial permeability and cell necrosis can result from a rapid activation of PARP and deplete the intracellular concentration of its substrate, which results from DNA strand breakage [401-404]. PARP also appears to influence inflammation by regulating the ICAM-1 gene expression [401]. Activation of PARP is essential for activation of the necrosis factor kappaB (NF-kappaB), which plays a main role in inflammation by controlling the expression of ICAM-1 [405]. In wild-type C57BL/6J mice, a study showed that ICAM-1 was upregulated by laser photocoagulation [406] .

1.14.4.1.6 Ligands for ICAM-1

Two types of ligand for ICAM-1 are well known as either cell-associated or soluble ligands. ICAM-1 binds to two integrins belonging to the beta2 subfamily CDlla/CD18 (LFA-I) and CDllb/CD18 (Mac-l) which is expressed by leukocytes [407-409]. Another well described membrane receptor for ICAM-1, profusely expressed by leukocytes and platelets, is CD43 (sialophorin) [410, 411]. Furthermore, ICAM-1 also operates as receptor for soluble fibrinogen and for the extracellular matrix hyaluronan to stimulate cell-cell adhesion [412, 413]. Human ICAM-1 also works as receptor for the several group of rhinoviruses [414, 415] and coxsackie A13 virus [416]. It is considered that LFA-1 as the most important ligand *in vivo* [372, 417, 418].

1.14.4.2 PECAM-1

Platelet endothelial cell adhesion molecule-1 or PECAM-1 is type 1 trans-membrane cell adhesion molecule, a member of cell adhesion molecules of the immunoglobulin superfamily (Ig-CAMs). It has a molecular weight of 130 KD [419]. It is expressed on the external surface of platelets, monocytes, neutrophils and some T cells. It forms a part of the endothelial cell intercellular junction [420-422]. PECAM-1 is absent from some cells, including fibroblasts, epithelium, muscular cells and non-vascular cells [423].

1.14.4.2.1 Structure

The PECAM-1 gene is located on the long end of chromosome 17 and is encoded by a 17-kb gene. PECAM-1 in early reports was known as myeloid differentiation antigen, a homologue of platelet GPIIa [420]. The primary structure of the PECAM-1 was determined in 1990 [424-426]. The extracellular part of this molecule consists of 574-amino acids, which form six Ig-like homology domains; each domain is encoded by a single exon [427]. PECAM-1 consists of 118 intracyoplasmic amino acids that have a complex structure. The intracellular part is encoded by eight different exon [419] **(Figure 1-5)**.

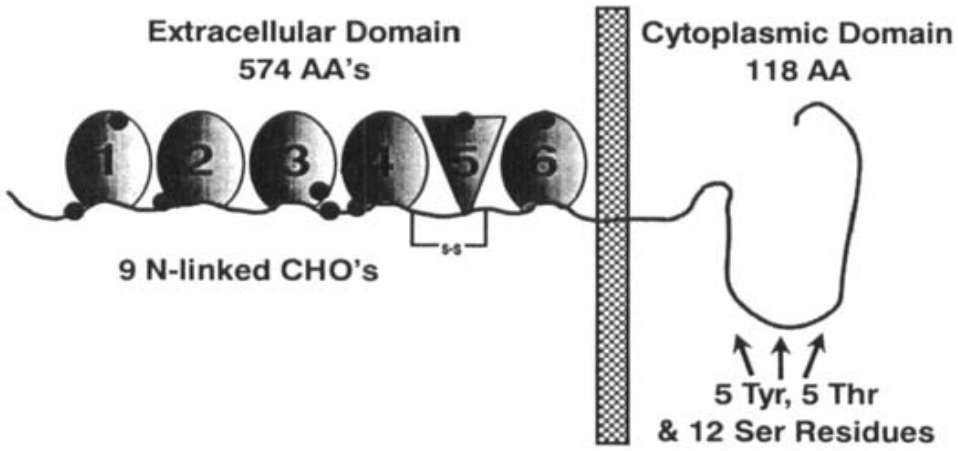

Figure 1-5 Schematic diagram of the structure of PECAM-I.

Adapted from Newman, P. J. 1994 [419]

1.14.4.2.2 Function

It well reported that PECAM-1 plays a role in the inflammation process. It plays a key role in the adhesion process which leads to extravasation of leucocytes. Inhibition of monocyte or neutrophil trans-endothelial emigration was achieved by using an anti-PECAM-1 antibody [428]. Leukocyte transmigration is inhibited by blocking endothelial cell junction PECAM-1 [428, 429]. Accumulation of neutrophils in the peritoneal cavity, the alveolar compartment, and human skin grafts in rat models of inflammation was prevented by using anti-PECAM-1 antibody [429]. In a mouse model of acute peritonitis, leukocyte migration to the peritoneal cavity was reduced by anti murine PECAM-1 antibody [430]. Myocardial infarction size is reduced by antagonising the adhesive and/or signalling function of PECAM-1 [431, 432]. A Less well-documented function for PECAM-1 is its role in chemotaxis. It was found that an antibody directed to PECAM-1 reduces neutrophil and monocyte chemotaxis [433]. Zehnder et al. [434] reported that it also has a role in alloimmune response by participating in T-lymphocyte function. In mixed T-lymphocyte reaction, blocking PECAM-1 with antibodies inhibit T-cell activation **(Table 1-4)**.

Table 1-4 Summary of alternative names and reported functions of PECAM-1.

Name	Antibody	Reported Function
gp120	TM2, TM3	Leukocyte chemotaxis
GPIla	HEC-75	Endothelial cell membrane
SG	SG 134	Myelomonocytic stem cell marker
GP130	Polyclonal	Platelet/endothelial cell shared antigen
hec 7	hec 7	Endothelial cell junction
CD3 1	Multiple	Leukocyte typing workshop
Endocam	Polyclonal	Endothelial cell adhesion molecule
PECAM-I	WM59	Cell adhesion molecule

Adapted from Newman, 1994 [419]

Formation of endothelial cell-cell contact requires the presence of functioning PECAM-1 [422]. Many studies have reported that PECAM-1 has a role in the process of angiogenesis. Studies of mouse brain endothelial cells indicate that PECAM-1 suppression decreases the ability of the cells to form three-dimensional vascular networks [435]. PECAM-1 was believed to have a positive a role in the early steps of clot formation [424], while the growth of platelet thrombi is negatively regulated by PECAM-1 [436]. An investigation of the prognostic significance of PECAM-1 antigens in patients with primary non-Hodgkin's gastric lymphoma found that PECAM-1is a representative marker of tumour expansion potential [437].

1.14.4.2.3 Ligand

It is generally believed that PECAM-1 is the principal ligand for itself. There are many indications that the cellular adhesive interaction of adjacent cells is mediated by PECAM-1 present in these cells, transforming PECAM-1 to PECAM-1 homophilic binding involving the distal N-terminal Ig-domain 1 and amino acid contact sites [438, 439]. Many ligands are known to interact with PECAM-1 in a heterophilic manner involving Ig-domains 1–3 of PECAM-1, including integrin $\alpha_v\beta_3$ which is expressed in many cell types such as endothelial, lymphoid, NK and mast cells[440] and also including CD38, 120-kDa ligands on T cells, and heparin-dependent-proteoglycans [440-443]. Cell surface glycosaminoglycans have also been reported as not serving as a ligand for PECAM-1 [444]. Changing the ligand binding ability of PECAM-1 from heterophilic to homophilic binding is also reported [445].

1.14.4.2.4 Radiation response

Unregulated CD31 expression on HUVECs has been achieved by using a single dose of gamma radiation (3.3 Gy/min) from a ^{137}Cs source [446]. A previous study on human AVM showed no significant change in expression of PECAM-1 after radiation [78]. Quarmby et al.

[447] investigated the effect of radiation on the expression of CD31 in cultured human dermal microvascular endothelial cells using flow cytometry and northern analysis. Dose-dependent increases in the surface expression of CD31 were observed and upregulation 72 hours after using 20 Gy was documented. In another study PECAM-1 expression increased in an irradiated human bone marrow EC line [448]. Upregulated PECAM-l expression has also been documented six days post-radiation, where a six-fold increase was observed compared to sham-irradiated mice [449]. The same group found that PECAM-l was upregulated in lung endothelial cells after total-body irradiation in mice [450].

1.14.4.3 Von Willebrand factor

The von Willebrand factor is a glycoprotein with an essential role in maintaining haemostasis. The gene for vWF is located on the tip of the short arm of chromosome 12 [451], is composed of about 180 kilobase and contains about 52 exons [452]. It is expressed in many different cells such as EC, and is also present in blood, plasma, platelets and the subendothelial matrix.

1.14.4.3.1 Structure

Purified vWF is seen under the electron microscope as a filamentous structure with a diameter ranging from 2–3 mm to 1300 nm. The largest oligomers, which are believed to be the most effective in cell aggregation and platelet adhesion, are detected in the blood of normal adults [453], the molecules present in plasma in variable size multimers. The pre-pro-vWF or the primary peptide translation is a polypeptide composed of 2813 amino acids and has a molecular mass of 307 kD [454]. Removal of signal peptide results in a pro-vWF subunit [455, 456]. The mature factor is a multimetric glycoprotein consisting of multiple subunits with identical structures. Each consists of 2,050 amino acid residues and up to 22 carbohydrate chains. The subunits are disulphide-bound to form dimers of 500 KDa, which in turn bond to form multimers of different sizes and may reach 20 MDa [457]. The

carbohydrate content of the molecules ranges from 10 – 19% of the total mass of the mature subunit [458].

1.14.4.3.2 Expression and radiation response

vWF is synthesised in endothelial cells and megakaryocytes exclusively. Endothelial cell vWF is secreted in two ways, a constitutive pathway or a regulated pathway [459]. A significant release of vWF in cultured endothelial cells irradiated with 20 Gy has been reported, but no significant change when they are irradiated with 10 Gy [460]. In irradiated mice kidneys with 16 Gy using a 250 kV x-ray, the glomerular expression of the protein decreases at 24 hours post-radiation, but is markedly increased at 40 weeks after radiation [461]. Using a single dose of 20 Gy to radiate a rat heart has been found to make no change in the expression of vWF mRNA [462]. Hong et al., [463] demonstrated that there was no change in expression of vWF mRNA in mice following whole body radiation or localised radiation of the midbrain. The same result has been documented in the radiation of mice kidneys, where 16 Gy radiation saw no change in the 10 – 30 weeks post-radiation level of vWF mRNA [464]. In another study there was an increase in production of vWF after irradiating HUVECs with 20Gy [460]. An increase in excretion of vWF after radiation of bone marrow has been linked to the increase in cell apoptosis [394]. Jahroudi et al. [465] investigated the effect of 20 Gy on human and bovine endothelial cells and found that ionising irradiation increased the procoagulant activity of the cells, including vWF. They concluded that vWF gene transcriptional activity is responsible for the higher levels of vWF mRNA accumulation; the promoter region of the vWF gene was shown to undergo increased activity after radiation. Verheij et al. [466] investigated ionising radiation on the release of vWF and documented that the release of vWF significantly increased at 48 hours after a single γ-radiation dose of 20 Gy in both the luminal and abluminal direction. In another study, vWF mRNA levels increased when either human or bovine endothelial cells were exposed to 20 Gy irradiation [467]. vWF positive stained vessels were slightly increased in irradiated sections compared to control sections in irradiated intestine [468].

1.14.4.4 Tissue factor

Tissue factor, also known as factor III, is a membrane glycoprotein that acts as a cofactor for factor VII in the extrinsic pathway of blood coagulation. It also participates in the conversion of factors X to Xa and IX to IXa, leading to the formation of thrombin. TF is highly expressed in cells such as astrocytes, trophoblasts, and alveolar cells. It is also highly expressed in myocytes, pericytes, fibroblasts, kidney, intestine, testes and uterus. Less TF expression was found in spleen, thymus, and liver [469]. Circulating TF mostly results from its expression in blood cells such as monocytes, macrophages and platelet free microparticles containing TF. The serum level can be measured by ELISA, and is related to procoagulant activity [470].

1.14.4.4.1 Structure

The tissue factor gene has been identified using cell hybridisation techniques; it is located on chromosome 1 [471].The primary structure of human TF has been deduced from a single 2,147-base pair cDNA insert derived from a placental library and cloned bacteriophage [472]. The protein consists of 263 residues; in its extracellular domain it contains three N-linked carbohydrate chains. It has a derived molecular weight of 29,593 [472]. One study has deduced the amino acid of the protein from human foetal lung fibroblast-derived cells, finding that the molecule consists of three domains: a short cytoplasmic domain composed of 21 residues, a transmembrane with domain 23 very hydrophobic residues, and a remarkably hydrophilic 219-residue extracellular domain [473].

1.14.4.4.2 Expression

Many tissues showing TF activity have been isolated and cloned, including adipose [474], fibroblast [475] and placental tissues [472, 473]. Structures corresponding to human TF mRNA have been identified in adipose tissue, small intestine, placenta, kidney [474] and brain [473]. Low levels of TF mRNA are documented as produced by cultured endothelial

cells [474]. One study using monocyte cell line U937 also identified TF mRNA [473]. Activation of monocytes with endotoxin or phorbol ester increases TF activity in the cells [476, 477]. The procoagulant of activity TF in endothelial cells is increased by the addition of endotoxin [478], thrombin [479], phorbol esters [478], interleukin 1 or tumour necrosis factor [480, 481] to the culture medium.

Wilcox et al. [482] investigated TF-producing cells in the normal vessel wall and in atherosclerotic plaques. They found that in all vascular tissues examined, the endothelial cells were negative for TF mRNA and protein, whereas large numbers of scattered cells in the tunica media of the saphenous vein were positive for TF mRNA. They also found that the adventitia had the strongest labelling for TF due to the presence of fibroblasts, which had the strongest TF staining.

Expression of TF in pancreatic neoplastic cells shows that TF was expressed in most non-invasive and invasive pancreatic neoplasia, of which about 54% tended to have both TF expression [483]. There has been a report that suggests that granulocytes acquire TF but do not synthesise. Whole-blood isolated granulocytes are reported that have very low or no TF activity or antigen, different from stimulated whole blood which contains very low levels of TF activity [484]. Similar data has shown that resting or stimulating eosinophil does not reveal TF antigens [485].

The expression of TF in endothelial cell is controversial. Many studies have found that HUVECs express TF [486] but Drake et al. [487] reported that endothelium does not show any expression of TF. Many factors are known to work as agonists for TF induction in the endothelial cells. In cultured endothelial cells, LPS is known to stimulate TF expression [488, 489]; VEGF and TNF also induce TF expression in HUVECs [319]. However, one study which investigated the presence of protein in saphenous veins and internal mammary arteries failed to find either endothelial TF expression [486] or any indication of TF in endothelial cells when inducted by thrombin [490]. In a diseased vessel wall the expression seems to be different, with atherosclerotic plaques characterised by significant TF in the extracellular matrix and in foam cell regions [491, 492]. The migratory smooth muscle cells in case of

restenosis of the coronary artery after angioplasty are associated with a marked increase in the synthesis of TF [493, 494].

1.14.4.4.3 Radiation response

Goldin-Lang et al. [495] investigated the effect of radiation on human peripheral blood mononuclear cells (PBMNCs) using 20 Gy and found a significant increase of PBMNC-associated procoagulant activity. This was associated with TF expression up to seven days post-radiation. IR has been documented to cause endothelial cell apoptosis, and increase endothelial permeability and thrombo-resistance by enhancing TF expression [496]. A transient increase in endothelial activity of TF 4–8 hours post-IR (20 Gy) has also been reported [496].

A study using mouse lungs to examine the expression of mRNA 10 to 18 days post-IR revealed 1.7-fold increase in mRNA expression in irradiated cells compared to non-irradiated controls [497]. An *in vivo* study of rat small intestine showed an increased TF expression up to 26 weeks post-radiation [498]. Finkelstein et al. [499] investigated the effect of intracoronary brachytherapy on TF, finding that the protein expresseion, with the TF procoagulant activity of PBMNCs elevated up to seven fold post-IR, indicating an increase in TF procoagulant activity associated with PBMNCs at that stage. TF was found to be the major contributor to extracellular thrombo-genicity in HUVECs post-IR [500]. In another study, the effect of Ionising radiation on endothelial TF activity and its cellular localisation also led to upregulation of TF [496], and upregulation of tissue factor receptor and protease-activated receptor 1 in irradiated intestine have been determined [501].

1.14.4.5 Thrombomodulin

TM, also known as fetomodulin, CD141, and BDCA3trans-, is a glycoprotein expressed on the surface of all vascular endothelial cells. It has a multidomain structure and is involved in

complex interactions with thrombin and protein C. The glycoprotein has many roles in regulating haemostasis as an anticoagulant, exhibits a range of physiological functions as an anti-inflammatory, and is an essential cofactor in a range of biologic processes and has anti-fibrinolysis properties.

1.14.4.5.1 Structure and Function of TM

In 1981 Esmon and Owen identified and isolated TM to determine how Vitamin K functioned [502], and to understand the molecular mechanism behind this molecule's coagulation, inflammation and fibrinolysis properties. Originally the molecule was believed to be a vascular endothelial cell receptor [503-505], but lately the molecule has been found to demonstrate many functions of coagulation.

In humans, TM is encoded by a gene that has been localised to chromosome 20 [506]. The human mature protein is a single-chain trans-membrane glycoprotein 557 amino acid residues long. In mice, the intracellular or C-terminus has no effect on development, survival, coagulation or inflammation [507]. A serine/threonine-rich domain has sites for O-linked glycosylation and supports the attachment of chondroitin sulphate. An *in vivo* study showed that the chondroitin sulphate of TM enhances the protein C cofactor activity of TM [508] and enhances the process of neutralisation of thrombin, therefore facilitating the binding of platelets factor 4 to protein C to increase its activation.

Another domain comprises six repeats of epidermal growth factor (EGF)-like units. In cultured fibroblasts and vascular smooth muscle cells, this domain is believed to have a mitogenic function that might play a role in cellular proliferation and atherogenesis [509, 510]. It is also essential for activation of protein C and the thrombin activatable fibrinolysis inhibitor by thrombin [511-513]. Such antifibrinolytic activity is supported by the EGF-like repeats of TM [514] and interference with the production of plasmin [515, 516].

At the N-terminus of the molecule there is a 154-amino acid residue module [517, 518]. The lectin-like domain of TM is spherical and sited furthest from the plasma membrane as is seen

under electron microscopy and in computer models [519, 520]. The domain plays a major role in inflammation and cell survival, and participates in innate immune functions such as complement activation, leukocyte trafficking and regulation of apoptosis [521, 522].

1.14.4.5.2 Expression of TM

TM is expressed in the vascular endothelium of all arteries, veins, capillaries and lymphatic endothelium, and is also found on the syncytiotrophoblasts of the human placenta [523]. Kawanami et al. [524] showed that in the alveolar zones of the lungs, the expression is high in capillary endothelial cells. Many other cells have been shown to express TM, such as astrocytes, keratinocytes, mesothelial cells, synovial lining cells, alveolar epithelial cells, ciliary non-pigmented epithelial cells of the eye [525, 526], and dendritic cells [527]. Many studies have shown that it also is produced by giant trophoblasts where it plays an important role in embryo survival [528, 529]. Proteolysis of the membrane-bound protein results in soluble forms of thrombomodulin, which circulate in the blood [530, 531] and are excreted in the urine [532].

TM has been found to be expressed in intimal monocytes and macrophages, smooth muscle cells of the intima and media, and vascular endothelial cells of the vasa vasorum in humans, and in rabbit atherosclerotic lesions [533]. One study has demonstrated that TM is downregulated in atherosclerotic coronary arteries that predispose to further inflammation and thrombosis [534]. Much evidence indicates that TM plays an important part in the inflammatory response in arthritis; TM has been seen expressed in the synovial lining cells of inflamed joints of rabbits and humans [535, 536]. This is evident in rheumatoid arthritis, where there is a marked elevation in synovial fluid TM [537].

Internalisation of TM via endocytosis in response to the pro-inflammatory cytokine shows that tumour necrosis factor (TNF) has links to inflammation [538, 539]. A reduction in the expression of TM at a site of injury may increase inflammation and coagulation responses, and may also have a role in removing thrombin from the circulation [540]. Beretz et al. [541]

and Brisson et al. [542] indicate that internalisation of thrombin–TM does not occur in human saphenous vein endothelial cells and the endothelial cell line.

Many factors are known to have a downregulation effect on TM, including fluid shear stress [543], hypoxia, oxidised LDL, free fatty acids, transforming growth factor beta [544-546] and C-reactive protein [547]. However, an *in vitro* study of monocyte-like cells demonstrated that TNF and IL-1β upregulate the expression of TM in these cells [548] and LPS downregulates it in monocytes [549]. Conway et al. [550] noted that in endothelial cells these cytokines significantly suppress TM mRNA. Infusion of LPS is shown cause a significant reduction in TM expression in aged mice [551]. This may somewhat explain the heightened sensitivity of elderly patients to infections and chronic inflammatory diseases such as atherosclerosis. Other experiments [552] have shown that NF-κB mediates TNF-induced suppression of TM.

Conway et al. [553] investigated the effect of heat shock on TM expression, showing that it upregulates the protein. They concluded that stress-induced upregulation of TM may be important during inflammation and ischemia–reperfusion. In an *in vivo* study of baboons, although there was a significant increase of TNF level after a lethal dose of Escherichia coli, expression of endothelial cell surface TM remained unchanged [550, 554, 555]. More studies supporting these findings come from a rat model of sepsis-induced thrombotic microaniopathy in which TM levels were not suppressed [556]. TM or its mRNA are also upregulated by other factors, including thrombin, vascular endothelial growth factor (VEGF), histamine, dibutyryl cyclic AMP, 1,25-dihydroxyvitamin D3, retinoic acid, prostaglandin E1, IL-4, theophylline and statins [541, 550, 557, 558].

1.14.4.5.3 Radiation response

Hauer-Jensen et al. [501] investigated acute and chronic radiation responses in normal tissues and the consequence of radiation injury on expression of the TM-protein C system. They documented that ionising radiation causes a pronounced, sustained deficiency of endothelial TM in normal tissues and concluded that this was likely due to initial inactivation of TM by

reactive oxygen species, reduced transcription of TM, and release of TM into the circulation. In another study cultured confluent HUVECs were treated with 60 Co γ rays at doses ranging from 0 to 50 Gy; an increase in the release of TM from irradiated endothelial cells and an increase in the number of molecules and the activity of TM on the surface of the cells were observed 24 hours post-irradiation. The release was time- and radiation dose-dependent [559]. A markedly significant decrease in TM immunoreactivity in irradiated intestine was also reported [468].

Circulating TM during radiation therapy of lung cancer was also investigated. The TM level was not significantly changed in patients with radiation pneumonitis, but a moderately significant decrease in plasma TM antigen during the initial 1–2 weeks was noted in pneumonitis-free patients [560]. Radiation caused a sustained, dose-dependent decrease in microvascular TM in irradiated rat intestine [561].

1.14.4.6 Integrins

Integrins are type I trans-membrane cell adhesion receptors composed of α and β chains. They play roles in developmental and pathological processes such as cancer, osteoporosis and autoimmune diseases, mediating the attachment of cells to the extracellular matrix (ECM) and contributing to specialised cell–cell interactions.

1.14.4.6.1 Structure

With the emergence of antibodies to integrin α subunits, and with evolution of the technology that allowed affinity purification of pure receptors, it has become clear that functional receptors are heterodimers comprised of non-covalently connected α and β chains [562]. Takada et al. discovered that integrins in vertebrates consist of 18 α subunits and 8 β subunits that can form 24 distinctive heterodimers for different ECM proteins [563]. Integrins are classified according to ligand-binding properties, or the composition of the subunit. The three

largest groups according to this classification are β1 integrins, β2 integrins, and αv-containing integrins.

1.14.4.6.2 Integrin expression and function

Integrins are expressed in the vast majority of human cells. Of several studies that have examined the role of integrin in angiogenesis, one found that αvβ3 and αvβ5 integrins are not fundamental for vascular growth or in pathological angiogenesis [564]. It identified that mice deficient in β3 integrins or both β3 and β5 display enhanced angiogenesis, suggesting that neither β3 nor β5 integrins are essential for neovascularisation, while using monoclonal antibodies or low-molecular-weight antagonists to block αvβ3 inhibits blood vessel formation in *in vivo* models [565] and tumour angiogenesis [566].

Epidermal stem cells express high levels of β1 integrins [567]. In some mammals, limited quantities of integrin are expressed in certain cell types or tissues; for instance, αIIbβ3 is only expressed on platelets, α6β4 is restricted to keratinocytes, αEβ7 to T cells, dendritic cells and mast cells in mucosal tissues, α4β1 to leukocytes, α4β7 to memory T cells, and the β2 integrins to leukocytes; αVβ3 integrins are largely expressed in endothelium [568]. Integrin has many functions depending on its localisation; for example, leucocyte-limited β2 integrins play an essential role in immune reaction [569]. Severe leucocyte adhesion deficiency type I results from a genetic anomaly of the β2 integrin [570]. Antonin et al. [571] suggest that it is involved in critical processes in the creation of the immunological synapse in immune response. It is also believed to have a function in leucocyte adhesion and extravasation through the endothelium [569, 572]. α4β1 is essentially expressed on the surface of lymphocytes, eosinophils, monocytes, basophils and mast cells, while α4β7 exists on subpopulations of T- and B-lymphocytes and on eosinophils [573, 574]. Both α4β1 and α4β7 contribute to leukocyte adhesion, migration, and activation [575]. It is believed that both α4β1 and α4β7 are linked to diseases such as inflammatory bowel disease, rheumatoid arthritis, asthma, Crohn’s disease and multiple sclerosis (MS), in which they are connected to activated leukocytes in the diseased tissue [569]. Integrin subtypes α1β1, α2β1, α10β1, and α11β1 are collagen integrin receptors bound to helical collagen expressed in fibrous tissues such skin, cartilage and bone [576]; it has been suggested that they participate in cell adhesion,

migration, and proliferation, in immune response [577]. Researchers investigating the role of α1β1 and α2β1 in several animal models of inflammation report that using mAb against murine α1 and α2 was found to significantly inhibit effector phase inflammatory responses in animal models [577]. White et al. [576] found that α1β1 may be involved in proliferation and α2β1 in matrix remodelling. α1β1 may also play a role in angiogenesis in cancer [578]. A high expression of α2β1 has been associated with a higher risk of stroke and myocardial infarction [579].

1.14.4.6.3 Radiation exposure

In one study the level of α2bβ3 integrin within tumour blood vessels after radiation was investigated using immunohistochemical staining and Western immunoblots. At six hours after irradiation, increased levels of the β3 and α2b chains of integrin α2bβ3 and integrin αvβ3 were reported; however, there was no significant increase in expression of the αv chain post-radiation. The study also showed an increase of the α2b chain of the α2bβ3 integrin, beginning at 3 h and persisting at 6 h after tumour irradiation [580]. The effect of ionising radiation on functional β1-integrin in human lung tumour cell lines *in vitro* has also been studied. Lung carcinoma cell lines A549 and SKMES1 cells grown on fibronectin, laminin, or plastic were exposed to 2 Gy or 6 Gy, and β1-integrin radiation-induced upregulation was observed [581]. An investigation of the effects of l Gy radiation on B16 melanoma reported a radiation-induced increase in expression of the αIIbβ3 integrin in melanoma cells [582]; after 0.5 Gy radiation, 99% of radiated B16 tumour cells were positively stained with monoclonal antibodies directed against αIIbβ3, compared with 22% of sham-irradiated cells.

1.14.4.7 Vascular endothelial (VE)-cadherins

VE-Cadherins are a superfamily of Ca2+dependent cell surface transmembrane adhesive glycoproteins including epithelial (E)-, neuronal (N)- and placental (P)-cadherins [583]. In vertebrates and invertebrates, vascular endothelial (VE)-cadherin is an endothelial specific

adhesion molecule found at junctions among ECs, and is a constitutive endothelial-specific marker [584]. It has a fundamental adhesive function with an important role in the maintenance and control of EC contacts. They also regulate cellular proliferation and apoptosis, modulate vascular endothelial growth factor receptor functions, and are necessary during embryonic angiogenesis [585].

1.14.4.7.1 Structure

More than 350 cadherins have been recognised and classified into subfamilies: the vertebrate classical cadherin subfamily includes type I and type II classical cadherins; and in mice and humans, 5 type I cadherins and 13 type II cadherins have been described [586].

Structurally both type I and type II classical cadherins have an ectodomain area comprising five extracellular cadherin domains, each consisting of about 110 amino acids. The extracellular cadherin domain are rigidified by calcium ion binding [586, 587]. Cadherins are mostly transmembrane proteins that contain a small cytoplasmic domain with binding places for β / γ -catenins and p120 catenins that mediate attachment to the cytoskeleton and control cadherin trafficking [588, 589].

1.14.4.7.2 Function

VE-cadherin is crucial for embryonic angiogenesis, vascular maintenance, and the restoration of vascular integrity after injury [590-592]. Cadherins have been documented as vital in different organs' morphogenesis [593, 594]. Gulino et al. [591] used a polyclonal anti-VE-cadherin antibody to block VE-cadherin in human endothelial cell culture, finding that the VE-cadherin antibody interrupts confluent endothelial cell monolayers and generates several gaps at cell-cell junctions. The destruction of interactions among the extracellular domains of VE-cadherins provokes a quick reproduction of VE-cadherins. Vittet et al. [595] found that in VE–cadherin-negative mouse embryonic stem cells, endothelial cells remained dispersed and

lacked an organised vasculature in embryonic bodies. Inactivation of the beta-catenin-binding cytosolic domain of the VE-cadherin gene in mice impairs EC remodelling and maturation; mice were found to die during development due to disintegration of the vasculature [596]. Antibodies directed against VE-cadherin cause disassembly of the vasculature in wild-type adult mice [597]. VE-cadherin also has been found to play a role in cellular processes such as leukocyte trafficking [598] and vascular permeability [599].

1.14.4.7.3 Expression

Expression varies for every individual cadherin, although different cadherins may be expressed concurrently within a tissue and the same cadherin can be found in a variety of embryonic cell types and tissues [584]. N-cadherin has been found expressed in human endothelial cells to a significant degree, and in other cell types such as in the nervous system and skeletal and cardiac muscle. M-cadherin is specifically found in skeletal muscle cells [600]. VE-cadherin (7B4 or cadherin-5) has been found exclusively in the cells of the adherens junctions of the vascular endothelium in vertebrate species [584, 588]. VE-cadherin can be found in all types of endothelium, in large and small vessels, arteries, veins, and the microvasculature of all tissues, but not in blood cells or in hematopoietic precursors [584].

1.14.4.7.4 Radiation response

A few studies have investigated the effect of radiation on VE-cadherin. In one study radiation was found to downregulate endothelial VE-cadherin in radiation of human aortic endothelial cells; the downregulation was dose-dependent [601]. Moriconi et al. [602] studied the effect of irradiation on gene expression of rat liver adhesion molecules, including E-cadherin. A real-time PCR analysis and northern blot study of the total RNA from rat liver *in vivo* showed that E-cadherin reached a significant peak 48 hours after irradiation. A significant downregulation of E-cadherin was detected by real-time PCR analysis of the total RNA from isolated rat hepatocytes *in vitro*. Gabryś et al. [603] studied radiation effects on human dermal

microvascular endothelial cells (DMECs) and HUVECs and found that within ten minutes of irradiation, significant dose-dependent VE-cadherin redistribution was observed, very prominently at 20 Gy, and persisting for up to 24 hours. After more than 24 hours the protein level was not changed, suggesting that irradiation primarily affects the distribution, but not the expression, of junctional proteins. Radiation was also found to increase expression of E-cadherin in laryngeal carcinoma [604], thyroid carcinoma [583] and human lung cancer cell lines *in vitro* where the expression increased six hours after irradiation with 10 Gy and reached its peak level at 24 hours [605].

Hypotheses and Aims

Hypotheses

The overall hypothesis: Radiosurgery induces changes in the molecular profile of the endothelial membrane that allow discrimination from normal endothelial cells, thereby providing molecular targets that can be used for a ligand-based vascular targeting thrombotic therapy for AVMs.

Aims of the study

1. To develop a suitable animal model for AVM molecular targeting, using Gamma Knife as the radiosurgery method;
2. To investigate the haemodynamics, morphological and histological changes that Gamma Knife induces on the animal model;
3. To investigate the expression of adhesive molecules in the animal model of AVM following Gamma Knife radiosurgery and to determine their cellular localization;
4. To investigate the expression of thrombotic molecules in an animal model of AVM following Gamma Knife radiosurgery.

Chapter 2

General methods.

2.1 Ethics

All animal experiments were approved by the Animal Care and Ethics Committee of Macquarie University (ACEC reference numbers 2011/011). Animal experimentation was performed within ACEC guidelines and the Australian Code of Practice for the Care and Use of Animals for Scientific Purposes (8th Edition, 2013). At 4-5 weeks of age, animals were obtained with average weights between 250 to 300 g. All rats were kept in standard rat cages, with a maximum of four per cage. Bedding was changed twice weekly. Animals were acclimatised for two weeks pre-operatively and were housed for two weeks post-operatively.

2.2 Morbidity and mortality

None of the animals had evidence of significant neurological morbidity at any stage of the experiments. One animal died during the Gamma Knife process due to an unknown reason and one animal died due to fistula occlusion. No complication was recorded after GKS. Mild haematuria was reported in some animals on the first day after GKS. None of the animals had to be euthanised in the post-procedure period.

2.3 Animal Experimental procedures

2.3.1 Anaesthesia and operative care

2.3.1.1 Inhalational anaesthesia

Animals were induced in an anaesthetic chamber using isoflurane (4%) and oxygen (1.5 L/min) and maintained with 2% isoflurane through a nose cone. Isoflurane was increased as

required to maintain an adequate level of anaesthesia. Respiratory rate and pedal reflex were used to check the depth of anaesthesia. Following surgery, the animals received oxygen through the nose cone until they recovered. The animals were kept under supervision for two hours post procedures. When there was no indication of morbidity, the animal was returned to the holding facility.

2.3.1.2 Intraperitoneal anaesthesia

Radiosurgery was performed under intraperitoneal anaesthesia. Ketamine and midazolam were used for all radiation experiments. Ten minutes prior to the procedure, ketamine (37.5 mg/kg) and midazolam (2.5 mg/kg) were given. The depth of the anaesthesia was tested in the same way as described previously in inhalation anaesthesia. After the procedure, animals were given atipamezole for recovery, and kept under observation for two hours and kept in a quiet area until recovery. If there was no evidence of significant morbidity, the animal was returned to the animal holding facility and kept in single boxes until the day after.

2.3.2 Operative and post-procedure care

All surgical procedures were done under general anaesthetic under aseptic conditions. The surgical site at the neck region was shaved and prepared with povidone-iodine. An implantable microchip was inserted subcutaneously and an alphabetical code was assigned to help with further animal identification. Animals were then observed daily for two weeks and then once weekly thereafter. Weight, assessment of motor function, behaviour and wound health were observed. Weight loss greater that 20% of pre-procedure body weight was an indication for animal euthanasia.

2.3.3 Fistula formation

Sixty-four male Sprague-Dawley rats were used to investigate the haemodynamic, angiographic and histological characteristics of AVMs. For the immunohistochemistry study, 50 male Sprague-Dawley rats were used to investigate the different molecules.

The model AVM was created using microsurgical techniques with the animal in a supine position. The rat's midline was identified using the sternum as a reference point, and a midline incision was made over the anterior neck. The left sternocleidomastoid muscle was identified and the left omohyoid muscle was divided to expose the left common carotid artery (LCCA). Haemostasis was secured using electro diathermy and pressure. Mobilisation of the left external jugular vein (LEJV) was performed by sacrificing the most caudal feeding veins. The caudal LEJV was ligated at the junction with the subclavian vein and the rostral end was clipped with an aneurysm clip. The LEJV was transected close to subclavian vein then mobilised to the lateral side of the LCCA.

The LCCA was clipped proximally and distally with Codman AVM clips. Then an elliptical hole was cut in the LCCA. After that the rostral end of the LEJV was anastomosed to the LCCA using running 10-0 prolene suture. If there was any bleeding after clip removal, gentle pressure was applied to the anastomosis site to stop further bleeding. The wound was closed with non-absorbable sutures **(Figures 2-1, 2-2)**. Sixty-four male Sprague-Dawley rats were used to investigate the haemodynamic, angiographic and histological studies. For the immunohistochemistry study 50 male Sprague-Dawley rats was used to investigate the different molecules.

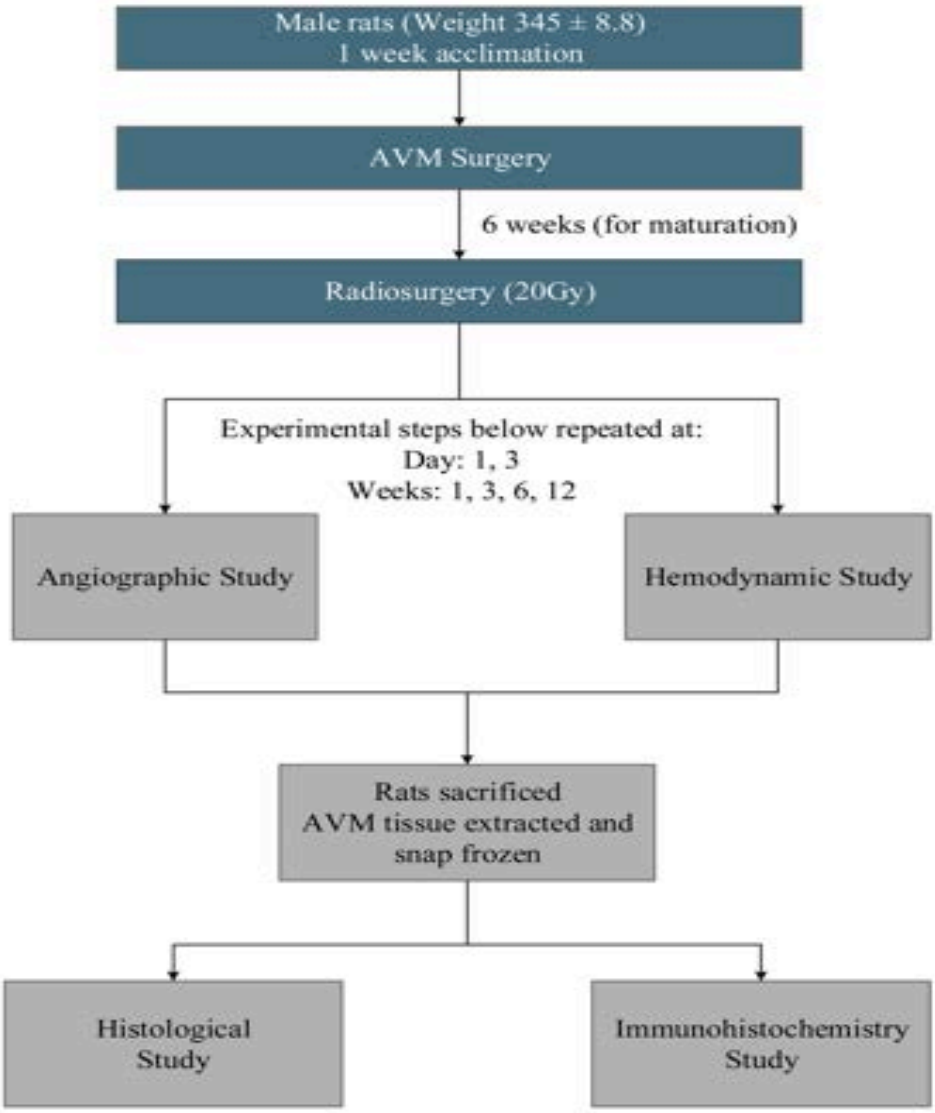

Figure 2-1 Schematic diagram illustrate the general methodology used in this study.

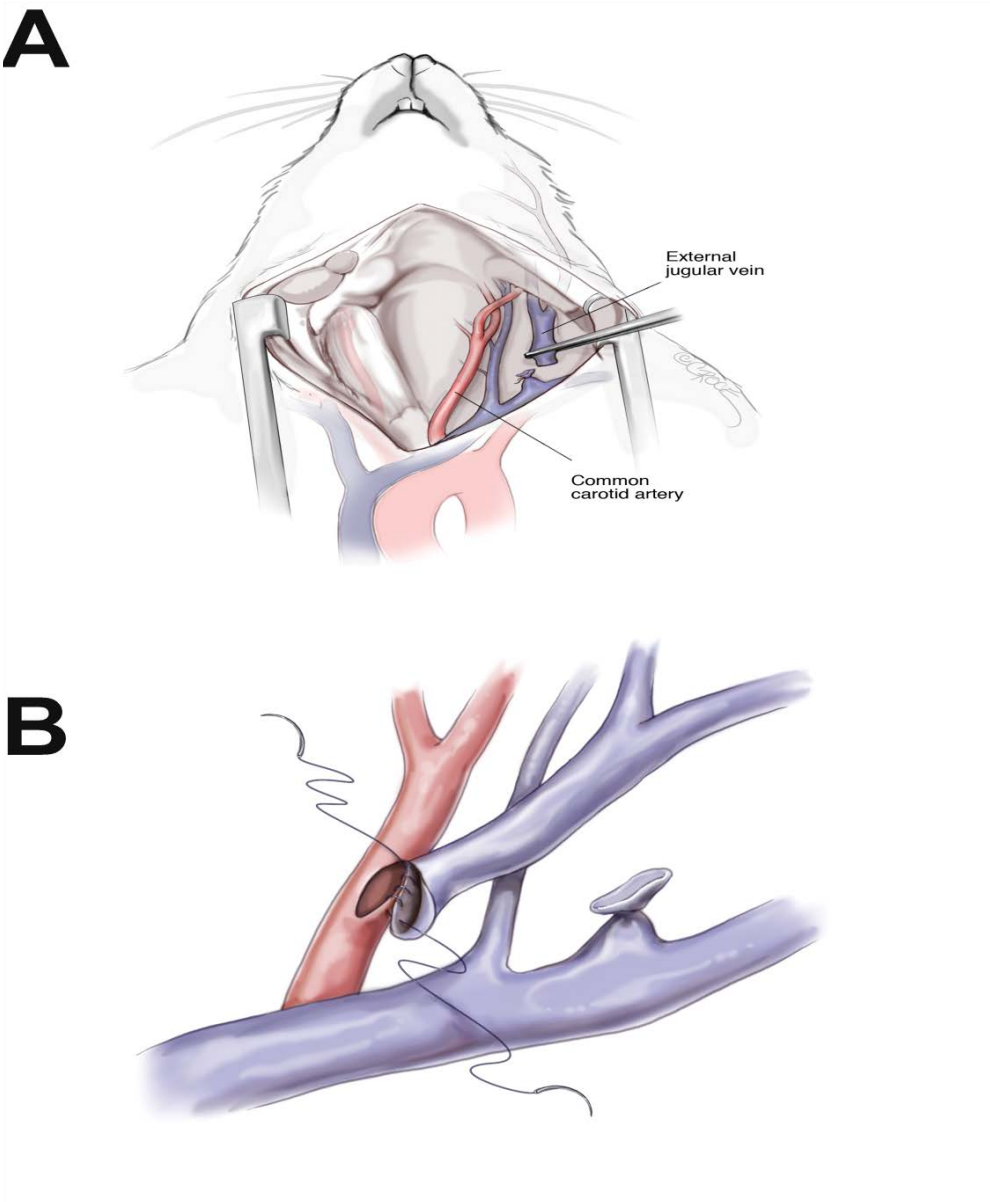

Figure 2-2 Drawing illustrates AVM creation.

(A) Surgical exposure of the rat neck area, showing LCCA and LEJV, (B) rostral end of the LEJV was anastomosed to the LCCA using running 10-0 Prolene suture.

2.3.4 Radiation planning and delivery

Each rat was anaesthetised using midazolam and ketamine for this procedure. Each rat underwent a multislice CT prior to Gamma Knife radiation. The rats were placed in a specially designed frame in a supine position (SC Medical biomedical engineering, Australia) **(Figure 2-3)**. The resulting image was reconstructed to a 3D image. The 3D images, axial and sagittal sections were used to determine the exact position of the created AVM. This information was used to plan the radiation that would be required to deliver a marginal dose of 20 Gy of gamma irradiation. Gamma Knife (Elekta) machine was then used to deliver 20 Gy gamma radiations to the AVM nidus.

2.3.5 Haemodynamic studies

Each fistula was carefully exposed under general anaesthesia after angiography. Blood flow measurements were obtained in the ipsilateral proximal and distal LCCA and the ipsilateral arterialised LEJV using a Doppler flowmeter **(Figure 2-4)**. Each measurement was recorded over an average of 10-minutes. Peri-vascular flow-probes (Transonic Systems, Australia) were selected to match the size of the vessel in which flow was being measured. Probes were connected to a transit time perivascular flow-meter (TS420, Transonic Systems, Australia), which was connected to a data acquisition system. Measurements of blood pressure were performed simultaneously in the ipsilateral left femoral artery (for mean systemic arterial pressure). A 0.58 mm polyethylene catheter was inserted into the vessel and pressure measured with a blood pressure transducer (Edwards Lifesciences, CA, USA). Flow and pressure data were acquired through a data acquisition system for off-line analysis (CED Limited, UK).

2.3.6 Angiography

Angiography was performed immediately prior to sacrifice. Eight control and eight GKS-treated animals were studied at each time point (1, 3, 6, and 12 weeks). Animals were placed under general anaesthesia using 2-3% Isoflurane (2 L/min). Under the operating microscope, the left femoral artery was exposed. A 0.8 mm Progreat microcatheter (TERUMO, Australia) was advanced through a small arteriotomy under a fluoroscopic C-arm (GE Healthcare, Australia) up to the left CCA. An arterial-phase anteroposterior angiogram was obtained by manual injection of 1 mL/kg contrast medium (Meglumine Iothalamate, 60% w/v. Covidien Pty Ltd, Australia) over three seconds. The catheter was withdrawn and the femoral artery was ligated after completion of angiography.

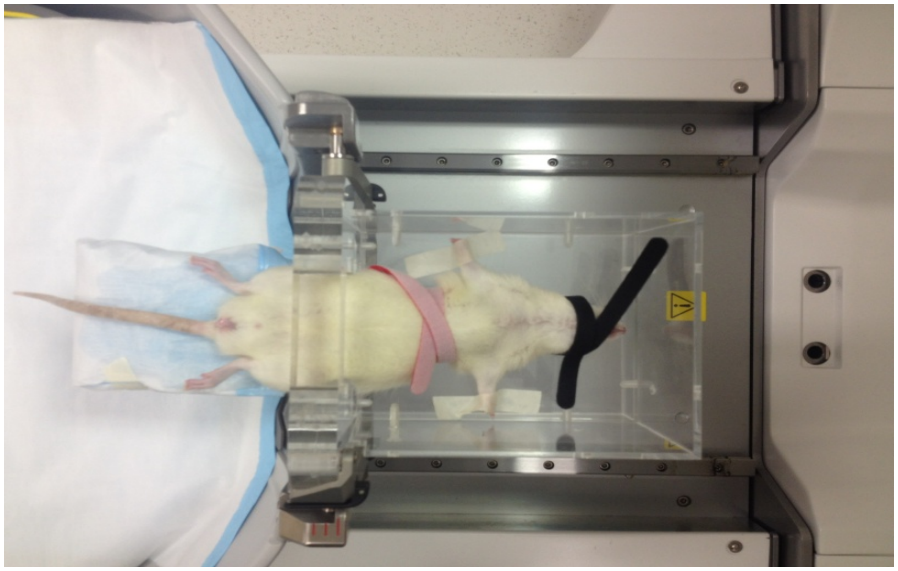

Figure 2-3. Anesthetized animal in supine position in GKS special designed frame.

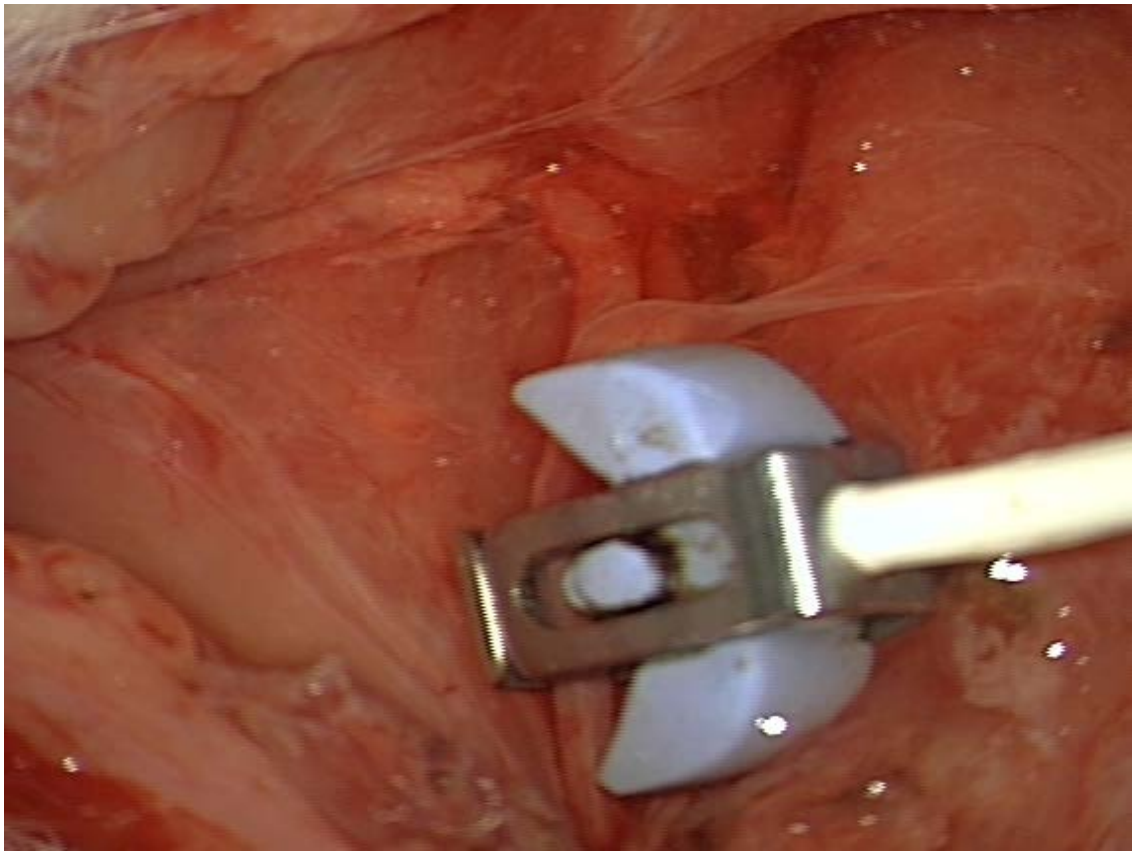

Figure 2-4. Placement of a perivascular flow-probe around the ipsilateral CCA for blood flow measurements.

2.3.7 External morphology study

After completion of angiography, a 4-0 silk suture was applied around the proximal segment of the arterialised LEJV. The fistula was exposed to measure the circumference and calculate the diameter (circumference/π) **(Figure 2-5).**

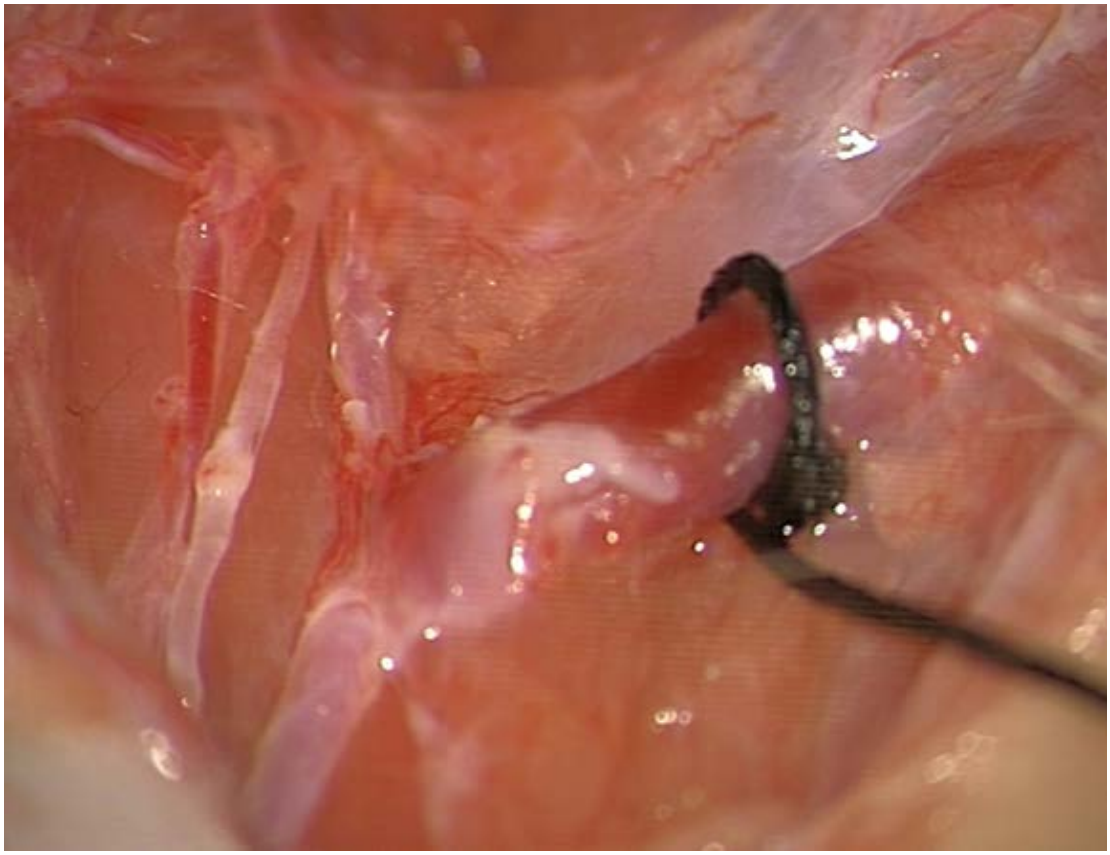

Figure 2-5. External morphology study. Measurement of the circumference of the proximal segment of the arterialised external jugular vein.

2.3.8 Perfusion-fixation

The animals were perfused at the end of each experiment. Animals were anaesthetised under general anaesthesia and the depth of anaesthesia was tested as described above. The animals were positioned supine. Laparotomy was performed and extended to a bilateral thoracotomy and the diaphragm was separated from the rib cage. The heart and great vessels were exposed. The heart was then cannulated through the left ventricle and the needle was carefully placed in the origin of the ascending aorta. A right atrium incision was made to allow out flow of blood and the perfusion solution. Phosphate buffered saline (PBS) was perfused through the heart using pulsatile delivery system. The fistula was exposed; ipsilateral CCA, ipsilateral

jugular vein and its small tributaries, contralateral CCA, contralateral jugular vein and contralateral femoral vein and artery, aorta and inferior vena cava were removed.

2.4 Tissue processing

Tissue was collected from the AVM animal model. The created AVM was taken and the LCCA, LEJV and the nidus were embedded in tissue freezing medium (ProSciTeck, Australia) and frozen in liquid nitrogen. Tissue was stored at –80°C until the time of staining. Tissues were sectioned (12 μm thickness) using a cryostat (Leica Microsystem, Germany), the proximal end of the vessels (towards the created AVM) was sectioned and stained with haematoxylin and eosin and Shikata Orcine for histological characterisation, with Martius Scarlet Blue staining for thrombus formation and for immunohistochemistry.

2.5 Staining

2.5.1.1 Haematoxylin and Eosin

Frozen sections were used for this study. The OCT medium was removed by rinsing the slides containing tissue in distilled water. The sections were deposited in haematoxylin for five minutes; the slides were then washed in distilled water. The slides were then dipped quickly in 2% of hydrochloric acid three times then rinsed in tap water. Lithium carbonate was used for bluing, by immersing the slide for 10 seconds in the solution. The slides were washed with tap water for three minutes. That was followed by counterstaining of the slides with eosin (alcoholic) for two minutes. Slides were dehydrated in serial alcohol (ethanol) concentration, 2 × 90% for 15 seconds, then 2 × 100% / 15 seconds and then washed in xylene for four minutes in two different baths. The slides were then covered with cover slips and left to dry at 37º C for two days.

2.5.1.2 Shikata Orcein staining

Frozen sections were used for this study. The OCT medium was removed by rinsing the slides containing tissue in distilled water. The sections then treated with acidified potassium permanganate for 3 minutes. After a second wash in water, decolourization of the tissue was performed by dipping the slides 7 times in 1% oxalic acid. The slides were washed in tap water again, and then slides stained with shikata orcein for 35 minutes. The slides were then washed in water, dehydrated, coverslipped and left to dry at 37º C for two days.

2.5.1.3 Immunohistochemistry

Sections were in dried at room temperature for 24 hours. A wax pen was used to place a border around the sections to help in applying the antibody on the tissue and to prevent loss of antibodies from the slides. Sections were then washed in PBS three times (3 × 5 min). The sections were permealised in 50% ethanol for 10 minutes then washed again with PBS (3 × 5 min). After that, sections were blocked in 10% donkey serum /PBS for 1 hr., RT. Then all slides were incubated overnight with primary antibody anti-vWF mixed with an antibody for the protein of interest in PBS humidifier (details of all antibodies in the following chapters) at 4°C, and washed with PBS (3 × 5 min). Then, the sections were incubated with the secondary antibody (Directed against the appropriate antibody isotype) (Details of all secondary antibody are given in the following chapters) in a dark humidifier for one hour at room temperature then washed with PBS (3 × 5 min). The slides were then incubated with DAPI for 1 minute and after that they were jet rinsed, cover-slipped (Dako, Carpinteria, CA) and cured for 24 hours in a dark room before microscopy. All chemicals used for immunofluorescence had a pH of 7.45 ± 0.1. Rat lymph node, liver and heart were used as a positive control for several antibodies and negative controls had the primary antibodies omitted from the staining procedure.

2.6 Microscopy

2.6.1 Light microscopy

For analysis of proteins expression microscopy was performed using a Zeiss microscope (Carl Zeiss, Germany). Digital images were captured under fixed parameters with an AxioCam HRc digital camera (Carl Zeiss, Germany).

2.6.2 Confocal microscope

Cellular localization of the protein was investigated using a confocal microscope (Leica TCS SP5 X, Leica Microsystems). Digital images were captured under fixed parameters with a digital camera (Leica TCS SP5 X).

2.6.3 Immunofluorescence

A grading system reported previously [82, 182] was used to evaluate the expression of each molecule. The immunofluorescence intensity of the proteins was semi-quantified by giving grade from 0-3 (0: no expression; 1: faint expression; 2: moderate but focal expression; and 3: generalized and intense expression. Sections were digitally photographed using each filter and then merged to allow visualization of dual staining (Carl Zeiss, Germany).

Preparation

Fixatives

Phosphate buffer stock

- dissolve 26.20 g $NaH_2PO_4.H_2O$ and 143.65 g $Na_2HPO_4.2H_2O$ in 5 L distilled water
- adjust pH to 7.45

Phosphate buffered saline (PBS)

PBS stock

- dissolve 1052 g NaCl in 3.250 L distilled water whilst stirring
- add 165.6 g $NaH_2PO_4.H_2O$
- once solution is clear, adjust pH to 6.33 using 5 M NaOH

PBS working solution (0.01 M)

- dilute 660 mL of PBS stock in 20 L distilled water
- adjust pH to 7.45

Chapter 3

Angiographic, haemodynamic and histological changes in an animal model of AVM treated with Gamma Knife radiosurgery

3.1 Abstract

Object: Brain arteriovenous malformations (AVMs) are a major cause of stroke. Many AVMs are effectively obliterated by stereotactic radiosurgery, but treatment of lesions larger than 3 cm is not as effective. Understanding the responses to radiosurgery may lead to new biological enhancements to this treatment modality. The aim of the present study was to investigate the hemodynamic, morphological and histological effects of Gamma Knife radiosurgery (GKS) in an animal model of brain AVM.

Methods: An arteriovenous fistula was created by anastomosing the left external jugular vein to the side of the common carotid artery in 64 male Sprague-Dawley rats (345 ± 8.8 g). Six weeks after AVM creation, 32 rats were treated with a single dose of GKS (20 Gy); 32 animals had sham irradiation. Eight irradiated and eight control animals were studied at 1, 3, 6 and 12 weeks for haemodynamic, morphological and histological characterization.

Results: Two AVMs had partial angiographic obliteration at 6 weeks. Angiography revealed complete obliteration in three irradiated rats at 12 weeks. Ipsilateral proximal carotid artery ($P<0.001$) and arterialized jugular vein ($P<0.05$) blood flow was significantly lower in the irradiated group than in the control group. The arterialized vein external diameter was significantly smaller in Gamma Knife-treated animals at 6 weeks ($P<0.05$) and 12 weeks ($P<0.001$). Histological changes included subendothelial cellular proliferation and luminal narrowing in irradiated animals. Neither luminal obliteration nor thrombus formation was identified at any of the time points in either irradiated or non-irradiated animals.

Conclusions: GKS produced morphological, angiographic and histological changes in the model of AVM as early as 6 weeks. These results support the use of this model for studying methods to enhance radiation response in AVMs.

3.2 Introduction

Brain arteriovenous malformation (AVMs) are a major cause of stroke in children and young adults. Surgical excision of an AVM offers immediate protection from haemorrhage and is suitable for small and superficial lesions. Approximately 70% of small AVMs (< 3 cm diameter) are completely obliterated by 2 – 3 years after Gamma Knife surgery (GKS) [606-608]. However, patients treated with GKS remain at risk of suffering hemorrhage during the latent period before AVM occlusion [609, 610]. A large number of patients who have large and/or deeply located AVMs are not treatable using current methods [609]. An improved method of treating AVMs is required for these patients.

One potential new treatment is to induce thrombosis in the AVM vessels using molecular techniques targeting endothelial changes induced by radiosurgery. Development of such a treatment requires an animal model that mimics the characteristics of human AVMs. An animal model has been developed that shares hemodynamic, structural, and molecular characteristics with human AVMs [72, 77]. However, the effects of GKS in this model have not been studied. The aim of this study was to investigate the morphological, haemodynamic and histological changes in the animal mode of AVM treated with GKS.

3.3 Materials and methods

3.3.1 Surgical fistula formation

All studies were approved by the Animal Care and Ethics Committee at Macquarie University (ACEC reference number 2011/011). Animal experimentation was performed in accordance with ACEC guidelines and the Australian Code of Practice for the Care and Use of Animals for Scientific Purposes, (ACEC reference numbers 2011/011).

The AVM model was created in 64 male Sprague-Dawley rats (345 ± 8.8 g). Creation of the AVM animal model was described previously [611]. Briefly, rats were anaesthetised by Isoflurane inhalation. The left common carotid artery (LCCA) and external jugular vein (LEJV) were exposed under an operating microscope (Carl Zeiss, Germany). The LEJV was ligated at its junction with the subclavian vein with 10-0 monofilament nylon suture (Ethicon, Ohio, USA). Mobilisation of the LEJV was achieved by coagulation of no more than two side branches with care taken not to injure the LEJV. The end of the LEJV was anastomosed to the side of the LCCA with continuous 10-0 monofilament nylon suture (Ethicon, Ohio, USA). A monofilament Vicryl suture (4-0) (Ethicon, Ohio, USA) was used to close the wound in a single layer.

3.3.2 Gamma Knife radiosurgery

Thirty-two male rats were treated with the Leksell Perfexion (Elekta Inc, Stockholm, Sweden) six weeks after AVM creation. The animals were sedated using ketamine (75 mg/kg) and medetomidine (0.5 mg/kg). Adequate anaesthesia was determined by the hind limb pinch test. Animals were then placed in the supine position in a specially designed frame (SC Medical Biomedical Engineering, Australia). An axial full body CT scan with 3D reconstruction was performed for AVM localisation **(Figure 3-1)**. The model AVM nidus was then treated with GKS with a marginal dose of 20 Gy. The non-irradiated animals had AVMs created but did not receive any radiation

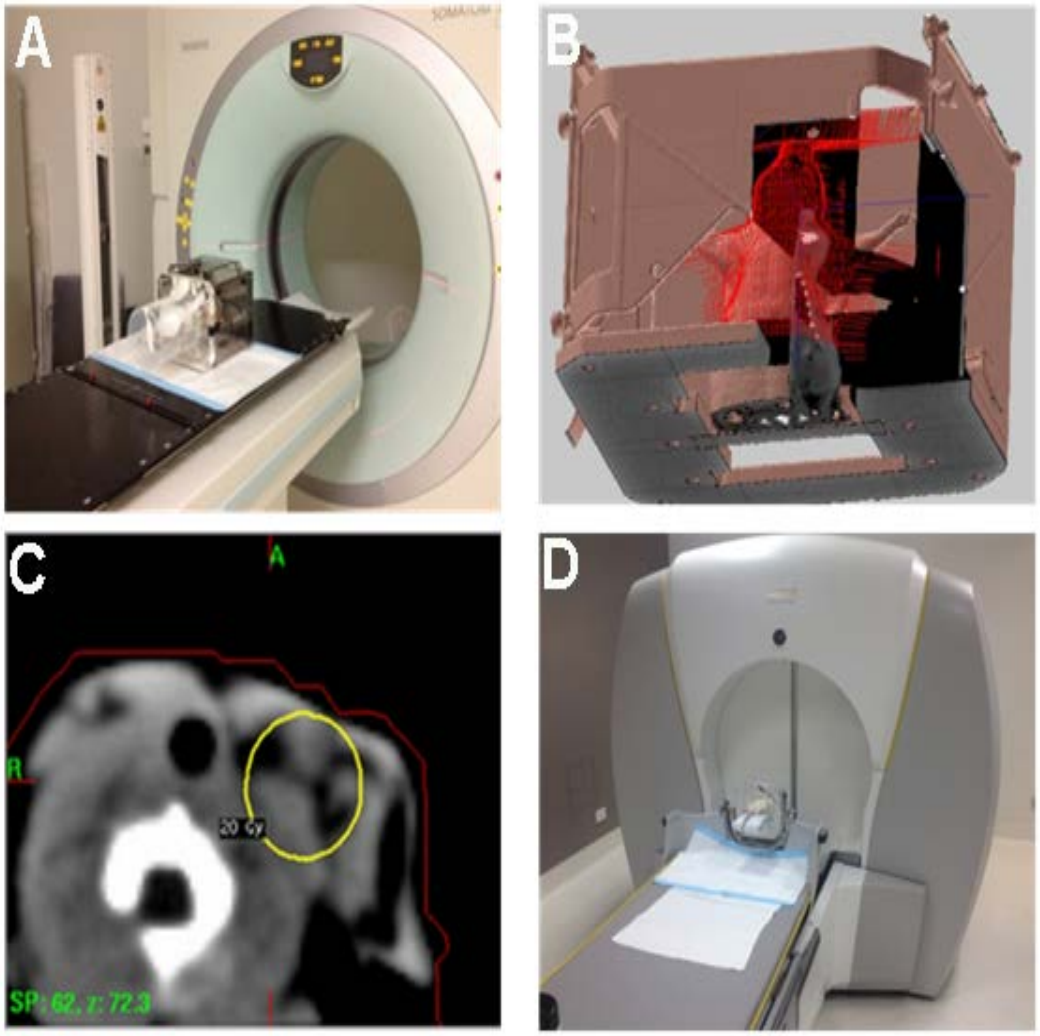

Figure 3-1. GKS planning and treatment.

A: each rat is placed in a frame and a CT scan is performed of the whole body. B: three-dimensional reconstruction demonstrating the position of the animal in the frame. C: Axial CT of the rat showing the marginal dose to the AVM nidus. D: Anaesthetised animal on frame about to enter the Gamma Knife for treatment.

3.3.3 Angiography

Eight control and eight GKS-treated animals were studied at each time point (1, 3, 6, and 12 weeks). Angiography was performed immediately prior to sacrifice. Animals were placed under general anaesthesia using 2 – 3% Isoflurane in oxygen. Under the operating microscope, the left femoral artery was exposed. A 0.8 mm Progreat microcatheter (TERUMO, Australia) was advanced through a small arteriotomy under fluoroscopic C-arm (GE Healthcare, Australia) control up to the LCCA. An arterial-phase antero-posterior angiogram was obtained by manual injection of 1 mL/kg contrast medium (Meglumine Iothalamate, 60% w/v Covidien Pty Ltd, Australia) over 3 s. The catheter was withdrawn and the femoral artery was ligated after completion of angiography.

3.3.4 Arterialised vein diameter

Each fistula was exposed after completion of angiography. A 4-0 silk suture was applied around the proximal segment of the arterialised external jugular vein to measure the circumference and calculate the diameter (circumference/π) **(Figure 2-5)**.

3.3.5 Haemodynamic studies

Blood flow measurements were obtained from the proximal LCCA and the LEJV using a Doppler flowmeter. Peri-vascular flow probes (Transonic Systems, Australia) were selected to match the size of the vessel in which flow was being measured. Probes were connected to a transit time perivascular flow meter (TS420, Transonic Systems, Australia). The average of a 10 min recording was used to determine the blood flow. Measurements of blood pressure were performed simultaneously in the left femoral artery (for mean systemic arterial pressure). A 0.58 mm polyethylene catheter was inserted into the vessel and pressure measured with a blood pressure transducer (Edwards Lifesciences, CA, USA). Flow and

pressure data were acquired through a data acquisition system for off-line analysis (CED Limited, UK).

3.3.6 Histological study

Eight irradiated and eight control animals were studied at 1, 3, 6 and 12 weeks following GKS for histological characterization. Histological sections were obtained from different parts of the AVM, including the LCCA, LEJV and the nidus. Animals were sacrificed by trans-cardiac perfusion of phosphate buffered saline. Different parts of the fistula were collected and embedded in freezing medium (ProSciTeck, Australia) and frozen in liquid nitrogen. The tissues were sectioned with a thickness of 10 micron and stained with haematoxylin and eosin or Shikata Orcein, or immunostained for vWF for endothelial staining.

3.3.7 Light microscope and data and statistical analysis

Microscopy was performed using a Zeiss microscope (Carl Zeiss, Germany). Digital images were captured under fixed parameters with an AxioCam HRc digital camera (Carl Zeiss, Germany). Image J was used to measure the diameters of the proximal and distal parts of the LEJV and proximal part of the LCCA. Blood flow analysis was performed using Spike (CED Limited, UK). All data are presented as mean ± SD. Statistical analysis was performed by 2-way analysis of variance (ANOVA). A P value < 0.05 was considered statistically significant.

3.4 Results

3.4.1 Angiography

The fistula was patent in all control animals. In the GKS treated group, two animals had partial obliteration at six weeks and three animals had complete obliteration at 12 weeks **(Figure 3-2)**. At the one week and three week time points, there were no significant differences between the control and treated groups in proximal and distal LEJV and LCCA diameters (Figure 3). Two rats had partial angiographic changes at 6 weeks and three rats had complete obliteration at 12 weeks, with statistically significant differences in proximal and distal LEJV diameters between the treatment group and the control group ($P < 0.05$) **(Figure 3-3)**.

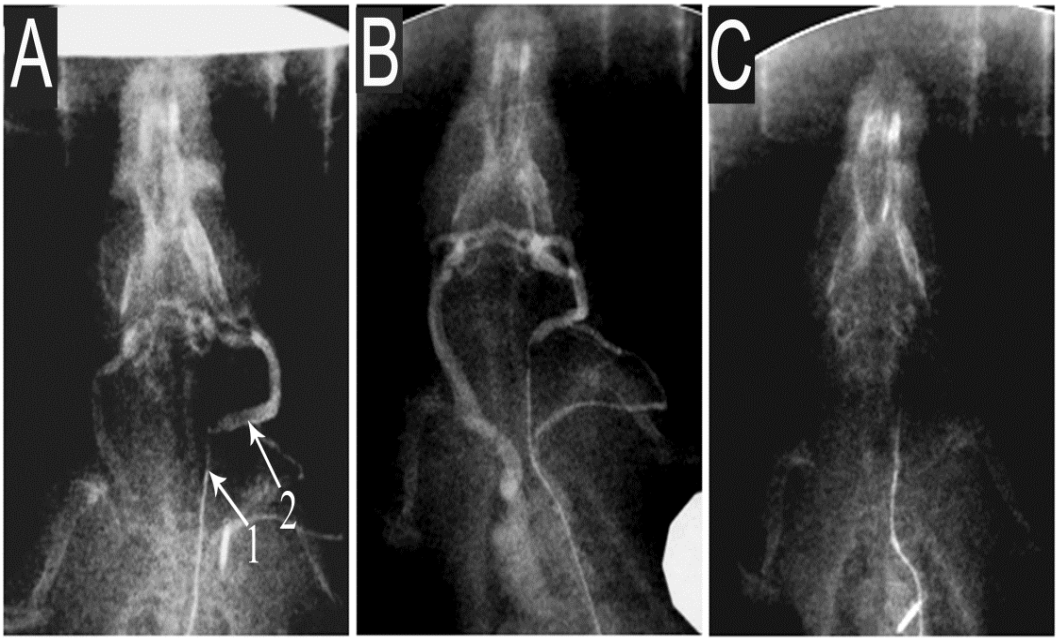

Figure 3-2. Angiography of the AVM model at 12 weeks.

A: Control animal. The fistula is patent and the jugular vein is enlarged. B: Animal treated with Gamma Knife radiosurgery. The fistula is patent but the jugular vein is narrowed. C: Animal treated with Gamma Knife radiosurgery. The fistula is occluded. 1: LCCA, 2: LEJV.

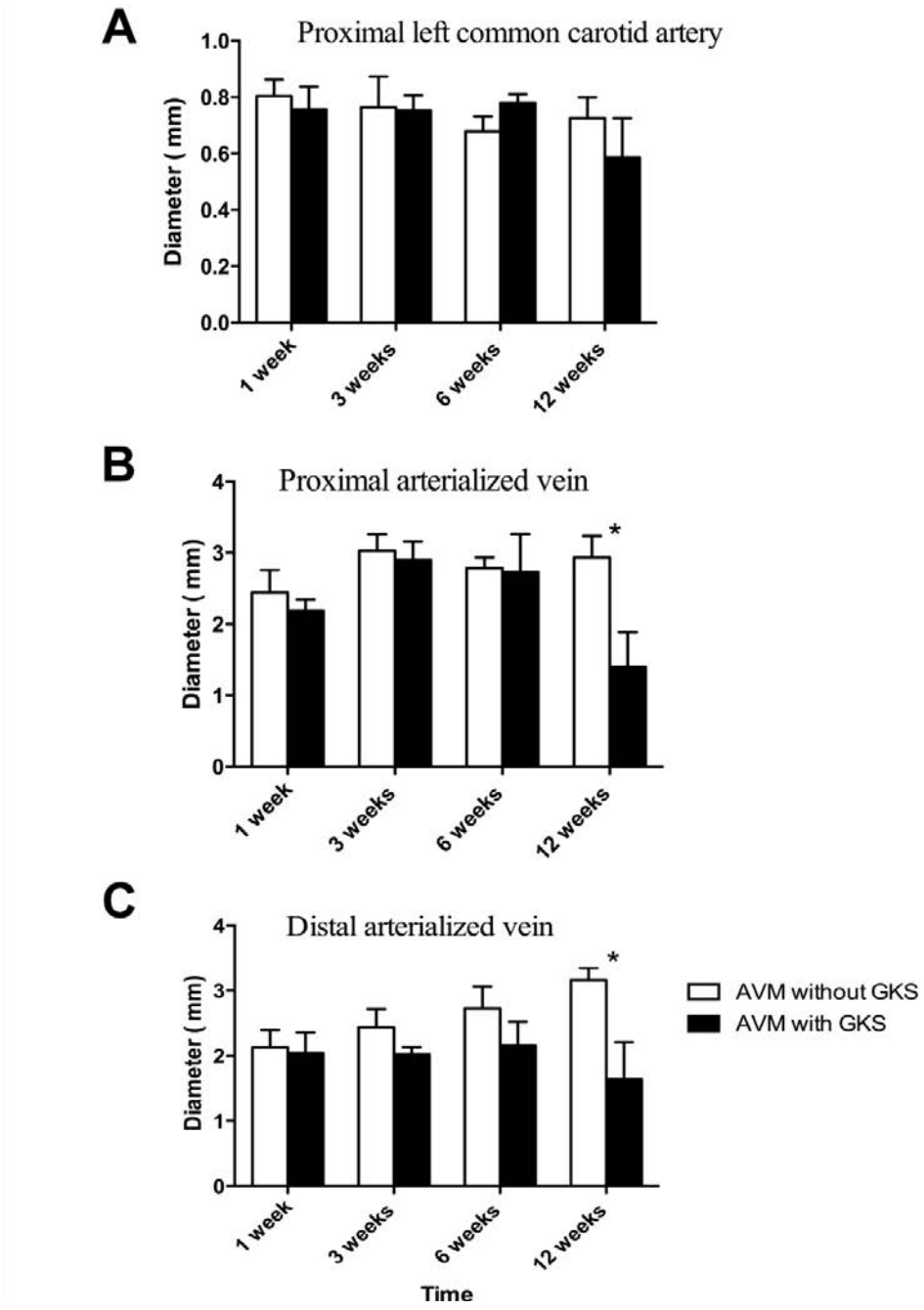

Figure 3-3. Angiographically-measured vessel diameters in control and irradiated animals.

(A) Proximal left carotid internal diameter ($P > 0.05$), (B) Proximal arterialised vein internal diameter ($P < 0.05$), and (C) Distal arterialised vein internal diameter ($P < 0.05$).

3.4.2 Haemodynamic study

Blood flow increased with time in the control group. However, in the GKS treated group the CCA flow increased until three weeks, and then decreased or stabilised **(Figure 3-4).** The treated group had a lower flow when assessed across all time points using ANOVA ($P < 0.001$). At 12 weeks, there was a significantly lower flow rate in the LCCA in the treated group compared with the control group ($P < 0.001$). There was a significant difference in flow in the LEJV in animals in the treated group compared to the control group using ANOVA ($P < 0.05$). However, individual time point comparisons between the two groups did not show any statistically significant differences **(Figure 3-4)**.

3.4.3 Histological changes

Radiated AVMs were not significantly different from the non-irradiated controls at 1 day, 3 days, or at 1 or 3 weeks. Concentric subendothelial cell growth was identified in some irradiated AVMs at 6 weeks and 12 weeks with vessel wall thickening and luminal narrowing. Although there was angiographic obliteration in some GKS treated AVMs, Neither luminal obliteration nor thrombus formation was identified at any of the time points on the histological analysis **(Figure 3-5)**. The elastic lamina had multiple layers in both groups with no changes in either group over time **(Figure 3-6)**. The endothelial lining remained intact in both groups at all time points **(Figure 3-7).**

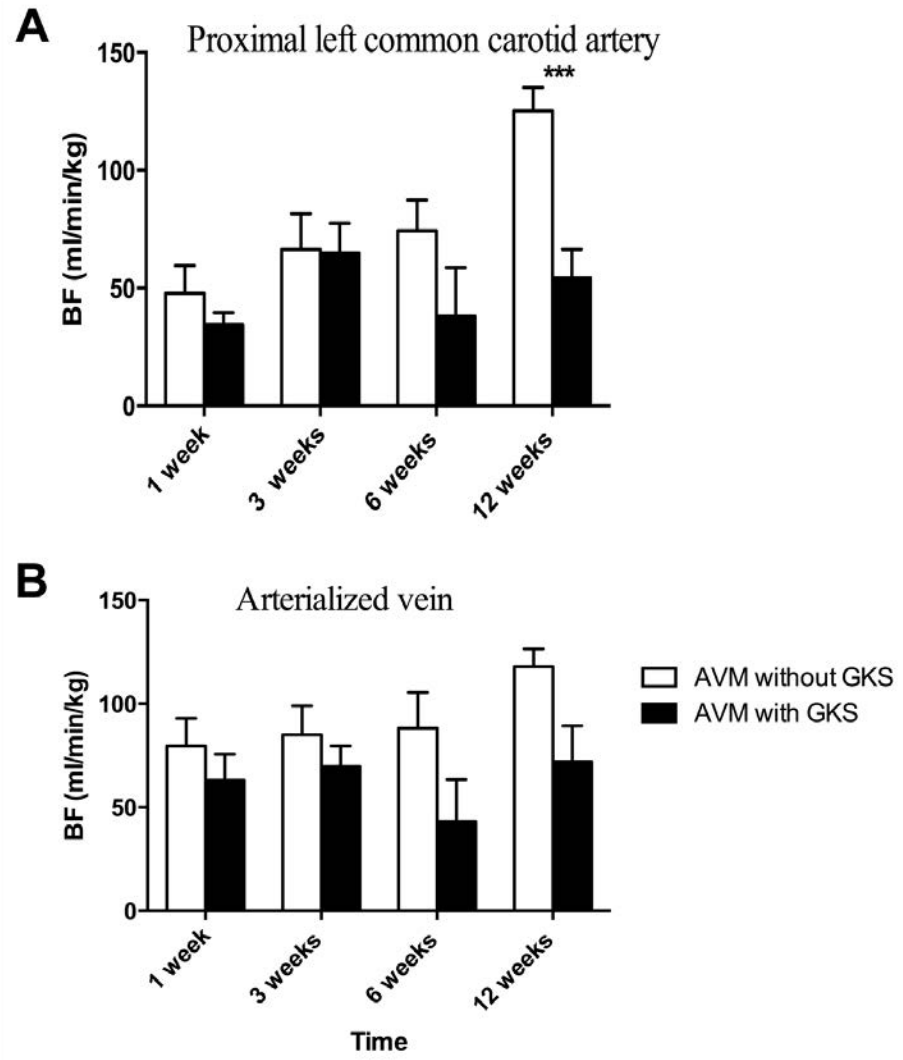

Figure 3-4. Blood flow measured with Doppler flowmeter.

(A) Proximal left common carotid artery flow. The flow was significantly lower in the treated group at 12 weeks ($P < 0.001$) and (B) flow in the left jugular vein. The treated group had a lower flow than the control group (ANOVA, $P < 0.05$).

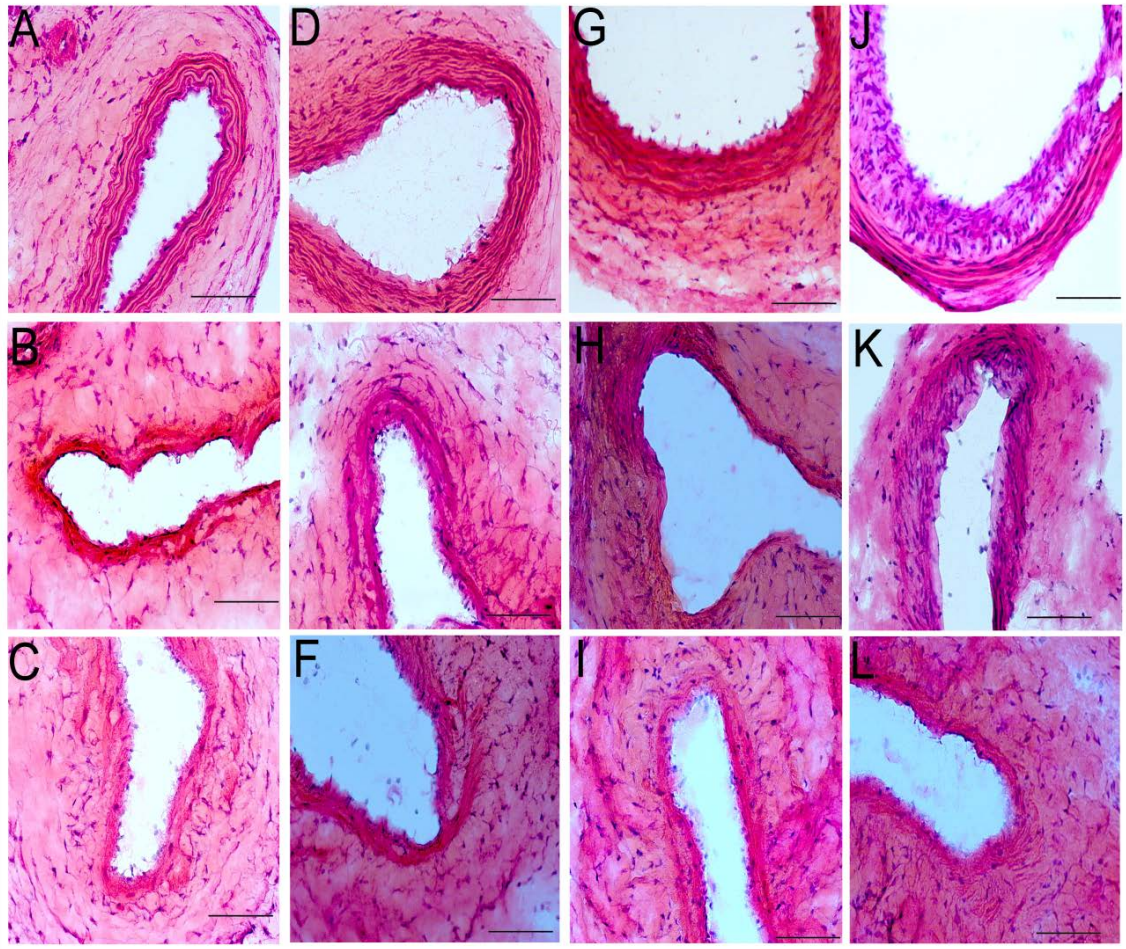

Figure 3-5. Histological study of model AVM.

(A) Non-irradiated animals, 12 weeks time point (A, D, G and J: LCCA. B, E, H and K: LEJV. C, F, I and L: nidus), (B) Irradiated animals, 12 weeks time point (A, D, G and J: LCCA. B, E, H and K: LEJV. C, F, L and I: nidus), (H and E; original magnification ✕ 20) (Scale bar: 200 μm).

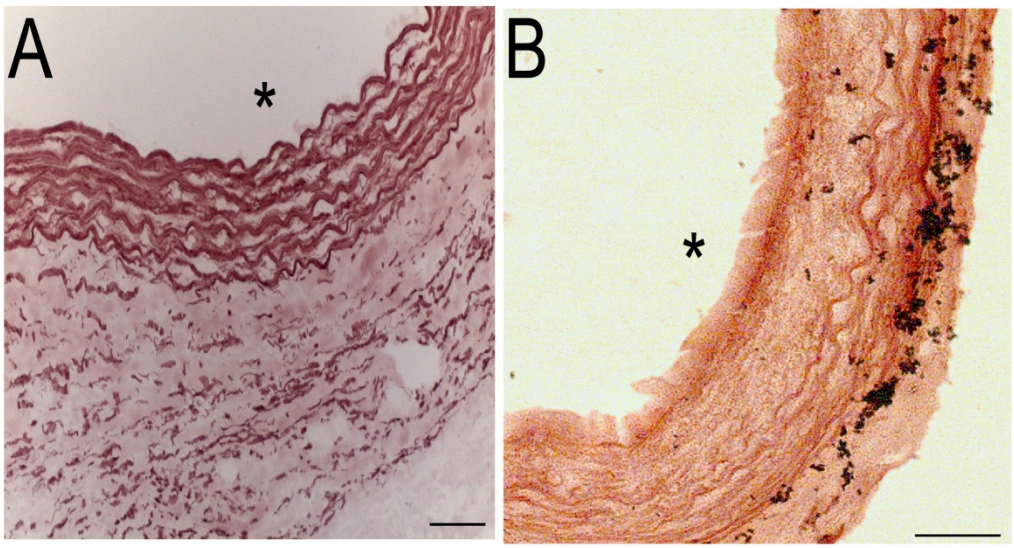

Figure 3-6. Left common carotid artery stained for elastin with Shikata Orcein.

(A) Control animal and (B) GKS-irradiated animal at 12 weeks. (Shikata Orcine stain, original magnification × 20) (Scale bar: 200 μm).

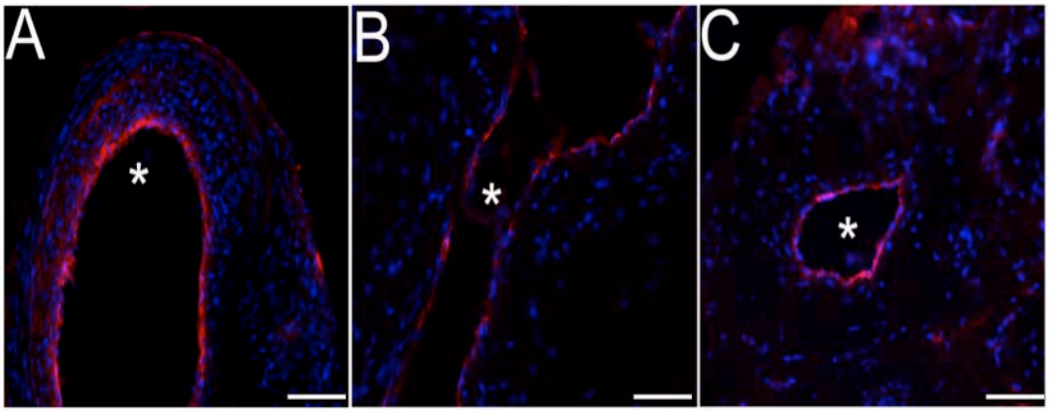

Figure 3-7. Endothelial staining for vWF.

vWF: red and DAPI: blue in an irradiated animal at 12 weeks. (A) Left common carotid artery, (B) arterialised jugular vein and (C) nidus. (* = lumen) (Scale bar: 200 μm).

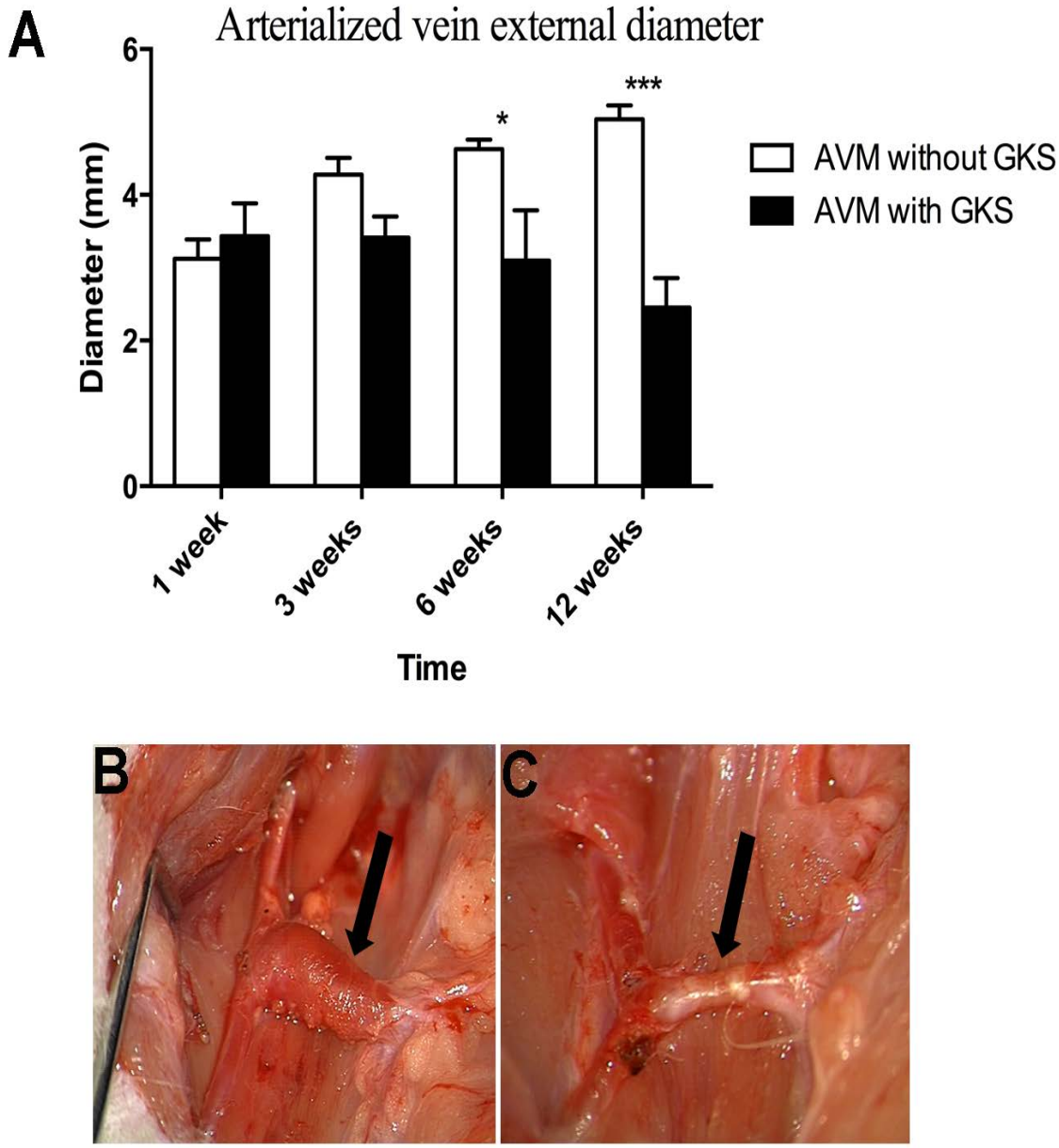

Figure 3-8. External diameter of the arterialised vein.

(A) Time-dependent external diameter changes of irradiated and non-irradiated animals, (B) Non- irradiated AVM model and (C) irradiated AVM showing narrowing of the external diameter of the jugular vein and whitish fibrinous material in the vessel wall. The vein diameter change was significantly smaller in the irradiated group at 6 weeks ($P < 0.05$) and at 12 weeks ($P < 0.001$) *Arrows: arterialised vein.*

3.4.4 Arterialised vein diameter and morphology

The LEJV external diameter was significantly smaller in the treated animals compared to the control group at 6 ($P < 0.05$) and 12 weeks ($P < 0.001$) **(Figure 3-8)**. Whitish fibrinous material was seen in the wall of the LEJV in the majority of treated animals; this was not seen in the control animals. Perivascular fibrous adhesions were seen in most of the treated animals at 6 weeks and 12 weeks. Hematoma was also seen in tissue around treated AVMs at 1 week and 3 weeks.

3.5 Discussion

Animal models of human AVMs are needed for a variety of reasons. Biological models can contribute to the understanding of AVM pathogenesis and rupture [72, 105]. They could also be used to study the effects of radiosurgery, since the mechanism of action of this treatment method is not well understood [612]. Models in large animals can be used to develop endovascular treatments and train operators in their use. Our need for an animal model is driven by our desire to develop a new molecular treatment for these lesions, many of which cannot be treated safely or effectively with current methods [125, 613-615].

The overall goal of our research is to develop a new treatment of AVMs that involves rapid stimulation of thrombosis within the abnormal vessels. Our proposal is that pro-thrombotic agents could be administered systemically, but accumulates selectively within AVM vessels by attaching them to antibodies (or other specific binding molecules) that target endothelial surface molecules that are expressed in the AVM vessels and not in normal vessels. As a powerful inducer of endothelial molecular change [183, 616] and with its precise spatial localisation, we suggest that radiosurgery be used as a first step in this treatment to stimulate discriminating endothelial molecular changes within only AVM vessels. The successful development of this treatment relies on an animal model that mimics the structural, haemodynamic, and molecular characteristics of human AVMs, and can be treated with radiosurgery. Endothelial phenotype varies widely depending on the organ of origin, and

AVM endothelium is also different to normal cerebral endothelium in its molecular characteristics [78, 182]. The response of endothelium to radiation may vary with different phenotypes, so it is essential that our research developing a molecular treatment targeting radiation-induced endothelial changes be done using a model that mimics the human AVM phenotype and its response to radiation.

The animal model used here has been shown previously to mimic human AVMs in its structural, haemodynamic, angiographic, and molecular characteristics [72]. We also developed a method to treat the model AVM with LINAC radiosurgery and studied adhesion molecule changes after radiation [616]. The feasibility of the proposed thrombotic treatment was demonstrated using LINAC as the radiosurgery priming method [198, 617]. We now have access to GKS and the facility to use 3D CT scan planning for each rat that is treated. Our intention is to continue this research using GKS rather than LINAC. However, the responses of the AVM model to GKS are not necessarily the same as to LINAC and a detailed study of responses to GKS was required before trialling new molecular treatments.

The change to GKS involved the development of a new frame and individual planning of the treatment based on 3D CT scans. The carotid artery and the arterialised jugular vein are readily identified on the non-contrast CT scans and treatment planning is relatively straightforward **(Figure 3-1)**.

GKS resulted in angiographic, haemodynamic, and structural changes that were evident by 6 weeks after treatment. Angiography revealed narrowing or occlusion of the arterialised vein in animals at 6 and 12 weeks, although complete occlusion of the vein was not confirmed histologically. Blood flow was lower at 6 weeks and 12 weeks in the GKS-treated animals. The diameter of the arterialised vein was also smaller in the later time points. Vessel wall thickening, perivascular fibrosis, and subendothelial cellular proliferation were observed at 6 and 12 weeks.

There have been very few studies of radiosurgery in animal models of AVM. De Salles et al. used LINAC doses from 20 – 90 Gy to treat the rete mirabilis in pigs. They found no angiographic changes by 2 months and substantial reductions in vascularity only with doses

of 50 Gy or more [110]. They reported histological effects similar to those reported here, with intimal proliferation that correlated with the dose of radiation. Reports of the effect of radiosurgery on normal vessels include a study of GKS on cat basilar artery [618] and rat anterior cerebral artery [619]. Findings included intimal proliferation, but no vessel occlusion except for one rat anterior cerebral artery 20 months after treatment with 100 Gy.

The morphological changes in our treated animals were similar to the reported effects of radiosurgery in human AVMs, which have shown perivascular fibrosis, subendothelial proliferation, and luminal narrowing [178, 181, 620]. Although it is not possible to perform a detailed study of the short-term effects of GKS in human AVMs, it seems reasonable to infer that the effects in our model simulate the processes occurring in human AVMs.

Development of a successful prothrombotic treatment strategy for AVMs will depend on identification of a highly discriminating endothelial surface marker in AVMs treated with radiosurgery. We are currently using the model described here, treated with GKS, in a search for the most prospective targets.

3.6 Conclusion

This study examined the haemodynamic and structural responses of the animal model to GKS treatment at different time points. This model may be suitable for further study seeking to identify highly discriminating endothelial molecular changes after radiosurgery that could be used as targets in prothrombotic molecular treatments.

Chapter 4

Gamma knife radiation injury in animal model of arteriovenous malformation leads to differential regulation of vascular endothelial cell adhesion molecules

4.1 Abstract

Introduction: Brain arteriovenous malformations (AVMs) are a major cause of stroke in children and young adults. Molecular targeting is a promising future therapy for large and deep AVMs, which cannot be treated with conventional therapy. Previous studies on irradiated human AVM endothelial tissue has shown that endothelial adhesion molecules such as intercellular adhesion molecule-1 (ICAM-1) were upregulated when compared with non-irradiated AVM and normal endothelial cells. The aim of this study was to investigate the changes in expression of ICAM-1 and platelet endothelial cell adhesion molecule-1 (PECAM-1) in an experimental model of AVM of rats after Gamma Knife irradiation.

Methods: Fifty male Sprague-Dawley rats (345 ± 8.8 g) were used for this study. The AVM Model was created by anastomosing the rostral part of the left external jugular vein to the left common carotid artery. The model nidus of thirty rats received a single dose of radiosurgery (20 Gy) using Gamma Knife six weeks after AVM creation. The rest of the rats were sham-irradiated animals. Animals were sacrificed at 1, 3 days and 1, 3, 6 and 12 weeks. Frozen sections were used for immunohistochemical analysis.

Results: ICAM-1 was significantly upregulated through all the time points in the irradiated AVM compared to the non-irradiated AVM. There were no significant changes when we compared the irradiated AVMs across different time points over a period of 12 weeks. The expression was observed to be similar in all examined regions of the AVM. When comparing the expression of ICAM-1 in the irradiated AVM to the contralateral jugular vein, inferior vena cava and abdominal aorta, the AVM specimen was significantly higher in GKS-treated AVM ($P < 0.05$). Confocal analysis indicated that the upregulation of ICAM-1 was primarily

confined to the endothelial cell surface. No significant differences in PECAM-1 expression between the irradiated and non-irradiated tissues were observed.

Conclusion: This study demonstrates that ICAM-1 is significantly upregulated in the irradiated AVM model and that this enhanced expression is localised on the surface of endothelial cells. PECAM-1 expression is not altered significantly. These results corroborate the previous findings and highlight the possibility of ICAM-1 being used for future ligand based therapy.

4.2 Introduction

Brain arteriovenous malformation (AVM) is a common cause of haemorrhage and strokes in children and adults [621, 622]. The morbidity and mortality rate from ruptured AVMs is high [49, 623, 624]. Around 35 percent of total AVMs are high grade and 90% of these are not manageable by conventional treatments [125, 625]. Vascular targeting is emerging as an attractive strategy to enhance the response of AVMs to radiosurgery and produce targeted thrombosis. Non-ligand vascular therapy using low dose lipopolysaccharide and soluble tissue factor (LPS+TF) to accelerate thrombosis after radiosurgery in animal models has been previously documented [198]. However, systemic use of LPS in humans may not be safe [626]. Alternatively, ligand-based therapies have the potential to overcome safety concerns and can utilise a range of effector molecules to alter vascular endothelial function as well as induce localised thrombosis. Developing a ligand based vascular targeting therapy for brain AVMs requires identification and detailed characterisation of specific endothelial cell surface molecules that distinguish AVMs from the normal vessels. Unlike the tumour vascular targeting therapies in practice, endothelial cells of AVMs do not appear to have a specific constitutive marker that distinguishes them from the endothelial cells of normal blood vessels [78, 627].

Exposing cells to drugs, stress and different types of radiation can alter proteins expression pattern. Inducing AVM endothelial cell surface molecular changes using radiosurgery might

be able to distinguish AVMs from other vessels for vascular targeting. The key to developing a successful molecular targeting treatment will be to identify the molecules that are respond on the endothelial surface after radiation and are highly discriminating from normal vessels. We have shown previously that expression of E-selectin and vascular cell adhesion molecule-1 is significantly altered after radiosurgery [182, 183, 616].

Understanding the changes in the expression pattern of other endothelial adhesion molecules such as ICAM-1 and PECAM-1 to radiosurgery treatment will be an important step forward to develop the proposed treatment. Although expression of ICAM-1 and PECAM-1 in brain AVM has been investigated [78], what happens to the relative expression of these molecules post radiation treatment is not known. In this study we have investigated the expression of ICAM-1 and PECAM-1 in an animal model of AVM and the effect of radiosurgery on their expression.

4.3 Materials and methods.

4.3.1 AVM model

All studies were approved by the Animal Care and Ethics Committee at Macquarie University. Animal experimentation was performed in accordance with the Australian Code of Practice for the Care and Use of animals for Scientific Purposes, (ACEC reference numbers 2011/011).

A model of AVM was created in 50 male Sprague-Dawley rats (345 ± 8 g). Animals were anesthetised using isoflourane inhalation as described previously in Chapter 2. An anastomosis was created surgically between the left common carotid artery LCCA and LEJV as previously described [105].

4.3.2 Gamma knife radiaosurgery

A Perfexion Leksell Gamma Knife (Elekta Inc) was used to deliver gamma radiation to each treated rat 6six weeks after creating the AVM. All radiation procedures were performed under general anaesthesia using ketamine (75 mg/kg) and medetomidin (0.5 mg/kg). Hind limb pinch was used to determine the depth of the anaesthesia. Animals were placed in a radiation frame (SC Medical biomedical engineering, Australia). The position of the created AVM nidus was confirmed using an axial neck CT scan and 3D reconstructed image. Gamma radiation (20 Gy marginal dose) was delivered to the model nidus of thirty animals (GKS Group); the other 20 animals were used as controls.

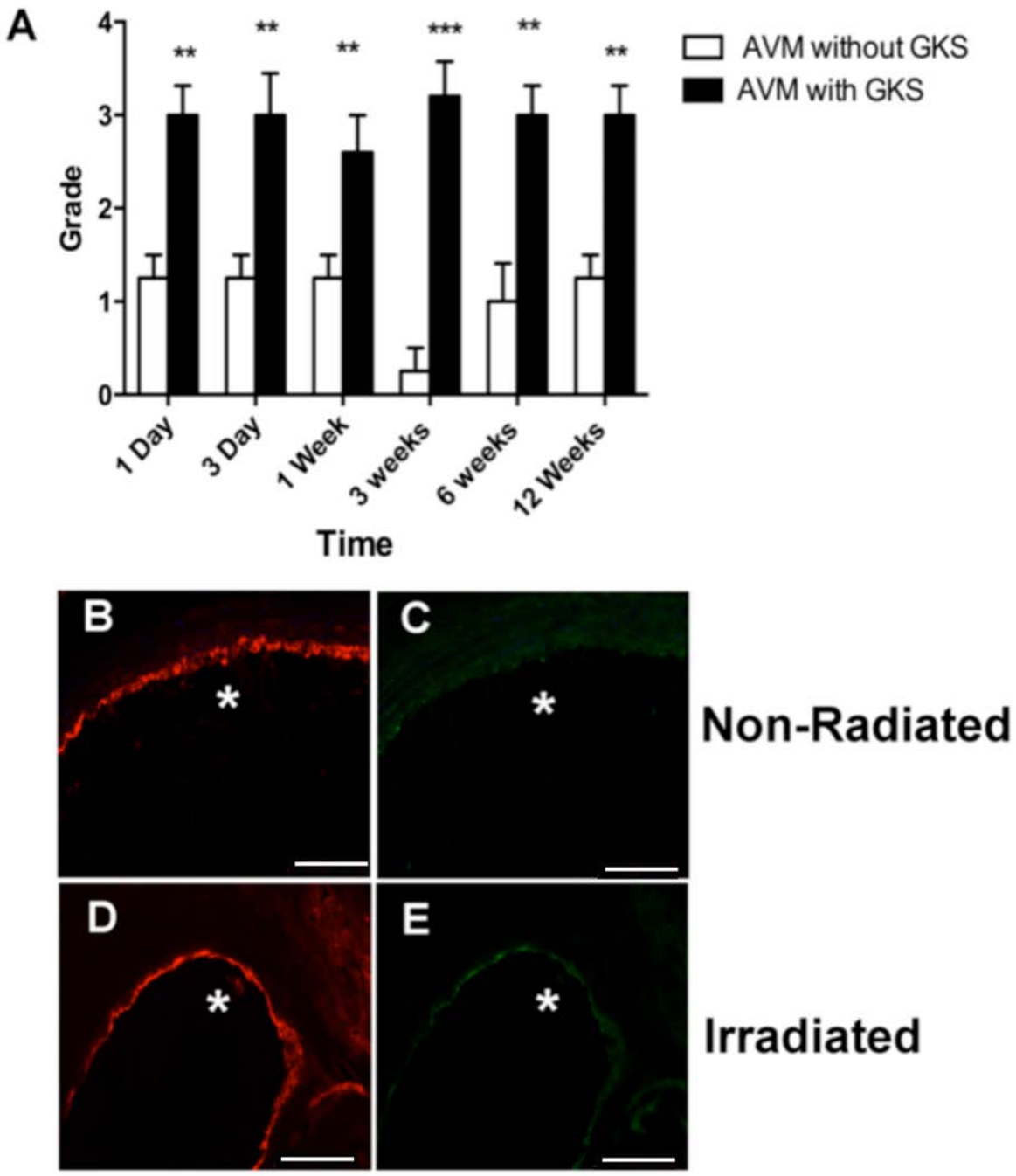

Figure 4-1 ICAM-1 expression in left carotid artery.

(A) Expression level in the GKS group compared to the control group. (B) and (D): vWF staining. (C) and (E): ICAM-1 staining in the same sections as (B) and (D). (* = lumen) (Scale bar: 200 μm).

4.3.3 Immunohistochemistry

Animals were sacrificed at 1 day, 3 days, 1week, 3 weeks, 6 weeks and 12 weeks. The model AVM was collected, embedded in freezing medium (ProSciTeck, Australia) and frozen in liquid nitrogen. The tissues were sectioned with a thickness of 18 micron and stained using immunohistochemistry protocols. The slides were left at room temperature for 24 hours, washed using PBS and permeabilised with 50% ethanol in PBS for 10 minutes. After another washing with PBS, the sections were blocked in 10% donkey serum for 1 hour at room temperature. This was followed by overnight incubation at 4ºC with anti Von Willebrand factor (vWF) rabbit polyclonal antibody (Abcam, ab6994) (dilution 1:500) and with anti ICAM-1 goat polyclonal antibody (Santa Cruze, sc-1511) (dilution 1:50). The slides were then washed and incubated with Anti-rabbit IgG-Alexa Flour 594 Molecular Probe, A21207) (dilution 1:500) and anti-goat IgG-DyLt 650 (Abcam, ab 98517, dilution 1:500) for one hour in the dark at room temperature. Slides were washed thoroughly and incubated with DAPI (Molecular Probes) for nuclear staining for 1 minute, coverslipped and cured for 48 hours before subjecting to fluorescence microscopy. A similar protocol was used for PECAM-1 except that the slides were incubated with anti PECAM-1 mouse monoclonal antibody (Abcam, ab64543, dilution 1:250) and polyclonal secondary antibody IgG-DyLt 650 (Abcam, ab98769, dilution 1:500).

4.3.4 Light microscopy

Microscopy was performed using a Zeiss microscope (Carl Zeiss, Germany). Digital images were captured under fixed parameters with an AxioCam HRc digital camera (Carl Zeiss, Germany) for intensity expression and with a confocal microscope (Leica Germany) for cellular anatomical expression to investigate the localisation of proteins.

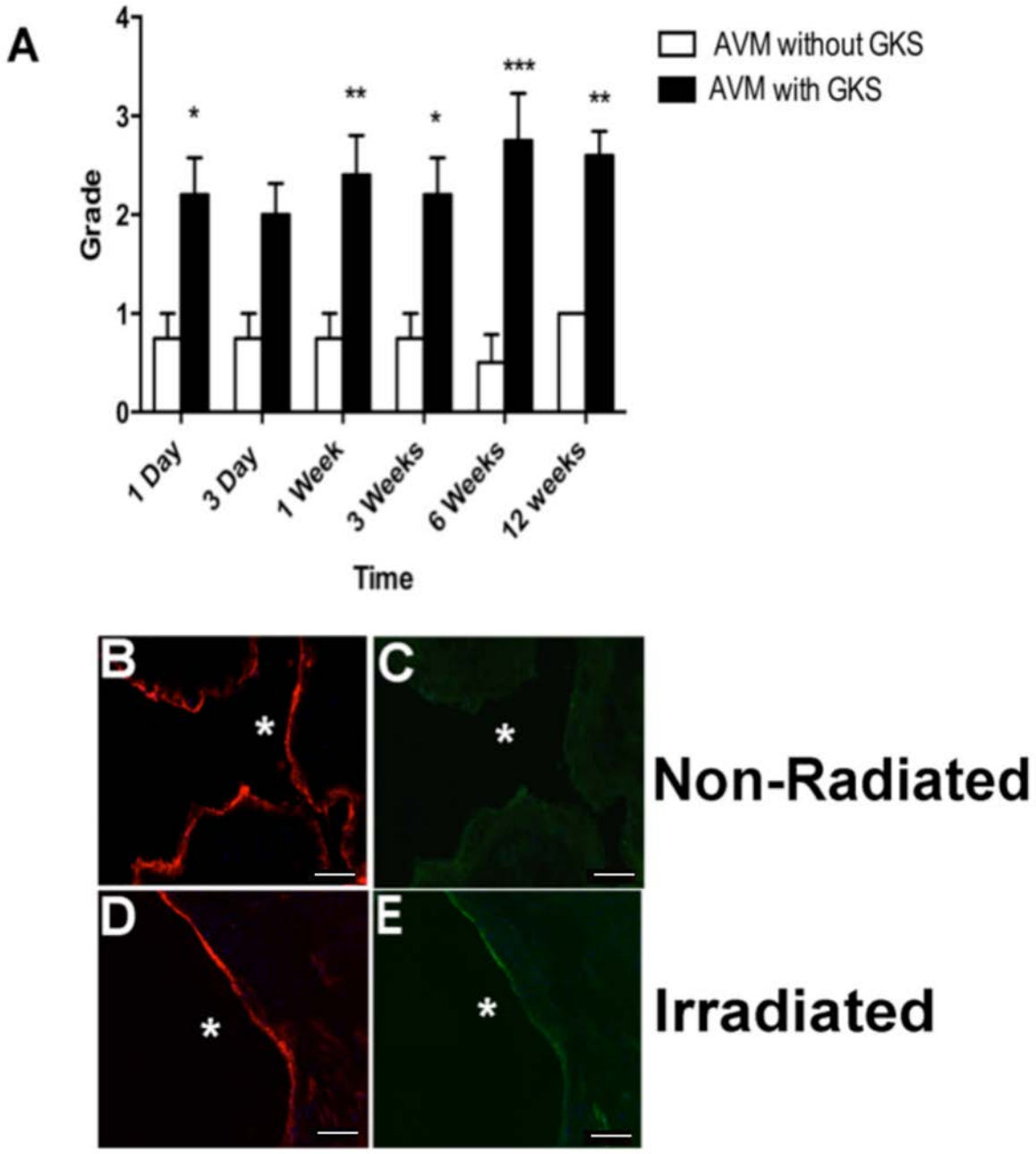

Figure 4-2 Expression of ICAM-1 in the left jugular vein.

(A) Expression in the GKS group compared to the control group. (B) and (D): vWF staining. (C) and (E): ICAM-1 staining in the same sections as (B) and (D). (* = lumen) (Scale bar: 200 μm).

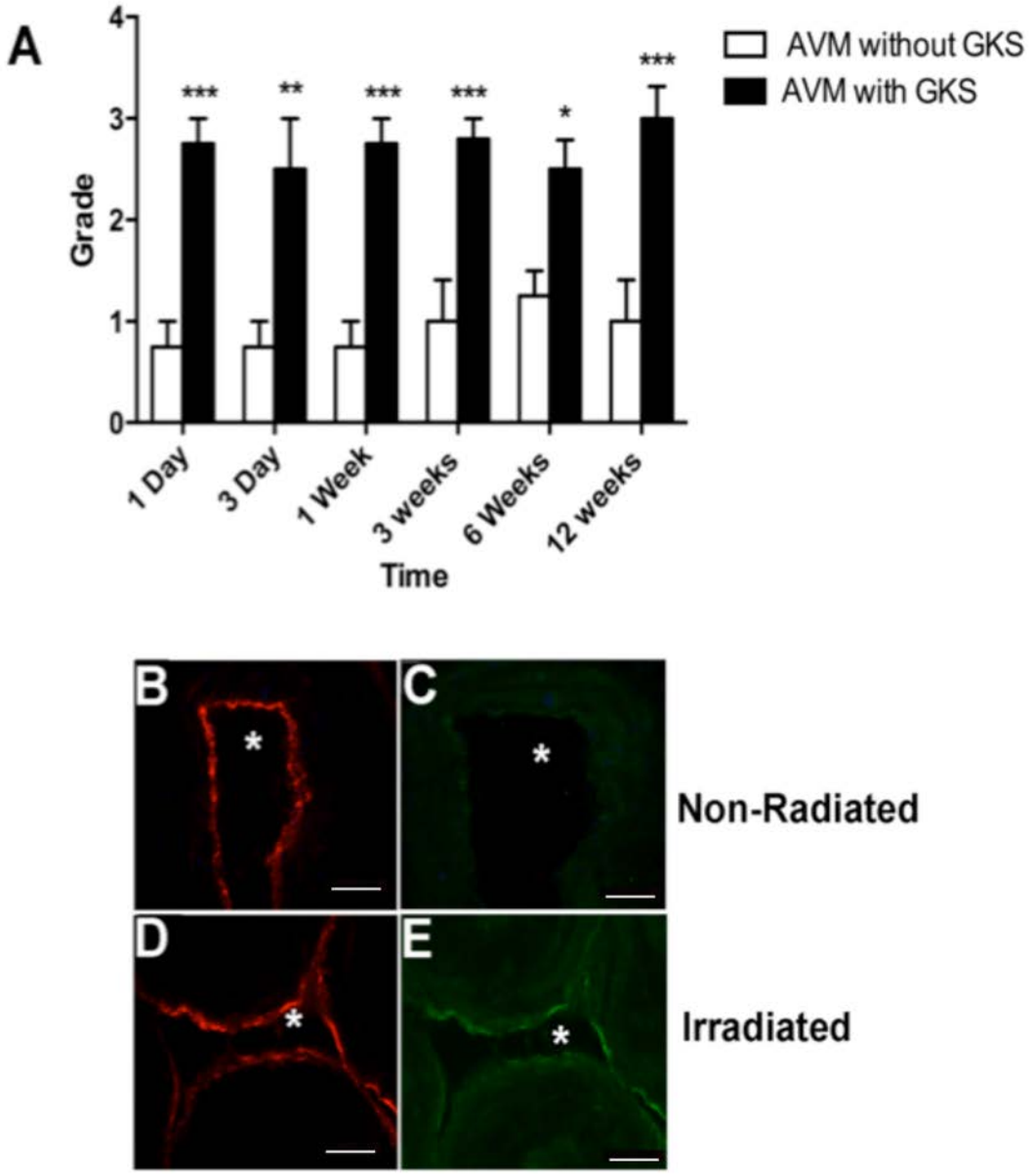

Figure 4-3 Expression of ICAM-1 in the AVM nidus.

(A) Expression in the GKS group compared to the control group. (B) and (D): vWF staining. (C) and (E): ICAM-1 staining in the same sections as (B) and (D). (* = lumen) (Scale bar: 200 μm).

4.3.5 Data and statistical analysis

All data are presented as mean ± SD. Statistical analysis was performed using Graphpad Prism by 2-way analysis of variance (ANOVA). A P value < 0.05 was considered statistically significant. Protein expression was evaluated using a grading system reported previously [82, 182].

The expression in vessels was examined according to the location in four histological layers: endothelium, subendothelium, tunica media, and tunica adventitia.

4.4 Results

Overall ICAM-1 expression was significantly increased in the GKS treated group compared to the non-irradiated group ANOVA (P < 0.001). An increase was detected starting at 1 day, persisting throughout the time points in the irradiated animals. When comparing the expression of ICAM-1 in the arterialised vein to the contralateral jugular vein, inferior vena cava and abdominal aorta, the increase was significant (P < 0.05). Expression of ICAM-1 was only in the endothelial cells; it was absent from the subendothelial and the other layers examined **(Figure 4-1, 4-2 and 4-3)**. Confocal microscopy confirmed that the expression was mainly on the endothelial cell surface **(Figure 4-4)**. In the control animals, ICAM-1 expression did not significantly change over the time points (P > 0.05).

PECAM-1 expression was unchanged in response to radiation. PECAM-1 staining was confined to the endothelial cells and was intense in the endothelial cell of the tissues examined. There was no significant difference in the expression of PECAM-1 in the GKS and control groups in the AVM or non-AVM vessels ANOVA (P > 0.05), **(Figure 4-5, 4-6 and 4-7)**.

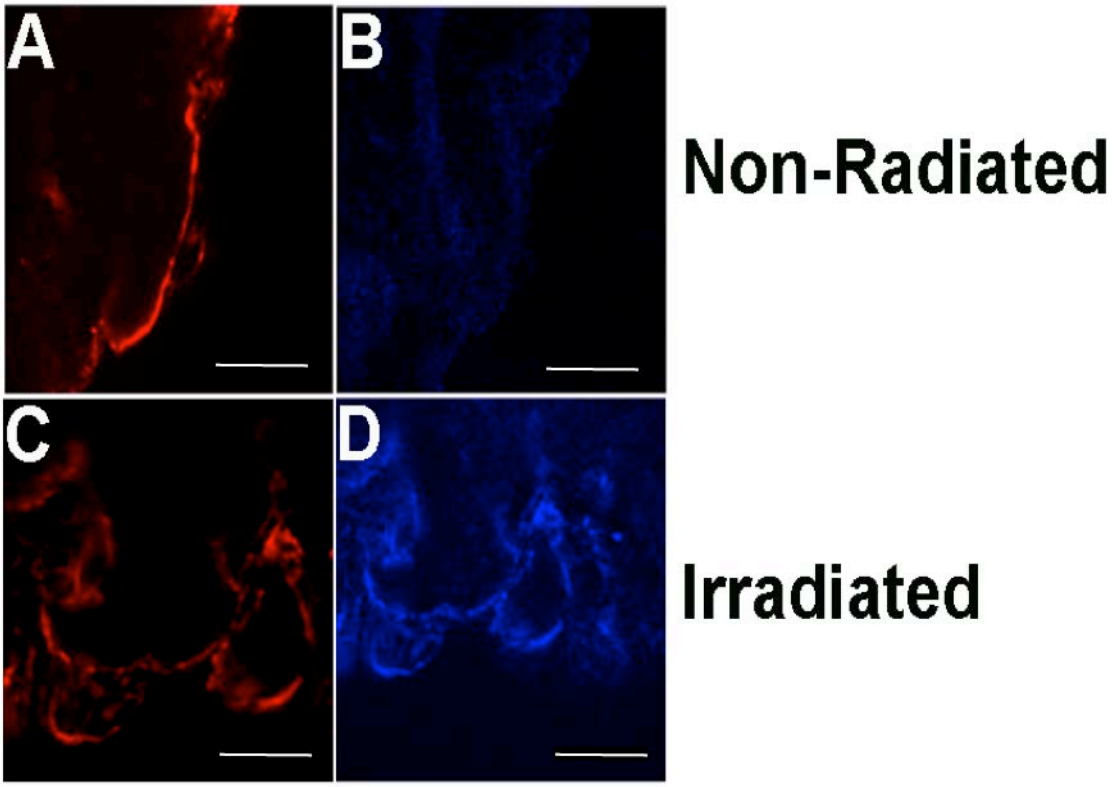

Figure 4-4 Cellular location of ICAM-1 expression.

Confocal images of individual endothelial cells of the left jugular vein. The endothelial cell surface is stained with vWF in red (A) and (C). (B) and (D): ICAM-1 staining (blue) (double labelling) (Scale bar: 5 μm).

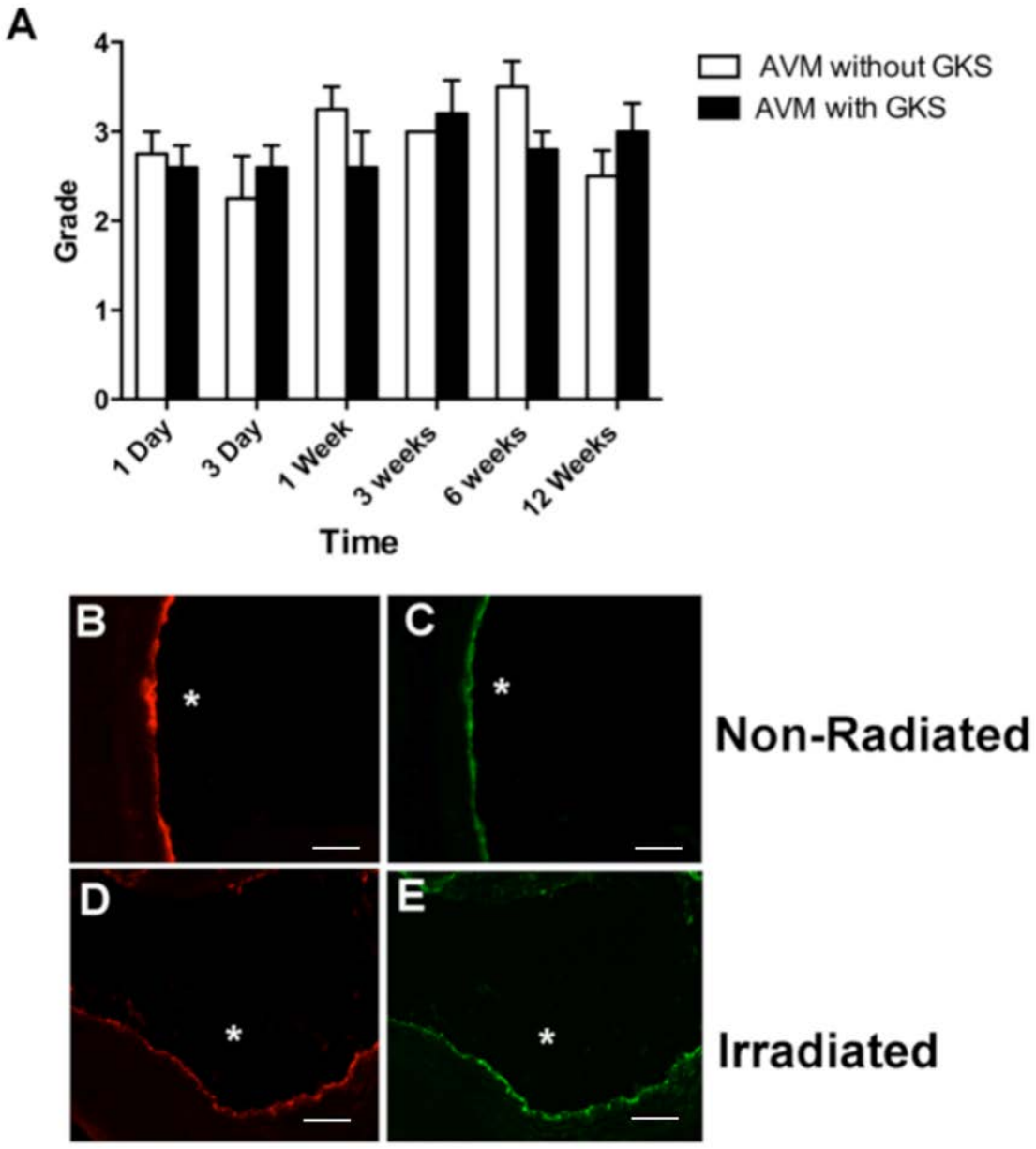

Figure 4-5 Expression of PECAM-1 in the left carotid artery.

(A) Expression in the GKS group compared to the control group. (B) and (D): vWF staining. (C) and (E): PECAM-1 staining in the same sections as (B) and (D). (* = lumen) (Scale bar: 200 μm).

4.5 Discussion

AVMs remain a problem; the pathogenesis is poorly understood and many are untreatable. Radiosurgery (RS) is a good treatment for some AVMs, but the mechanism of action is unknown [628].Understanding the molecular characteristic of AVMs and their response to RS would be beneficial for improving our understanding of AVM pathogenesis and mechanism of action of RS. However, our focus is on developing vascular targeting as a new treatment for AVM.

Application of ligand-based vascular targeting therapy to AVMs would require identification of an endothelial surface molecule that is highly expressed in AVM vessels and not in normal vessels, so that selective thrombosis is induced in only the AVM vessels. In the absence of a constitutively expressed discriminating surface molecule, we have proposed that radiosurgery be used to alter endothelial expression in the prescribed volume of the AVM, allowing the use of specific ligand targeting agents.

Adhesion molecules are highly prospective targets because they are known to have increased expression in many endothelial phenotypes in response to external stimuli including radiation. The purpose of this study was to determine whether ICAM-1 and PECAM-1 are upregulated on the EC surface in the AVM endothelial phenotype. Responses to radiation vary by phenotype, hence the need for an animal model that replicates the AVM phenotype.

This study showed an increase in ICAM-1 expression but not PECAM-1 after GKS. Our study showed that ICAM-1 is expressed on the surface of the endothelial cells of irradiated, non-irradiated tissue and non-AVM tissue. The level of the expression in non-irradiated tissue was low. We demonstrated that there is a significant upregulation of ICAM-1 in the irradiated AVM starting 24 hours after radiation and continuing up to 12 weeks after radiation. Over the time course there were no changes in the expression of ICAM-1 in the irradiated tissue. It has been reported that ICAM-1 expression is increased in irradiated cells 24 hours after radiation [391] and 7 days after radiation of cultured human bone marrow [394]. Upregulation of ICAM-1 in human umbilical cord as a response to radiation is also reported [392]. Upregulation of ICAM-1 in first few hours after radiation and returning to the baseline within

days to weeks is well documented [392]. Late upregulated of ICAM-1 on pulmonary vascular endothelium of mice 80 days after thoracic irradiation is also reported [398, 629]. Previous work on human AVMs also found an upregulation of ICAM-1 in the irradiated tissue compared with non irradiated controls [78].

Our study demonstrated that PECAM-1 is strongly expressed on the endothelial cells of all tissue examined. There was no significant upregulation in the irradiated tissue. These results are consistent with previous reports that PECAM-1 in human AVM [78] and also in cultured HUVEC at 5 or 10 Gy is not upregulated. Other studies have documented that PECAM-1 is upregulated significantly after exposure to 5 Gy [447, 448, 630].

An increase in ICAM-1 expression in irradiated AVM EC demonstrated here means that ICAM-1 is a potential target for vascular targeting therapy to accelerate thrombosis after radiosurgery. ICAM-1 expression suggests that an anti–ICAM-1 could be injected one day after radiosurgery. Even though ICAM-1 is expressed on the surface of normal endothelial and endothelial cell of AVM without radiation, the level of expression is low and we do not expect induced thrombosis to happen anywhere else except in the irradiated vessels. Studies have shown that binding of anti-ICAM-1 (aICAM-1) antibodies to ICAM-1 is dependent on the level of ICAM-1 expression on the endothelial cell [631]. Kiani et al. [324] demonstrated that the number of anti-ICAM-1 microspheres binding to HUVECs was increased after irradiation by 4.8 times compared to non irradiated cells. The number was increased by 8 and 13 times relative to controls at 24 hours and 48 hours post-irradiation within the irradiated tissue after augmentation of rate of adhesion by addition of erythrocytes to the media. This indicates that many factors play a role in ligand directed vascular targeting. Study demonstrated that a co-ligand directed against tumour endothelium VCAM-1 for example, does not cause thrombosis in other area that express VACM-1 such as heart and lung. The answer was that present antiVCAM-1 vecam-1 interaction this does not seem to be the only factor. They found that presence of externalized PS is important in may paly a role in activation of coagulation complexes [632].

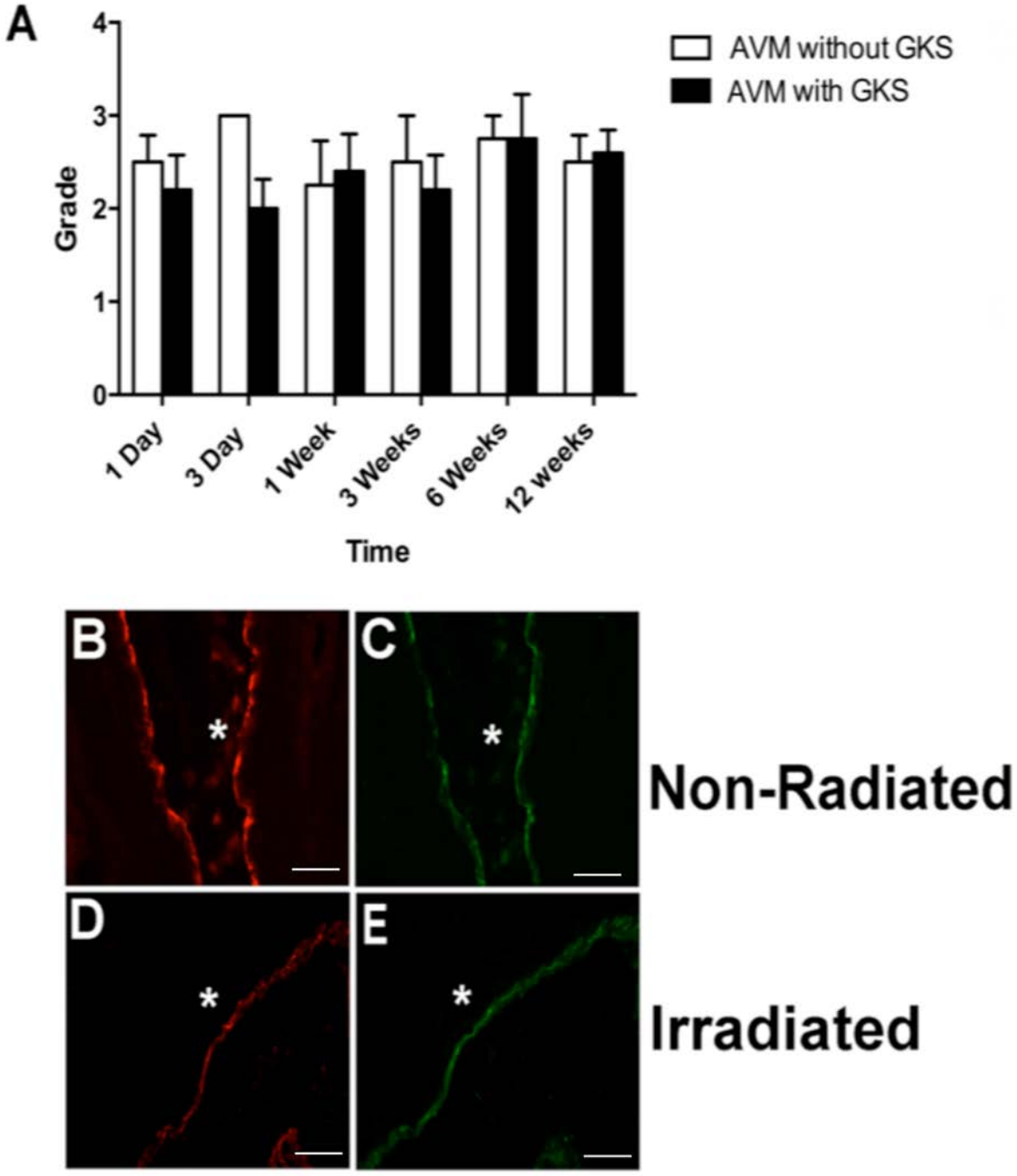

Figure 4-6 Expression of PECAM-1 in the left jugular vein.

(A) Expression in the GKS group compared to the control group. (B) and (D): vWF staining. (C) and (E): PECAM-1 staining in the same sections as (B) and (D). (* = lumen) (Scale bar: 200 μm).

ICAM-1 expression is sustained over a period of time indicating that any time between 1 day and 12 weeks may be optimum for recognition of these targets by antibodies and associated therapeutics such as beads and toxins. There is a possibility that more than one antibody dosage can be given as the ICAM-1 expression will be sustained and there is no need to irradiate the tissues again and again. Even at an extended time of 12 weeks there was no sign of decreasing ICAM-1 expression. At this dosage we did not observe any deterioration of the blood vessels either indicating it is a good strategy. When the expression comes down is not known—longer studies will be required to test this. This strategy may also help other diseases such as tumour treatments. Whether an enhanced ICAM-1 expression will lead to recruitment of inflammatory molecules and fibrosis is not known. Also it is not known how it will affect the biomechanical properties of the vessels.

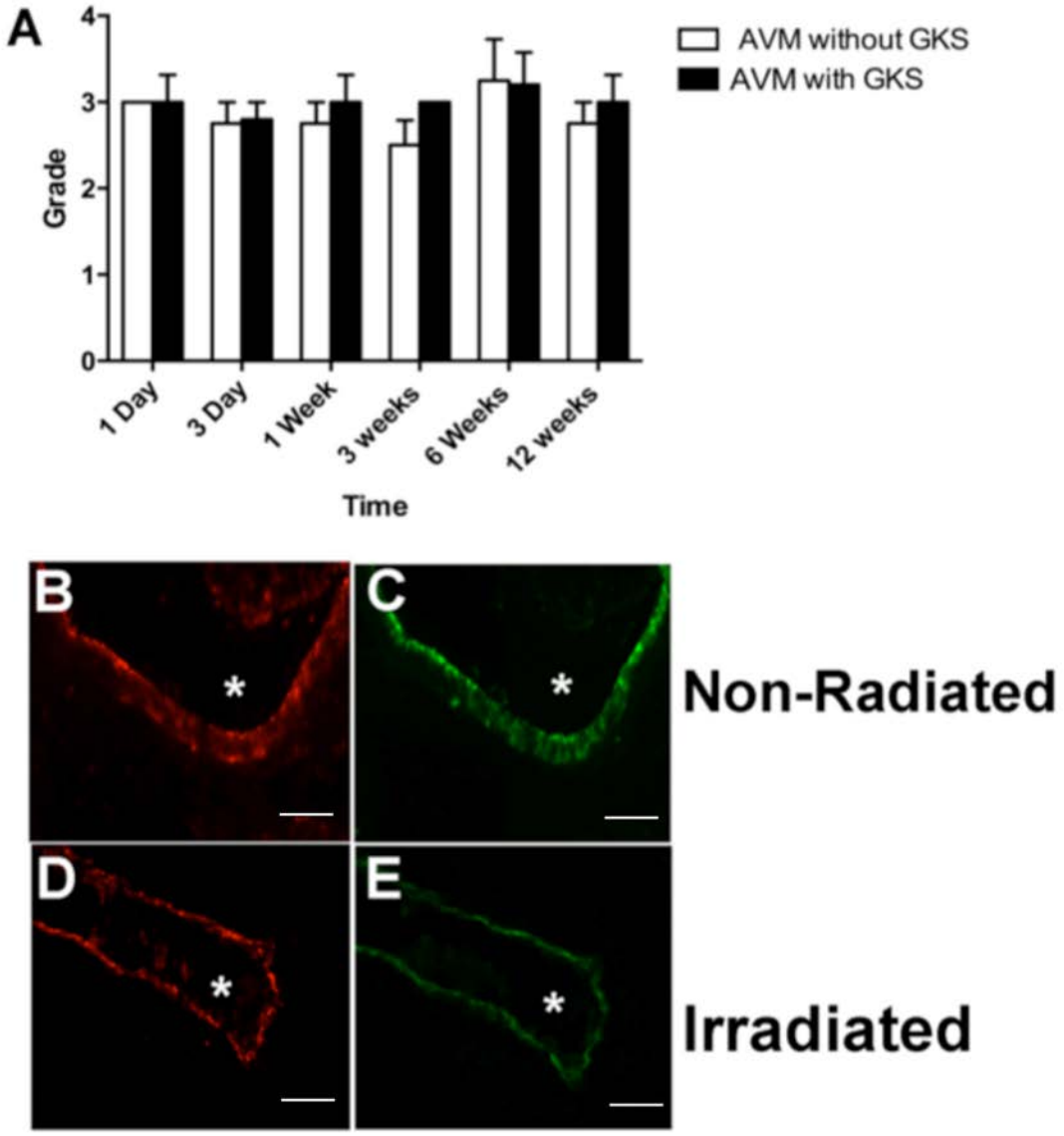

Figure 4-7 Expression of PECAM-1 in the nidus.

(A) Expression in the GKS group compared to the control group. (B) and (D): vWF staining. (C) and (E): PECAM-1 staining in the same sections as (B) and (D). (* = lumen) (Scale bar: 200 μm).

4.6 Conclusion

This study demonstrates that ICAM-1 is significantly upregulated in the irradiated AVM model. Moreover, ICAM-1 enhanced expression is localised on the surface of endothelial cells. This study shows a high potential of ICAM-1 as a radiation-induced target in deep brain tissues where conventional surgery is not possible.

Chapter 5

Thrombotic molecule expression after Gamma knife radiosurgery in animal model of AVM.

5.1 Abstract

Introduction: Over 90% of large AVMs are untreatable with current treatment methods. Molecular targeting is a prospective new treatment for these lesions. Understanding the endothelial response to radiosurgery is crucial in developing this technique. The aim of this study was to elucidate endothelial thrombotic molecules (tissue factor, thrombomodulin and von willebrand factor) expression changes after radiosurgery.

Methods: The following study was carried out using tissue extracted from the rats used in chapter 4. Fifty male Sprague-Dawley rats (345 ± 8.8 g) underwent AVM creation by connecting the rostral part of the left external jugular vein to left common carotid artery. The created AVMs in 30 rats were exposed to a single dose of radiosurgery (20 Gy) using the Gamma Knife after six weeks. The rest of the rats were sham-irradiated. Animals were sacrificed at 1 and 3 days, and at 1, 3, 6 and 12 weeks; tissue was frozen and used for the immunohistochemistry study.

Results: A slight upregulation in TF expression in irradiated AVMs was identified at one, three, six and twelve weeks after radiation. Thrombomodulin and von Willebrand factor expression did not change after radiation exposure any time.

Conclusion: The up-regulation of TF, although not significant, suggests that the pro-thrombotic effect of radiation starts at approximately one-week post-gamma knife radiosurgery. The results indicate that TF is unlikely to be a good candidate for vascular targeting, as expression was not significantly up regulated in the irradiated samples compared to controls. However, the timing of these expression changes may still be important when considering the optimal timing for applying pro-thrombotic strategies targeting E-selectin or ICAM-1.

5.2 Introduction

Brain arteriovenous malformation (AVM) is a common cause of haemorrhage and stroke in children and adults [621, 622]. High grade cerebral AVMs make up around one third of lesions, 90% of which are not treatable by surgery or radiosurgery [125, 625]. Most of these AVMs are larger than 3cm making radiosurgery ineffective for most cases [125, 625, 633]. Although the precise mechanism of action of radiosurgery is not known [628], EC damage, smooth muscle cells (SMC) and myofibroblast proliferation and also intraluminal thrombosis are part of the radiosurgery process [181].

Accelerating thrombus formation after radiosurgery has been proposed as a new method of AVM treatment, and has shown promising results in an animal model of AVM [634]. Further development of this strategy require a thorough understanding of endothelial molecular changes after radiosurgery, especially with regard to molecules involved in the thrombotic process.

The aim of this study was to investigate the effect of Gamma Knife radiosurgery on thrombotic molecules in an AVM model including the time course of expression changes.

5.3 Materials and methods

The Animal Care and Ethics Committee at Macquarie University approved all studies. Animal experimentation was performed in accordance with the Australian Code of Practice for the Care and Use of Animals for Scientific Purposes.

5.3.1 AVM formation

Fifty male Sprague-Dawley rats (345 ± 8 g) were used in this study. They were put under general anaesthesia using inhaled isoflurane and underwent surgery under surgical microscopes (Carl Zeiss, Germany) as described in chapter 2. Left common carotid artery was

anastomosed to left external jugular vein using a 10-0 monofilament nylon suture (Ethicon, Ohio, USA). After securing the patency of the fistulae, the wound was closed using (4-0) (Ethicon, Ohio, USA).

5.3.2 Gamma knife radiation

After maturation period of 6 weeks, the rats underwent radiosurgery or sham radiosurgery. Under general anaesthesia using ketamine (75 mg/kg) and medetomidine (0.5 mg/kg), thirty male Sprague Dawley rats received a single dose of gamma radiation using a Perfexion Leksell machine (Elekta Inc.). Animals were placed in a radiation frame (SC Medical biomedical engineering, Australia). A CT scan and 3D reconstructive image **(Figure 3-1)** were used for visualising the AVM, and for planning treatment. Gamma radiation (20 Gy marginal dose) was then delivered to the model nidus of thirty animals; the other 20 were a sham control. Hind limb pinch was used to determine the depth of the anaesthesia before and after the procedure.

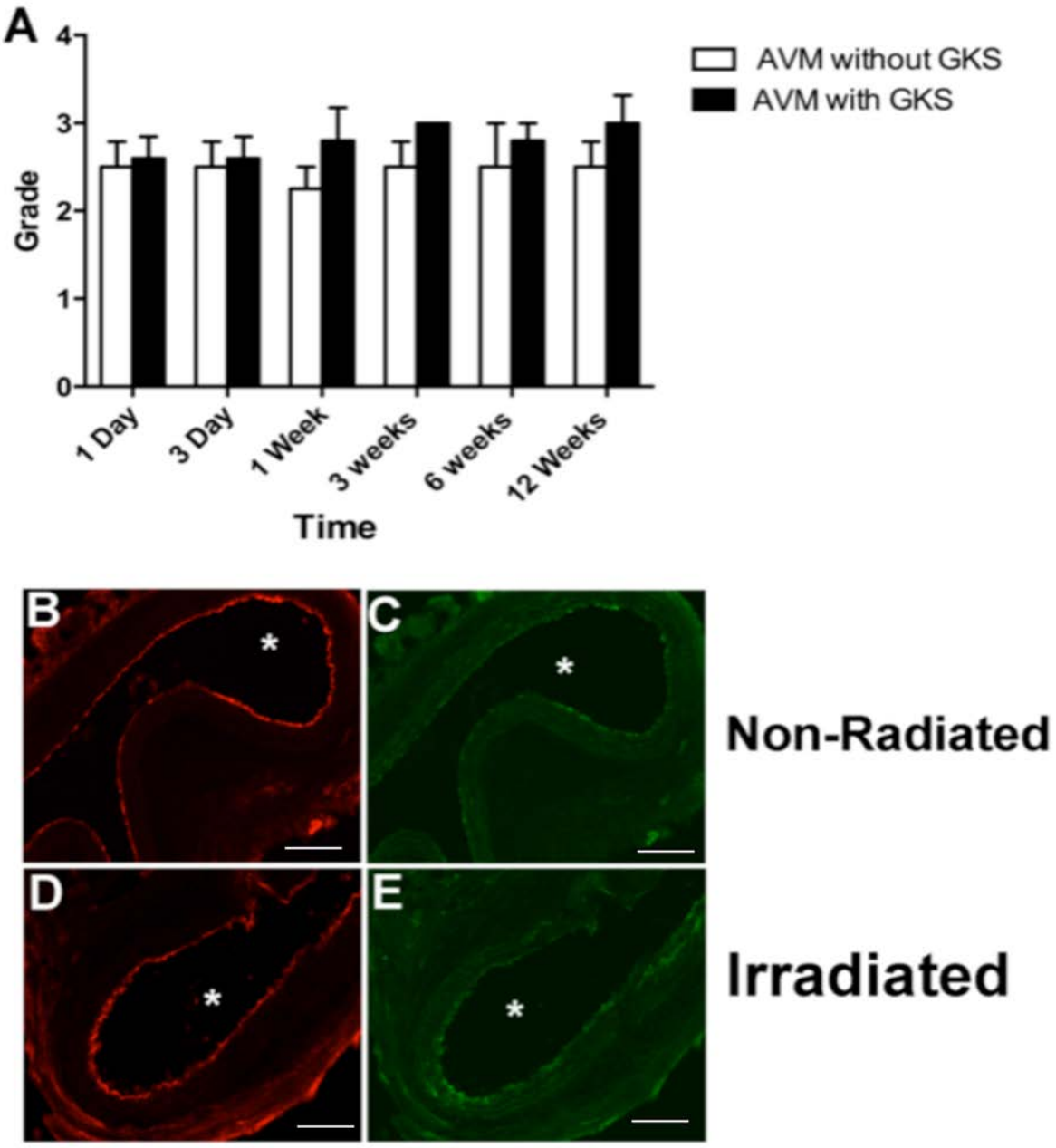

Figure 5-1 TF expression in left carotid artery.

(A) Expression in the GKS group compared to the control group. (B) and (D): vWF staining. (C) and (E): TF staining in the same sections as (B) and (D). (* = lumen) (Scale bar: 200 μm).

5.3.3 Immunohistochemistry

At the different time points mentioned before, animals were sacrificed. Ipsilateral LCCA, LEJV and nidus were collected then embedded in freezing media (ProSciTeck, Australia) and frozen in liquid nitrogen. Using cryostat, 18-micron tissue thicknesses were sectioned and placed on positive charged slides, and stained using protocols described in the immunohistochemistry technique. The slides were left at room temperature for 24 hours, and then washed using PBS and permeabilised with 50% ethanol in PBS for 10 minutes. After another washing with PBS, the sections were blocked in 10% donkey serum for one hour at room temperature. This was followed by overnight incubation at 4ºC anti-vWF rabbit polyclonal antibody (Abcam, ab6994, dilution 1:500) and with TM goat polyclonal IgG (SANTA CRUZ, sc-7097, dilution 1:50). The slides were then washed and incubated with anti-rabbit IgG-Alexa Fluor 594 (Molecular Probe, A21207, dilution 1:500) and anti-goat IgG-DyLt 650 (Abcam, Ab98517, dilution 1:500) for one hour in the dark at room temperature. Slides were washed thoroughly and incubated with DAPI (Molecular Probes) for nuclear staining for one minute, cover-slipped and cured for 48 hours before being subjected to fluorescence microscopy. A similar protocol were used for TF: the slides were incubated with vWF rabbit polyclonal antibody (Abcam, ab6994, dilution 1:500) and then with TF goat polyclonal IgG (SANTA CRUZ, sc-23596, dilution 1:50). Anti-rabbit IgG-Alexa Fluor 594 (Molecular Probe, A21207)(dilution 1:500) and anti-goat IgG-DyLt 650 (Abcam, ab 98517, dilution 1:500) were used as a secondary antibody. Expression of vWF was examined using a single labelling technique; the slides were stained with vWF rabbit polyclonal antibody (Abcam, ab6994, dilution 1:500) and anti-rabbit IgG-Alexa Fluor 594 (Molecular Probe, A21207, dilution 1:500).

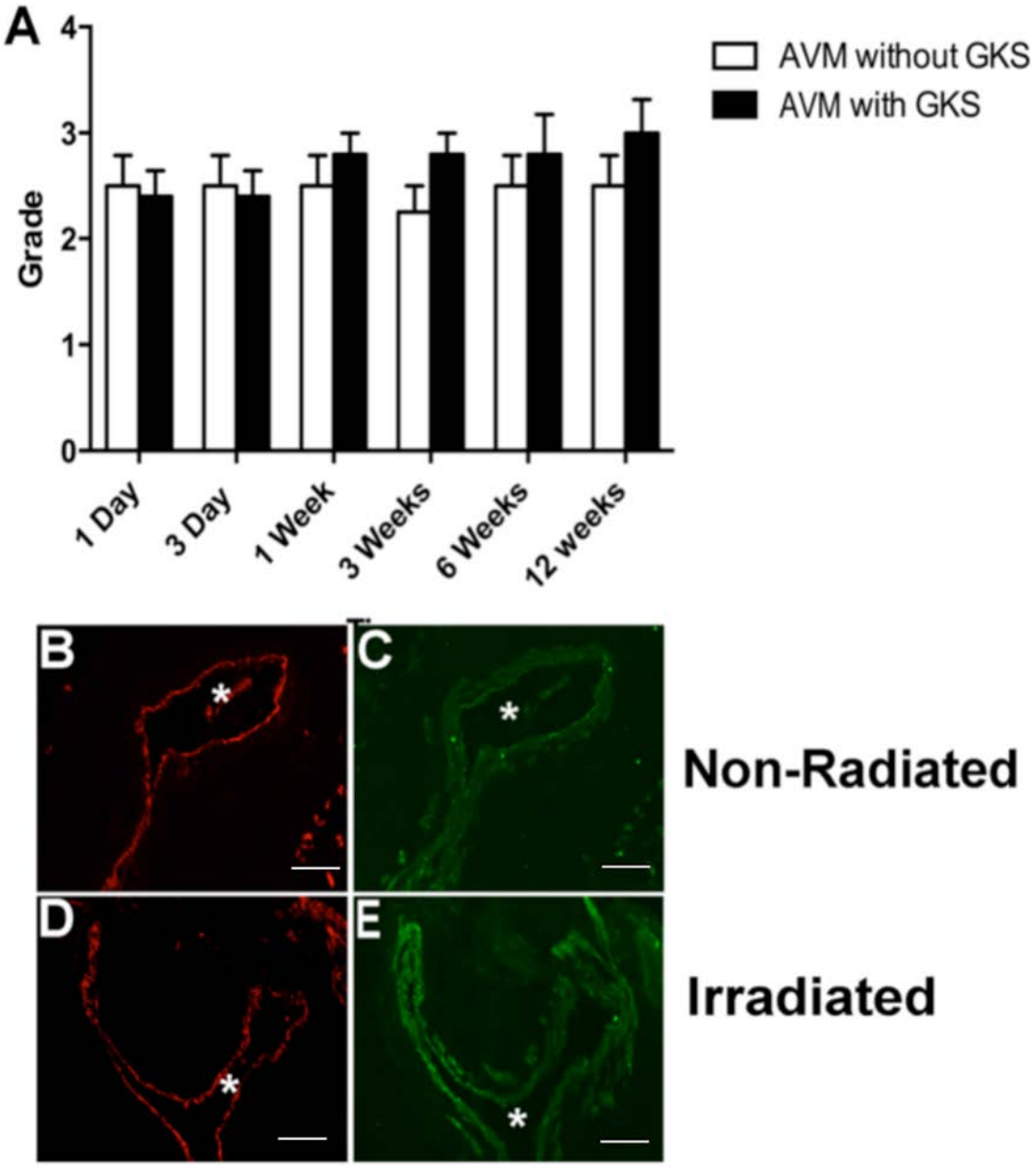

Figure 5-2. TF expression in the left external jugular vein.

(A) Expression in the GKS group compared to the control group. (B) and (D): vWF staining. (C) and (E): TF staining in the same sections as (B) and (D). (* = lumen) (Scale bar: 200 μm).

5.3.4 Light microscopy

Digital images were captured under fixed parameters with an AxioCam HRc digital camera (Zeiss, Germany) on a Zeiss microscope.

5.3.5 Data and statistical analysis

Protein expressions were evaluated using a grading system reported previously [82, 182], according to intensity and histological location in four histological layers: endothelium, subendothelium, tunica media, and tunica adventitia.

5.4 Results

5.4.1 Tissue factor

TF was expressed in the adventitial and perivascular layers in all tissues examined endothelial staining was detected in some sections. TF expression in irradiated tissue did not differ significantly from non-irradiated controls at any time point, although the expression was slightly higher at 1, 3, 6 and 12 weeks ($P>0.05$). However, analysis of all time points using ANOVA showed a significant change in LCCA ($P<0.05$) and nidus ($P<0.01$), and in the LEJV ($P>0.05$). **(Figures 5-1, 5-2, 5-3).**

5.4.2 Thrombomodulin

TM was observed in all AVM tissue, in both endothelial and sub-endothelial layers. The expression ranged from faint to moderate. No significant changes in expression of TM were found when comparing the irradiated with non-irradiated tissue at different time points or across all time points in the various parts of the created AVM. ($P>0.05$), ANOVA was ($P>0.05$). **(Figures 5-4, 5-5, 5-6)**.

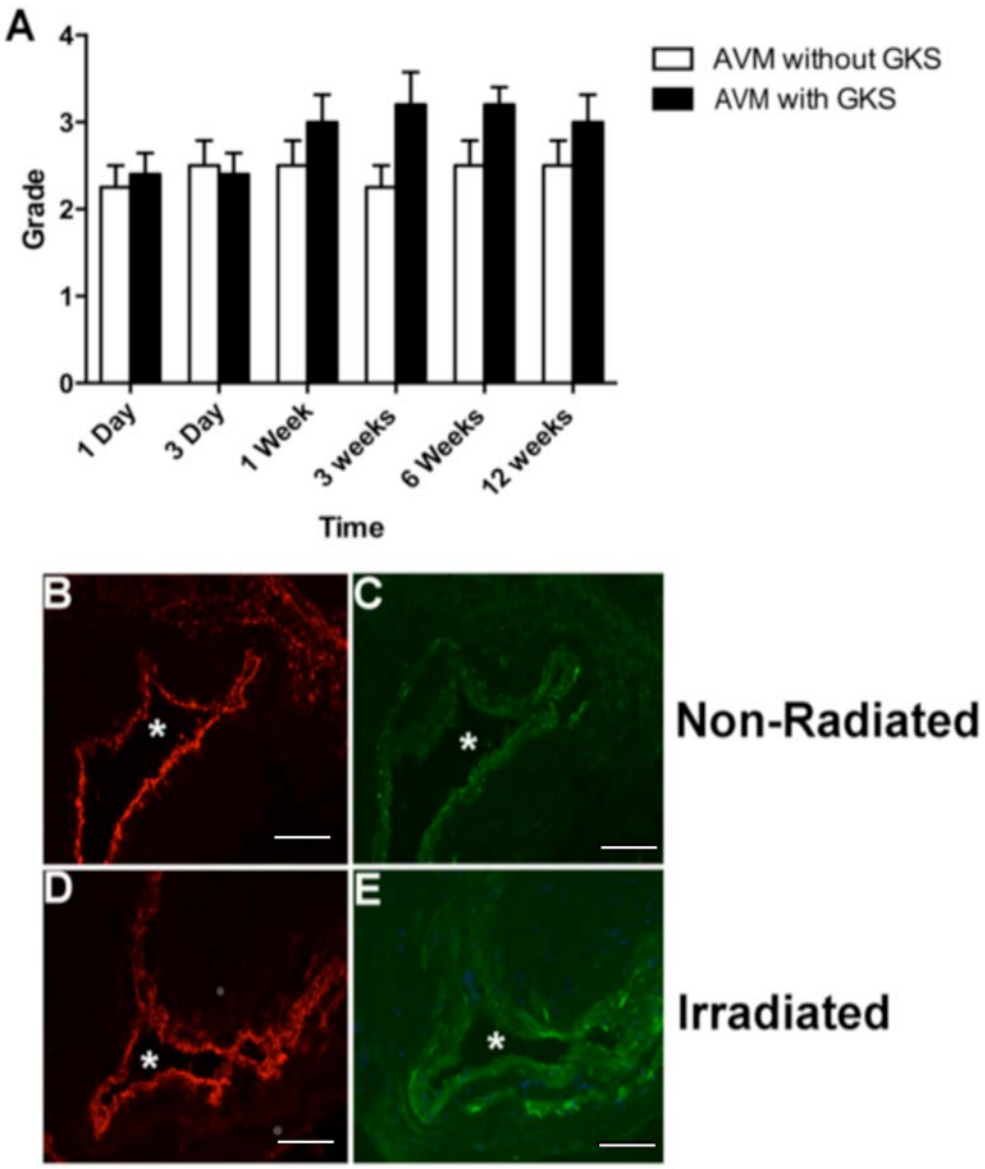

Figure 5-3 TF expression in the AVM nidus.

(A) Expression in the GKS group compared to the control group. (B) and (D): vWF staining. (C) and (E): TF staining in the same sections as (B) and (D). (* = lumen) (Scale bar: 200 μm).

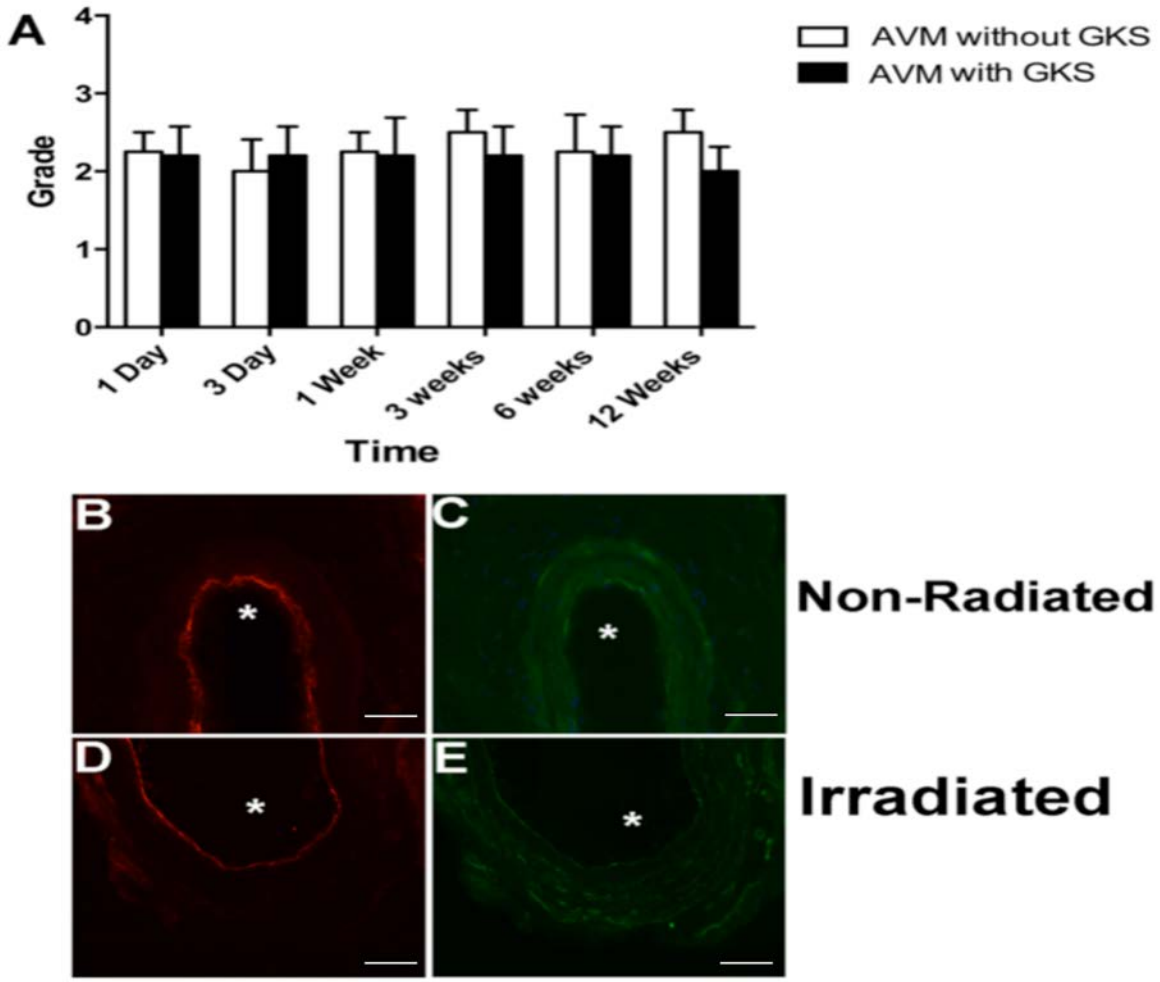

Figure 5-4 TM expression in left carotid artery.

(A) Expression in the GKS group compared to the control group. (B) and (D): vWF staining. (C) and (E): TM staining in the same sections as (B) and (D). (* = lumen) (Scale bar: 200 μm).

5.4.3 von Willebrand factor

All irradiated and non-irradiated tissues expressed vWF, the expression ranging from moderate to strong and mostly confined to the endothelial cells, with some subendothelial layer staining. Expression in irradiated tissue was not significantly different from the non-irradiated controls at different time points ($P > 0.05$) or across all time points ANOVA ($P > 0.05$). **(Figures 5-7, 5-8, 5-9).**

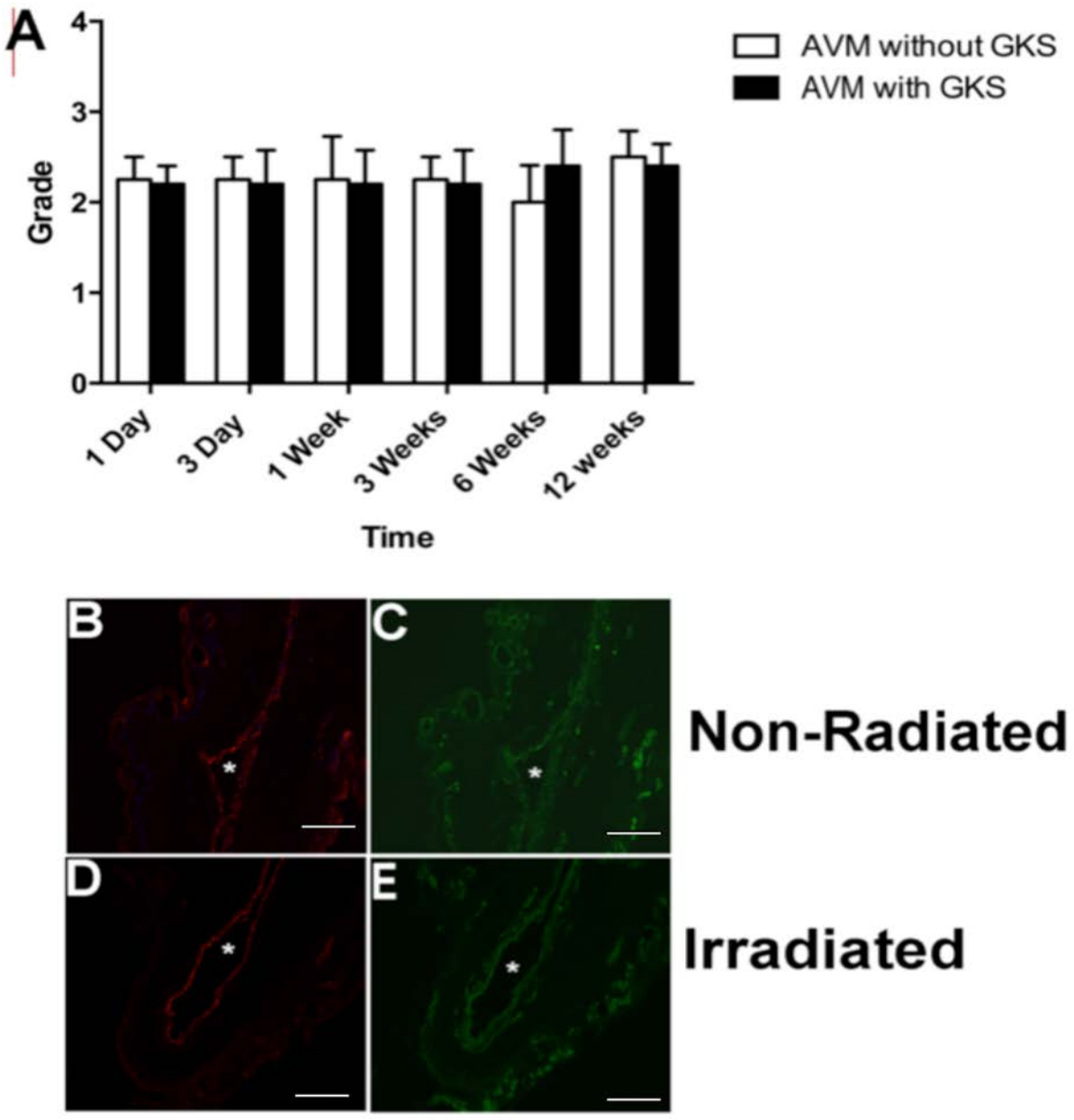

Figure 5-5. TM expression in the left jugular vein.

(A) Expression in the GKS group compared to the control group. (B) and (D): vWF staining. (C) and (E): TM staining in the same sections as (B) and (D). (* = lumen) (Scale bar: 200 μm).

5.5 Discussion

Radiosurgery is one treatment option for brain AVMs. Complete obliteration of a lesion may take up to three years and does not occur in all cases. Although the GKS process involves cell proliferation and thrombus formation, the exact mechanism is not well understood [635].

Molecular targeting therapy may be an alternative treatment for AVMs that are not able to be safely or effectively treated using surgery or radiosurgery. Previous work has shown that selective thrombosis can be achieved in animal models of AVM using a non-ligand targeting therapy [198, 636]. However, there are safety concerns using LPS in humans. Ligand-based molecular targeting therapy could overcome the safety limitations of LPS, but this type of treatment requires a highly discriminatory molecule that differentiation the ECs of AVM from normal ECs to allow selective accumulation of the pro-thrombotic agents in the AVM area. Unfortunately, the molecular expression of AVM endothelium is not significantly different from normal endothelium [78, 627]. We therefore used radiosurgery as a first step to stimulate discriminating endothelial molecular changes within AVM vessels only.

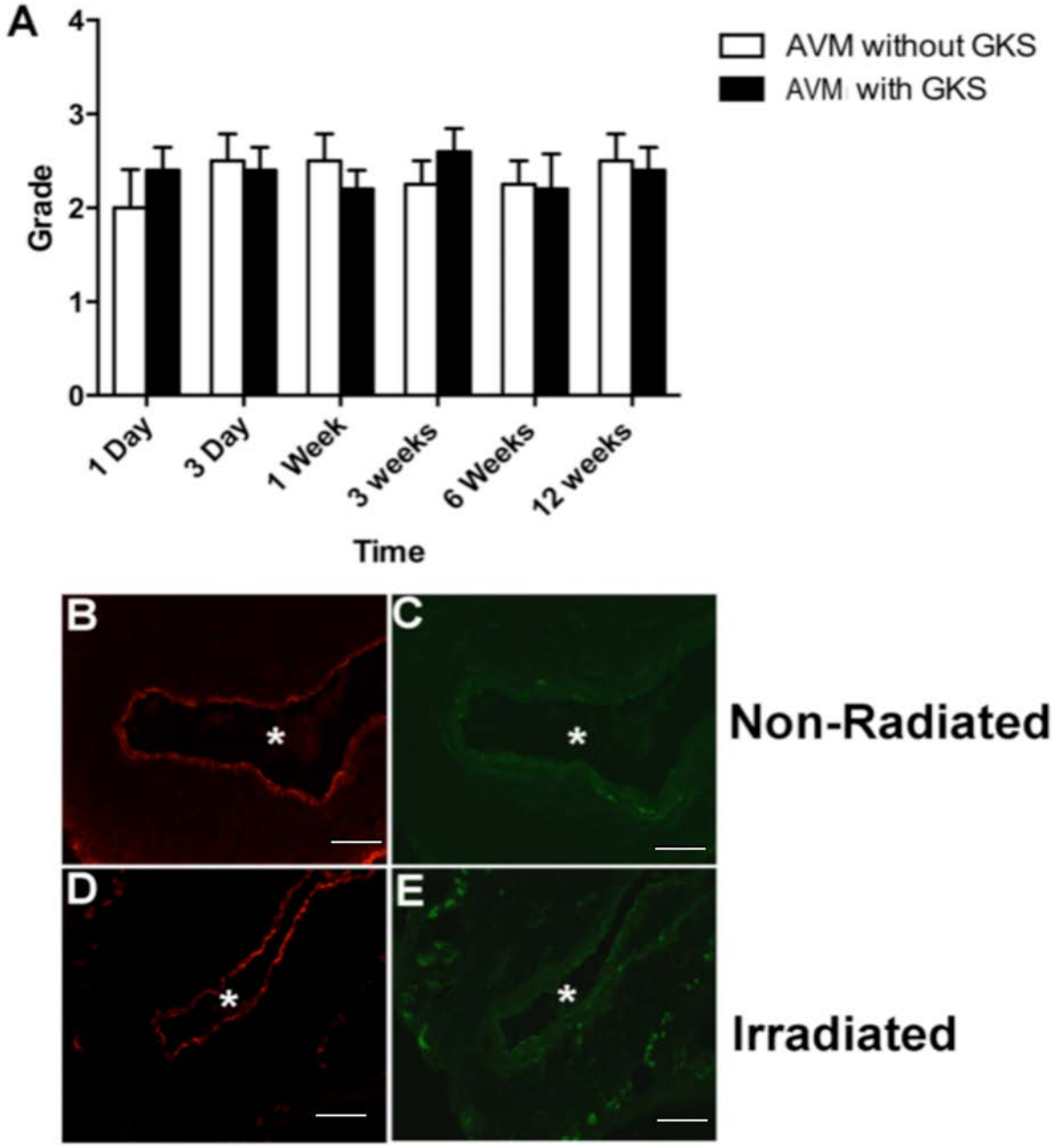

Figure 5-6. TM expression in the AVM nidus.

(A) Expression in the GKS group compared to the control group. (B) and (D): vWF staining. (C) and (E): TM staining in the same sections as (B) and (D). (* = lumen) (Scale bar: 200 μm).

Investigating the expression of both adhesion and thrombotic molecules in endothelium after radiosurgery help to identify the most suitable targeting molecule and choose the best time for treatment.

5.5.1.1 Tissue factor

The results indicate that upregulation of TF starts at one week and continues to 12 weeks post-GKS treatment. Expression of TF was found predominately in subendothelial cells, namely the media and adventitia of the vascular wall [637]. Other studies have found expression of TF in activated endothelial cells and cultured HUVECs [469, 637]. Tissue factor was found not significantly changed after radiation of human cerebral AVMs [182]. In another study, ionised radiation (IR) was shown to cause endothelial cell apoptosis, enhancing TF by a three- to four-fold increase [496]; while Liu et al. [183] found that TF expression is not significantly affected by radiation and was expressed mainly on the cell membrane. He also indicated that at 12, 24 and 72 post radiation there was cytoplasmic expressions of TF.

5.5.1.2 Thrombomodulin

The current study identified no change in expression of TM in acute and chronic time after radiation exposure. A previous study on cultured murine cerebral EC showed that a single dose of 25 Gy increase expression of TM [183]. Hauer-Jensen et al. [501] investigated the effect of radiation injury on expression of thrombomodulin (TM)-protein C system, and found exposure of normal tissues to ionising radiation causes a pronounced, sustained deficiency of endothelial TM. Cultured confluent HUVECs showed an increase in the release of TM from irradiated endothelial cells when treated with 60 Co γ rays at doses ranging from 0 to 50 Gy [559].

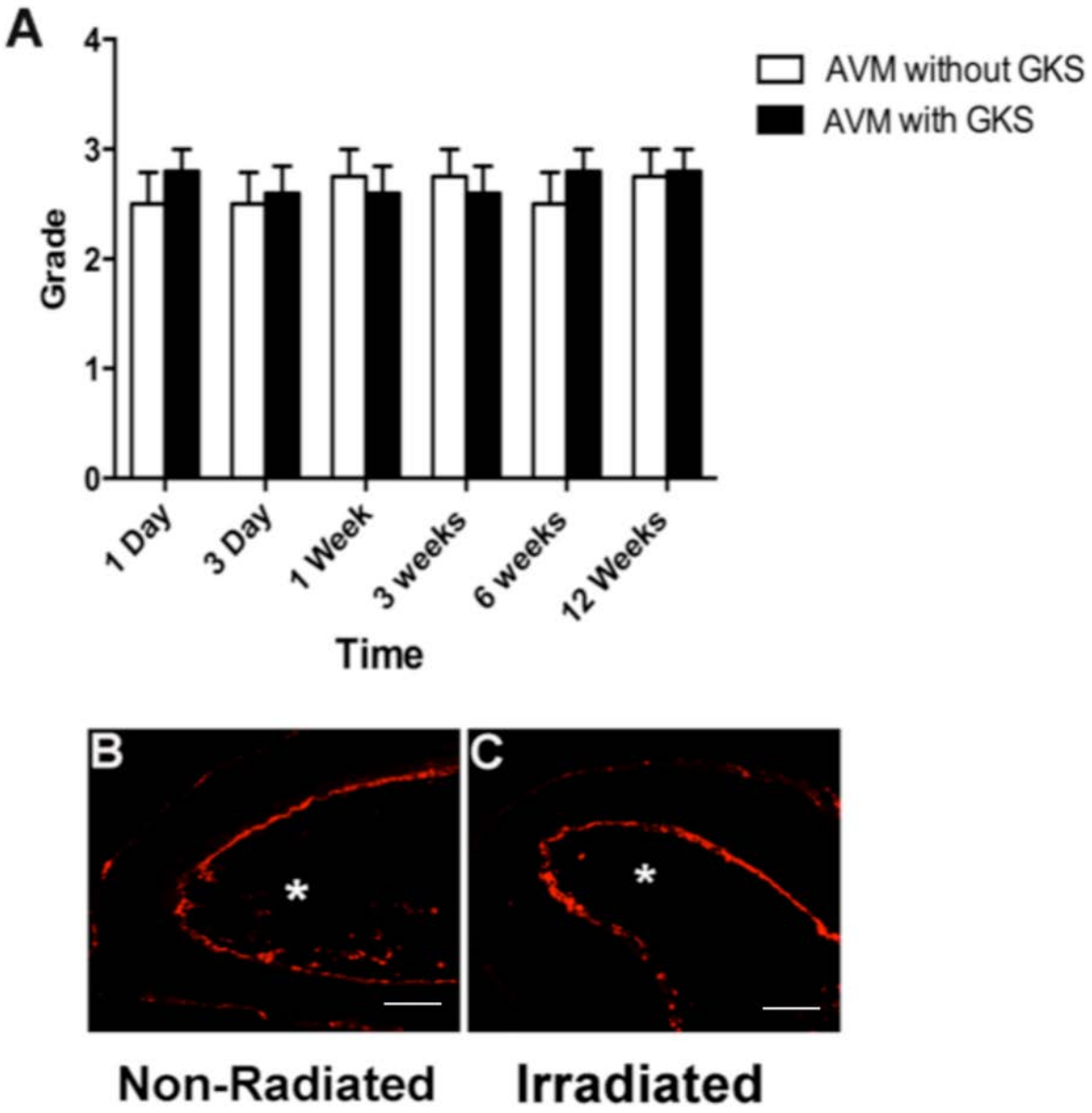

Figure 5-7. vWF expression in left carotid artery.

(A) Expression in the GKS group compared to the control group. (B) vWF staining in non-irradiated control. (C) vWF staining in irradiated treated. (* = lumen) (Scale bar: 200 μm).

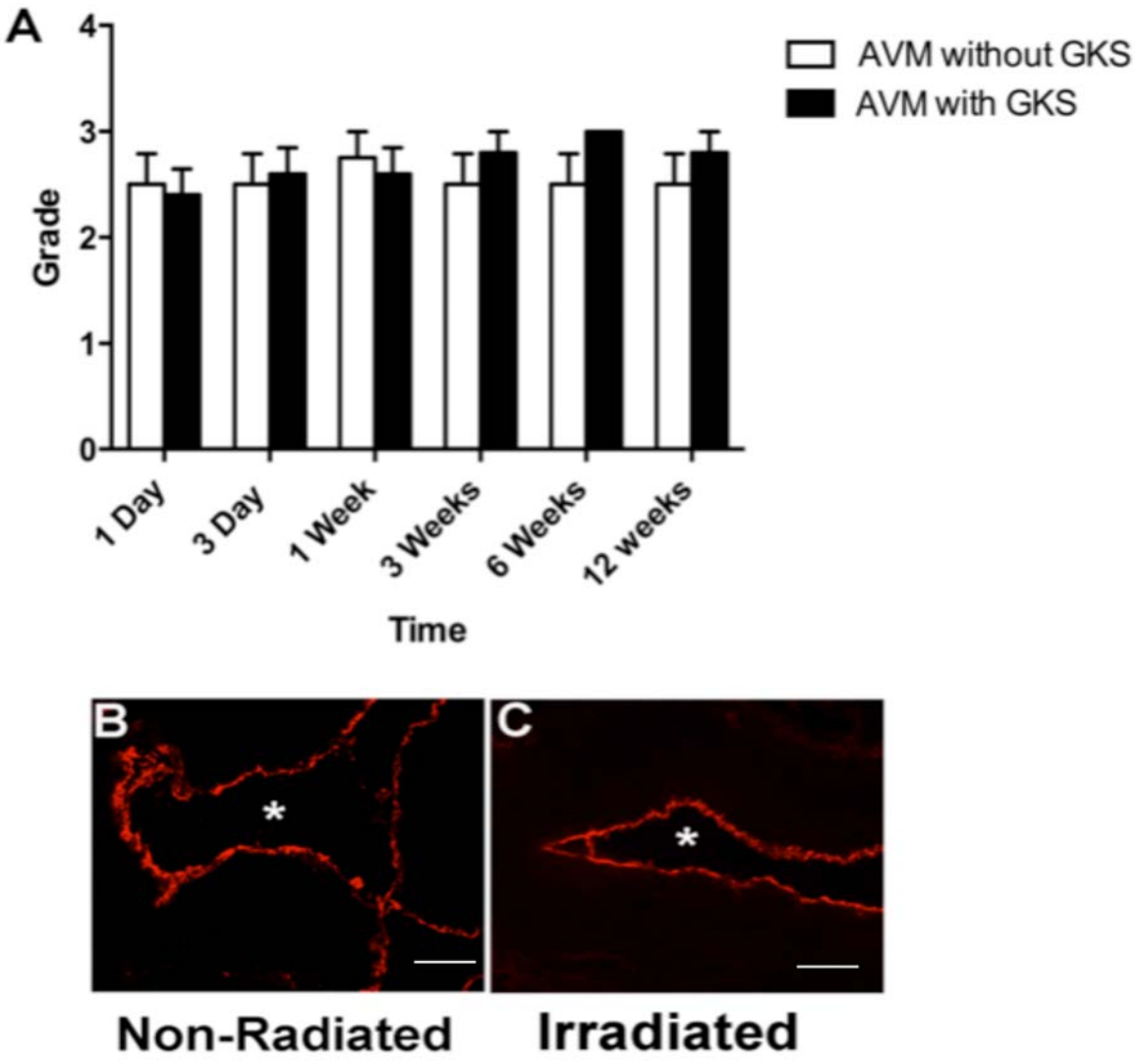

Figure 5-8. vWF expression in the left jugular vein.

(A) Expression in the GKS group compared to the control group. (B) vWF staining in non-irradiated control. (C) vWF staining in irradiated treated. (* = lumen) (Scale bar: 200 μm).

5.5.1.3 The Von Willebrand factor

We demonstrated that all irradiated and non-irradiated samples stained with vWF, the expression was not significantly different between the groups. Storer et al. [182] showed that irradiated samples frequently have no staining for vWF in the intima, indicating loss of the endothelium. Other studies have shown that radiation produces a significant release of vWF in cultured endothelial cells treated with 20 Gy [460]. An increase in production of vWF after radiating HUVECs with 20 Gy has also been reported [460].

5.6 Conclusion

This study indicates that level of TF expression is unlikely to be sufficient to be used as a target. However, acceleration of thrombus formation using a ligand vascular targeting such as E-selectin or ICAM1-1 for example, might be more effective when the pro-thrombotic effects of radiation are at their maximum effect. We demonstrated that there is an upregulation in TF, beginning at 1 week. Injecting a ligand might be more effective if performed after one week of radiation exposure.

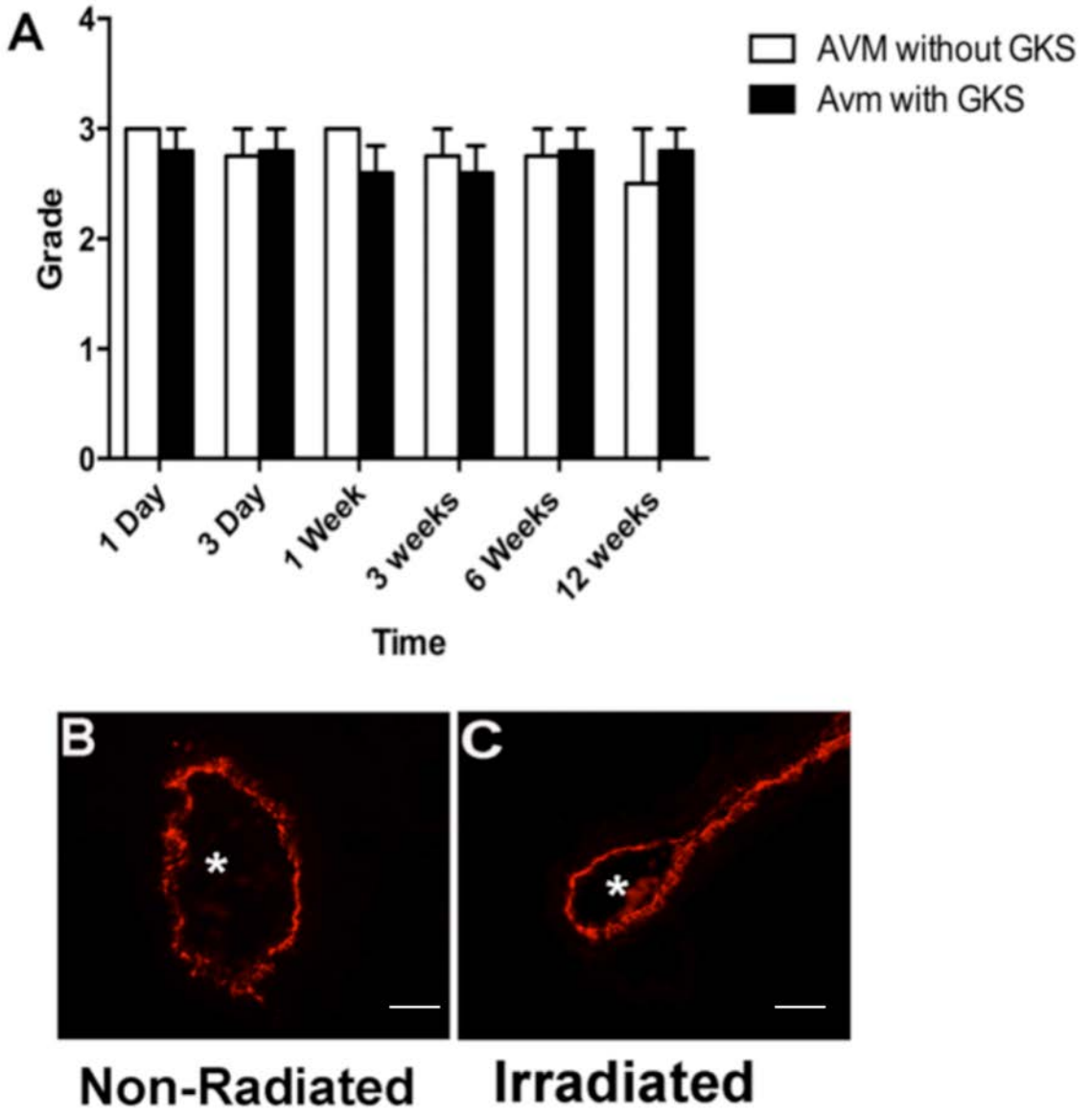

Figure 5-9. vWF expression in the nidus.

(A) Expression in the GKS group compared to the control group. (B) vWF staining in non-irradiated control. (C) vWF staining in irradiated treated. (* = lumen) (Scale bar: 200 μm).

Chapter 6

Expression of Integrin beta 1 in a rat model of AVM after Gamma knife radiosurgery.

6.1 Abstract

Introduction: A large percentage of high -grade deeply located AVMs are not treated with surgery or radiosurgery. Investigating different endothelial molecules expressed on the surface of endothelial cells may help in developing a new molecular targeting therapy for AVMs. The aim of this study was to determine the changes in Integrin beta 1 expression after exposure to radiation.

Methods: A rat model of AVM was created by anastomosing the left external jugular vein to left common carotid artery of fifty Sprague-Dawley rats. After 6weeks of AVM creation, 30 model AVMs were irradiated with a single dose of radiosurgery (20 Gy) using the Gamma Knife. Twenty rats were used as non-irradiated controls. Animals were perfused with Phosphate buffered saline, then tissue was collected at 1and 3 days and 1, 3, 6 and 12 weeks. Frozen tissue was used for immunohistochemistry study.

Results: Integrin beta 1 was expressed in all examined tissue; expression was found in all vessel layers. In endothelial cells the expression was scattered and moderate to weak; it was diffuse in all other layers. Arteries tended to have stronger staining than other examined tissue. A reduction in expression of beta 1 integrin in irradiated tissues compared to non-irradiated controls was identified at 1 and 3 days and 1 week, returning to normal by 3 weeks to 12 weeks: (ANOVA $P < 0.05$).

Conclusion: The study illustrates response of the protein to GKS; the protein is not suitable for the proposed molecular targeting therapy at the time points were described.

6.2 Introduction

Brain AVMs are abnormal conglomerations of dilated arteries and veins connected by single or multiple fistulae [124]. Surgery is suitable for small superficially located AVMs; however, grades IV and V are not surgically treated without high risk [125, 638]. Radiosurgery is suitable for AVMs under 3 cm [124], with a latency period that may extend to three years [639] in which the patient remains at risk of haemorrhage [640, 641].

Molecular targeting therapy is a promising new treatment for previously non-treatable AVMs. Work in animal model of AVM has shown that molecular targeting therapy is possible with non -ligand methods [634, 636], although, non-ligand vascular targeting is not effective in larger vessels and might not be safe for use in humans [634].

Developing ligand vascular targeting for AVMs requires choosing the most suitable EC molecule that can discriminate AVM ECs from normal ECs. The expression of EC molecules in AVM is not significantly different from normal ECs [78, 627]. Radiation is a powerful stimulator for of endothelial molecular changes [616]. We propose that radiosurgery can stimulate the cell surface expression of discriminating proteins that would then enable molecular targeting therapy.

Several AVM endothelial proteins have been identified [642] including E-selectin, ICAM-1, VCAM-1 and Integrin beta 1. The effect of radiation on E-selectin, ICAM-1 and VCAM-1 has been documented [333, 616]. Also, Integrin beta 1 is upregulated in lung tumour cell lines after radiation [581].

The aim of this experiment was to study the time course of the expression of Integrin beta 1 in a rodent model of arteriovenous fistula following radiosurgery, and to determine its suitability for targeting by a coaguligand.

6.3 Materials and methods

6.3.1 Surgical fistula formation

All animal experiments were approved by The Animal Care and Ethics Committee at Macquarie University and were conducted in accordance with the Australian Code of Practice for the Care and Use of Animals for Scientific Purposes, (ACEC reference numbers 2011/011).

Fifty rats underwent AVM creation surgery. Animal care, anaesthesia and the surgical procedure for anastomosing LEJV and LCCA were as described in the previous chapter.

6.3.2 Gamma Knife radiation

Radiosurgery was performed under intraperitoneal ketamine and midazolam anaesthesia. Non-irradiated animal models were treated in the same manner but did not receive any radiation. At the time points described previously, animals were anaesthetised and perfused with phosphate buffered saline. Six weeks post-AVM creation, the rats underwent the radiosurgical procedure, in which thirty male Sprague Dawley rats received a single dose of gamma radiation as described in the previous chapter. CT scan and 3D reconstructive images were used for visualising AVM and planning the treatment, then 20 Gy gamma radiation was delivered to the model nidus of thirty animals, the other 20 animals were sham controls.

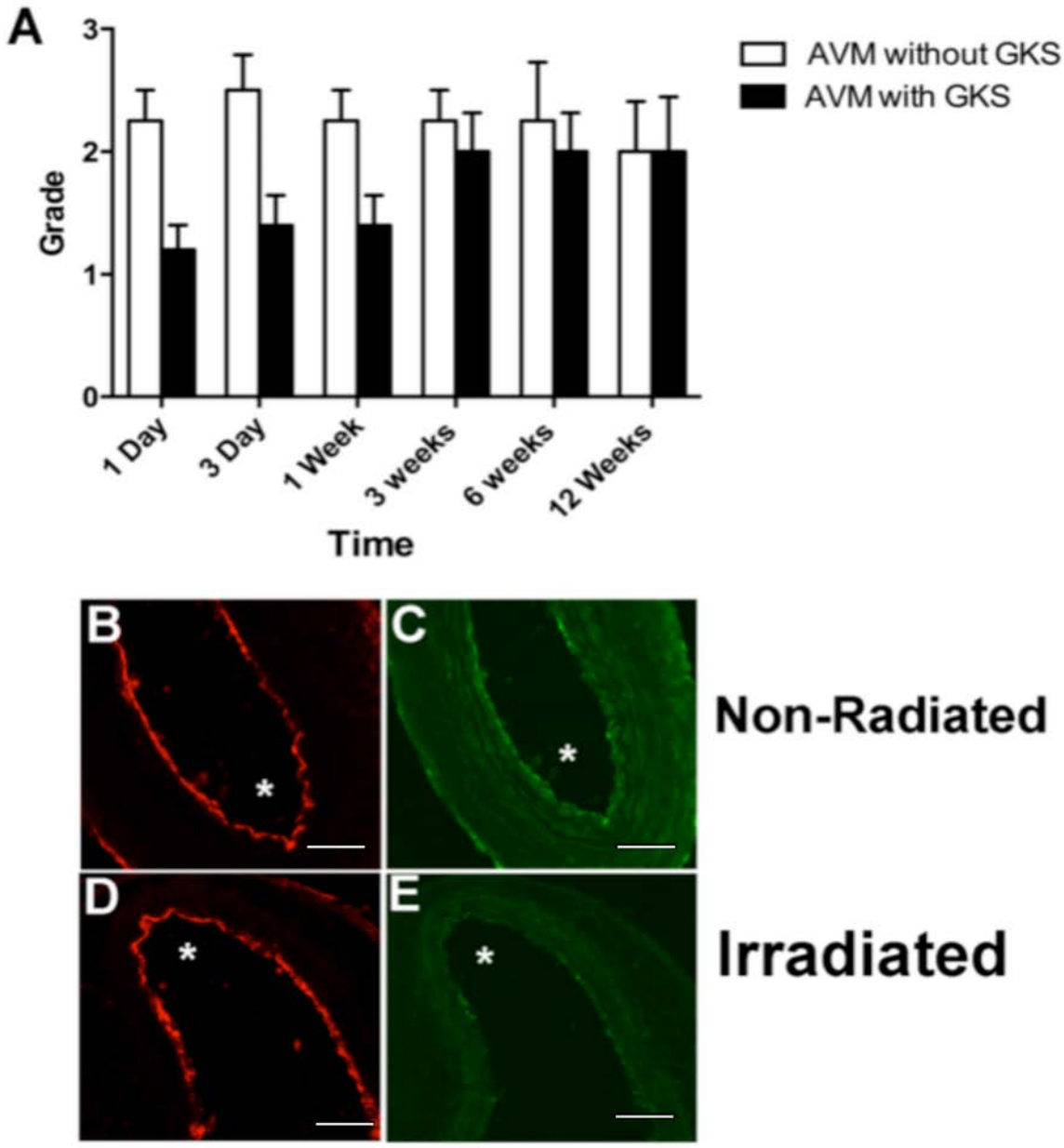

Figure 6-1. Integrin beta 1 expression in left carotid artery.

(A) Expression in the GKS group compared to the control group. (B) and (D) vWF staining. (C) and (E) Integrin beta 1 staining in the same sections as (B) and (D). (* = lumen) (Scale bar: 200 μm).

6.3.3 Immunohistochemistry

Animals were sacrificed at 1 and 3 days and 1, 3, 6 and 12 weeks. For each time point, 5 irradiated and 4 non-irradiated rats were used for the immunohistochemistry study. Tissue was collected and embedded in freezing media (ProSciTeck, Australia) and frozen in liquid nitrogen. Sections were cut 18-micron and placed on positively charged slides, and stained using the protocols described before. The slides were left at room temperature for 24 hours, washed using PBS and permeabilised with 50% ethanol in PBS for 10 minutes. After another washing with PBS, the sections were blocked in 10% donkey serum for one hour at room temperature. This was followed by overnight incubation at 4ºC anti-vWF antibody rabbit polyclonal antibody (Abcam, ab6994, dilution 1:500) and with anti-Integrin beta 1 (sc-6622, dilution 1:100) goat polyclonal antibody. The slides were then washed again and incubated with anti-rabbit IgG-Alexa Fluor 594 (Molecular Probe, A21207, dilution 1:500) and anti-goat IgG-DyLt 650 (Abcam, Ab98517, dilution 1:500) for one hour in the dark at room temperature. Slides were washed thoroughly and incubated with DAPI (Molecular Probes) for nuclear staining for one minute, cover-slipped and cured for 48 hours before being subjected to fluorescence microscopy.

6.3.4 Light microscopy, data and statistical analysis

Digital images were captured under fixed parameters as explained above; the same grading system was used to evaluate the protein expressions [82, 182].

6.4 Results

Integrin beta 1 was expressed in all examined tissue; the expression was found in all vessel layers. In ECs the expression was scattered and moderate to weak, but was diffuse in all other layers. The LCCA tended to have stronger staining than other tissues examined **(Figures 6-1, 6-2, 6-3)**. Reduced expression of the examined molecule in irradiated tissues compared to

non-irradiated controls was identified at 1 and 3 days and 1 week ($P > 0.05$). At 3, 6, and 12 weeks, the expression in the irradiated tissue was normalised ($P > 0.05$). Although the expression was not significant each time point ($P > 0.05$), overall ANOVA was ($P < 0.05$).

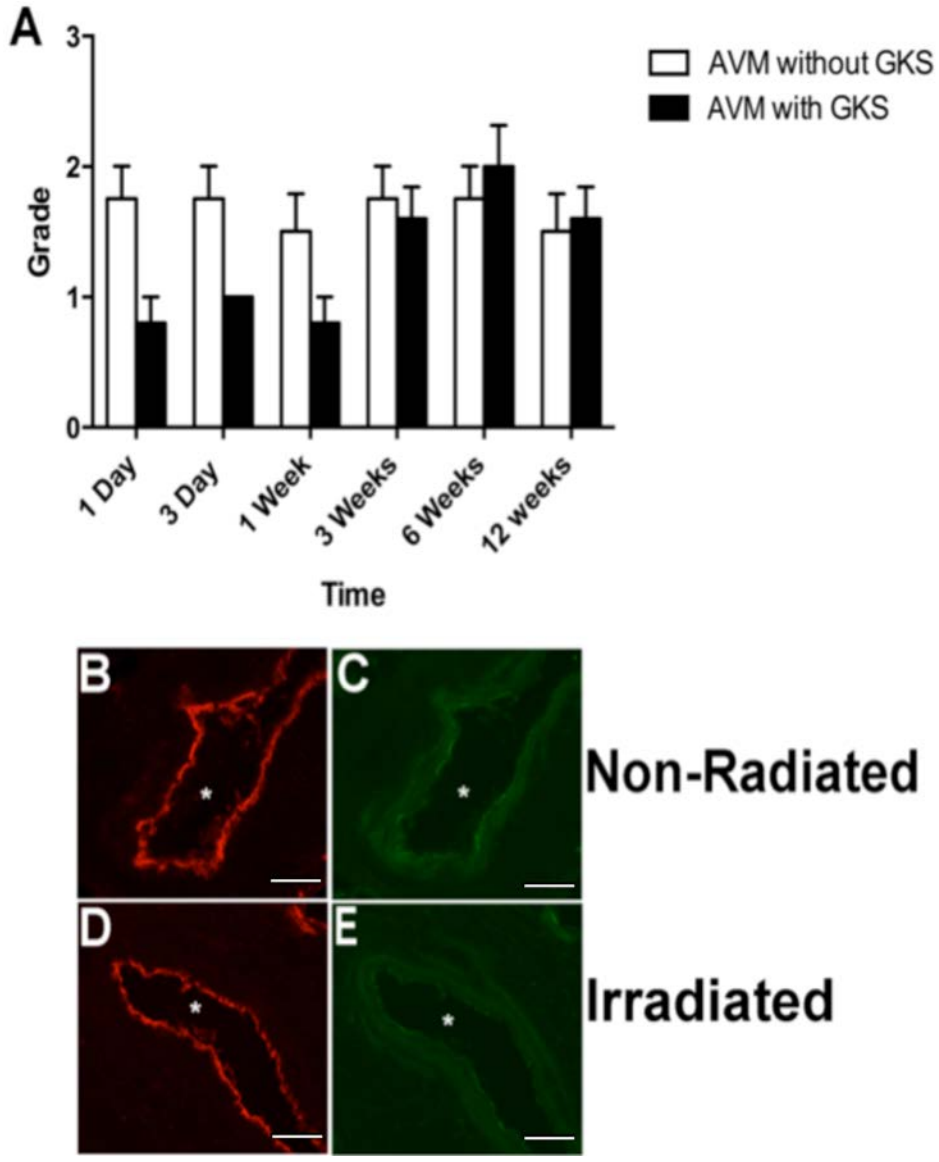

Figure 6-2. Expression of Integrin beta one in the left jugular vein.

(A) Expression in the GKS group compared to the control group. (B) and (D) vWF staining. (C) and (E) Integrin beta 1 staining in the same sections as (B) and (D). (* = lumen) (Scale bar: 200 μm).

6.5 Discussion

Integrin beta one is a type I transmembrane cell adhesion receptor. It plays an important role in immune responses [569], leukocyte adhesion, migration and activation [575], and has a role in cancer angiogenesis [578]. The family of integrin receptors mediate the attachment of cells to the extracellular matrix [581]. Simonian et al. [642] have determined several surface membrane proteins expressed in an AVM rat model, including Integrin beta 1, Integrin beta 4 and Integrin alpha 6.

The results of this study suggest that Integrin beta one is expressed in all layers of the created AVM including ECs. The protein was downregulated during the first week following GKS treatment, then the expression normalised up to 12 weeks. In contrast, other study have indicated that Integrin beta 1 is upregulated in lung tumour cell lines within 48 hours after radiosurgery exposure [581], and in irradiated epidermis cells at the end of five weeks of radiotherapy compared to the non-irradiated controls.

6.6 Conclusion

This study gives more detail about the molecular characteristic of AVMs and their response to radiosurgery. The results of this study suggest the response of cells to radiation might vary according to cell phenotype; however, our focus is on developing vascular targeting as a new treatment for AVM. The study suggests that the response of this protein to GKS is not enough to discriminate the ECs of AVM from normal ECs.

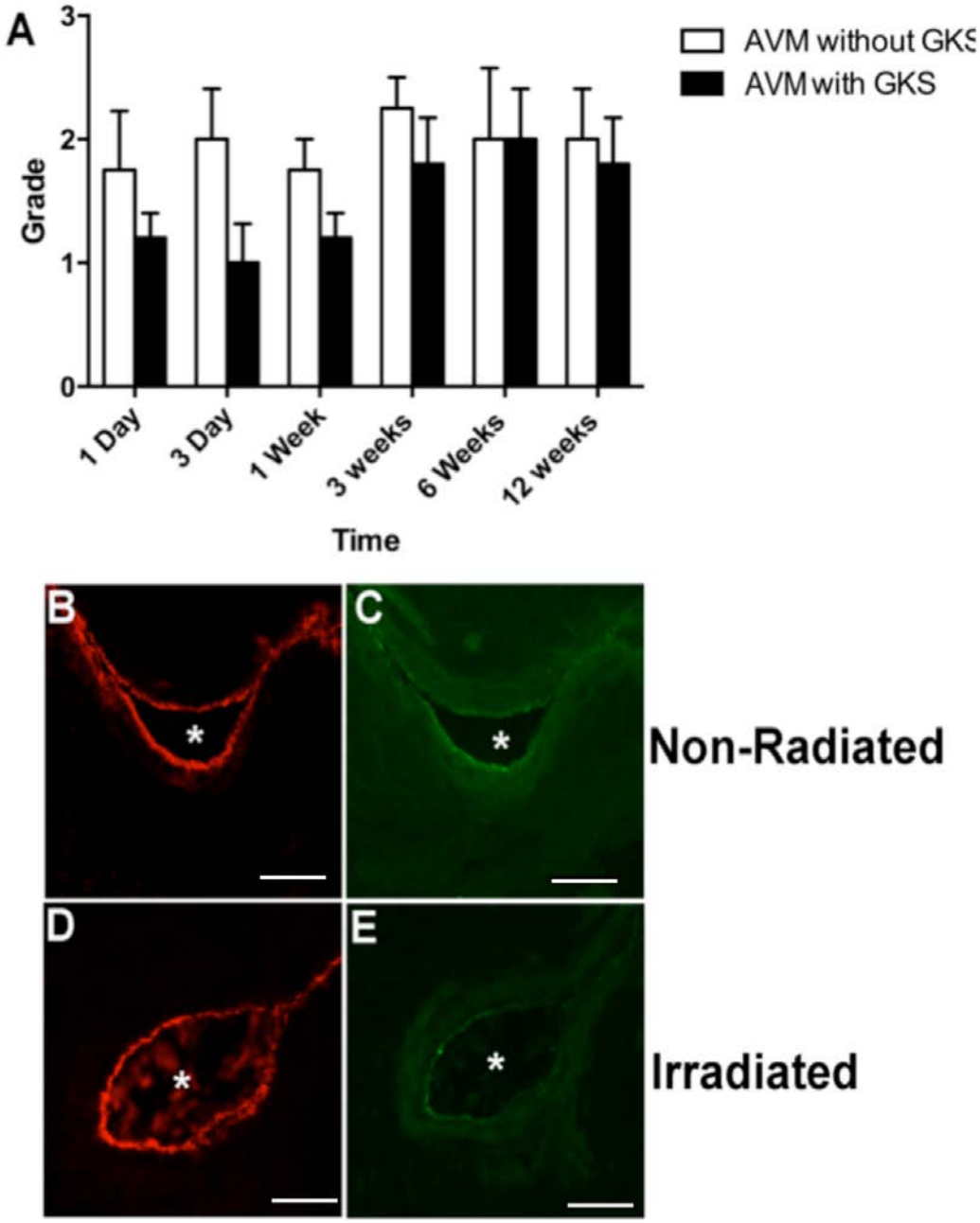

Figure 6-3. Expression of Integrin beta 1 in the AVM nidus.

(A) Expression in the GKS group compared to the control group. (B) and (D) vWF staining. (C) and (E) Integrin beta 1 staining in the same sections as (B) and (D). (* = lumen) (Scale bar: 200 μm).

Chapter 7

General discussion and future directions

7.1 What are cerebral AVMs?

Brain arteriovenous malformation is a common cause of haemorrhage and strokes in children and adults [621, 622]. Al-Shahi et al. reported that AVM prevalence varies between 15 and 18 per 100,000 adults [643]. The morbidity and mortality rate from ruptured AVMs is considerable [49, 623, 624]. Around 35% of total AVMs are high grade, and 90% are not manageable by conventional treatments [125, 625]; the partial treatment of a large and deeply located AVM can compound risks [125]. Ruptured brain AVMs has higher haemorrhage risk (4.5%–34%) than previously unruptured ones (0.9%–8%) [644]. Statistically significant risk factors for haemorrhage are previous haemorrhage (HR 3.2, 95% CI 2.1–4.3), deeply located AVM (HR 2.4, 95% CI 1.4–3.4), AVM with exclusively deep venous drainage (HR 2.4, 95% CI 1.1–3.8), and association with aneurysms (HR 1.8, 95% CI 1.6–2.0) [645]. Death from AVM haemorrhages are high, accounting for 10% to 30% of patients [36, 37, 646], and the risk of permanent morbidity ranges from 5% to 20% [646].

The goals of brain AVM treatment are to prevent haemorrhage, control seizures, and prevent the progress of neurological deficits [647]. Almost all AVMs of grades I to III can be treated surgically with relative safety; however, surgery for grade IV and V AVMs carries a risk of permanent neurological disability or death ranging from 12% to almost 40% [127, 648]. A subtotal resection or obliteration can increase the risk of haemorrhage [125].

Endovascular treatment of AVMs involves intra-arterial injection of occluding substances. The indications for this type of therapy may include preoperative and pre-radiosurgery reduction of AVM size or flow, obliterating a source of haemorrhage as targeted embolisation, attempting curative modality for small lesions, and using palliative embolisation to relieve shunting related symptoms. Endovascular treatment is used most commonly as an adjunct to surgery or radiosurgery to reduce the size of the AVM nidus to a range that is amenable to radiosurgical ablation [649].

Stereotactic radiosurgery is a relatively non-invasive approach suitable for small AVMs (<3 cm) where surgery is not suitable because the AVM is located in an eloquent area of the brain or patients are unable to go through surgery because of comorbidity issues [650]. The AVM obliteration rate following radiosurgery is hard to determine with certainty, as obliteration rates are based only on patients who had late angiography. Although the obliteration rate is high in lesions that are less than 10 ml, it is as much as 47% in lesions larger than this [651].

Radiosurgery has many disadvantages. The latency period in patients whose AVM is eventually obliterated may extend from one to many years, during which the risk of haemorrhage remains at 3–4% per year as it is not treated. Radiosurgery is not therapeutically effective in about 10–15% of small lesions [633]; and the reappearance of AVMs has been reported after totally obliteration by radiosurgery [652].

Although there have been considerable advances in terms of AVM treatment, a large number of patients still cannot be treated without risk. Low grade AVMs comprise approximately 40% of AVMs and can be managed with low risk [123, 653], but over 90% of high grade lesions (IV-V) are untreatable [125, 625] and 25% of grade III AVMs cannot be treated without high risk. Current treatments are safe and effective for small AVMs, but over one third of all AVM patients cannot be effectively treated [625, 654].

Molecular targeting therapy is an attractive new treatment for AVMs that are not treated with currently available therapies. In this technique, intravascular thrombosis is stimulated and complete obliteration could be achieved. By exploiting the differences resulting from radiosurgery, thrombosis can be enhanced.

Radiosurgery enhancing vascular targeting has been developed before, in cancer treatments where intravascular thrombosis has been stimulated to achieve tumour necrosis [200, 655, 656]. Selective vascular thrombosis was achieved in an AVM animal model [198] using lipopolysaccharide (LPS) and soluble tissue factor (sTF).

LPS is the major component of the outer membrane of gram-negative bacteria such as E. coli. This is localised in the outer layer of the membrane and is, in noncapsulated strains, exposed

on the cell surface. Non-damaged bacterial lipopolysaccharides are macromolecules with the molecular mass 10−20 kDa. They consist of a hydrophobic lipid section, a hydrophilic core polysaccharide chain and a repeating hydrophilic O-antigenic oligosaccharide side chain [657], and are known to have prothrombotic and proinflammatory effects. LPS directly stimulates expression of TF, interstitial and vascular cell adhesion molecules, and E-selectin [658-660].

Using LPS combined with soluble TF to initiate coagulation has shown that it is possible to selectively induce thrombosis of irradiated vessels in a rat model of arteriovenous malformation [634]. Reddy et al. [636] investigated vascular targeting enhancement of radiosurgery in an animal model of AVM up to 90 days after treatment with LPS and soluble TF, reporting that histologically, durable micro vessel thrombosis was achieved following radiosurgery and coadministration of LPS/sTF.

Although the reported result is promising as thrombosis was selectivity induced without any evidence of LPS toxicity in the animals, no systemic thrombosis occurred anywhere except in the AVM areas. Inducing thrombosis using a non-ligand strategy (LPS and sTF) has many limitations. LPS is known to cause leukopenia in animals [661] and has been reported to induce DIC and septic shock [662]. Another study has shown decreased survival of newborn neurons in the dorsal hippocampus after neonatal LPS exposure in mice [663]. Furthermore, the approach lacks clear specificity and it is not certainly known that the method is safe or effective for use in humans: already it has been documented to cause transient renal and hepatic toxicities, fever, chills and hypotension [664]. Many other adverse effects may limit the use of LPS for molecular targeting in humans. Another limitation is that thrombosis induced by the administration of LPS and sTF is not radiation-specific and may lead to secondary high blood flow and shear stress. Thrombosis occurs even in AVMs that do not receive radiation, following administration of the targeting agent; this is more significant in small vessels (< 50 μm) [634]. The thrombosis in non-irradiated vessels could be explained by the fact that non-irradiated fistula vessels tend to overexpress VCAM and might externalise phosphatidylserine [77], allowing the LPS and sTF to cause thrombosis.

A ligand-based vascular targeting strategy is an alternative technique to the non-ligand strategy and would overcome the difficulties that arise from that therapy in animal models of AVM. The strategy uses a combination of a targeting moiety and an effector moiety. Radiosurgery has been proposed to induce molecular changes that allow discrimination of the endothelium of AVM vessels from those of non-AVM vessels, thus allowing successful selective targeting of the vascular lesions.

Different methods are been used to investigate the molecular expression of endothelial cell. These methods include immunohistochemistry, western blotting, polymerase chain reaction and proteomics technique. Imunohischemistry on fresh frozen as gives good morphologic features, and clean background. The Morphologic features for frozen tissue sections demonstrated apparently better cell and tissue features. Western blotting is not appropriate in the animal model because the protein changes on the endothelial surface are a very small fraction of the total proteins that would be obtained in any tissue sample. Both polymerase chain reaction and proteomics technique is been used to investigate the similar molecules in our laboratories

7.2 Reponses of the animal model to radiation

7.2.1 Developing the radiation technique for the animal model

GKS irradiated animal model was developed in this study. A pilot study of 3 animals was used to adjust the rat position in the animal frame, obtain CT images to locate the AVM and adjust the dose delivered to the model. No animal death was reported as a consequence of Gamma Knife treatment. With the help of radiosurgical experts we developed the animal frame, a critical requirement to allow for targeted radiosurgery. We are confident that using this technique we can identify the exact position of the AVM using CT and three-dimensional re-constructed images and administer highly targeted radiation to the AVM, an achievement not possible without planning for each animal. The dose to adjacent structures can be

controlled to minimise adverse effects. No neurological- surgical- or radiation-related complications were observed in any animals.

7.2.2 Angiographic changes

Our study was able to demonstrate that angiographic evaluation of the fistula in the created animal model of the AVM could be performed. Although the angiographic features observed in this model do not completely resemble human AVMs, many similarities are present, such as a feeding artery and a draining vein (Figure 3.2). The angiography revealed narrowing and occlusion of the arterialised vein in animals at six and twelve weeks, although complete occlusion of the vein was not confirmed histologically. We believe that with the angiographic study we will be able to use this technique and progress to evaluating molecular targeting therapy at different time points without sacrificing the animals.

The primary limitation of the angiographic study was visualization of the nidus. The nidus in our model consisted of many small ipsilateral external jugular vein tributaries that could not be seen on the angiographic study.

7.2.3 Histological study

The histological study and immunohistochemistry with vWF provide more information about the characteristics of the animal model and how AVMs respond to radiation over different time points. We conclude that our AVM animal model responds to radiation in the same ways as have been documented in human studies. Neither the irradiated or non-irradiated animals showed any lumen obliteration or thrombosis. The endothelial cells were strongly stained with vWF, indicating that the endothelium was intact. We have confidence that the GKS irradiated model is suitable for future targeting therapy.

7.2.4 Blood flow measurement

This study provides some new insights into AVM haemodynamic changes resulting from GKS treatment. Our study supports our previous published results in non-irradiating AVM animal model, in that the blood flow increased over the time period. It incorporated a high flow shunt, and had an anatomic arrangement that resembles the human AVM [72]. More importantly, our study demonstrates a decrease in the blood flow after radiation at early time points, which becomes significant at 12 weeks, and shows that blood flow decreases before any histological or angiographic changes become evident. A decrease in blood flow before a significant anatomic change is apparent is well documented [151, 191, 665]. Again with this technique we will be able to measure the flow in several time points without the need to sacrifice the animals.

7.2.5 Vascular malformation endothelium molecular response

Several adhesive and thrombotic molecules have been investigated in this study. ICAM-1 expression was significantly increased in the GKS-treated group compared to the non-irradiated group; the expression was on the surface of the endothelial cell of irradiated tissue. PECAM-1 expression was unchanged in response to radiation. Early downregulation of Integrin beta 1 in irradiated tissues was observed compared to the non-irradiated controls. The upregulation of ICAM-1 expression in irradiated AVM ECs compared to PECAM-1 and Integrin beta 1 means that ICAM-1 is a potential target for vascular targeting therapy to accelerate thrombosis after radiosurgery.

Choosing the time for injection of anti–ICAM-1, for example after radiosurgery procedure, could be subject to change. The drug should be injected where there is a prothrombotic environment to ensure the best result. We have shown that TF a coagulation factor, starts to increase slightly one week after radiosurgery, and continues up to 12 weeks. Although other thrombotic molecules have not shown any changes, according to these results giving anti–

ICAM-1 after one week of radiosurgery procedure might produce a better thrombotic effect than injection at earlier time points.

7.3 Future directions

Several studies will follow this work. Many other EC molecules remains be investigated. These molecules include E-Selectin, VCAM-1, ESAM, Hmga2, Cadherin 5 and 13, and the spectrin beta chain. Molecular imaging study will further help to investigate the different molecules and their response to radiosurgery.

Primary AVM EC cultures and investigating the levels of circulating soluble adhesion and coagulation factors in AVM-irradiated patients will provide information about the expression of several molecules and their suitability for targeting. Also, a larger animal model study is needed to examine the effect of radiosurgery and to test the proposed molecular therapy.

Future steps in this project will be to prepare and optimise conjugates of anti-target antibodies with thrombotic agents. For example, the E-selectin: thrombin co-ligand and the I-CAM-1: thrombin co-ligand are being developed and will be tested using *in vivo* and *in vitro* studies. In addition, the conjugates will be tested using an *in vitro* thrombus formation system to determine their efficacy in inducing thrombus around irradiated human AVM endothelial cells. The conjugates will also be tested using *in vitro* cultured AVM vessels and *in vivo* animal models (small and large animals) for their efficacy in inducing thrombus after irradiation. Finally, clinical trials of this technique in AVM patients need to be conducted.

7.4 Conclusion

In the GKS treated group, two animals had partial angiographic obliteration of the AVM at six weeks and three animals had complete obliteration at 12 weeks. There was a statistically significant difference in the angiographic diameters in proximal and distal LEJV between the

treatment group and the control group ($P < 0.05$). Individual time point comparisons between the two groups did not show any statistically significant differences in the blood flow. Concentric subendothelial cell growth was identified in the irradiated AVMs at 6 weeks and 12 weeks with vessel wall thickening and luminal narrowing. However, the endothelial lining remained intact in both groups at all time points. The immunohistochemistry study revealed significant up regulation of ICAM-1 at all time points in the irradiated AVM compared to the non-irradiated AVM ($P < 0.05$). ICAM-1 was confined to the endothelial cell surface. Up regulation of TF expression in irradiated AVMs was identified at 1, 3, 6 and 12 weeks after irradiation. However, this did not reach significance.

This thesis demonstrates that the GKS-treated rat model is suitable for studying methods to enhance radiation response in AVMs. The experiment suggests that I-CAM-1 may be a suitable candidate for VTs. As TF starts to increase one week after GKS, co-ligand may be better injected at that time, which may help to achieve maximum prothrombotic effect.

References

1. Choi, J.H. and J.P. Mohr, *Brain arteriovenous malformations in adults.* The Lancet Neurology, 2005. **4**(5): p. 299-308.
2. Courville, C.B., *Intracranial tumors. Notes upon a series of three thousand verified cases with some current observations pertaining to their mortality.* Bull Los Angeles Neurol Soc, 1967. **32**(3): p. Suppl 2:1-80.
3. Stapf, C., et al., *Epidemiology and natural history of arteriovenous malformations.* Neurosurg Focus, 2001. **11**(5): p. e1.
4. Jellinger, K., *Vascular malformations of the central nervous system: A morphological overview.* Neurosurgical Review, 1986. **9**(3): p. 177-216.
5. McCormick, W.F., *The Pathology of Vascular ("Arteriovenous") Malformations.* Journal of Neurosurgery, 1966. **24**(4): p. 807-816.
6. Jessurun, G.A., et al., *Cerebral arteriovenous malformations in The Netherlands Antilles. High prevalence of hereditary hemorrhagic telangiectasia-related single and multiple cerebral arteriovenous malformations.* Clin Neurol Neurosurg, 1993. **95**(3): p. 193-8.
7. McCORMICK, W.F. and D.B. ROSENFIELD, *Massive Brain Hemorrhage: A Review of 144 Cases and an Examination of Their Causes.* Stroke, 1973. **4**(6): p. 946-954.
8. ApSimon, H.T., et al., *A Population-Based Study of Brain Arteriovenous Malformation: Long-Term Treatment Outcomes.* Stroke, 2002. **33**(12): p. 2794-2800.
9. Stapf, C., et al., *The New York Islands AVM Study: Design, Study Progress, and Initial Results.* Stroke, 2003. **34**(5): p. e29-e33.
10. Laakso, A. and J. Hernesniemi, *Arteriovenous Malformations: Epidemiology and Clinical Presentation.* Neurosurgery Clinics of North America, 2012. **23**(1): p. 1-6.
11. Bulsara, K.R., et al., *De novo cerebral arteriovenous malformation: case report.* Neurosurgery, 2002. **50**(5): p. 1137-40; discussion 1140-1.
12. Gonzalez, L.F., et al., *De novo presentation of an arteriovenous malformation. Case report and review of the literature.* J Neurosurg, 2005. **102**(4): p. 726-9.
13. Kim, H., et al., *Common variants in interleukin-1-Beta gene are associated with intracranial hemorrhage and susceptibility to brain arteriovenous malformation.* Cerebrovasc Dis, 2009. **27**(2): p. 176-82.
14. Achrol, A.S., et al., *Tumor necrosis factor-alpha-238G>A promoter polymorphism is associated with increased risk of new hemorrhage in the natural course of patients with brain arteriovenous malformations.* Stroke, 2006. **37**(1): p. 231-4.
15. Brouillard, P. and M. Vikkula, *Genetic causes of vascular malformations.* Human Molecular Genetics, 2007. **16**(R2): p. R140-R149.
16. Letteboer, T.G., et al., *Genotype-phenotype relationship in hereditary haemorrhagic telangiectasia.* J Med Genet, 2006. **43**(4): p. 371-7.
17. Pawlikowska, L., et al., *Polymorphisms in transforming growth factor-beta-related genes ALK1 and ENG are associated with sporadic brain arteriovenous malformations.* Stroke, 2005. **36**(10): p. 2278-80.

18. McAllister, K.A., et al., *Endoglin, a TGF-beta binding protein of endothelial cells, is the gene for hereditary haemorrhagic telangiectasia type 1.* Nat Genet, 1994. **8**(4): p. 345-51.
19. Johnson, D.W., et al., *Mutations in the activin receptor-like kinase 1 gene in hereditary haemorrhagic telangiectasia type 2.* Nat Genet, 1996. **13**(2): p. 189-95.
20. Mahmoud, M., et al., *Pathogenesis of Arteriovenous Malformations in the Absence of Endoglin.* Circulation Research, 2010. **106**(8): p. 1425-1433.
21. Park, S.O., et al., *Real-time imaging of de novo arteriovenous malformation in a mouse model of hereditary hemorrhagic telangiectasia.* J Clin Invest, 2009. **119**(11): p. 3487-96.
22. Roman, B.L., et al., *Disruption of acvrl1 increases endothelial cell number in zebrafish cranial vessels.* Development, 2002. **129**(12): p. 3009-19.
23. Chen, Y., et al., *MMP-9 expression is associated with leukocytic but not endothelial markers in brain arteriovenous malformations.* Front Biosci, 2006. **11**: p. 3121-8.
24. Chen, Y., et al., *Interleukin-6 involvement in brain arteriovenous malformations.* Ann Neurol, 2006. **59**(1): p. 72-80.
25. Chen, Y., et al., *Evidence of inflammatory cell involvement in brain arteriovenous malformations.* Neurosurgery, 2008. **62**(6): p. 1340-9; discussion 1349-50.
26. Hashimoto, T., et al., *Abnormal pattern of Tie-2 and vascular endothelial growth factor receptor expression in human cerebral arteriovenous malformations.* Neurosurgery, 2000. **47**(4): p. 910-8; discussion 918-9.
27. Hashimoto, T., et al., *Abnormal balance in the angiopoietin-tie2 system in human brain arteriovenous malformations.* Circ Res, 2001. **89**(2): p. 111-3.
28. Ceradini, D.J. and G.C. Gurtner, *Homing to hypoxia: HIF-1 as a mediator of progenitor cell recruitment to injured tissue.* Trends Cardiovasc Med, 2005. **15**(2): p. 57-63.
29. Ceradini, D.J., et al., *Progenitor cell trafficking is regulated by hypoxic gradients through HIF-1 induction of SDF-1.* Nat Med, 2004. **10**(8): p. 858-64.
30. Hashimoto, T., et al., *Evidence of increased endothelial cell turnover in brain arteriovenous malformations.* Neurosurgery, 2001. **49**(1): p. 124-31; discussion 131-2.
31. Heissig, B., et al., *Recruitment of stem and progenitor cells from the bone marrow niche requires MMP-9 mediated release of kit-ligand.* Cell, 2002. **109**(5): p. 625-37.
32. Crawford, P.M., et al., *Arteriovenous malformations of the brain: natural history in unoperated patients.* J Neurol Neurosurg Psychiatry, 1986. **49**(1): p. 1-10.
33. Itoyama, Y., et al., *Natural course of unoperated intracranial arteriovenous malformations: study of 50 cases.* J Neurosurg, 1989. **71**(6): p. 805-9.
34. Ondra, S.L., et al., *The natural history of symptomatic arteriovenous malformations of the brain: a 24-year follow-up assessment.* Journal of Neurosurgery, 1990. **73**(3): p. 387-391.
35. Yamada, S., et al., *Risk factors for subsequent hemorrhage in patients with cerebral arteriovenous malformations.* Journal of Neurosurgery, 2007. **107**(5): p. 965-972.
36. Brown, R.D., et al., *The natural history of unruptured intracranial arteriovenous malformations.* Journal of Neurosurgery, 1988. **68**(3): p. 352-357.

37. Brown, R.D., Jr., et al., *Incidence and prevalence of intracranial vascular malformations in Olmsted County, Minnesota, 1965 to 1992.* Neurology, 1996. **46**(4): p. 949-52.
38. Fults, D. and D.L. Kelly, Jr., *Natural history of arteriovenous malformations of the brain: a clinical study.* Neurosurgery, 1984. **15**(5): p. 658-62.
39. Turjman, F., et al., *Epilepsy associated with cerebral arteriovenous malformations: a multivariate analysis of angioarchitectural characteristics.* AJNR Am J Neuroradiol, 1995. **16**(2): p. 345-50.
40. Halim, A.X., et al., *Longitudinal risk of intracranial hemorrhage in patients with arteriovenous malformation of the brain within a defined population.* Stroke, 2004. **35**(7): p. 1697-1702.
41. Al-Shahi, R., et al., *Prospective, population-based detection of intracranial vascular malformations in adults: the Scottish Intracranial Vascular Malformation Study (SIVMS).* Stroke, 2003. **34**(5): p. 1163-9.
42. Stapf, C., et al., *Incidence of Adult Brain Arteriovenous Malformation Hemorrhage in a Prospective Population-Based Stroke Survey.* Cerebrovascular Diseases, 2002. **13**(1): p. 43-46.
43. Stapf, C., et al., *Invasive treatment of unruptured brain arteriovenous malformations is experimental therapy.* Curr Opin Neurol, 2006. **19**(1): p. 63-8.
44. Graf, C.J., G.E. Perret, and J.C. Torner, *Bleeding from cerebral arteriovenous malformations as part of their natural history.* J Neurosurg, 1983. **58**(3): p. 331-7.
45. Hillman, J., *Population-based analysis of arteriovenous malformation treatment.* Journal of Neurosurgery, 2001. **95**(4): p. 633-637.
46. Svien, H.J. and J.A. Mcrae, *Arteriovenous Anomalies of the Brain.* Journal of Neurosurgery, 1965. **23**(1): p. 23-28.
47. Crawford, P.M., et al., *Arteriovenous malformations of the brain: natural history in unoperated patients.* Journal of Neurology, Neurosurgery & Psychiatry, 1986. **49**(1): p. 1-10.
48. Morgan, M.K., et al., *Delayed neurological deterioration following resection of arteriovenous malformations of the brain.* Journal of Neurosurgery, 1999. **90**(4): p. 695-701.
49. Hartmann, A., et al., *Morbidity of Intracranial Hemorrhage in Patients With Cerebral Arteriovenous Malformation.* Stroke, 1998. **29**(5): p. 931-934.
50. Khaw, A.V., et al., *Association of Infratentorial Brain Arteriovenous Malformations With Hemorrhage at Initial Presentation.* Stroke, 2004. **35**(3): p. 660-663.
51. Hofmeister, C., et al., *Demographic, Morphological, and Clinical Characteristics of 1289 Patients With Brain Arteriovenous Malformation.* Stroke, 2000. **31**(6): p. 1307-1310.
52. Kondziolka, D., L.D. Lunsford, and J.R.W. Kestle, *The natural history of cerebral cavernous malformations.* Journal of Neurosurgery, 1995. **83**(5): p. 820-824.
53. Mast, H., et al., *Risk of spontaneous haemorrhage after diagnosis of cerebral arteriovenous malformation.* Lancet, 1997. **350**(9084): p. 1065-1068.
54. Pellettieri, L., et al., *Surgical versus conservative treatment of intracranial arteriovenous malformations: a study in surgical decision-making.* Acta Neurochirurgica, Supplement, 1979. **29**: p. 1-86.

55. Graf, C.J., G.E. Perret, and J.C. Torner, *Bleeding from cerebral AVM's as part of their natural history.* J Neurosurg, 1983. **58**: p. 331.
56. Crawford, P.M., et al., *Arteriovenous malformations of the brain: Natural history in unoperated patients.* Journal of Neurology Neurosurgery and Psychiatry, 1986. **49**(1): p. 1-10.
57. Stefani, M.A., et al., *Large and deep brain arteriovenous malformations are associated with risk of future hemorrhage.* Stroke, 2002. **33**(5): p. 1220-1224.
58. Fults, D. and D.L. Kelly Jr, *Natural history of arteriovenous malformations of the brain: A clinical study.* Neurosurgery, 1984. **15**(5): p. 658-662.
59. Brown Jr, R.D., D.O. Wiebers, and G.S. Forbes, *Unruptured intracranial aneurysms and arteriovenous malformations: Frequency of intracranial hemorrhage and relationship of lesions.* Journal of Neurosurgery, 1990. **73**(6): p. 859-863.
60. Hartmann, A., et al., *Morbidity of intracranial hemorrhage in patients with cerebral arteriovenous malformation.* Stroke, 1998. **29**(5): p. 931-934.
61. Turjman, F., et al., *Correlation of the angioarchitectural features of cerebral arteriovenous malformations with clinical presentation of hemorrhage.* Neurosurgery, 1995. **37**(5): p. 856-862.
62. Choi, J.H. and J.P. Mohr, *Brain arteriovenous malformations in adults.* Lancet Neurol, 2005. **4**(5): p. 299-308.
63. Zabramski, J.M., J.S. Henn, and S. Coons, *Pathology of cerebral vascular malformations.* Neurosurg Clin N Am, 1999. **10**(3): p. 395-410.
64. Doppaman J, L.L., Ommaya A, Kondzziolka D, , *obliteration of spinal-cord arteriovenous malformations with bucrylate: experience in 46 cases* Lancet Neurol, 1968: p. 477.
65. Grzyska, U. and J. Fiehler, *Pathophysiology and treatment of brain AVMs.* Klin Neuroradiol, 2009. **19**(1): p. 82-90.
66. Challa, V.R., D.M. Moody, and W.R. Brown, *Vascular malformations of the central nervous system.* J Neuropathol Exp Neurol, 1995. **54**(5): p. 609-21.
67. Yamada, S., et al., *Concept of arteriovenous malformation compartments and surgical management.* Neurol Res, 2004. **26**(3): p. 288-300.
68. Drake, C.G., *Cerebral arteriovenous malformations: considerations for and experience with surgical treatment in 166 cases.* Clin Neurosurg, 1979. **26**: p. 145-208.
69. SM, Y., *Arteriovenous Malformations in Functional Areas of the Brain*. 1990, Armonk: Futura.
70. Hecht, S.T., J.A. Horton, and C.W. Kerber, *Hemodynamics of the central nervous system arteriovenous malformation nidus during particulate embolization. A computer model.* Neuroradiology, 1991. **33**(1): p. 62-4.
71. Okazaki H, S.B., *Atlas of neuropathology*, in *Atlas of neuropathology*. 1988, gower: New york.
72. Tu, J., et al., *Comparison of an animal model of arteriovenous malformation with human arteriovenous malformation.* Journal of Clinical Neuroscience, 2010. **17**(1): p. 96-102.

73. Takashima, S. and L.E. Becker, *Neuropathology of cerebral arteriovenous malformations in children.* Journal of Neurology, Neurosurgery & Psychiatry, 1980. **43**(5): p. 380-385.
74. Bradac, G.B., *Cerebral Angiography, Normal Anatomy and Vascular Pathology*. 2011: springer-verlag Berlin Heidelberg.
75. Tu, J., et al., *Ultrastructure of Perinidal Capillaries in Cerebral Arteriovenous Malformations.* Neurosurgery, 2006. **58**(5): p. 961-970 10.1227/01.NEU.0000210248.39504.B5.
76. Koch, A.E., et al., *Angiogenesis mediated by soluble forms of E-selectin and vascular cell adhesion molecule-1*. Nature, 1995. **376**(6540): p. 517-9.
77. Karunanyaka A, T.J., Watling AM, Storer KP, Windsor AA, Stoodley MA, *Endothelial molecular changes in a rodent model of arteriovenous malformation Laboratory investigation.* Journal of neurosurgery, 2008. **109**(6): p. 1165-1172.
78. Storer, K.P., et al., *Inflammatory molecule expression in cerebral arteriovenous malformations.* Journal of Clinical Neuroscience, 2008. **15**(2): p. 179-184.
79. Uranishi, R., *Further Study of CD31 Protein and Messenger Ribonucleic Acid Expression in Human Cerebral Vascular Malformations.* Neurosurgery, 2002. **50**(1): p. 110-115.
80. Shenkar, R., *Differential gene expression in human cerebrovascular malformations.* Neurosurgery, 2003. **52**(2): p. 465-478.
81. Koizumi, T., *Expression of Vascular Endothelial Growth Factors and Their Receptors in and around Intracranial Arteriovenous Malformations.* Neurosurgery, 2002. **50**(1): p. 117-124.
82. Kiliç, T., *Expression of structural proteins and angiogenic factors in cerebrovascular anomalies.* Neurosurgery, 2000. **46**(5): p. 1179.
83. Rothbart, D., et al., *Expression of angiogenic factors and structural proteins in central nervous system vascular malformations.* Neurosurgery, 1996. **38**(5): p. 915-24; discussion 924-5.
84. Sonstein, W.J., et al., *Expression of vascular endothelial growth factor in pediatric and adult cerebral arteriovenous malformations: an immunocytochemical study.* J Neurosurg, 1996. **85**(5): p. 838-45.
85. Hashimoto, T., et al., *Abnormal Balance in the Angiopoietin-Tie2 System in Human Brain Arteriovenous Malformations.* Circulation Research, 2001. **89**(2): p. 111-113.
86. Isoda, K., et al., *Arteriovenous malformation of the brain. Histological study and micrometric measurement of abnormal vessels.* Acta Pathologica Japonica, 1981. **31**(5): p. 883-893.
87. Yamada, S., *Arteriovenous malformations in the functional area: Surgical treatment and regional cerebral blood flow.* Neurological Research, 1982. **4**(3-4): p. 283-322.
88. Wolpert, S.M., F.J. Barnett, and R.J. Prager, *Benefits of embolization without surgery for cerebral arteriovenous malformations.* American Journal of Roentgenology, 1982. **138**(1): p. 99-102.
89. Nichols WW, O.R.M., *McDonald's blood flow in arteries. Theoretic, experimental and clinical principles, third edn. London Edward Arnold.* 1990. **62**.

90. Holman, E., *The development of arterial aneurysms.* Surgery, gynecology & obstetrics, 1955. **100**(5): p. 599.
91. Nornes, H. and A. Grip, *Hemodynamic aspects of cerebral arteriovenous malformations.* Journal of Neurosurgery, 1980. **53**(4): p. 456-464.
92. Davies, P.F., et al., *Turbulent fluid shear stress induces vascular endothelial cell turnover in vitro.* Proceedings of the National Academy of Sciences of the United States of America, 1986. **83**(7): p. 2114-2117.
93. Davies, P.F., et al., *Influence of hemodynamic forces on vascular endothelial function. In vitro studies of shear stress and pinocytosis in bovine aortic cells.* Journal of Clinical Investigation, 1984. **73**(4): p. 1121-1129.
94. Masuda, H., et al., *Flow loaded canine carotid artery. I. A morphometric study of microfilament bundles in endothelial cells.* Acta Pathologica Japonica, 1986. **36**(12): p. 1833-1842.
95. Masuda, H., et al., *Flow loaded canine carotid artery. II. Ultrastructural changes in the subendothelial layer.* Acta Pathologica Japonica, 1987. **37**(2): p. 239-251.
96. Smith, R.L., et al., *Thrombus production by turbulence.* Journal of applied physiology, 1972. **32**(2): p. 261-264.
97. Hassler, W. and H. Steinmetz, *Cerebral hemodynamics in angioma patients: An intraoperative study.* Journal of Neurosurgery, 1987. **67**(6): p. 822-831.
98. Young, W.L., et al., *Evidence for adaptive autoregulatory displacement in hypotensive cortical territories adjacent to arteriovenous malformations.* Neurosurgery, 1994. **34**(4): p. 601-611.
99. Sorimachi, T., et al., *Blood pressure monitoring in feeding arteries of cerebral arteriovenous malformations during embolization: A preventive role in hemodynamic complications.* Neurosurgery, 1995. **37**(6): p. 1041-1048.
100. Fogarty-Mack, P., et al., *The effect of arteriovenous malformations on the distribution of intracerebral arterial pressures.* American Journal of Neuroradiology, 1996. **17**(8): p. 1443-1449.
101. Fleischer, L.H., et al., *Relationship of transcranial Doppler flow velocities and arteriovenous malformation feeding artery pressures.* Stroke, 1993. **24**(12): p. 1897-1902.
102. Morgan, M. and M. Winder, *Haemodynamics of arteriovenous malformations of the brain and consequences of resection: a review.* Journal of Clinical Neuroscience, 2001. **8**(3): p. 216-224.
103. Young, W.L., et al., *Arteriovenous malformation draining vein physiology and determinants of transnidal pressure gradients.* Neurosurgery, 1994. **35**(3): p. 389-396.
104. Murayama, Y., et al., *Transvenous hemodynamic assessment of arteriovenous malformations and fistulas: Preliminary clinical experience in Doppler guidewire monitoring of embolotherapy.* Stroke, 1996. **27**(8): p. 1358-1364.
105. Yassari, R., et al., *Angiographic, hemodynamic and histological characterization of an arteriovenous fistula in rats.* Acta Neurochirurgica, 2004. **146**(5): p. 495-504.
106. Massoud, T.F., *Histopathologic characteristics of a chronic arteriovenous malformation in a swine model: Preliminary study.* American journal of neuroradiology : AJNR, 2000. **21**(7): p. 1268-1276.

107. Qian, Z., *A simplified arteriovenous malformation model in sheep: Feasibility study.* American journal of neuroradiology : AJNR, 1999. **20**(5): p. 765-770.
108. Pietil, x000E, and T. A., *Animal Model for Cerebral Arteriovenous Malformation.* Acta neurochirurgica, 2000. **142**(11): p. 1231-1240.
109. Lemson, M.S., *A New Animal Model to Study Intimal Hyperplasia in Arteriovenous Fistulas.* The Journal of surgical research, 1999. **85**(1): p. 51-58.
110. De Salles, A.A., et al., *Arteriovenous malformation animal model for radiosurgery: the rete mirabile.* American Journal of Neuroradiology, 1996. **17**(8): p. 1451-8.
111. Becker, T.A., *In Vivo Assessment of Calcium Alginate Gel for Endovascular Embolization of a Cerebral Arteriovenous Malformation Model Using the Swine Rete Mirabile.* Neurosurgery, 2002. **51**(2): p. 453-459.
112. Altschuler, E., *Radiobiologic models for radiosurgery.* Neurosurgery clinics of North America, 1992. **3**(1): p. 61-77.
113. Baker, S.R., *Radiation effects on microvascular anastomosis.* Archives of oto-rhino-laryngology, 1978. **104**(2): p. 103-107.
114. Bederson, J.B., *Intracranial venous hypertension and the effects of venous outflow obstruction in a rat model of arteriovenous fistula.* Neurosurgery, 1991. **29**(3): p. 341-350.
115. Hai, J., et al., *A new rat model of chronic cerebral hypoperfusion associated with arteriovenous malformations.* Journal of Neurosurgery, 2002. **97**(5): p. 1198-1202.
116. Yamada, M., et al., *Chronic cerebral venous hypertension model in rats.* Neurological Research, 2003. **25**(7): p. 694-696.
117. Sho, E., *Arterial enlargement, tortuosity, and intimal thickening in response to sequential exposure to high and low wall shear stress.* Journal of vascular surgery, 2004. **39**(3): p. 601-612.
118. Scott, B.B., *Vascular dynamics of an experimental cerebral arteriovenous shunt in the primate.* Surgical neurology, 1978. **10**(1): p. 34-38.
119. Morgan, M.K., *The effects of hyperventilation on cerebral blood flow in the rat with an open and closed carotid-jugular fistula.* Neurosurgery, 1989. **25**(4): p. 606-612.
120. Stüer, C., *Evidence for a Predominant Intrinsic Sympathetic Control of Cerebral Blood Flow Alterations in an Animal Model of Cerebral Arteriovenous Malformation.* Translational stroke research, 2010. **1**(3): p. 210-219.
121. Hashimoto, N., et al., *Surgery of cerebral arteriovenous malformations.* Neurosurgery, 2007. **61**(1): p. SHC-375-SHC-389.
122. Surdell, D.L., S. Bhattacharjee, and C.M. Loftus, *Pros, cons, and current indications of open craniotomy <i xmlns="*http://pub2web.metastore.ingenta.com/ns/*> gamma knife in the treatment of arteriovenous malformations and the role of endovascular embolization.* Neurological Research, 2002. **24**(4): p. 347-353.
123. Spetzler, R.F. and N.A. Martin, *A proposed grading system for arteriovenous malformations.* Journal of Neurosurgery, 1986. **65**(4): p. 476-483.
124. Friedlander, R.M., *Arteriovenous malformations of the brain.* New England Journal of Medicine, 2007. **356**(26): p. 2704-2712.
125. Han, P.P., F.A. Ponce, and R.F. Spetzler, *Intention-to-treat analysis of Spetzler-Martin grades IV and V arteriovenous malformations: natural history and treatment paradigm.* J Neurosurg, 2003. **98**(1): p. 3-7.

126. Hamilton, M.G., et al., *The prospective application of a grading system for arteriovenous malformations.* Neurosurgery, 1994. **34**(1): p. 2-7.
127. Heros, R.C., K. Korosue, and P.M. Diebold, *Surgical excision of cerebral arteriovenous malformations: late results.* Neurosurgery, 1990. **26**(4): p. 570-578.
128. Sisti, M.B., A. Kader, and B.M. Stein, *Microsurgery for 67 intracranial arteriovenous malformations less than 3 cm in diameter.* Journal of Neurosurgery, 1993. **79**(5): p. 653-660.
129. Pasqualin, A., et al., *The relevance of anatomic and hemodynamic factors to a classification of Cerebral arteriovenous malformations.* Neurosurgery, 1991. **28**(3): p. 370-379.
130. Clarke, R. and V. Horsley, *On a method of investigating the deep ganglia and tracts of the central nervous system (cerebellum).* The British Medical Journal, 1906. **2**(2399): p. 1799-1800.
131. Horsley, V., *The Linacre Lecture ON THE FUNCTION OF THE SO-CALLED MOTOR AREA OF THE BRAIN: Delivered to the Master and Fellows of St. John's College, Cambridge, May 6th, 1909.* Br Med J, 1909. **2**(2533): p. 121-32.
132. Schaltenbrand, G., *Personal Observations on the Development of Stereotaxy.* Stereotactic and Functional Neurosurgery, 1975. **37**(4): p. 410-416.
133. Spiegel, E.A., et al., *Stereotaxic Apparatus for Operations on the Human Brain.* Science, 1947. **106**(2754): p. 349-50.
134. Spiegel, E.A., *Methodological problems in stereoencephalotomy.* Confin Neurol, 1965. **26**(3): p. 125-32.
135. Gildenberg, P.L. and J.K. Krauss, *History of Stereotactic Surgery*, in *Textbook of Stereotactic and Functional Neurosurgery*, A. Lozano, P. Gildenberg, and R. Tasker, Editors. 2009, Springer Berlin Heidelberg. p. 1-33.
136. Leksell, L., *The stereotaxic method and radiosurgery of the brain.* Acta Chir Scand, 1951. **102**(4): p. 316-9.
137. Leksell, L., et al., *Lesions in the depth of the brain produced by a beam of high energy protons.* Acta radiol, 1960. **54**: p. 251-64.
138. Woodruff, K.H., et al., *Delayed sequelae of pituitary irradiation.* Hum Pathol, 1984. **15**(1): p. 48-54.
139. Betti, O.O. and V.E. Derechinsky, *Hyperselective Encephalic Irradiation with Linear Accelerator*, in *Advances in Stereotactic and Functional Neurosurgery 6*, J. Gybels, et al., Editors. 1984, Springer Vienna. p. 385-390.
140. Lutz, W., K.R. Winston, and N. Maleki, *A system for stereotactic radiosurgery with a linear accelerator.* Int J Radiat Oncol Biol Phys, 1988. **14**(2): p. 373-81.
141. Adler, J.R., Jr., et al., *The Cyberknife: a frameless robotic system for radiosurgery.* Stereotact Funct Neurosurg, 1997. **69**(1-4 Pt 2): p. 124-8.
142. Giorgi, C. and A. Cossu, *Robotics and Radiosurgery*, in *Principles and Practice of Stereotactic Radiosurgery*, L. Chin and W. Regine, Editors. 2008, Springer New York. p. 163-170.
143. Chang, S.D. and J.R. Adler, *Robotics and radiosurgery–the cyberknife.* Stereotactic and functional neurosurgery, 2002. **76**(3-4): p. 204-208.
144. Schweikard, A., et al., *Robotic motion compensation for respiratory movement during radiosurgery.* Computer Aided Surgery, 2000. **5**(4): p. 263-277.

145. Steiner, L., et al., *Stereotaxic radiosurgery for cerebral arteriovenous malformations. Report of a case.* Acta Chir Scand, 1972. **138**(5): p. 459-64.
146. Colombo, F., et al., *Early results of CyberKnife radiosurgery for arteriovenous malformations.* Journal of Neurosurgery, 2009. **111**(4): p. 807-819.
147. National Guideline, C. *Stereotactic radiosurgery for patients with intracranial arteriovenous malformations (AVM).* 10/17/2013]; Available from: http://www.guideline.gov/content.aspx?id=14723.
148. Steinberg, G.K., et al., *Stereotactic heavy-charged-particle Bragg-peak radiation for intracranial arteriovenous malformations.* New England Journal of Medicine, 1990. **323**(2): p. 96-101.
149. Lunsford, L.D., et al., *Stereotactic radiosurgery for arteriovenous malformations of the brain.* Journal of Neurosurgery, 1991. **75**(4): p. 512-524.
150. Yamamoto, Y., et al., *Interim report on the radiosurgical treatment of cerebral arteriovenous malformations. The influence of size, dose, time, and technical factors on obliteration rate.* Journal of Neurosurgery, 1995. **83**(5): p. 832-837.
151. Pollock, B.E., et al., *Hemorrhage risk after stereotactic radiosurgery of cerebral arteriovenous malformations.* Neurosurgery, 1996. **38**(4): p. 652-661.
152. Ellis, T.L., et al., *Analysis of treatment failure after radiosurgery for arteriovenous malformations.* Journal of Neurosurgery, 1998. **89**(1): p. 104-110.
153. Kwon, Y., et al., *Analysis of the causes of treatment failure in gamma knife radiosurgery for intracranial arteriovenous malformations.* Journal of Neurosurgery, 2000. **93**(SUPPL. 3): p. 104-106.
154. Colombo, F., et al., *Three-dimensional angiography for radiosurgical treatment planning for arteriovenous malformations.* J Neurosurg, 2003. **98**(3): p. 536-43.
155. Karlsson, B., I. Lax, and M. Soderman, *Risk for hemorrhage during the 2-year latency period following gamma knife radiosurgery for arteriovenous malformations.* Int J Radiat Oncol Biol Phys, 2001. **49**(4): p. 1045-51.
156. Pollock, B.E., et al., *Factors associated with successful arteriovenous malformation radiosurgery.* Neurosurgery, 1998. **42**(6): p. 1239-44; discussion 1244-7.
157. Flickinger, J.C., et al., *An analysis of the dose-response for arteriovenous malformation radiosurgery and other factors affecting obliteration.* Radiother Oncol, 2002. **63**(3): p. 347-54.
158. Friedman, W.A., et al., *Analysis of factors predictive of success or complications in arteriovenous malformation radiosurgery.* Neurosurgery, 2003. **52**(2): p. 296-307; discussion 307-8.
159. Pollock, B.E., et al., *Hemorrhage risk after stereotactic radiosurgery of cerebral arteriovenous malformations.* Neurosurgery, 1996. **38**(4): p. 652-9; discussion 659-61.
160. Friedman, W.A., *Stereotactic Radiosurgery of Intracranial Arteriovenous Malformations.* Neurosurgery Clinics of North America, 2013. **24**(4): p. 561-574.
161. Steiner, L., *Treatment of arteriovenous malformations by radiosurgery.* Intracranial Arteriovenous Malformations. Baltimore: Williams & Wilkins, 1984: p. 295-313.
162. Steiner, L., et al., *Stereotactic radiosurgery in intracranial arterio-venous malformations.* Acta Neurochirurgica, 1974. **Suppl 21**: p. 195-209.
163. Steiner, L., et al., *Stereotaxic radiosurgery for cerebral arteriovenous malformations. Report of a case.* Acta Chirurgica Scandinavica, 1972. **138**(5): p. 459-464.

164. Germano, I., *LINAC and gamma knife radiosurgery*. 2000: Thieme.
165. Karlsson, B., C. Lindquist, and L. Steiner, *Prediction of obliteration after gamma knife surgery for cerebral arteriovenous malformations.* Neurosurgery, 1997. **40**(3): p. 425-431.
166. Shin, M., et al., *Analysis of nidus obliteration rates after gamma knife surgery for arteriovenous malformations based on long-term follow-up data: The University of Tokyo experience.* Journal of Neurosurgery, 2004. **101**(1): p. 18-24.
167. Kemeny, A.A., P.S. Dias, and D.M.C. Forster, *Results of stereotactic radiosurgery of arteriovenous malformations: An analysis of 52 cases.* Journal of Neurology Neurosurgery and Psychiatry, 1989. **52**(5): p. 554-558.
168. Pollock, B., *Intracranial Stereotactic Radiosurgery, an Issue of Neurosurgery Clinics*. 2013: Elsevier - Health Sciences Division.
169. Betti, O.O., C. Munari, and R. Rosler, *Stereotactic radiosurgery with the linear accelerator: treatment of arteriovenous malformations.* Neurosurgery, 1989. **24**(3): p. 311-321.
170. Betti, O.O., *Treatment of arteriovenous malformations with the linear accelerator.* Applied Neurophysiology, 1987. **50**(1-6): p. 262.
171. Andrade-Souza, Y.M., et al., *Radiosurgical treatment for rolandic arteriovenous malformations.* Journal of Neurosurgery, 2006. **105**(5): p. 689-697.
172. Colombo, F., et al., *Linear accelerator radiosurgery of cerebral arteriovenous malformations.* Neurosurgery, 1989. **24**(6): p. 833-840.
173. Souhami, L., et al., *Radiosurgery of cerebral arteriovenous malformations with the dynamic stereotactic irradiation.* International Journal of Radiation Oncology Biology Physics, 1990. **19**(3): p. 775-782.
174. Loeffler, J.S., et al., *Stereotactic radiosurgery for intracranial arteriovenous malformations using a standard linear accelerator.* International Journal of Radiation Oncology Biology Physics, 1989. **17**(3): p. 673-677.
175. Kjellberg, R.N., et al., *Bragg-peak proton-beam therapy for arteriovenous malformations of the brain.* New England Journal of Medicine, 1983. **309**(5): p. 269-274.
176. Szeifert, G.T., O. Major, and A.A. Kemeny, *Ultrastructural changes in arteriovenous malformations after gamma knife surgery: an electron microscopic study.* Special Supplements, 2005. **102**(s_supplement): p. 289-292.
177. Oppenheim, C., et al., *Radiosurgery of cerebral arteriovenous malformations: is an early angiogram needed?* AJNR Am J Neuroradiol, 1999. **20**(3): p. 475-81.
178. Tu, J., et al., *Responses of arteriovenous malformations to radiosurgery: Ultrastructural changes.* Neurosurgery, 2006. **58**(4): p. 749-757.
179. Yamamoto, M., et al., *Gamma knife radiosurgery for cerebral arteriovenous malformations: An autopsy report focusing on irradiation-induced changes observed in nidus- unrelated arteries.* Surgical Neurology, 1995. **44**(5): p. 421-427.
180. Yamamoto, M., *Long-term results of radiosurgery for arteriovenous malformation: Neurodiagnostic imaging and histological studies of angiographically confirmed nidus obliteration.* Surgical neurology, 1992. **37**(3): p. 219-230.

181. Schneider, B.F., D.A. Eberhard, and L.E. Steiner, *Histopathology of arteriovenous malformations after gamma knife radiosurgery.* Journal of Neurosurgery, 1997. **87**(3): p. 352-357.
182. Storer, K.P., et al., *Thrombotic molecule expression in cerebral vascular malformations.* Journal of Clinical Neuroscience, 2007. **14**(10): p. 975-980.
183. Liu, S., et al., *Molecular responses of brain endothelial cells to radiation in a mouse model.* Journal of Clinical Neuroscience, 2012. **19**(8): p. 1154-1158.
184. Simonian, M., *Detection of endothelial cell surface proteins following irradiation as potential targets for brain arteriovenous malformations.* 2nd internation Confernce and exhibition on metabolomics and system bilology 2013.
185. Ellis, T.L., et al., *Analysis of treatment failure after radiosurgery for arteriovenous malformations.* Journal of Neurosurgery, 1998. **89**(1): p. 104-111.
186. Pollock, B.E., et al., *Factors associated with successful arteriovenous malformation radiosurgery.* Neurosurgery, 1998. **42**(6): p. 1239-1244.
187. Pollock, B.E., et al., *Repeat stereotactic radiosurgery of arteriovenous malformations: Factors associated with incomplete obliteration.* Neurosurgery, 1996. **38**(2): p. 318-324.
188. Karlsson, B., I. Lax, and M. Söderman, *Factors influencing the risk for complications following Gamma Knife radiosurgery of cerebral arteriovenous malformations.* Radiotherapy and Oncology, 1997. **43**(3): p. 275-280.
189. Yamamoto, M., et al., *Gamma knife radiosurgery for arteriovenous malformations: Long-term follow-up results focusing on complications occurring more than 5 years after irradiation.* Neurosurgery, 1996. **38**(5): p. 906-914.
190. Gallina, P., et al., *Failure in radiosurgery treatment of cerebral arteriovenous malformations.* Neurosurgery, 1998. **42**(5): p. 996-1002; discussion 1002-4.
191. Zipfel, G.J., et al., *Do the morphological characteristics of arteriovenous malformations affect the results of radiosurgery?* Journal of Neurosurgery, 2004. **101**(3): p. 393-401.
192. Pollock, B.E. and J.C. Flickinger, *A proposed radiosurgery-based grading system for arteriovenous malformations.* Journal of Neurosurgery, 2002. **96**(1): p. 79-85.
193. Pollock, B.E., D.A. Gorman, and R.J. Coffey, *Patient outcomes after arteriovenous malformation radiosurgical management: results based on a 5-to 14-year follow-up study.* Neurosurgery, 2003. **52**(6): p. 1291-1297.
194. Han, P.P., F.A. Ponce, and R.F. Spetzler, *Intention-to-treat analysis of Spetzler—Martin Grades IV and V arteriovenous malformations: natural history and treatment paradigm.* Journal of Neurosurgery, 2003. **98**(1): p. 3-7.
195. Ferch, R.D. and M.K. Morgan, *High-grade arteriovenous malformations andtheir management.* Journal of Clinical Neuroscience, 2002. **9**(1): p. 37-40.
196. Hoh, D.J., et al., *Chained lightning: part III--Emerging technology, novel therapeutic strategies, and new energy modalities for radiosurgery.* Neurosurgery. **61**(6): p. 1111-29; discussion 1129-30.
197. Thorpe, P.E., *Vascular Targeting Agents as Cancer Therapeutics.* Clinical Cancer Research, 2004. **10**(2): p. 415-427.

198. Storer, K., et al., *Coadministration of Low‐Dose Lipopolysaccharide and Soluble Tissue Factor Induces Thrombosis After Radiosurgery in An Animal Arteriovenous Malformation Model.* Neurosurgery, 2007. **61**(3): p. 604-611 10.1227/01.NEU.0000290909.32600.A8.
199. Ran, S. and P.E. Thorpe, *Phosphatidylserine is a marker of tumor vasculature and a potential target for cancer imaging and therapy.* International Journal of Radiation Oncology*Biology*Physics, 2002. **54**(5): p. 1479-1484.
200. He, J., T.A. Luster, and P.E. Thorpe, *Radiation-Enhanced Vascular Targeting of Human Lung Cancers in Mice with a Monoclonal Antibody That Binds Anionic Phospholipids.* Clinical Cancer Research, 2007. **13**(17): p. 5211-5218.
201. Otto, F., et al., *Phase II trial of intravenous endotoxin in patients with colorectal and non-small cell lung cancer.* European Journal of Cancer, 1996. **32**(10): p. 1712-1718.
202. Levi, M. and H. ten Cate, *Disseminated Intravascular Coagulation.* New England Journal of Medicine, 1999. **341**(8): p. 586-592.
203. Shenkar, R., et al., *Differential gene expression in human cerebrovascular malformations.* Neurosurgery, 2003. **52**(2): p. 465.
204. Awad, I.A., *Unfolding knowledge on cerebral cavernous malformations.* Surgical neurology, 2005. **63**(4): p. 317-318.
205. Tu, J., et al., *Responses of Arteriovenous Malformations to Radiosurgery: Ultrastructural Changes.* Neurosurgery, 2006. **58**(4): p. 749-758 10.1227/01.NEU.0000192360.87083.90.
206. Heidelberger, C., et al., *Fluorinated pyrimidines. VI. Effects of 5-fluorouridine and 5-fluoro-2'-deoxyuridine on transplanted tumors.* Proc Soc Exp Biol Med, 1958. **97**(2): p. 470-5.
207. Nigro, N.D., V.K. Vaitkevicius, and B. Considine, Jr., *Combined therapy for cancer of the anal canal: a preliminary report. 1974.* Dis Colon Rectum, 1993. **36**(7): p. 709-11.
208. Lawrence, T.S., J.E. Tepper, and A.W. Blackstock, *Fluoropyrimidine-Radiation Interactions in Cells and Tumors.* Semin Radiat Oncol, 1997. **7**(4): p. 260-266.
209. Rich, T.A., *Infusional chemoradiation for rectal and anal cancers.* Oncology (Williston Park), 1999. **13**(10 Suppl 5): p. 131-4.
210. Whittington, R., et al., *Protracted intravenous fluorouracil infusion with radiation therapy in the management of localized pancreaticobiliary carcinoma: a phase I Eastern Cooperative Oncology Group Trial.* Journal of Clinical Oncology, 1995. **13**(1): p. 227-32.
211. Richmond, R.C., *Toxic variability and radiation sensitization by dichlorodiammineplatinum(II) complexes in Salmonella typhimurium cells.* Radiat Res, 1984. **99**(3): p. 596-608.
212. Amorino, G.P., et al., *Radiopotentiation by the oral platinum agent, JM216: role of repair inhibition.* Int J Radiat Oncol Biol Phys, 1999. **44**(2): p. 399-405.
213. J. Moreland, N., et al., *Modulation of Drug Resistance Mediated by Loss of Mismatch Repair by the DNA Polymerase Inhibitor Aphidicolin.* Cancer Research, 1999. **59**(9): p. 2102-2106.
214. Yang, L.X., E.B. Douple, and H.J. Wang, *Irradiation enhances cellular uptake of carboplatin.* Int J Radiat Oncol Biol Phys, 1995. **33**(3): p. 641-6.

215. Prost, P., M. Ychou, and D. Azria, *[Gemcitabine and pancreatic cancer]*. Bull Cancer, 2002. **89 Spec No**: p. S91-5.
216. Rothenberg, M.L., et al., *A phase II trial of gemcitabine in patients with 5-FU-refractory pancreas cancer.* Ann Oncol, 1996. **7**(4): p. 347-53.
217. Sandler AB, A.R., McClean J, *A Hoosier Oncology Group phase II study of gemcitabine plus cisplatin in non-small-cell lung cancer.* Proc Am Soc Clin Oncol . , 1995.
218. Iaffaioli, R.V., et al., *Phase I-II Study of Gemcitabine and Carboplatin in Stage IIIB-IV Non–Small-Cell Lung Cancer.* Journal of Clinical Oncology, 1999. **17**(3): p. 921.
219. Chen, A.Y., H. Choy, and M.L. Rothenberg, *DNA topoisomerase I-targeting drugs as radiation sensitizers.* Oncology-Huntington, 1999. **13**(5): p. 39-46.
220. Chen, A.Y., et al., *Mammalian DNA Topoisomerase I Mediates the Enhancement of Radiation Cytotoxicity by Camptothecin Derivatives.* Cancer Research, 1997. **57**(8): p. 1529-1536.
221. Huang, S.M. and P.M. Harari, *Epidermal growth factor receptor inhibition in cancer therapy: biology, rationale and preliminary clinical results.* Invest New Drugs, 1999. **17**(3): p. 259-69.
222. Huang, S.-M. and P.M. Harari, *Modulation of Radiation Response after Epidermal Growth Factor Receptor Blockade in Squamous Cell Carcinomas: Inhibition of Damage Repair, Cell Cycle Kinetics, and Tumor Angiogenesis.* Clinical Cancer Research, 2000. **6**(6): p. 2166-2174.
223. McKenna, W.G., et al., *Synergistic effect of the v-myc oncogene with H-ras on radioresistance.* Cancer Res, 1990. **50**(1): p. 97-102.
224. Bos, J.L., *ras oncogenes in human cancer: a review.* Cancer Res, 1989. **49**(17): p. 4682-9.
225. Davis, T.W., et al., *COX-2 inhibitors as radiosensitizing agents for cancer therapy.* Am J Clin Oncol, 2003. **26**(4): p. S58-61.
226. Bernhard, E.J., et al., *Inhibiting Ras prenylation increases the radiosensitivity of human tumor cell lines with activating mutations of ras oncogenes.* Cancer Res, 1998. **58**(8): p. 1754-61.
227. Cohen-Jonathan, E., et al., *Farnesyltransferase inhibitors potentiate the antitumor effect of radiation on a human tumor xenograft expressing activated HRAS.* Radiat Res, 2000. **154**(2): p. 125-32.
228. Hanson, W.R. and C. Thomas, *16, 16-dimethyl prostaglandin E2 increases survival of murine intestinal stem cells when given before photon radiation.* Radiat Res, 1983. **96**(2): p. 393-8.
229. Riehl, T., et al., *Lipopolysaccharide is radioprotective in the mouse intestine through a prostaglandin-mediated mechanism.* Gastroenterology, 2000. **118**(6): p. 1106-16.
230. Furuta, Y., et al., *Increase in radioresponse of murine tumors by treatment with indomethacin.* Cancer Res, 1988. **48**(11): p. 3008-13.
231. Besa, P.C., N.R. Hunter, and L. Milas, *Improvement in radiotherapy for a murine sarcoma by indomethacin plus WR-2721.* Radiat Res, 1993. **135**(1): p. 93-7.
232. Bolten, W.W., *Scientific rationale for specific inhibition of COX-2.* J Rheumatol Suppl, 1998. **51**: p. 2-7.

233. Hicklin, D.J., *Role of the Vascular Endothelial Growth Factor Pathway in Tumor Growth and Angiogenesis.* Journal of clinical oncology, 2004. **23**(5): p. 1011-1027.
234. Dvorak, H.F., *Vascular Permeability Factor/Vascular Endothelial Growth Factor: A Critical Cytokine in Tumor Angiogenesis and a Potential Target for Diagnosis and Therapy.* Journal of clinical oncology, 2002. **20**(21): p. 4368-4380.
235. Ferrara, N. and W.J. Henzel, *Pituitary follicular cells secrete a novel heparin-binding growth factor specific for vascular endothelial cells.* Biochemical and Biophysical Research Communications, 1989. **161**(2): p. 851-858.
236. Senger, D.R., *Tumor cells secrete a vascular permeability factor that promotes accumulation of ascites fluid.* Science (New York, N.Y.), 1983. **219**(4587): p. 983-985.
237. Robles Irizarry, L., et al., *Therapeutic targeting of VEGF in the treatment of glioblastoma.* Expert Opinion on Therapeutic Targets, 2012. **16**(10): p. 973-984.
238. Carmeliet, P., et al., *Abnormal blood vessel development and lethality in embryos lacking a single VEGF allele.* Nature, 1996. **380**(6573): p. 435-9.
239. Ferrara, N., et al., *Heterozygous embryonic lethality induced by targeted inactivation of the VEGF gene.* Nature, 1996. **380**(6573): p. 439-42.
240. Dvorak, H.F., *Vascular permeability factor/vascular endothelial growth factor: a critical cytokine in tumor angiogenesis and a potential target for diagnosis and therapy.* J Clin Oncol, 2002. **20**(21): p. 4368-80.
241. Ferrara, N., H.P. Gerber, and J. LeCouter, *The biology of VEGF and its receptors.* Nat Med, 2003. **9**(6): p. 669-76.
242. Rafii, S., *Therapeutic stem and progenitor cell transplantation for organ vascularization and regeneration.* Nature medicine, 2003. **9**(6): p. 702-712.
243. Jain, R.K., et al., *Lessons from phase III clinical trials on anti-VEGF therapy for cancer.* Nat Clin Pract Oncol, 2006. **3**(1): p. 24-40.
244. Casanovas, O., *Drug resistance by evasion of antiangiogenic targeting of VEGF signaling in late-stage pancreatic islet tumors.* Cancer cell, 2005. **8**(4): p. 299-309.
245. Bergers, G., *Modes of resistance to anti-angiogenic therapy.* Nature reviews. Cancer, 2008. **8**(8): p. 592-603.
246. Ellis, L.M. and D.J. Hicklin, *VEGF-targeted therapy: Mechanisms of anti-tumour activity.* Nature Reviews Cancer, 2008. **8**(8): p. 579-591.
247. Fujio, Y. and K. Walsh, *Akt mediates cytoprotection of endothelial cells by vascular endothelial growth factor in an anchorage-dependent manner.* J Biol Chem, 1999. **274**(23): p. 16349-54.
248. Gerber, H.P., et al., *Vascular endothelial growth factor regulates endothelial cell survival through the phosphatidylinositol 3'-kinase/Akt signal transduction pathway. Requirement for Flk-1/KDR activation.* J Biol Chem, 1998. **273**(46): p. 30336-43.
249. Bruns, C.J., et al., *Vascular endothelial growth factor is an in vivo survival factor for tumor endothelium in a murine model of colorectal carcinoma liver metastases.* Cancer, 2000. **89**(3): p. 488-99.
250. Laird, A.D., et al., *SU6668 inhibits Flk-1/KDR and PDGFRbeta in vivo, resulting in rapid apoptosis of tumor vasculature and tumor regression in mice.* FASEB J, 2002. **16**(7): p. 681-90.

251. Motzer, R.J., et al., *Sunitinib versus interferon alfa in metastatic renal-cell carcinoma.* New England Journal of Medicine, 2007. **356**(2): p. 115-124.
252. Miller, K., *Paclitaxel plus Bevacizumab versus Paclitaxel Alone for Metastatic Breast Cancer.* The New England journal of medicine, 2007. **357**(26): p. 2666-2676.
253. Sandler, A., *Paclitaxel–Carboplatin Alone or with Bevacizumab for Non–Small-Cell Lung Cancer.* The New England journal of medicine, 2006. **355**(24): p. 2542-2550.
254. Hurwitz, H., *Bevacizumab plus Irinotecan, Fluorouracil, and Leucovorin for Metastatic Colorectal Cancer.* The New England journal of medicine, 2004. **350**(23): p. 2335-2342.
255. Escudier, B., *Sorafenib in Advanced Clear-Cell Renal-Cell Carcinoma.* The New England journal of medicine, 2007. **356**(2): p. 125-134.
256. Motzer, R.J., *Sunitinib versus Interferon Alfa in Metastatic Renal-Cell Carcinoma.* The New England journal of medicine, 2007. **356**(2): p. 115-124.
257. Llovet, J., et al., *Sorafenib improves survival in advanced hepatocellular carcinoma (HCC): results of a phase III randomized placebo-controlled trial (SHARP trial)(abstract LBA1).* J Clin Oncol, 2007. **25**.
258. LAIRD, A.D., et al., *SU6668 inhibits Flk-1/KDR and PDGFRβ in vivo, resulting in rapid apoptosis of tumor vasculature and tumor regression in mice.* The FASEB Journal, 2002. **16**(7): p. 681-690.
259. Geng, L., et al., *Inhibition of vascular endothelial growth factor receptor signaling leads to reversal of tumor resistance to radiotherapy.* Cancer Res, 2001. **61**(6): p. 2413-9.
260. Schuuring, J., et al., *Irradiation combined with SU5416: microvascular changes and growth delay in a human xenograft glioblastoma tumor line.* Int J Radiat Oncol Biol Phys, 2005. **61**(2): p. 529-34.
261. Fishman, M.N., et al., *Phase Ib study of tivozanib (AV-951) in combination with temsirolimus in patients with renal cell carcinoma.* European Journal of Cancer, 2013. **49**(13): p. 2841-2850.
262. Hari, D., et al., *Angiostatin induces mitotic cell death of proliferating endothelial cells.* Mol Cell Biol Res Commun, 2000. **3**(5): p. 277-82.
263. Mauceri, H.J., et al., *Combined effects of angiostatin and ionizing radiation in antitumour therapy.* Nature, 1998. **394**(6690): p. 287-91.
264. Tanaka, T., et al., *Viral vector-targeted antiangiogenic gene therapy utilizing an angiostatin complementary DNA.* Cancer Res, 1998. **58**(15): p. 3362-9.
265. Drevs, J., et al., *Antiangiogenesis: current clinical data and future perspectives.* Onkologie, 2002. **25**(6): p. 520-7.
266. Hynes, R.O., *A reevaluation of integrins as regulators of angiogenesis.* Nat Med, 2002. **8**(9): p. 918-21.
267. Ruegg, C., O. Dormond, and A. Mariotti, *Endothelial cell integrins and COX-2: mediators and therapeutic targets of tumor angiogenesis.* Biochim Biophys Acta, 2004. **1654**(1): p. 51-67.
268. Liekens, S., *Angiogenesis: regulators and clinical applications.* Biochemical pharmacology, 2001. **61**(3): p. 253-270.
269. Eliceiri, B.P., *Adhesion events in angiogenesis.* Current opinion in cell biology, 2001. **13**(5): p. 563-568.

270. Kerbel, R.S., *The anti-angiogenic basis of metronomic chemotherapy.* Nature reviews. Cancer, 2004. **4**(6): p. 423-436.
271. Aboody, K., J. Najbauer, and M. Danks, *Stem and progenitor cell-mediated tumor selective gene therapy.* Gene therapy, 2008. **15**(10): p. 739-752.
272. Masood, R., et al., *Retroviral vectors bearing IgG-binding motifs for antibody-mediated targeting of vascular endothelial growth factor receptors.* Int J Mol Med, 2001. **8**(4): p. 335-43.
273. Jin, N., et al., *Gene therapy of murine solid tumors with T cells transduced with a retroviral vascular endothelial growth factor--immunotoxin target gene.* Hum Gene Ther, 2002. **13**(4): p. 497-508.
274. Ma, H.I., et al., *Suppression of intracranial human glioma growth after intramuscular administration of an adeno-associated viral vector expressing angiostatin.* Cancer Res, 2002. **62**(3): p. 756-63.
275. Vigna, E., et al., *Targeted therapy by gene transfer of a monovalent antibody fragment against the Met oncogenic receptor.* Journal of Molecular Medicine, 2013: p. 1-12.
276. Akhtar, J., et al., *Lentiviral-mediated RNA interference targeting stathmin1 gene in human gastric cancer cells inhibits proliferation in vitro and tumor growth in vivo.* Journal of Translational Medicine, 2013. **11**(1): p. 212.
277. He, B., et al., *Cancer targeting gene-viro-therapy for pancreatic cancer using oncolytic adenovirus ZD55-IL-24 in immune-competent mice.* Molecular Biology Reports, 2013. **40**(9): p. 5397-5405.
278. Denekamp, J., *Endothelial cell proliferation as a novel approach to targeting tumour therapy.* Br J Cancer, 1982. **45**(1): p. 136-9.
279. Denekamp, J., *Angiogenesis, neovascular proliferation and vascular pathophysiology as targets for cancer therapy.* British Journal of Radiology, 1993. **66**(783): p. 181-196.
280. Siemann, D.W. and A.M. Rojiani, *The vascular disrupting agent ZD6126 shows increased antitumor efficacy and enhanced radiation response in large, advanced tumors.* International Journal of Radiation Oncology*Biology*Physics, 2005. **62**(3): p. 846-853.
281. Landuyt, W., et al., *Vascular targeting of solid tumoursa major 'inverse' volume-response relationship following combretastatin A-4 phosphate treatment of rat rhabdomyosarcomas.* European Journal of Cancer, 2000. **36**(14): p. 1833-1843.
282. Fox, S.B., et al., *Relationship of Endothelial Cell Proliferation to Tumor Vascularity in Human Breast Cancer.* Cancer Research, 1993. **53**(18): p. 4161-4163.
283. Siemann, D.W., et al., *Vascular targeting agents enhance chemotherapeutic agent activities in solid tumor therapy.* Int J Cancer, 2002. **99**(1): p. 1-6.
284. Siim, B.G., et al., *Marked potentiation of the antitumour activity of chemotherapeutic drugs by the antivascular agent 5,6-dimethylxanthenone-4-acetic acid (DMXAA).* Cancer Chemother Pharmacol, 2003. **51**(1): p. 43-52.
285. Wedge, S., et al. *Combination of the VEGF receptor tyrosine kinase inhibitor ZD6474 and vascular-targeting agent ZD6126 produces an enhanced anti-tumor response*. in *Proc Am Assoc Cancer Res*. 2002.
286. Thorpe, P.E., D.J. Chaplin, and D.C. Blakey, *The First International Conference on Vascular Targeting: Meeting Overview.* Cancer Research, 2003. **63**(5): p. 1144-1147.

287. Denekamp, J. and B. Hobson, *Endothelial-cell proliferation in experimental tumours.* Br J Cancer, 1982. **46**(5): p. 711-20.
288. Denekamp, J., *Vascular attack as a therapeutic strategy for cancer.* Cancer Metastasis Rev, 1990. **9**(3): p. 267-82.
289. Nihei, Y., et al., *Evaluation of antivascular and antimitotic effects of tubulin binding agents in solid tumor therapy.* Jpn J Cancer Res, 1999. **90**(12): p. 1387-95.
290. Dark, G.G., et al., *Combretastatin A-4, an Agent That Displays Potent and Selective Toxicity toward Tumor Vasculature.* Cancer Research, 1997. **57**(10): p. 1829-1834.
291. Beauregard, D.A., et al., *Magnetic resonance imaging and spectroscopy of combretastatin A4 prodrug-induced disruption of tumour perfusion and energetic status.* Br J Cancer, 1998. **77**(11): p. 1761-7.
292. Malcontenti-Wilson, C., et al., *Combretastatin A4 Prodrug Study of Effect on the Growth and the Microvasculature of Colorectal Liver Metastases in a Murine Model.* Clinical Cancer Research, 2001. **7**(4): p. 1052-1060.
293. Horsman, M.R., et al., *The effect of combretastatin A-4 disodium phosphate in a C3H mouse mammary carcinoma and a variety of murine spontaneous tumors.* Int J Radiat Oncol Biol Phys, 1998. **42**(4): p. 895-8.
294. Tozer, G.M., et al., *Mechanisms Associated with Tumor Vascular Shut-Down Induced by Combretastatin A-4 Phosphate: Intravital Microscopy and Measurement of Vascular Permeability.* Cancer Research, 2001. **61**(17): p. 6413-6422.
295. Davis, P.D., et al., *Enhancement of vascular targeting by inhibitors of nitric oxide synthase.* Int J Radiat Oncol Biol Phys, 2002. **54**(5): p. 1532-6.
296. Li, L., A. Rojiani, and D.W. Siemann, *Targeting the tumor vasculature with combretastatin A-4 disodium phosphate: effects on radiation therapy.* Int J Radiat Oncol Biol Phys, 1998. **42**(4): p. 899-903.
297. Chaplin, D.J., G.R. Pettit, and S.A. Hill, *Anti-vascular approaches to solid tumour therapy: evaluation of combretastatin A4 phosphate.* Anticancer Res, 1999. **19**(1A): p. 189-95.
298. Landuyt, W., et al., *In vivo antitumor effect of vascular targeting combined with either ionizing radiation or anti-angiogenesis treatment.* Int J Radiat Oncol Biol Phys, 2001. **49**(2): p. 443-50.
299. Murata, R., et al., *Interaction between combretastatin A-4 disodium phosphate and radiation in murine tumors.* Radiother Oncol, 2001. **60**(2): p. 155-61.
300. Murata, R., et al., *Improved tumor response by combining radiation and the vascular-damaging drug 5,6-dimethylxanthenone-4-acetic acid.* Radiat Res, 2001. **156**(5 Pt 1): p. 503-9.
301. Pedley, R.B., et al., *Eradication of Colorectal Xenografts by Combined Radioimmunotherapy and Combretastatin A-4 3-O-Phosphate.* Cancer Research, 2001. **61**(12): p. 4716-4722.
302. Pedley, R.B., et al., *Synergy between vascular targeting agents and antibody-directed therapy.* Int J Radiat Oncol Biol Phys, 2002. **54**(5): p. 1524-31.
303. Ohno, T., et al., *Antitumor and antivascular effects of AC-7700, a combretastatin A-4 derivative, against rat liver cancer.* Int J Clin Oncol, 2002. **7**(3): p. 171-6.

304. Hori, K., S. Saito, and K. Kubota, *A novel combretastatin A-4 derivative, AC7700, strongly stanches tumour blood flow and inhibits growth of tumours developing in various tissues and organs.* Br J Cancer, 2002. **86**(10): p. 1604-14.
305. Chaplin, D.J., et al., *Antivascular approaches to solid tumour therapy: evaluation of tubulin binding agents.* The British journal of cancer. Supplement, 1996. **27**: p. S86-88.
306. Natsume, T., et al., *Enhanced antitumor activities of TZT-1027 against TNF-alpha or IL-6 secreting Lewis lung carcinoma in vivo.* Cancer Chemother Pharmacol, 2002. **49**(1): p. 35-47.
307. Kobayashi, M., et al., *Antitumor activity of TZT-1027, a novel dolastatin 10 derivative.* Jpn J Cancer Res, 1997. **88**(3): p. 316-27.
308. Blakey, D.C., et al., *ZD6126: a novel small molecule vascular targeting agent.* Int J Radiat Oncol Biol Phys, 2002. **54**(5): p. 1497-502.
309. Blakey, D., et al., *The novel vascular targeting agent ZD6126 causes rapid morphology changes leading to endothelial cell detachment at non-cytotoxic concentrations.* Clin. Exp. Metastasis, 1999. **17**: p. 776.
310. Blakey, D.C., et al., *Antitumor Activity of the Novel Vascular Targeting Agent ZD6126 in a Panel of Tumor Models.* Clinical Cancer Research, 2002. **8**(6): p. 1974-1983.
311. Goertz, D.E., et al., *High-Frequency Doppler Ultrasound Monitors the Effects of Antivascular Therapy on Tumor Blood Flow.* Cancer Research, 2002. **62**(22): p. 6371-6375.
312. Siemann, D.W. and A.M. Rojiani, *Antitumor efficacy of conventional anticancer drugs is enhanced by the vascular targeting agent ZD6126.* Int J Radiat Oncol Biol Phys, 2002. **54**(5): p. 1512-7.
313. Goto, H., et al., *Activity of a New Vascular Targeting Agent, ZD6126, in Pulmonary Metastases by Human Lung Adenocarcinoma in Nude Mice.* Cancer Research, 2002. **62**(13): p. 3711-3715.
314. Burrows, F.J., Y. Watanabe, and P.E. Thorpe, *A Murine Model for Antibody-directed Targeting of Vascular Endothelial Cells in Solid Tumors.* Cancer Research, 1992. **52**(21): p. 5954-5962.
315. Burrows, F.J. and P.E. Thorpe, *Eradication of large solid tumors in mice with an immunotoxin directed against tumor vasculature.* Proceedings of the National Academy of Sciences, 1993. **90**(19): p. 8996-9000.
316. Cines, D.B., *Endothelial cells in physiology and in the pathophysiology of vascular disorders.* Blood, 1998. **91**(10): p. 3527-3561.
317. Clark, P., et al., *Intercellular adhesion molecule-1 (ICAM-1) expression is upregulated by thrombin in human monocytes and THP-1 cells in vitro and in pregnant subjects in vivo.* Thromb Haemost, 2003. **89**(6): p. 1043-51.
318. Clatterbuck, R.E., et al., *Dynamic nature of cavernous malformations: a prospective magnetic resonance imaging study with volumetric analysis.* J Neurosurg, 2000. **93**(6): p. 981-6.
319. Clauss, M., et al., *Synergistic induction of endothelial tissue factor by tumor necrosis factor and vascular endothelial growth factor: Functional analysis of the tumor necrosis factor receptors.* FEBS Letters, 1996. **390**(3): p. 334-338.

320. Crompton, N.E., *Telomeres, senescence and cellular radiation response.* Cell Mol Life Sci, 1997. **53**(7): p. 568-75.
321. Cronstein, B.N., et al., *A mechanism for the antiinflammatory effects of corticosteroids: the glucocorticoid receptor regulates leukocyte adhesion to endothelial cells and expression of endothelial-leukocyte adhesion molecule 1 and intercellular adhesion molecule 1.* Proc Natl Acad Sci U S A, 1992. **89**(21): p. 9991-5.
322. Hallahan, D.E., et al., *Targeting drug delivery to radiation-induced neoantigens in tumor microvasculature.* Journal of Controlled Release, 2001. **74**(1–3): p. 183-191.
323. He, J., T.A. Luster, and P.E. Thorpe, *Radiation-enhanced vascular targeting of human lung cancers in mice with a monoclonal antibody that binds anionic phospholipids.* Clin Cancer Res, 2007. **13**(17): p. 5211-8.
324. Kiani, M.F., *Targeting microparticles to select tissue via radiation-induced upregulation of endothelial cell adhesion molecules.* Pharmaceutical research, 2002. **19**(9): p. 1317-1322.
325. Hashimoto, T.M.D.L., Michael T. M.D.; Wen, Gen M.D.; Yang, Guo-Yuan M.D., Ph.D.; Chaly, Thomas Jr. B.S.; Stewart, Campbell L. B.A.; Dressman, Holly K. Ph.D.; Barbaro, Nicholas M. M.D.; Marchuk, Douglas A. Ph.D.; Young, William L. M.D., *Gene Microarray Analysis of Human Brain Arteriovenous Malformations.* Congress of Neurological Surgeons, 2004. **54**(2): p. 410-425.
326. Hallahan, D., et al., *E-selectin gene induction by ionizing radiation is independent of cytokine induction.* Biochem Biophys Res Commun, 1995. **217**(3): p. 784-95.
327. Hallahan, D., J. Kuchibhotla, and C. Wyble, *Cell adhesion molecules mediate radiation-induced leukocyte adhesion to the vascular endothelium.* Cancer Res, 1996. **56**(22): p. 5150-5.
328. Hallahan, D.E. and S. Virudachalam, *Intercellular adhesion molecule 1 knockout abrogates radiation induced pulmonary inflammation.* Proc Natl Acad Sci U S A, 1997. **94**(12): p. 6432-7.
329. Hallahan, D.E. and S. Virudachalam, *Ionizing radiation mediates expression of cell adhesion molecules in distinct histological patterns within the lung.* Cancer Res, 1997. **57**(11): p. 2096-9.
330. Handschel, J., et al., *Irradiation induces increase of adhesion molecules and accumulation of beta2-integrin-expressing cells in humans.* Int J Radiat Oncol Biol Phys, 1999. **45**(2): p. 475-81.
331. Heckmann, M., et al., *Vascular activation of adhesion molecule mRNA and cell surface expression by ionizing radiation.* Exp Cell Res, 1998. **238**(1): p. 148-54.
332. Yuan, H., et al., *Radiation-induced up-regulation of adhesion molecules in brain microvasculature and their modulation by dexamethasone.* Radiation Research, 2005. **163**(5): p. 544-551.
333. Sharp, C.D.B.S.E.J., Ajay M.D.; Warren, April C. B.S.; Elrod, John W. B.S.; Nanda, Anil M.D.; Alexander, J. Steven Ph.D., *Gamma Knife Irradiation Increases Cerebral Endothelial Expression of Intercellular Adhesion Molecule 1 and E-selectin.* Congress of Neurological Surgeons, 2003. **53**(1): p. 154-161.
334. Voisard, R., et al., *Low-dose irradiation stimulates TNF-α-induced ICAM-1 mRNA expression in human coronary vascular cells.* Medical Science Monitor, 2007. **13**(5): p. BR107-BR111.

335. Ning, S., et al., *Targeting Integrins and PI3K/Akt-Mediated Signal Transduction Pathways Enhances Radiation-Induced Anti-angiogenesis.* Radiation Research, 2007. **168**(1): p. 125-133.
336. Augustin, H.G., D.H. Kozian, and R.C. Johnson, *Differentiation of endothelial cells: analysis of the constitutive and activated endothelial cell phenotypes.* Bioessays, 1994. **16**(12): p. 901-6.
337. Stetler-Stevenson, W.G., *Matrix metalloproteinases in angiogenesis: A moving target for therapeutic intervention.* The Journal of clinical investigation, 1999. **103**(9): p. 1237-1241.
338. Gale, N.W., *Growth factors acting via endothelial cell-specific receptor tyrosine kinases: VEGFs, angiopoietins, and ephrins in vascular development.* Genes & development, 1999. **13**(9): p. 1055-1066.
339. Pohlman, T.H. and J.M. Harlan, *Adaptive responses of the endothelium to stress.* Journal of Surgical Research, 2000. **89**(1): p. 85-119.
340. Liu, Y., *Hypoxia regulates vascular endothelial growth factor gene expression in endothelial cells: Identification of a 5' enhancer.* Circulation research, 1995. **77**(3): p. 638-643.
341. Wang, D., *Induction of vascular endothelial growth factor expression in endothelial cells by platelet-derived growth factor through the activation of phosphatidylinositol 3-kinase.* Cancer research (Baltimore), 1999. **59**(7): p. 1464-1472.
342. Abedi, H., *Vascular Endothelial Growth Factor Stimulates Tyrosine Phosphorylation and Recruitment to New Focal Adhesions of Focal Adhesion Kinase and Paxillin in Endothelial Cells.* The Journal of biological chemistry, 1997. **272**(24): p. 15442-15451.
343. Rousseau, S., *P38 MAP kinase activation by vascular endothelial growth factor mediates actin reorganization and cell migration in human endothelial cells.* Oncogene, 1997. **15**(18): p. 2169-2177.
344. Dejana, E., *Endothelial adherens junctions: implications in the control of vascular permeability and angiogenesis.* J Clin Invest, 1996. **98**(9): p. 1949-53.
345. Kumar, S., D.C. West, and A. Ager, *Heterogeneity in endothelial cells from large vessels and microvessels.* Differentiation, 1987. **36**(1): p. 57-70.
346. Levin, E.G., L. Santell, and K.G. Osborn, *The expression of endothelial tissue plasminogen activator in vivo: a function defined by vessel size and anatomic location.* J Cell Sci, 1997. **110 (Pt 2)**: p. 139-48.
347. Mitra, D., et al., *Thrombotic Thrombocytopenic Purpura and Sporadic Hemolytic-Uremic Syndrome Plasmas Induce Apoptosis in Restricted Lineages of Human Microvascular Endothelial Cells.* Blood, 1997. **89**(4): p. 1224-1234.
348. Zhu, D.Z., C.F. Cheng, and B.U. Pauli, *Mediation of lung metastasis of murine melanomas by a lung-specific endothelial cell adhesion molecule.* Proceedings of the National Academy of Sciences, 1991. **88**(21): p. 9568-9572.
349. Butcher, E.C. and L.J. Picker, *Lymphocyte Homing and Homeostasis.* Science, 1996. **272**(5258): p. 60-67.
350. Rafii, S., et al., *Human bone marrow microvascular endothelial cells support long-term proliferation and differentiation of myeloid and megakaryocytic progenitors.* Blood, 1995. **86**(9): p. 3353-3363.

351. Morin, O., P. Patry, and L. Lafleur, *Heterogeneity of endothelial cells of adult rat liver as resolved by sedimentation velocity and flow cytometry.* J Cell Physiol, 1984. **119**(3): p. 327-34.
352. Ku, D.N., *Pulsatile flow and atherosclerosis in the human carotid bifurcation. Positive correlation between plaque location and low and oscillating shear stress.* Arteriosclerosis (Dallas, Tex.), 1985. **5**(3): p. 293-302.
353. Gimbrone Jr, M.A., *Biomechanical activation: An emerging paradigm in endothelial adhesion biology.* The Journal of clinical investigation, 1997. **100**(11 suppl.): p. S61-S65.
354. Zhao, S., *Synergistic effects of fluid shear stress and cyclic circumferential stretch on vascular endothelial cell morphology and cytoskeleton.* Arteriosclerosis, thrombosis, and vascular biology, 1995. **15**(10): p. 1781-1786.
355. Ziegler, T., *Influence of oscillatory and unidirectional flow environments on the expression of endothelin and nitric oxide synthase in cultured endothelial cells.* Arteriosclerosis, thrombosis, and vascular biology, 1998. **18**(5): p. 686-692.
356. Carosi, J.A., *Modulation of secretion of vasoactive materials from human and bovine endothelial cells by cyclic strain.* Biotechnology and bioengineering, 1994. **43**(7): p. 615-621.
357. Sumpio, B.E., *Prostacyclin synthetic activity in cultured aortic endothelial cells undergoing cyclic mechanical deformation.* Surgery, 1988. **104**(2): p. 383-389.
358. Iba, T., *Tissue plasminogen activator expression in endothelial cells exposed to cyclic strain in vitro.* Cell transplantation, 1992. **1**(1): p. 43-50.
359. Awolesi, M.A., *Cyclic strain upregulates nitric oxide synthase in cultured bovine aortic endothelial cells.* The Journal of clinical investigation, 1995. **96**(3): p. 1449-1454.
360. Mitsumata, M., *Fluid shear stress stimulates platelet-derived growth factor expression in endothelial cells.* The American journal of physiology, 1993. **265**(1 34-1): p. H3-H8.
361. Nishida, K., *Molecular cloning and characterization of the constitutive bovine aortic endothelial cell nitric oxide synthase.* The Journal of clinical investigation, 1992. **90**(5): p. 2092-2096.
362. Chiu, J.J., *Shear Stress Increases ICAM-1 and Decreases VCAM-1 and E-selectin Expressions Induced by Tumor Necrosis Factor- in Endothelial Cells.* Arteriosclerosis, thrombosis, and vascular biology, 2004. **24**(1): p. 73-79.
363. Chappell, D.C., et al., *Oscillatory Shear Stress Stimulates Adhesion Molecule Expression in Cultured Human Endothelium.* Circulation Research, 1998. **82**(5): p. 532-539.
364. Cui, X., et al., *Shear stress augments the endothelial cell differentiation marker expression in late EPCs by upregulating integrins.* Biochemical and Biophysical Research Communications, 2012. **425**(2): p. 419-425.
365. Dustin, M.L., et al., *Induction by IL 1 and interferon-gamma: tissue distribution, biochemistry, and function of a natural adherence molecule (ICAM-1).* The Journal of Immunology, 1986. **137**(1): p. 245-54.

366. Staunton, D.E., et al., *Primary structure of ICAM-1 demonstrates interaction between members of the immunoglobulin and integrin supergene families.* Cell, 1988. **52**(6): p. 925-33.
367. Charlotte Lawson, S.W., *ICAM-1 signaling in endothelial cells.* Pharmacological Reports, 2009. **61**(22–32): p. 1734-1140.
368. Scholer, A., et al., *Intercellular adhesion molecule-1-dependent stable interactions between T cells and dendritic cells determine CD8+ T cell memory.* Immunity, 2008. **28**(2): p. 258-70.
369. Lawson, C. and S. Wolf, *ICAM-1 signaling in endothelial cells.* Pharmacol Rep, 2009. **61**(1): p. 22-32.
370. Wang, S.C., et al., *Evidence for LFA-1/ICAM-1 dependent stimulation of protein tyrosine phosphorylation in human B lymphoid cell lines during homotypic adhesion.* J Leukoc Biol, 1995. **57**(2): p. 343-51.
371. Naoyuki Kondo, G.B.M., *Intercellular Adhesion Molecule 1 Promotes HIV-1 Attachment but Not Fusion to Target Cells.* PLoS One, 2012. **7**(9).
372. Stolpe, A. and P.T. Saag, *Intercellular adhesion molecule-1.* Journal of Molecular Medicine, 1996. **74**(1): p. 13-33.
373. Xu, H., et al., *Leukocytosis and resistance to septic shock in intercellular adhesion molecule 1-deficient mice.* J Exp Med, 1994. **180**(1): p. 95-109.
374. Lawrence, M.B., et al., *Effect of venous shear stress on CD18-mediated neutrophil adhesion to cultured endothelium.* Blood, 1990. **75**(1): p. 227-37.
375. Carlos, T.M. and J.M. Harlan, *Leukocyte-endothelial adhesion molecules.* Blood, 1994. **84**(7): p. 2068-101.
376. Oppenheimer-Marks, N., et al., *Differential utilization of ICAM-1 and VCAM-1 during the adhesion and transendothelial migration of human T lymphocytes.* J Immunol, 1991. **147**(9): p. 2913-21.
377. Fine, J.S. and A.M. Kruisbeek, *The role of LFA-1/ICAM-1 interactions during murine T lymphocyte development.* J Immunol, 1991. **147**(9): p. 2852-9.
378. Geissler, D., et al., *A monoclonal antibody directed against the human intercellular adhesion molecule (ICAM-1) modulates the release of tumor necrosis factor-alpha, interferon-gamma and interleukin 1.* Eur J Immunol, 1990. **20**(12): p. 2591-6.
379. Durieu-Trautmann, O., et al., *Intercellular adhesion molecule 1 activation induces tyrosine phosphorylation of the cytoskeleton-associated protein cortactin in brain microvessel endothelial cells.* J Biol Chem, 1994. **269**(17): p. 12536-40.
380. van Horssen, M., et al., *Co-ligation of ICAM-1 (CD54) and membrane IgM negatively affects B cell receptor signaling.* Eur J Immunol, 1995. **25**(1): p. 154-8.
381. Arroyo, A.G., et al., *Induction of tyrosine phosphorylation during ICAM-3 and LFA-1-mediated intercellular adhesion, and its regulation by the CD45 tyrosine phosphatase.* J Cell Biol, 1994. **126**(5): p. 1277-86.
382. Campanero, M.R., et al., *ICAM-3 regulates lymphocyte morphology and integrin-mediated T cell interaction with endothelial cell and extracellular matrix ligands.* J Cell Biol, 1994. **127**(3): p. 867-78.
383. Juan, M., et al., *CD50 (intercellular adhesion molecule 3) stimulation induces calcium mobilization and tyrosine phosphorylation through p59fyn and p56lck in Jurkat T cell line.* J Exp Med, 1994. **179**(6): p. 1747-56.

384. van de Stolpe, A., et al., *Fibrinogen binding to ICAM-1 on EA.hy 926 endothelial cells is dependent on an intact cytoskeleton.* Thromb Haemost, 1996. **75**(1): p. 182-9.
385. Lord, K.A., B. Hoffman-Liebermann, and D.A. Liebermann, *Complexity of the immediate early response of myeloid cells to terminal differentiation and growth arrest includes ICAM-1, Jun-B and histone variants.* Oncogene, 1990. **5**(3): p. 387-96.
386. Greve, J.M., et al., *Mechanisms of receptor-mediated rhinovirus neutralization defined by two soluble forms of ICAM-1.* J Virol, 1991. **65**(11): p. 6015-23.
387. Ockenhouse, C.F., et al., *Plasmodium falciparum-infected erythrocytes bind ICAM-1 at a site distinct from LFA-1, Mac-1, and human rhinovirus.* Cell, 1992. **68**(1): p. 63-9.
388. Wegner, C., et al., *Intercellular adhesion molecule-1 (ICAM-1) in the pathogenesis of asthma.* Science, 1990. **247**(4941): p. 456-459.
389. Müller, A.M., et al., *Comparative Study of Adhesion Molecule Expression in Cultured Human Macro- and Microvascular Endothelial Cells.* Experimental and Molecular Pathology, 2002. **73**(3): p. 171-180.
390. Shen, J., R.G. Ham, and S. Karmiol, *Expression of Adhesion Molecules in Cultured Human Pulmonary Microvascular Endothelial Cells.* Microvascular Research, 1995. **50**(3): p. 360-372.
391. Hallahan, D.E. and S. Virudachalam, *Ionizing Radiation Mediates Expression of Cell Adhesion Molecules in Distinct Histological Patterns within the Lung.* Cancer Research, 1997. **57**(11): p. 2096-2099.
392. Hallahan, D., J. Kuchibhotla, and C. Wyble, *Cell Adhesion Molecules Mediate Radiation-induced Leukocyte Adhesion to the Vascular Endothelium.* Cancer Research, 1996. **56**(22): p. 5150-5155.
393. Hashimoto, T., et al., *Gene microarray analysis of human brain arteriovenous malformations.* Neurosurgery, 2004. **54**(2): p. 410-23; discussion 423-5.
394. Gaugler, M.H., et al., *Characterization of the response of human bone marrow endothelial cells to in vitro irradiation.* Br J Haematol, 1998. **103**(4): p. 980-9.
395. Panes, J., et al., *Role of leukocyte-endothelial cell adhesion in radiation-induced microvascular dysfunction in rats.* Gastroenterology, 1995. **108**(6): p. 1761-9.
396. Molla, M., et al., *Influence of dose-rate on inflammatory damage and adhesion molecule expression after abdominal radiation in the rat.* Int J Radiat Oncol Biol Phys, 1999. **45**(4): p. 1011-8.
397. Ishii, Y. and S. Kitamura, *Soluble intercellular adhesion molecule-1 as an early detection marker for radiation pneumonitis.* Eur Respir J, 1999. **13**(4): p. 733-8.
398. Epperly, M.W., et al., *Pulmonary irradiation-induced expression of VCAM-I and ICAM-I is decreased by manganese superoxide dismutase-plasmid/liposome (MnSOD-PL) gene therapy.* Biol Blood Marrow Transplant, 2002. **8**(4): p. 175-87.
399. Gianetti, J., et al., *Inverse association between carotid intima-media thickness and the antioxidant lycopene in atherosclerosis.* American Heart Journal, 2002. **143**(3): p. 467-474.
400. N Marui, M.K.O., R Swerlick, C Kunsch, C A Rosen, M Ahmad, R W Alexander, R M Medford and J.C. Invest, *Vascular cell adhesion molecule-1 (VCAM-1) gene transcription and expression are regulated through an antioxidant-sensitive*

mechanism in human vascular endothelial cells. journal of clinical investigation 1993. **92**(4): p. 1866–1874.
401. Sharp, C., et al., *Poly ADP Ribose-Polymerase Inhibitors Prevent the Upregulation of ICAM-1 and E-selectin in Response to Th1 Cytokine Stimulation.* Inflammation, 2001. **25**(3): p. 157-163.
402. Virág, L. and C. Szabó, *Inhibition of poly(ADP-ribose) synthetase (PARS) and protection against peroxynitrite-induced cytotoxicity by zinc chelation.* British Journal of Pharmacology, 1999. **126**(3): p. 769-777.
403. Zingarelli, B., A.L. Salzman, and C. Szabó, *Genetic Disruption of Poly (ADP-Ribose) Synthetase Inhibits the Expression of P-Selectin and Intercellular Adhesion Molecule-1 in Myocardial Ischemia/Reperfusion Injury.* Circulation Research, 1998. **83**(1): p. 85-94.
404. Zingarelli, B., C. Szabó, and A.L. Salzman, *Blockade of poly(ADP-ribose) synthetase inhibits neutrophil recruitment, oxidant generation, and mucosal injury in murine colitis.* Gastroenterology, 1999. **116**(2): p. 335-345.
405. P. O. Hassa, M.O.H., *A Role of Poly (ADP-Ribose) Polymerase in NF- B Transcriptional Activation.* biological chemistry 2005. **380**(7-8): p. 953–959.
406. Sakurai, E., et al., *Targeted Disruption of the CD18 or ICAM-1 Gene Inhibits Choroidal Neovascularization.* Investigative Ophthalmology & Visual Science, 2003. **44**(6): p. 2743-2749.
407. Marlin, S.D. and T.A. Springer, *Purified intercellular adhesion molecule-1 (ICAM-1) is a ligand for lymphocyte function-associated antigen 1 (LFA-1).* Cell, 1987. **51**(5): p. 813-9.
408. Diamond, M.S., et al., *ICAM-1 (CD54): a counter-receptor for Mac-1 (CD11b/CD18).* J Cell Biol, 1990. **111**(6 Pt 2): p. 3129-39.
409. Diamond, M.S., et al., *Binding of the integrin Mac-1 (CD11b/CD18) to the third immunoglobulin-like domain of ICAM-1 (CD54) and its regulation by glycosylation.* Cell, 1991. **65**(6): p. 961-71.
410. Remold-O'Donnell, E., et al., *Expression on blood cells of sialophorin, the surface glycoprotein that is defective in Wiskott-Aldrich syndrome.* Blood, 1987. **70**(1): p. 104-9.
411. Rosenstein, Y., et al., *CD43, a molecule defective in Wiskott-Aldrich syndrome, binds ICAM-1.* Nature, 1991. **354**(6350): p. 233-5.
412. Languino, L.R., et al., *Fibrinogen mediates leukocyte adhesion to vascular endothelium through an ICAM-1-dependent pathway.* Cell, 1993. **73**(7): p. 1423-34.
413. McCourt, P.A., et al., *Intercellular adhesion molecule-1 is a cell surface receptor for hyaluronan.* J Biol Chem, 1994. **269**(48): p. 30081-4.
414. Greve, J.M., et al., *The major human rhinovirus receptor is ICAM-1.* Cell, 1989. **56**(5): p. 839-47.
415. Staunton, D.E., et al., *A cell adhesion molecule, ICAM-1, is the major surface receptor for rhinoviruses.* Cell, 1989. **56**(5): p. 849-53.
416. Marlin, S.D., et al., *A soluble form of intercellular adhesion molecule-1 inhibits rhinovirus infection.* Nature, 1990. **344**(6261): p. 70-2.

417. Manning, A.M., et al., *Cloning and comparative sequence analysis of the gene encoding canine intercellular adhesion molecule-1 (ICAM-1).* Gene, 1995. **156**(2): p. 291-5.
418. Voraberger, G., R. Schafer, and C. Stratowa, *Cloning of the human gene for intercellular adhesion molecule 1 and analysis of its 5'-regulatory region. Induction by cytokines and phorbol ester.* J Immunol, 1991. **147**(8): p. 2777-86.
419. Newman, P.J., *The role of PECAM-1 in vascular cell biology.* Ann N Y Acad Sci, 1994. **714**: p. 165-74.
420. van Mourik, J.A., et al., *Vascular endothelial cells synthesize a plasma membrane protein indistinguishable from the platelet membrane glycoprotein IIa.* J Biol Chem, 1985. **260**(20): p. 11300-6.
421. Muller, W.A., et al., *A human endothelial cell-restricted, externally disposed plasmalemmal protein enriched in intercellular junctions.* J Exp Med, 1989. **170**(2): p. 399-414.
422. Albelda, S.M., et al., *EndoCAM: a novel endothelial cell-cell adhesion molecule.* J Cell Biol, 1990. **110**(4): p. 1227-37.
423. Jackson, D.E., *The unfolding tale of PECAM-1.* FEBS Lett, 2003. **540**(1-3): p. 7-14.
424. Newman, P.J., et al., *PECAM-1 (CD31) cloning and relation to adhesion molecules of the immunoglobulin gene superfamily.* Science, 1990. **247**(4947): p. 1219-22.
425. Stockinger, H., et al., *Molecular characterization and functional analysis of the leukocyte surface protein CD31.* J Immunol, 1990. **145**(11): p. 3889-97.
426. Simmons, D.L., et al., *Molecular cloning of CD31, a putative intercellular adhesion molecule closely related to carcinoembryonic antigen.* J Exp Med, 1990. **171**(6): p. 2147-52.
427. Kirschbaum, N.E., R.J. Gumina, and P.J. Newman, *Organization of the gene for human platelet/endothelial cell adhesion molecule-1 shows alternatively spliced isoforms and a functionally complex cytoplasmic domain.* Blood, 1994. **84**(12): p. 4028-37.
428. Muller, W.A., et al., *PECAM-1 is required for transendothelial migration of leukocytes.* J Exp Med, 1993. **178**(2): p. 449-60.
429. Vaporciyan, A.A., et al., *Involvement of platelet-endothelial cell adhesion molecule-1 in neutrophil recruitment in vivo.* Science, 1993. **262**(5139): p. 1580-2.
430. Bogen, S., et al., *Monoclonal antibody to murine PECAM-1 (CD31) blocks acute inflammation in vivo.* J Exp Med, 1994. **179**(3): p. 1059-64.
431. Gumina, R.J., et al., *Antibody to platelet/endothelial cell adhesion molecule-1 reduces myocardial infarct size in a rat model of ischemia-reperfusion injury.* Circulation, 1996. **94**(12): p. 3327-33.
432. Murohara, T., et al., *Blockade of platelet endothelial cell adhesion molecule-1 protects against myocardial ischemia and reperfusion injury in cats.* J Immunol, 1996. **156**(9): p. 3550-7.
433. Ohto, H., et al., *A novel leukocyte differentiation antigen: two monoclonal antibodies TM2 and TM3 define a 120-kd molecule present on neutrophils, monocytes, platelets, and activated lymphoblasts.* Blood, 1985. **66**(4): p. 873-81.

434. Zehnder, J.L., et al., *Involvement of CD31 in lymphocyte-mediated immune responses: importance of the membrane-proximal immunoglobulin domain and identification of an inhibiting CD31 peptide.* Blood, 1995. **85**(5): p. 1282-8.
435. Sheibani, N., P.J. Newman, and W.A. Frazier, *Thrombospondin-1, a natural inhibitor of angiogenesis, regulates platelet-endothelial cell adhesion molecule-1 expression and endothelial cell morphogenesis.* Mol Biol Cell, 1997. **8**(7): p. 1329-41.
436. Jones, K.L., et al., *Platelet endothelial cell adhesion molecule-1 is a negative regulator of platelet-collagen interactions.* Blood, 2001. **98**(5): p. 1456-63.
437. Darom, A., et al., *Molecular markers (PECAM-1, ICAM-3, HLA-DR) determine prognosis in primary non-Hodgkin's gastric lymphoma patients.* World J Gastroenterol, 2006. **12**(12): p. 1924-32.
438. Sun, Q.H., et al., *Individually distinct Ig homology domains in PECAM-1 regulate homophilic binding and modulate receptor affinity.* J Biol Chem, 1996. **271**(19): p. 11090-8.
439. Sun, J., et al., *Platelet endothelial cell adhesion molecule-1 (PECAM-1) homophilic adhesion is mediated by immunoglobulin-like domains 1 and 2 and depends on the cytoplasmic domain and the level of surface expression.* J Biol Chem, 1996. **271**(31): p. 18561-70.
440. Piali, L., et al., *CD31/PECAM-1 is a ligand for alpha v beta 3 integrin involved in adhesion of leukocytes to endothelium.* J Cell Biol, 1995. **130**(2): p. 451-60.
441. Deaglio, S., et al., *Human CD38 (ADP-ribosyl cyclase) is a counter-receptor of CD31, an Ig superfamily member.* J Immunol, 1998. **160**(1): p. 395-402.
442. Prager, E., et al., *Interaction of CD31 with a heterophilic counterreceptor involved in downregulation of human T cell responses.* J Exp Med, 1996. **184**(1): p. 41-50.
443. DeLisser, H.M., et al., *Platelet/endothelial cell adhesion molecule-1 (CD31)-mediated cellular aggregation involves cell surface glycosaminoglycans.* Journal of Biological Chemistry, 1993. **268**(21): p. 16037-16046.
444. Sun, Q.H., et al., *Cell surface glycosaminoglycans do not serve as ligands for PECAM-1. PECAM-1 is not a heparin-binding protein.* Journal of Biological Chemistry, 1998. **273**(19): p. 11483-11490.
445. Famiglietti, J., et al., *Tyrosine residue in exon 14 of the cytoplasmic domain of platelet endothelial cell adhesion molecule-1 (PECAM-1/CD31) regulates ligand binding specificity.* Journal of Cell Biology, 1997. **138**(6): p. 1425-1435.
446. Quarmby, S., et al., *Irradiation Induces Upregulation of CD31 in Human Endothelial Cells.* Arteriosclerosis, Thrombosis, and Vascular Biology, 1999. **19**(3): p. 588-597.
447. QUARMBY, et al., *Irradiation induced expression of CD31, ICAM-1 and VCAM-1 in human microvascular endothelial cells*. Vol. 20. 2000, Attiki, GRECE: International Institute of Anticancer Research.
448. Gaugler, M.-H., et al., *Irradiation enhances the support of haemopoietic cell transmigration, proliferation and differentiation by endothelial cells.* British Journal of Haematology, 2001. **113**(4): p. 940-950.
449. Van der Meeren, A., *Abdominal Radiation Exposure Elicits Inflammatory Responses and Abscopal Effects in the Lungs of Mice.* Radiation research, 2005. **163**(2): p. 144-152.

450. Van Der Meeren, A., *Inflammatory Reaction and Changes in Expression of Coagulation Proteins on Lung Endothelial Cells after Total-Body Irradiation in Mice.* Radiation research, 2003. **160**(6): p. 637-646.
451. Ginsburg, D., et al., *Human von Willebrand factor (vWF): isolation of complementary DNA (cDNA) clones and chromosomal localization.* Science, 1985. **228**(4706): p. 1401-6.
452. Mancuso, D.J., et al., *Structure of the gene for human von Willebrand factor.* J Biol Chem, 1989. **264**(33): p. 19514-27.
453. Weinstein, M.J., et al., *Fetal and neonatal von Willebrand factor (vWF) is unusually large and similar to the vWF in patients with thrombotic thrombocytopenic purpura.* Br J Haematol, 1989. **72**(1): p. 68-72.
454. Bonthron, D., et al., *Nucleotide sequence of pre-pro-von Willebrand factor cDNA.* Nucleic Acids Res, 1986. **14**(17): p. 7125-7.
455. Lynch, D.C., et al., *Biosynthesis of the subunits of factor VIIIR by bovine aortic endothelial cells.* Proc Natl Acad Sci U S A, 1983. **80**(9): p. 2738-42.
456. Wagner, D.D. and V.J. Marder, *Biosynthesis of von Willebrand protein by human endothelial cells. Identification of a large precursor polypeptide chain.* J Biol Chem, 1983. **258**(4): p. 2065-7.
457. Titani, K., *Amino acid sequence of human von Willebrand factor.* Biochemistry (Easton), 1986. **25**(11): p. 3171-3184.
458. Titani, K., et al., *Amino acid sequence of human von Willebrand factor.* Biochemistry, 1986. **25**(11): p. 3171-84.
459. Ruggeri, Z.M., *Structure and Function of von Willebrand Factor.* Thrombosis and Haemostasis, 1999. **165-1004**(576-584): p. 165-1004.
460. Verheij, M., et al., *Ionizing Radiation Enhances Platelet Adhesion to the Extracellular Matrix of Human Endothelial Cells by an Increase in the Release of von Willebrand Factor.* Radiation Research, 1994. **137**(2): p. 202-207.
461. Kleef, E.M.v., et al., *Increased Expression of Glomerular von Willebrand Factor after Irradiation of the Mouse Kidney.* Radiation Research, 1998. **150**(5): p. 528-534.
462. Boerma, M., et al., *Increased deposition of von Willebrand factor in the rat heart after local ionizing irradiation.* Strahlenther Onkol, 2004. **180**(2): p. 109-16.
463. Hong, J.-H., *Induction of acute phase gene expression by brain irradiation.* International journal of radiation oncology, biology, physics, 1995. **33**(3): p. 619-626.
464. Kuin, A., *Increased glomerular Vwf after kidney irradiation is not due to increased biosynthesis or endothelial cell proliferation.* Radiation research, 2001. **156**(1): p. 20-27.
465. Jahroudi, N., A. Ardekani, and J. Greenberger, *Ionizing irradiation increases transcription of the von Willebrand factor gene in endothelial cells.* Blood, 1996. **88**(10): p. 3801-3814.
466. Verheij, M., et al., *Ionizing radiation enhances platelet adhesion to the extracellular matrix of human endothelial cells by an increase in the release of von Willebrand factor.* Radiation Research, 1994. **137**(2): p. 202-207.
467. Jahroudi, N., A.M. Ardekani, and J.S. Greenberger, *Ionizing irradiation increases transcription of the von Willebrand factor gene in endothelial cells.* Blood, 1996. **88**(10): p. 3801-3814.

468. Richter, K.K., *Is the loss of endothelial thrombomodulin involved in the mechanism of chronicity in late radiation enteropathy?* Radiotherapy and oncology, 1997. **44**(1): p. 65-71.
469. Østerud, B. and E. Bjørklid. *Sources of tissue factor*. in *Seminars in thrombosis and hemostasis*. 2006. New York: Stratton Intercontinental Medical Book Corporation, c1974-.
470. Key, N.S. and N. Mackman, *Tissue factor and its measurement in whole blood, plasma, and microparticles.* Semin Thromb Hemost, 2010. **36**(8): p. 865-75.
471. Carson, S., W. Henry, and T. Shows, *Tissue factor gene localized to human chromosome 1 (1pter----1p21).* Science, 1985. **229**(4717): p. 991-993.
472. Spicer, E.K., et al., *Isolation of cDNA clones coding for human tissue factor: primary structure of the protein and cDNA.* Proceedings of the National Academy of Sciences, 1987. **84**(15): p. 5148-5152.
473. Scarpati, E.M., et al., *Human tissue factor: cDNA sequence and chromosome localization of the gene.* Biochemistry, 1987. **26**(17): p. 5234-5238.
474. Fisher, K.L., et al., *Cloning and expression of human tissue factor cDNA.* Thrombosis Research, 1987. **48**(1): p. 89-99.
475. Morrissey, J.H., H. Fakhrai, and T.S. Edgington, *Molecular cloning of the cDNA for tissue factor, the cellular receptor for the initiation of the coagulation protease cascade.* Cell, 1987. **50**(1): p. 129-135.
476. Bjørklid, E., T. Holm, and B. Østerud, *The development of monospecific antibodies against human thrombo-plastin apoprotein (apoprotein III) and their application in the immunocytochemical detection of the antigen in blood cells.* Thrombosis Research, 1987. **45**(5): p. 609-624.
477. Lyberg, T., K. Nilsson, and H. Prydz, *Synthesis of thromboplastin by U-937 cells.* British Journal of Haematology, 1982. **51**(4): p. 631-641.
478. Lyberg, T., et al., *Cellular cooperation in endothelial cell thromboplastin synthesis.* British Journal of Haematology, 1983. **53**(1): p. 85-95.
479. Brox, J.H., et al., *Production and availability of thromboplastin in endothelial cells: the effects of thrombin, endotoxin and platelets.* British Journal of Haematology, 1984. **57**(2): p. 239-246.
480. Nawroth, P.P. and D.M. Stern, *Modulation of endothelial cell hemostatic properties by tumor necrosis factor.* The Journal of Experimental Medicine, 1986. **163**(3): p. 740-745.
481. Nawroth, P.P., et al., *Interleukin 1 induces endothelial cell procoagulant while suppressing cell-surface anticoagulant activity.* Proceedings of the National Academy of Sciences, 1986. **83**(10): p. 3460-3464.
482. Wilcox, J.N., et al., *Localization of tissue factor in the normal vessel wall and in the atherosclerotic plaque.* Proceedings of the National Academy of Sciences, 1989. **86**(8): p. 2839-2843.
483. Khorana, A.A., et al., *Tissue Factor Expression, Angiogenesis, and Thrombosis in Pancreatic Cancer.* Clinical Cancer Research, 2007. **13**(10): p. 2870-2875.
484. Egorina, E.M., et al., *Granulocytes do not express but acquire monocyte-derived tissue factor in whole blood: evidence for a direct transfer.* Blood, 2008. **111**(3): p. 1208-1216.

485. Sovershaev, M.A., et al., *No evidence for the presence of tissue factor in high-purity preparations of immunologically isolated eosinophils.* Journal of Thrombosis and Haemostasis, 2008. **6**(10): p. 1742-1749.
486. Østerud, B., *Tissue factor expression in blood cells.* Thrombosis Research, 2010. **125, Supplement 1**(0): p. S31-S34.
487. Drake, T.A., et al., *Functional tissue factor is entirely cell surface expressed on lipopolysaccharide-stimulated human blood monocytes and a constitutively tissue factor-producing neoplastic cell line.* The Journal of cell biology, 1989. **109**(1): p. 389-395.
488. Drake, T.A., *Expression of tissue factor, thrombomodulin, and E-selectin in baboons with lethal Escherichia coli sepsis.* The American journal of pathology, 1993. **142**(5): p. 1458-1470.
489. Roth, R., *Hemoglobin enhances the production of tissue factor by endothelial cells in response to bacterial endotoxin.* Blood, 1994. **83**(10): p. 2860-2865.
490. Solberg, S., et al., *Lack of ability to synthesize tissue factor by endothelial cells in intact human saphenous veins.* Blood Coagul Fibrinolysis, 1990. **1**(6): p. 595-600.
491. Alexander, B., et al., *Congenital SPCA deficiency: a hitherto unrecognized coagulation defect with hemorrhage rectified by serum and serum fractions.* J Clin Invest, 1951. **30**(6): p. 596-608.
492. Koller, F., A. Loeliger, and F. Duckert, *Experiments on a new Clotting Factor (Factor VII).* Acta Haematologica, 1951. **6**(1): p. 1-18.
493. Jang, Y., et al., *Influence of Blockade at Specific Levels of the Coagulation Cascade on Restenosis in a Rabbit Atherosclerotic Femoral Artery Injury Model.* Circulation, 1995. **92**(10): p. 3041-3050.
494. Oltrona, L., et al., *Inhibition of Tissue Factor–Mediated Coagulation Markedly Attenuates Stenosis After Balloon-Induced Arterial Injury in Minipigs.* Circulation, 1997. **96**(2): p. 646-652.
495. Goldin-Lang, P., et al., *Ionizing radiation induces upregulation of cellular procoagulability and tissue factor expression in human peripheral blood mononuclear cells.* Thrombosis Research, 2007. **120**(6): p. 857-864.
496. Verheij, M., L.G.H. Dewit, and J.A. Van Mourik, *The effect of ionizing radiation on endothelial tissue factor activity and its cellular localization.* Thrombosis and Haemostasis, 1995. **73**(5): p. 894-895.
497. Van Der Meeren, A., et al., *Inflammatory Reaction and Changes in Expression of Coagulation Proteins on Lung Endothelial Cells after Total-Body Irradiation in Mice.* Radiation Research, 2003. **160**(6): p. 637-646.
498. Wang, J., et al., *Hirudin ameliorates intestinal radiation toxicity in the rat: support for thrombin inhibition as strategy to minimize side-effects after radiation therapy and as countermeasure against radiation exposure.* Journal of Thrombosis and Haemostasis, 2004. **2**(11): p. 2027-2035.
499. Finkelstein, A., et al., *Intracoronary β-irradiation enhances balloon-injury-induced tissue factor expression in the porcine injury model.* International Journal of Cardiovascular Interventions, 2004. **6**(1): p. 20-27.

500. Szotowski, B., et al., *Antioxidative treatment inhibits the release of thrombogenic tissue factor from irradiation- and cytokine-induced endothelial cells.* Cardiovascular Research, 2007. **73**(4): p. 806-812.
501. Hauer-Jensen, M., *Radiation injury and the protein C pathway.* Critical care medicine, 2004. **32**(supplement): p. S325-S330.
502. Esmon, C.T. and W.G. Owen, *The discovery of thrombomodulin.* Journal of Thrombosis and Haemostasis, 2004. **2**(2): p. 209-213.
503. Suzuki, K., et al., *Functionally Active Thrombomodulin Is Present in Human Platelets.* Journal of Biochemistry, 1988. **104**(4): p. 628-632.
504. McCachren, S., et al., *Thrombomodulin expression by human blood monocytes and by human synovial tissue lining macrophages.* Blood, 1991. **78**(12): p. 3128-3132.
505. Wong, V.L.Y., et al., *Regional distribution of thrombomodulin in human brain.* Brain Research, 1991. **556**(1): p. 1-5.
506. Wen, D., et al., *Human thrombomodulin: Complete cDNA sequence and chromosome localization of the gene.* Biochemistry, 1987. **26**(14): p. 4350-4357.
507. Conway, E.M., et al., *Structure-Function Analyses of Thrombomodulin by Gene-Targeting in Mice: The Cytoplasmic Domain Is Not Required for Normal Fetal Development.* Blood, 1999. **93**(10): p. 3442-3450.
508. Koyama, T., et al., *Different glycoforms of human thrombomodulin. Their glycosaminoglycan-dependent modulatory effects on thrombin inactivation by heparin cofactor II and antithrombin III.* Eur J Biochem, 1991. **198**(3): p. 563-70.
509. Hamada, H., et al., *The epidermal growth factor-like domain of recombinant human thrombomodulin exhibits mitogenic activity for Swiss 3T3 cells.* Blood, 1995. **86**(1): p. 225-233.
510. Tohda, G., et al., *Expression of Thrombomodulin in Atherosclerotic Lesions and Mitogenic Activity of Recombinant Thrombomodulin in Vascular Smooth Muscle Cells.* Arteriosclerosis, Thrombosis, and Vascular Biology, 1998. **18**(12): p. 1861-1869.
511. Wang, W., et al., *Elements of the Primary Structure of Thrombomodulin Required for Efficient Thrombin-activable Fibrinolysis Inhibitor Activation.* Journal of Biological Chemistry, 2000. **275**(30): p. 22942-22947.
512. Zushi, M., et al., *The last three consecutive epidermal growth factor-like structures of human thrombomodulin comprise the minimum functional domain for protein C-activating cofactor activity and anticoagulant activity.* Journal of Biological Chemistry, 1989. **264**(18): p. 10351-10353.
513. Suzuki, K., et al., *A domain composed of epidermal growth factor-like structures of human thrombomodulin is essential for thrombin binding and for protein C activation.* Journal of Biological Chemistry, 1989. **264**(9): p. 4872-6.
514. Schenk-Braat, E.A., J. Morser, and D.C. Rijken, *Identification of the epidermal growth factor-like domains of thrombomodulin essential for the acceleration of thrombin-mediated inactivation of single-chain urokinase-type plasminogen activator.* Eur J Biochem, 2001. **268**(21): p. 5562-9.
515. de Munk, G.A., E. Groeneveld, and D.C. Rijken, *Acceleration of the thrombin inactivation of single chain urokinase-type plasminogen activator (pro-urokinase) by thrombomodulin.* J Clin Invest, 1991. **88**(5): p. 1680-4.

516. Molinari, A., et al., *Thrombomodulin is a cofactor for thrombin degradation of recombinant single-chain urokinase plasminogen activator "in vitro" and in a perfused rabbit heart model.* Thromb Haemost, 1992. **67**(2): p. 226-32.
517. Lu, R.L., et al., *The active site of the thrombin-thrombomodulin complex. A fluorescence energy transfer measurement of its distance above the membrane surface.* Journal of Biological Chemistry, 1989. **264**(22): p. 12956-12962.
518. Suzuki, K., et al., *Structure and expression of human thrombomodulin, a thrombin receptor on endothelium acting as a cofactor for protein C activation.* EMBO J, 1987. **6**(7): p. 1891-7.
519. Villoutreix, B.O. and B. Dahlbäck, *Molecular Model for the C-type Lectin Domain of Human Thrombomodulin.* Molecular modeling annual, 1998. **4**(10): p. 310-322.
520. Weisel, J.W., et al., *The Shape of Thrombomodulin and Interactions with Thrombin as Determined by Electron Microscopy.* Journal of Biological Chemistry, 1996. **271**(49): p. 31485-31490.
521. Dodd, R.B. and K. Drickamer, *Lectin-like proteins in model organisms: implications for evolution of carbohydrate-binding activity.* Glycobiology, 2001. **11**(5): p. 71R-79R.
522. Vasta, G.R., et al., *C-type lectins and galectins mediate innate and adaptive immune functions: their roles in the complement activation pathway.* Dev Comp Immunol, 1999. **23**(4-5): p. 401-20.
523. Maruyama, I., C.E. Bell, and P.W. Majerus, *Thrombomodulin is found on endothelium of arteries, veins, capillaries, and lymphatics, and on syncytiotrophoblast of human placenta.* J Cell Biol, 1985. **101**(2): p. 363-71.
524. Kawanami, O., et al., *Heterogeneous distribution of thrombomodulin and von Willebrand factor in endothelial cells in the human pulmonary microvessels.* Journal of Nippon Medical School = Nihon Ika Daigaku zasshi, 2000. **67**(2): p. 118-125.
525. Raife, T.J., et al., *Thrombomodulin expression by human keratinocytes. Induction of cofactor activity during epidermal differentiation.* J Clin Invest, 1994. **93**(4): p. 1846-51.
526. Kawamura, H., Y. Hiramatsu, and I. Watanabe, *Localization of thrombomodulin in a rabbit eye.* Curr Eye Res, 1996. **15**(9): p. 938-42.
527. Yerkovich, S.T., et al., *Allergen-enhanced thrombomodulin (blood dendritic cell antigen 3, CD141) expression on dendritic cells is associated with a TH2-skewed immune response.* J Allergy Clin Immunol, 2009. **123**(1): p. 209-216 e4.
528. Isermann, B., et al., *Tissue-restricted expression of thrombomodulin in the placenta rescues thrombomodulin-deficient mice from early lethality and reveals a secondary developmental block.* Development, 2001. **128**(6): p. 827-38.
529. Isermann, B., et al., *The thrombomodulin-protein C system is essential for the maintenance of pregnancy.* Nat Med, 2003. **9**(3): p. 331-7.
530. Boehme, M.W., et al., *Release of thrombomodulin from endothelial cells by concerted action of TNF-alpha and neutrophils: in vivo and in vitro studies.* Immunology, 1996. **87**(1): p. 134-40.
531. Lohi, O., S. Urban, and M. Freeman, *Diverse substrate recognition mechanisms for rhomboids; thrombomodulin is cleaved by Mammalian rhomboids.* Curr Biol, 2004. **14**(3): p. 236-41.

532. Yamamoto, S., et al., *Urinary thrombomodulin, its isolation and characterization.* J Biochem, 1993. **113**(4): p. 433-40.
533. Tohda, G., et al., *Expression of thrombomodulin in atherosclerotic lesions and mitogenic activity of recombinant thrombomodulin in vascular smooth muscle cells.* Arterioscler Thromb Vasc Biol, 1998. **18**(12): p. 1861-9.
534. Laszik, Z.G., et al., *Down-regulation of endothelial expression of endothelial cell protein C receptor and thrombomodulin in coronary atherosclerosis.* Am J Pathol, 2001. **159**(3): p. 797-802.
535. McCachren, S.S., et al., *Thrombomodulin expression by human blood monocytes and by human synovial tissue lining macrophages.* Blood, 1991. **78**(12): p. 3128-32.
536. Boffa, M.C., B. Burke, and C.C. Haudenschild, *Preservation of thrombomodulin antigen on vascular and extravascular surfaces.* J Histochem Cytochem, 1987. **35**(11): p. 1267-76.
537. Conway, E.M. and B. Nowakowski, *Biologically active thrombomodulin is synthesized by adherent synovial fluid cells and is elevated in synovial fluid of patients with rheumatoid arthritis.* Blood, 1993. **81**(3): p. 726-33.
538. Moore, K.L., C.T. Esmon, and N.L. Esmon, *Tumor necrosis factor leads to the internalization and degradation of thrombomodulin from the surface of bovine aortic endothelial cells in culture.* Blood, 1989. **73**(1): p. 159-65.
539. Conway, E.M., *Thrombomodulin and its role in inflammation.* Seminars in Immunopathology, 2012. **34**(1): p. 107-125.
540. Maruyama, I. and P.W. Majerus, *The turnover of thrombin-thrombomodulin complex in cultured human umbilical vein endothelial cells and A549 lung cancer cells. Endocytosis and degradation of thrombin.* J Biol Chem, 1985. **260**(29): p. 15432-8.
541. Beretz, A., et al., *Stability of the thrombin-thrombomodulin complex on the surface of endothelial cells from human saphenous vein or from the cell line EA.hy 926.* Biochem J, 1989. **259**(1): p. 35-40.
542. Brisson, C., et al., *Antibodies to thrombomodulin induce receptor-mediated endocytosis in human saphenous vein endothelial cells.* Thrombosis and haemostasis, 1992. **68**(6): p. 737-743.
543. Malek, A.M., et al., *Endothelial expression of thrombomodulin is reversibly regulated by fluid shear stress.* Circ Res, 1994. **74**(5): p. 852-60.
544. Ohji, T., et al., *Transforming growth factor beta 1 and beta 2 induce down-modulation of thrombomodulin in human umbilical vein endothelial cells.* Thromb Haemost, 1995. **73**(5): p. 812-8.
545. Rong, Y., et al., *JNK-ATF-2 inhibits thrombomodulin (TM) expression by recruiting histone deacetylase4 (HDAC4) and forming a transcriptional repression complex in the TM promoter.* FEBS Lett, 2010. **584**(5): p. 852-8.
546. Ishii, H., et al., *Oxidized phospholipids in oxidized low-density lipoprotein down-regulate thrombomodulin transcription in vascular endothelial cells through a decrease in the binding of RARbeta-RXRalpha heterodimers and Sp1 and Sp3 to their binding sequences in the TM promoter.* Blood, 2003. **101**(12): p. 4765-74.
547. Nan, B., et al., *C-reactive protein decreases expression of thrombomodulin and endothelial protein C receptor in human endothelial cells.* Surgery, 2005. **138**(2): p. 212-22.

548. Grey, S.T., V. Csizmadia, and W.W. Hancock, *Differential effect of tumor necrosis factor-alpha on thrombomodulin gene expression by human monocytoid (THP-1) cell versus endothelial cells.* Int J Hematol, 1998. **67**(1): p. 53-62.
549. Kim, H.K., et al., *Lipopolysaccharide down-regulates the thrombomodulin expression of peripheral blood monocytes: Effect of serum on thrombomodulin expression in the THP-1 monocytic cell line.* Blood Coagulation and Fibrinolysis, 2007. **18**(2): p. 157-164.
550. Conway, E.M. and R.D. Rosenberg, *Tumor necrosis factor suppresses transcription of the thrombomodulin gene in endothelial cells.* Mol Cell Biol, 1988. **8**(12): p. 5588-92.
551. Starr, M.E., et al., *Age-dependent vulnerability to endotoxemia is associated with reduction of anticoagulant factors activated protein C and thrombomodulin.* Blood, 2010. **115**(23): p. 4886-93.
552. Sohn, R.H., et al., *Regulation of endothelial thrombomodulin expression by inflammatory cytokines is mediated by activation of nuclear factor-kappa B.* Blood, 2005. **105**(10): p. 3910-7.
553. Conway, E.M., et al., *Heat shock of vascular endothelial cells induces an up-regulatory transcriptional response of the thrombomodulin gene that is delayed in onset and does not attenuate.* J Biol Chem, 1994. **269**(36): p. 22804-10.
554. Nawroth, P.P. and D.M. Stern, *Modulation of endothelial cell hemostatic properties by tumor necrosis factor.* J Exp Med, 1986. **163**(3): p. 740-5.
555. Drake, T.A., et al., *Expression of tissue factor, thrombomodulin, and E-selectin in baboons with lethal Escherichia coli sepsis.* Am J Pathol, 1993. **142**(5): p. 1458-70.
556. Laszik, Z., et al., *Lack of suppressed renal thrombomodulin expression in a septic rat model with glomerular thrombotic microangiopathy.* Lab Invest, 1994. **70**(6): p. 862-7.
557. Shi, J., et al., *Statins increase thrombomodulin expression and function in human endothelial cells by a nitric oxide-dependent mechanism and counteract tumor necrosis factor alpha-induced thrombomodulin downregulation.* Blood Coagul Fibrinolysis, 2003. **14**(6): p. 575-85.
558. Maruyama, I., et al., *Increased expression of thrombomodulin on the cultured human umbilical vein endothelial cells and mouse hemangioma cells by cyclic AMP.* Thromb Res, 1991. **61**(3): p. 301-10.
559. Zhou, Q., *Thrombomodulin as a Marker of Radiation-Induced Endothelial Cell Injury.* Radiation research, 1992. **131**(3): p. 285.
560. Hauer-Jensen, M., et al., *Circulating thrombomodulin during radiation therapy of lung cancer.* Radiat Oncol Investig, 1999. **7**(4): p. 238-42.
561. Wang, J., et al., *Deficiency of microvascular thrombomodulin and up-regulation of protease-activated receptor-1 in irradiated rat intestine: possible link between endothelial dysfunction and chronic radiation fibrosis.* Am J Pathol, 2002. **160**(6): p. 2063-72.
562. Hynes, R.O., *Integrins: bidirectional, allosteric signaling machines.* Cell, 2002. **110**(6): p. 673-87.
563. Takada, Y., X. Ye, and S. Simon, *The integrins.* Genome Biol, 2007. **8**(5): p. 215.
564. Reynolds, L.E., et al., *Enhanced pathological angiogenesis in mice lacking β3 integrin or β3 and β5 integrins.* Nature Medicine, 2002. **8**(1): p. 27-34.

565. Eliceiri, B.P. and D.A. Cheresh, *The role of αv integrins during angiogenesis: Insights into potential mechanisms of action and clinical development.* Journal of Clinical Investigation, 1999. **103**(9): p. 1227-1230.
566. Brooks, P.C., et al., *Antiintegrin αvβ3 blocks human breast cancer growth and angiogenesis in human skin.* Journal of Clinical Investigation, 1995. **96**(4): p. 1815-1822.
567. Jensen, U.B., S. Lowell, and F.M. Watt, *The spatial relationship between stem cells and their progeny in the basal layer of human epidermis: a new view based on whole-mount labelling and lineage analysis.* Development, 1999. **126**(11): p. 2409-18.
568. Takada, Y., X. Ye, and S. Simon, *The integrins.* Genome Biology, 2007. **8**(5): p. 215.
569. Vanderslice, P. and D.G. Woodside, *Integrin antagonists as therapeutics for inflammatory diseases.* Expert Opin Investig Drugs, 2006. **15**(10): p. 1235-55.
570. Kuijpers, T.W., et al., *Leukocyte adhesion deficiency type 1 (LAD-1)/variant. A novel immunodeficiency syndrome characterized by dysfunctional beta2 integrins.* J Clin Invest, 1997. **100**(7): p. 1725-33.
571. de Fougerolles, A.R. and T.A. Springer, *Intercellular adhesion molecule 3, a third adhesion counter-receptor for lymphocyte function-associated molecule 1 on resting lymphocytes.* J Exp Med, 1992. **175**(1): p. 185-90.
572. Dustin, M.L. and T.A. Springer, *Lymphocyte function-associated antigen-1 (LFA-1) interaction with intercellular adhesion molecule-1 (ICAM-1) is one of at least three mechanisms for lymphocyte adhesion to cultured endothelial cells.* J Cell Biol, 1988. **107**(1): p. 321-31.
573. Erle, D.J., et al., *Expression and function of the MAdCAM-1 receptor, integrin alpha 4 beta 7, on human leukocytes.* J Immunol, 1994. **153**(2): p. 517-28.
574. Bochner, B.S., et al., *Adhesion of human basophils, eosinophils, and neutrophils to interleukin 1-activated human vascular endothelial cells: contributions of endothelial cell adhesion molecules.* J Exp Med, 1991. **173**(6): p. 1553-7.
575. Kinashi, T., *Overview of integrin signaling in the immune system.* Methods Mol Biol, 2012. **757**: p. 261-78.
576. White, D.J., et al., *The collagen receptor subfamily of the integrins.* Int J Biochem Cell Biol, 2004. **36**(8): p. 1405-10.
577. de Fougerolles, A.R., et al., *Regulation of inflammation by collagen-binding integrins alpha1beta1 and alpha2beta1 in models of hypersensitivity and arthritis.* J Clin Invest, 2000. **105**(6): p. 721-9.
578. Pozzi, A., et al., *Elevated matrix metalloprotease and angiostatin levels in integrin alpha 1 knockout mice cause reduced tumor vascularization.* Proc Natl Acad Sci U S A, 2000. **97**(5): p. 2202-7.
579. Moshfegh, K., et al., *Association of two silent polymorphisms of platelet glycoprotein Ia/IIa receptor with risk of myocardial infarction: a case-control study.* Lancet, 1999. **353**(9150): p. 351-4.
580. Hallahan, D., et al., *Integrin-mediated targeting of drug delivery to irradiated tumor blood vessels.* Cancer Cell, 2003. **3**(1): p. 63-74.
581. Cordes, N., et al., *Ionizing radiation induces up-regulation of functional beta1-integrin in human lung tumour cell lines in vitro.* Int J Radiat Biol, 2002. **78**(5): p. 347-57.

582. Onoda, J.M., *Radiation-Induced Increase in Expression of the α IIb β 3 Integrin in Melanoma Cells: Effects on Metastatic Potential.* Radiation research, 1992. **130**(3): p. 281.
583. Baluna, R.G., T.Y. Eng, and C.R. Thomas Jr, *Adhesion molecules in radiotherapy.* Radiation Research, 2006. **166**(6): p. 819-831.
584. Breier, G., et al., *Molecular cloning and expression of murine vascular endothelial-cadherin in early stage development of cardiovascular system.* Blood, 1996. **87**(2): p. 630-41.
585. Vestweber, D., *VE-cadherin: the major endothelial adhesion molecule controlling cellular junctions and blood vessel formation.* Arterioscler Thromb Vasc Biol, 2008. **28**(2): p. 223-32.
586. Posy, S., *Sequence and Structural Determinants of Strand Swapping in Cadherin Domains: Do All Cadherins Bind Through the Same Adhesive Interface?* Journal of molecular biology, 2008. **378**(4): p. 954-966.
587. Boggon, T.J., et al., *C-Cadherin Ectodomain Structure and Implications for Cell Adhesion Mechanisms.* Science, 2002. **296**(5571): p. 1308-1313.
588. Brasch, J., et al., *Structure and Binding Mechanism of Vascular Endothelial Cadherin: A Divergent Classical Cadherin.* Journal of Molecular Biology, 2011. **408**(1): p. 57-73.
589. Lampugnani, M.G., et al., *The molecular organization of endothelial cell to cell junctions: differential association of plakoglobin, beta-catenin, and alpha-catenin with vascular endothelial cadherin (VE-cadherin).* J Cell Biol, 1995. **129**(1): p. 203-17.
590. Gentil-dit-Maurin, A., et al., *Unraveling the distinct distributions of VE- and N-cadherins in endothelial cells: A key role for p120-catenin.* Experimental Cell Research, 2010. **316**(16): p. 2587-2599.
591. Gulino, D., et al., *Alteration of endothelial cell monolayer integrity triggers resynthesis of vascular endothelium cadherin.* Journal of Biological Chemistry, 1998. **273**(45): p. 29786-29793.
592. Wallez, Y., I. Vilgrain, and P. Huber, *Angiogenesis: the VE-cadherin switch.* Trends Cardiovasc Med, 2006. **16**(2): p. 55-9.
593. Ranscht, B., *Cadherins and catenins: interactions and functions in embryonic development.* Curr Opin Cell Biol, 1994. **6**(5): p. 740-6.
594. Takeichi, M., *Morphogenetic roles of classic cadherins.* Curr Opin Cell Biol, 1995. **7**(5): p. 619-27.
595. Vittet, D., et al., *Targeted null-mutation in the vascular endothelial-cadherin gene impairs the organization of vascular-like structures in embryoid bodies.* Proceedings of the National Academy of Sciences of the United States of America, 1997. **94**(12): p. 6273-6278.
596. Carmeliet, P., et al., *Targeted deficiency or cytosolic truncation of the VE-cadherin gene in mice impairs VEGF-mediated endothelial survival and angiogenesis.* Cell, 1999. **98**(2): p. 147-157.
597. Corada, M., et al., *Vascular endothelial-cadherin is an important determinant of microvascular integrity in vivo.* Proceedings of the National Academy of Sciences of the United States of America, 1999. **96**(17): p. 9815-9820.

598. Navarro, P., et al., *Catenin-dependent and -independent functions of vascular endothelial cadherin.* Journal of Biological Chemistry, 1995. **270**(52): p. 30965-30972.
599. Corada, M., et al., *Monoclonal antibodies directed to different regions of vascular endothelial cadherin extracellular domain affect adhesion and clustering of the protein and modulate endothelial permeability.* Blood, 2001. **97**(6): p. 1679-1684.
600. Moore, R. and F.S. Walsh, *The cell adhesion molecule M-cadherin is specifically expressed in developing and regenerating, but not denervated skeletal muscle.* Development, 1993. **117**(4): p. 1409-20.
601. Kim, M., et al., *The effect of oxidized low-density lipoprotein (ox-LDL) on radiation-induced endothelial-to-mesenchymal transition.* Int J Radiat Biol, 2013. **89**(5): p. 356-63.
602. Moriconi, F., et al., *Effect of irradiation on gene expression of rat liver adhesion molecules : iiin vivo and in vitro studies.* Strahlentherapie und Onkologie, 2009. **185**(7): p. 460-468.
603. Gabryś, D., et al., *Radiation Effects on the Cytoskeleton of Endothelial Cells and Endothelial Monolayer Permeability.* International Journal of Radiation Oncology*Biology*Physics, 2007. **69**(5): p. 1553-1562.
604. Pomp, J., et al., *The influence of pre-operative radiotherapy on the expression of p53 and adhesion molecules: correlation with treatment results in patients with squamous cell carcinoma or adenocarcinoma.* Oncol Rep, 2002. **9**(3): p. 621-5.
605. Akimoto, T., et al., *Effect of radiation on the expression of E-cadherin and alpha-catenin and invasive capacity in human lung cancer cell line in vitro.* Int J Radiat Oncol Biol Phys, 1998. **41**(5): p. 1171-6.
606. Guo, W.Y., et al., *Gamma knife surgery of cerebral arteriovenous malformations: serial MR imaging studies after radiosurgery.* Int J Radiat Oncol Biol Phys, 1993. **25**(2): p. 315-23.
607. Coffey, R.J., D.A. Nichols, and E.G. Shaw, *Stereotactic radiosurgical treatment of cerebral arteriovenous malformations. Gamma Unit Radiosurgery Study Group.* Mayo Clin Proc, 1995. **70**(3): p. 214-22.
608. Yamamoto, M., et al., *Long-term results of radiosurgery for arteriovenous malformation: neurodiagnostic imaging and histological studies of angiographically confirmed nidus obliteration.* Surg Neurol, 1992. **37**(3): p. 219-30.
609. Maruyama, K., et al., *The risk of hemorrhage after radiosurgery for cerebral arteriovenous malformations.* N Engl J Med, 2005. **352**(2): p. 146-53.
610. Shin, M., et al., *Risk of hemorrhage from an arteriovenous malformation confirmed to have been obliterated on angiography after stereotactic radiosurgery.* J Neurosurg, 2005. **102**(5): p. 842-6.
611. Yassari, R., et al., *Angiographic, hemodynamic and histological characterization of an arteriovenous fistula in rats.*
612. O'Connor MM, M.M., *Effects of radiation on cerebral vasculature: A review.* Neurosurgery, 2000. **46**(1): p. 138-151.
613. Nozaki K, H.N., Miyamoto S, Kikuchi H., *Resectability of Spetzler-Martin grade IV and V cerebral arteriovenous malformations.* 2000. **7**: p. 78-81.

614. Klopfenstein JD, S.R., *Cerebral arteriovenous malformations: when is surgery indicated?* Acta neurochirurgica, 2005. **147**(7): p. 693-695.
615. Maruyama, K., *The Risk of Hemorrhage after Radiosurgery for Cerebral Arteriovenous Malformations.* The New England journal of medicine, 2005. **352**(2): p. 146-153.
616. Storer Kp, T.J., Stoodley MA, Smee RI., *Expression of Endothelial Adhesion Molecules After Radiosurgery in an Animal Model of Arteriovenous Malformation.* Neurosurgery, 2010. **67**(4): p. 976-983.
617. Reddy, R., et al., *Durable thrombosis in a rat model of arteriovenous malformation treated with radiosurgery and vascular targeting.* J Neurosurg, 2014. **120**(1): p. 113-9.
618. Nilsson, A., et al., *Stereotactic gamma irradiation of basilar artery in cat: Preliminary experiences.* Acta Oncologica, 1978. **17**(2): p. 150-160.
619. Kamiryo, T., et al., *Occlusion of the anterior cerebral artery after Gamma Knife irradiation in a rat.* Acta Neurochirurgica, 1996. **138**(8): p. 983-991.
620. Tu, J., et al., *Different responses of cavernous malformations and arteriovenous malformations to radiosurgery.* Journal of Clinical Neuroscience, 2009. **16**(7): p. 945-949.
621. Ruiz-Sandoval, J.L., C. Cantu, and F. Barinagarrementeria, *Intracerebral hemorrhage in young people: analysis of risk factors, location, causes, and prognosis.* Stroke, 1999. **30**(3): p. 537-41.
622. Toffol, G.J., J. Biller, and H.P. Adams, Jr., *Nontraumatic intracerebral hemorrhage in young adults.* Arch Neurol, 1987. **44**(5): p. 483-5.
623. Brown, R.D., Jr., et al., *Frequency of intracranial hemorrhage as a presenting symptom and subtype analysis: a population-based study of intracranial vascular malformations in Olmsted Country, Minnesota.* J Neurosurg, 1996. **85**(1): p. 29-32.
624. Brown, R.D., Jr., et al., *Natural history, evaluation, and management of intracranial vascular malformations.* Mayo Clin Proc, 2005. **80**(2): p. 269-81.
625. Heros, R.C., *Spetzler-Martin grades IV and V arteriovenous malformations.* J Neurosurg, 2003. **98**(1): p. 1-2; discussion 2.
626. Yin, G.Q., *Endotoxic shock model with fluid resuscitation in Macaca mulatta.* Laboratory animals (London), 2005. **39**(3): p. 269-279.
627. Shenkar, R., et al., *Variations in Structural Protein Expression and Endothelial Cell Proliferation in Relation to Clinical Manifestations of Cerebral Cavernous Malformations.* Neurosurgery, 2005. **56**(2): p. 343-354 10.1227/01.NEU.0000148903.11469.E9.
628. O'Connor, M.M. and M.R. Mayberg, *Effects of radiation on cerebral vasculature: a review.* Neurosurgery, 2000. **46**(1): p. 138-49; discussion 150-1.
629. Epperly, M.W., et al., *Pulmonary irradiation-induced expression of VCAM-I and ICAM-I is decreased by manganese superoxide dismutase-plasmid/liposome (MnSOD-PL) gene therapy.* Biology of Blood and Marrow Transplantation, 2002. **8**(4): p. 175-187.
630. Van der Meeren, A., et al., *Inflammatory Reaction and Changes in Expression of Coagulation Proteins on Lung Endothelial Cells after Total-Body Irradiation in Mice.* Radiation Research, 2003. **160**(6): p. 637-646.

631. Paulis, L., et al., *Targeting of ICAM-1 on vascular endothelium under static and shear stress conditions using a liposomal Gd-based MRI contrast agent.* Journal of Nanobiotechnology, 2012. **10**(1): p. 25.
632. Ran, S., *Increased exposure of anionic phospholipids on the surface of tumor blood vessels.* Cancer research (Baltimore), 2002. **62**(21): p. 6132.
633. Barrow, D.L., *Controversies in neurosurgery: microsurgery versus radiosurgery for arteriovenous malformations--the case for microsurgery.* Clinical neurosurgery, 2000. **46**: p. 285-294.
634. Storer, K., et al., *Coadministration of low-dose lipopolysaccharide and soluble tissue factor induces thrombosis after radiosurgery in an animal arteriovenous malformation model.* Neurosurgery, 2007. **61**(3): p. 604-10; discussion 610-1.
635. Chang, S.D., et al., *Stereotactic radiosurgery of arteriovenous malformations: pathologic changes in resected tissue.* Clin Neuropathol, 1997. **16**(2): p. 111-6.
636. Reddy, R., et al., *Durable thrombosis in a rat model of arteriovenous malformation treated with radiosurgery and vascular targeting.* Journal of Neurosurgery. **0**(0): p. 1-7.
637. Lorenzet, R., et al., *Cell-cell interaction and tissue factor expression.* Blood Coagulation and Fibrinolysis, 1998. **9**(SUPPL. 1): p. S49-S59.
638. *Arteriovenous malformations of the brain in adults.* N Engl J Med, 1999. **340**(23): p. 1812-8.
639. Heffez, D.S., et al., *The effect of incomplete patient follow-up on the reported results of AVM radiosurgery.* Surg Neurol, 1998. **49**(4): p. 373-81; discussion 381-4.
640. Friedman, W.A., et al., *The risk of hemorrhage after radiosurgery for arteriovenous malformations.* Journal of neurosurgery, 1996. **84**(6): p. 912-919.
641. Yen, C.P., D. Schlesinger, and J.P. Sheehan, *Natural history of cerebral arteriovenous malformations and the risk of hemorrhage after radiosurgery*, 2013. p. 5-21.
642. Margaret Simonian, M.P.M.a.M.A.S., *In vitro and in vivo biotinylation of endothelial cell surface proteins in the pursuit of targets for molecular therapies for brain AVMs.* Metabolomics : open access, 2012.
643. Al-Shahi, R., et al., *Prevalence of adults with brain arteriovenous malformations: a community based study in Scotland using capture-recapture analysis.* J Neurol Neurosurg Psychiatry, 2002. **73**(5): p. 547-51.
644. Stapf, C., et al., *Predictors of hemorrhage in patients with untreated brain arteriovenous malformation.* Neurology, 2006. **66**(9): p. 1350-5.
645. Gross, B.A. and R. Du, *Natural history of cerebral arteriovenous malformations: a meta-analysis.* Journal of Neurosurgery, 2013. **118**(2): p. 437-443.
646. Laakso, A., *Risk of Hemorrhage in Patients With Untreated Spetzler-Martin Grade IV and V Arteriovenous Malformations: A Long-term Follow-up Study in 63 Patients.* Neurosurgery, 2011. **68**(2): p. 372-377.
647. Ogilvy, C.S., et al., *AHA Scientific Statement: Recommendations for the management of intracranial arteriovenous malformations: a statement for healthcare professionals from a special writing group of the Stroke Council, American Stroke Association.* Stroke, 2001. **32**(6): p. 1458-71.
648. Chang, S.D., et al., *Multimodality treatment of giant intracranial arteriovenous malformations.* Neurosurgery, 2003. **53**(1): p. 1-11; discussion 11-3.

649. Kalani, M.Y.S., et al., *Endovascular Treatment of Cerebral Arteriovenous Malformations.* Neuroimaging Clinics of North America, 2013. **23**(4): p. 605-624.
650. Farhat, H.I., *Cerebral Arteriovenous Malformations.* Disease-a-Month, 2011. **57**(10): p. 625-637.
651. Friedman, W.A., *Radiosurgery versus surgery for arteriovenous malformations: the case for radiosurgery.* Clin Neurosurg, 1999. **45**: p. 18-20.
652. Lindqvist, M., et al., *Angiographic long-term follow-up data for arteriovenous malformations previously proven to be obliterated after gamma knife radiosurgery.* Neurosurgery, 2000. **46**(4): p. 803-8; discussion 809-10.
653. Davidson, A.S. and M.K. Morgan, *How safe is arteriovenous malformation surgery? A prospective, observational study of surgery as first-line treatment for brain arteriovenous malformations.* Neurosurgery, 2010. **66**(3): p. 498-504; discussion 504-5.
654. McInerney, J., et al., *Decision analysis for small, asymptomatic intracranial arteriovenous malformations.* Neurosurg Focus, 2001. **11**(5): p. e7.
655. Baguley, B.C., *Antivascular therapy of cancer: DMXAA.* The Lancet Oncology, 2003. **4**(3): p. 141-148.
656. Carswell, E.A., et al., *An endotoxin-induced serum factor that causes necrosis of tumors.* Proc Natl Acad Sci U S A, 1975. **72**(9): p. 3666-70.
657. Rietschel, E.T., et al., *Bacterial endotoxin: molecular relationships of structure to activity and function.* FASEB J, 1994. **8**(2): p. 217-25.
658. Steinemann, S., R.J. Ulevitch, and N. Mackman, *Role of the lipopolysaccharide (LPS)-binding protein/CD14 pathway in LPS induction of tissue factor expression in monocytic cells.* Arterioscler Thromb, 1994. **14**(7): p. 1202-9.
659. Yang, Z., et al., *CD14 and tissue factor expression by bacterial lipopolysaccharide-stimulated bovine alveolar macrophages in vitro.* Infect Immun, 1995. **63**(1): p. 51-6.
660. Meszaros, K., et al., *Monocyte tissue factor induction by lipopolysaccharide (LPS): dependence on LPS-binding protein and CD14, and inhibition by a recombinant fragment of bactericidal/permeability-increasing protein.* Blood, 1994. **83**(9): p. 2516-25.
661. Tóth, F., et al., *Effects of an intravenous endotoxin challenge on glucose and insulin dynamics in horses.* American Journal of Veterinary Research, 2008. **69**(1): p. 82-88.
662. Yin, G.Q., et al., *Endotoxic shock model with fluid resuscitation in Macaca mulatta.* Laboratory Animals, 2005. **39**(3): p. 269-279.
663. Järlestedt, K., et al., *Decreased survival of newborn neurons in the dorsal hippocampus after neonatal LPS exposure in mice.* Neuroscience, 2013. **253**: p. 21-28.
664. Otto, F., *Phase II trial of intravenous endotoxin in patients with colorectal and non-small cell lung cancer.* European journal of cancer (1990), 1996. **32**(10): p. 1712-1718.
665. Shin, M., et al., *Retrospective analysis of a 10-year experience of stereotactic radiosurgery for arteriovenous malformations in children and adolescents.* Journal of Neurosurgery, 2002. **97**(4): p. 779-784.

MACQUARIE UNIVERSITY

ANIMAL RESEARCH AUTHORITY (ARA)

AEC Reference No.: 2011/011-14 **Date of Expiry:** 03 May 2014

Full Approval Duration: 04 May 2011 to 03 May 2014 (36 months)

This ARA remains in force until the Date of Expiry (unless suspended, cancelled or surrendered) **and will only be renewed upon receipt of a satisfactory Progress Report before expiry.**

Principal Investigator:
Dr Hong Duong
Australian School of Advanced Medicine
Macquarie University NSW 2109
0404 246 318
hong.duong@mq.edu.au

In case of emergency, please contact:
the Principal Investigator / Associate Investigator named above, or
Animal Welfare Officer 9850 7758 / 0439 497 383
Manager, CAF 9850 7780 / 0428 861 163

Associate Investigators:

Marcus Stoodley	0407 896 492
Andrew Davidson	0416 157 859
Vivienne Lee	0416 250 779
Jude Amalraj	0435 830 607
Saleh Kashba	0415 789 600
Newsha Raoufi-rad	0415 599 087
Zhenjun Zhao	0426 532 358
David Bervini	0452 497 513
Miikka Korja	0434 795 200
Rajesh Reddy	0412 725 577

Investigator:

Biyi Chen	0412 941 115

Visitor:

Nirav Patel	0415 946 569

The above-named are authorised by MACQUARIE UNIVERSITY ANIMAL ETHICS COMMITTEE to conduct the following research:

Title of the project: Developing new treatments for brain arteriovenous malformations: Characterisation of Gamma Knife Radiosurgery-induced endothelial molecular changes
Purpose: 4 - Research (human or animal biology)
Aims: This project aims to develop a new treatment for brain arteriovenous malformations (AVMs) that is safer and more effective than the current methods of surgery and Radiosurgery, using biological methods to promote intravascular thrombosis after Radiosurgery.
Surgical Procedures category: 5 (Major Surgery With Recovery)
All procedures must be performed as per the AEC-approved protocol, unless stated otherwise by the AEC and/or AWO.

Maximum numbers approved (for the Full Approval Duration):

Species	Strain	Sex	Weight	Age	Total	Supplier/Source
Rat	SD	male	250-500g	6-12 weeks	414	ARC Perth

Location of research:

Location	*Full street address*
Australian School of Advanced Medicine	Level 1, Clinic Building, 2 Technology Place, Macquarie University NSW 2109
Central Animal Facility	Building F9A, Research Park Drive, Macquarie University NSW 2109
Macquarie University Hospital	3 Technology Place, Macquarie University NSW 2109

Amendments approved by the AEC since initial approval:

1. *Addition of Dr Nirav J Patel as visitor assisting in the anastomosis (Approved 11 August 2011)*
2. *Addition of Dr Saleh Kashba as Associate Investigator (Approved 11 August 2011)*
3. *Amendment of technique – Addition of Doppler ultrasound to check vessel patency (Approved 11 August 2011)*
4. *Amendment of technique – Addition of angiography (Approved 8 September 2011)*
5. *Amendment of technique - Addition of Doppler ultrasound directly on vessel intraoperatively (Approved 20 October 2011)*
6. *Addition of Newsha Raoufi-rad as other personnel (Approved 8 December 2011)*
7. *Addition of Dr Zhenjun Zhao as Associate Investigator (Approved 16 February 2012)*
8. *Addition of David Bervini to the protocol (Approved 17 May 2012)*
9. *Addition of Miikka Korja to the protocol as Associate Investigator (Approved 4 Oct 2012)*
10. *Addition of Biyi Chen to the protocol as Investigator (Exec Approved 2 Apr 2013, ratified AEC 18 April 2013)*
11. *Addition of Rajesh Reddy as Associate Investigator (Approved & AEC ratified May 2013)*
12. *Addition of 10 male SD rats as negative control (Approved13 June 2013)*

Conditions of Approval:

1. *AEC Meeting 21 April 2011 - Animals must be acclimatised for seven days prior to treatment to reduce stress.*
2. *AEC Meeting 8 September 2011 - Please document the appropriate dosage of contrast in both mg/ml and mg/kg.*
3. *New rodent researchers must successfully complete the MQ rodent basic training courses*
   a. *Rodent Handling and Care*
   b. *Rodent anaesthesia with injectable and inhalant anaesthetics*
   c. *Clean and Aseptic surgical techniques*
   d. *Post-operative monitoring and pain relief*

Being animal research carried out in accordance with the Code of Practice for a recognised research purpose and in connection with animals (other than exempt animals) that have been obtained from the holder of an animal suppliers licence.

Prof Mark Connor (Chair, Animal Ethics Committee) **Approval Date:** 13 June 2013

Adapted from Form C (issued under part IV of the Animal Research Act, 1985)

MACQUARIE UNIVERSITY

ANIMAL RESEARCH AUTHORITY (ARA)

AEC Reference No.: 2011/012-9 **Date of Expiry:** 03 August 2014

Full Approval Duration: 04 May 2011 to 03 August 2014 (36 months+3months extension)

This ARA remains in force until the Date of Expiry (unless suspended, cancelled or surrendered) **and will only be renewed upon receipt of a satisfactory Progress Report before expiry.**

Principal Investigator:
Prof Marcus Stoodley
Australian School of Advanced Medicine
Macquarie University NSW 2109
0407 896 492
marcus@teamneuro.com

Associate Investigators:

Hong Duong	0404 246 318
Jude Amalraj	0435 830 607
Vivienne Lee	0416 250 779
Saleh Kashba	0415 789 600
Miikka Korja	0434 795 200
Santhosh Thomas	0422 585 653
Lucinda McRobb	0411 126 331
Ravi Dadlani	0420 275 599
Hari Bandi	0419 475 203

In case of emergency, please contact:
the Principal Investigator / Associate Investigator named above
or Manager, CAF: 9850 7780 / 0428 861 163 and Animal Welfare Officer: 9850 7758 / 0439 497 383

The above-named are authorised by MACQUARIE UNIVERSITY ANIMAL ETHICS COMMITTEE to conduct the following research:

Title of the project: Training new staff/students in the creation of an animal model of brain arteriovenous malformation (AVM)

Purpose: 3 - Education

Aims of project: To provide new research staff/PhD students with the skills necessary to perform the rodent model of brain AVM to carry out their research project.

Surgical Procedures category: 2 (Animal Unconscious Without Recovery)

All procedures must be performed as per the AEC-approved protocol, unless stated otherwise by the AEC and/or AWO.
Maximum numbers approved (for the Full Approval Duration):

Species	Strain	Sex	Weight	Age	Total	Supplier/Source
Rat	Any	male	250-500g	6-12 weeks	210	ARC Perth, or as determined by the CAF Manager
Rat	Any	male	250-500g	6-12 weeks	60	ARC Perth, or as determined by the CAF Manager
				TOTAL	270	

Location of research:

Location	*Full street address*
Australian School of Advanced Medicine	Level 1, Clinic Building, 2 Technology Place, Macquarie University NSW 2109
Central Animal Facility	Building F9A, Research Park Drive, Macquarie University NSW 2109

Amendments approved by the AEC since initial approval:

1. *Additional personnel – Saleh Kashba (Approved 11 August 2011)*
2. *(i) Addition of Vivienne Lee as Research Assistant, (ii) Addition of 60 animals (Approved 20 October 2011)*
3. *Additional Personnel - Miikka Korja (Approved 18 October 201)*
4. *Change of type of animal from SD to any strain (Approved May 2013)*
5. *Addition of SanthoshThomas as Associate Investigator (Exec approved 19 March 2014, ratified by AEC 20 March 2014)*
6. *Addition of Lucinda McRobb as Associate Investigator (Exec approved 19 March 2014, ratified by AEC 20 March 2014)*
7. *Addition of Ravi Dadlani as Associate Investigator (Exec approved 19 March 2014, ratified by AEC 20 March 2014)*
8. *Addition of Dr Hari Bandi as Associate Investigator (Exec approved 26 March 2014, ratified by AEC 17 April 2014)*
9. *Extension to approval duration – 3 months (Approved 17 April 2014)*

Conditions of Approval:

1. *The supervising Neurosurgeon must be present for all surgical procedures described in the application.*
2. *20 October 2011: The Committee agreed to approve the amendment subject to the attachment referred to in Section 4 – Experience of participant (checklist), being submitted to the Animal Ethics Committee*
3. *New rodent researchers must successfully complete the MQ rodent basic training courses*
   a. *Rodent Handling and Care*
   b. *Rodent anaesthesia with injectable and inhalant anaesthetics*
   c. *Clean and Aseptic surgical techniques*
   d. *Post-operative monitoring and pain relief.*

Being animal research carried out in accordance with the Code of Practice for a recognised research purpose and in connection with animals (other than exempt animals) that have been obtained from the holder of an animal suppliers licence.

Professor Mark Connor (Chair, Animal Ethics Committee) **Approval Date:** 17 April 2014

Adapted from Form C (issued under part IV of the Animal Research Act, 1985)